



***In vitro* analysis of the ABC transporter Pdr5**

Inaugural-Dissertation

zur Erlangung des Doktorgrades
der Mathematisch-Naturwissenschaftlichen Fakultät
der Heinrich-Heine-Universität Düsseldorf

vorgelegt von

Manuel Wagner

aus Mettingen

Düsseldorf, September 2019

aus dem Institut für Biochemie
der Heinrich-Heine-Universität Düsseldorf

Gedruckt mit der Genehmigung der
Mathematisch-Naturwissenschaftlichen Fakultät der
Heinrich-Heine-Universität Düsseldorf

Berichterstatter:

1. Prof. Dr. Lutz Schmitt

2. Prof. Dr. Georg Groth

Tag der mündlichen Prüfung: 17.12.2019

“Progress is made by trial and failure; the failures are generally a hundred times more numerous than the successes; yet they are usually left unchronicled.”

William Ramsay

Abstract

The overexpression of ATP-binding cassette (ABC) transporters is one of the main mechanisms that result in the phenomenon of multidrug resistance (MDR) existing across all organisms from man to bacteria. In *Saccharomyces cerevisiae*, the ABC transporters of the pleiotropic drug resistance (PDR) network are often involved in conferring MDR by lowering the cytosolic concentration of cytotoxic compounds. The key player of this network is Pdr5, a full-size ABC transporter that was discovered thirty years ago as a gene which's gene product confers cycloheximide resistance. Since then it has become an important model to study MDR in fungi, especially since its homologues like Cdr1 from pathogenic *Candida albicans* are conferring resistance towards the most commonly clinically used antifungals.

Mutational studies of Pdr5 mapped several key residues that are important for either its ATPase or transport activity. However, since it was not possible to investigate this efflux pump in an isolated form, many aspects of the molecular mechanism of the transport process remained elusive. Therefore, in a first step, a purification protocol was established that enabled in-depth biochemical, biophysical and structural analysis of Pdr5. It could be demonstrated that the detergent purified Pdr5 exhibits identical NTPase characteristics compared to Pdr5 located in the plasma membrane. Remarkably, using an electrophysiological approach, we could show that Pdr5 reconstituted into a planar lipid bilayer acts as a drug/proton symporter and can conduct ion currents. This has not been demonstrated for any other ABC exporter before.

Pdr5 belongs to the class of asymmetric ABC transporters that possess a degenerate nucleotide binding site (NBS). Mutational studies demonstrated that this degeneration is of crucial importance for the functionality of the protein. Based on the established purification protocol it was possible to perform structural analysis of Pdr5 using single particle cryo electron microscopy (cryo-EM). During this doctoral research, we were able to obtain the first electron density maps and the resulting model structure of Pdr5 in its apo and occluded state. This allowed to propose a mechanistic model that explains how the degenerate NBS forms the structural basis for the transport process, which does not fully follow the classical 'alternating access model' but rather indicates a 'twist-like' conformational shift of Pdr5 during the substrate efflux. Finally, based on the biochemical and biophysical data combined with the proposed transport model, it

can be concluded that cycloheximide, which initially led to the discovery of the ABC transporter Pdr5, might in fact not be a real substrate of Pdr5, but the observed cycloheximide-resistance is a byproduct of the proton pumping properties of Pdr5.

Zusammenfassung

Die Überexpression von *ATP-binding cassette* (ABC) Transportern ist einer der Hauptmechanismen, der in dem Phänomen der Multidrogenresistenz (MDR) resultiert und das in allen Organismen vom Menschen bis zur Bakterie existiert. In *Saccharomyces cerevisiae* sind die ABC Transporter des pleiotropen Drogenresistenz (PDR) Netzwerkes oft in die Vermittlung von MDR involviert, indem sie die zytosolische Konzentration zytotoxischer Stoffe reduzieren. Der Hauptakteur dieses Netzwerkes ist Pdr5, ein volllängen ABC Transporter, der vor dreißig Jahren als Gen entdeckt wurde, dessen Genprodukt Resistenz gegen Cycloheximid vermittelt. Seitdem ist es zu einem wichtigen Modell geworden, um MDR in Fungi zu untersuchen, vor allem, da seine Homologe wie Cdr1 von pathogenen *Candida albicans* Resistenz gegen die üblicherweise klinisch eingesetzten Fungizide vermitteln.

Mutationsstudien mit Pdr5 haben mehrere Schlüssel-Aminosäuren aufgezeigt, die wichtig sind für entweder seine ATPase- oder Transportaktivität. Dennoch, da es nicht möglich war diese Effluxpumpe in isolierter Form zu studieren, blieben viele Aspekte des molekularen Mechanismus des Transportprozesses ungeklärt. Folglich wurde in einem ersten Schritt ein Protokoll zur Reinigung des Proteins etabliert, das die tiefgehende biochemische, biophysische und strukturelle Analyse von Pdr5 ermöglicht. Es konnte gezeigt werden, dass das Detergenz-gereinigte Pdr5 identische NTPase Eigenschaften aufweist wie Pdr5, das in der Plasmamembran lokalisiert ist. Bemerkenswerterweise konnten wir mit einem elektrophysiologischen Ansatz zeigen, dass Pdr5 rekonstituiert in eine planare Lipid-Doppelschicht als Drogen/Proton Symporter agiert und Ionenströme leiten kann. Dies wurde noch für keinen anderen ABC Exporter zuvor demonstriert.

Pdr5 gehört zu der Klasse der asymmetrischen ABC Transporter, die eine degenerierte Nukleotidbindestelle (NBS) besitzen. Mutationsstudien zeigten, dass diese Degeneration von äußerster Wichtigkeit für die Funktionalität des Proteins ist. Basierend auf dem etablierten Protokoll für die Reinigung, war es möglich, Pdr5 strukturanalytisch mittels Einzelpartikel Kryoelektronenmikroskopie (cryo-EM) zu untersuchen. Während dieser Doktorarbeit konnten wir die ersten Elektronendichtekarten und die daraus resultierende Modellstruktur von Pdr5 in seiner apo und geschlossenen Form erhalten. Dies erlaubte ein mechanistisches Modell vorzuschlagen, das erklärt, wie die degenerierte NBS die strukturelle Basis für den Transportprozess bildet,

welcher nicht vollständig dem klassischen „abwechselnden Zugangsmodell“ folgt, sondern eher auf eine drehungsähnliche Konformationsänderung von Pdr5 während des Substrateffluxes hindeutet. Abschließend, basierend auf den biochemischen und biophysischen Daten zusammen mit dem vorgeschlagenen Transportmodell, kann geschlussfolgert werden, dass Cycloheximid, welches initial zu der Entdeckung des ABC Transporters Pdr5 geführt hat, tatsächlich kein echtes Substrat von Pdr5 ist, sondern die beobachtete Cycloheximidresistenz ein Nebenprodukt der Eigenschaft Pdr5 ist, Protonen zu pumpen.

Table of Contents

Abstract	I
Zusammenfassung	III
List of Figures	VII
List of Abbreviations	VIII
1. Introduction	1
1.1 Membrane transport	1
1.2 Structure of ABC transporters	2
1.3 Models, functions and mechanisms of ABC transporters	4
1.4 MDR ABC exporters – a special case	6
1.5 MDR in yeast – The pleiotropic drug resistance network	7
1.6 Pdr5 – The key player of the pleiotropic drug resistance	9
2. Aims	14
3. Publications	15
3.1 Chapter I	15
3.2 Chapter II	26
3.3 Chapter III	38
3.4 Chapter IV	61
3.5 Chapter V	98
4. Discussion	116
4.1 Pdr5 is an uncoupled transporter.....	118
4.2 Pdr5 as a proton pump and its implications.....	119
4.3 On the proposed R6G transport mechanism mediated by Pdr5.....	120

4.4	The structure of Pdr5.....	123
4.5	Asymmetry of the NBDs – A new constant contact model.....	123
4.6	Pdr5 – An ABC transporter with a twist	124
4.7	Cycloheximide – Transport or degradation?	127
5.	References.....	129
A.	Curriculum Vitae	140
B.	Acknowledgments	143
C.	Declaration	146

List of Figures

Figure 1 Schematic overview of the membrane transport types.	2
Figure 2 Structures of ABC transporters.	3
Figure 3 Schematic overview of target genes of the transcription factors PDR1 and PDR3 of the PDR network.....	8
Figure 4 Sequence alignment of the Walker A, C-loop, Walker B and H-loop motifs of the asymmetric ABC transporters Pdr5, Cdr1, ABCG5/G8 and TM287/288.....	10
Figure 5 Structural comparison of two maltosides.	117
Figure 6 Schematic overview of the R6G transport assay mediated by Pdr5.....	121
Figure 7 Simplified schematic representation of possible transport mechanisms.....	126

List of Abbreviations

Å	Ångstrom
ABC	ATP-binding cassette
ATP	Adenosine triphosphate
BEA	Beauvericin
CFTR	Cystic fibrosis transmembrane conductance regulator
CMC	Critical micellar concentration
Cryo-EM	Cryo-electron microscopy
CYH	Cycloheximide
DNA	Deoxyribonucleic acid
ECL	Extracellular loop
ICL	Intracellular loop
KA	Ketoconazole
kDa	Kilo Dalton
MDR	Multidrug resistance
µg	Microgram
mg	Milligram
min	Minute
µl	Microliter
ml	Milliliter
µM	Micromolar
mM	Millimolar
NBD	Nucleotide binding domain
NBS	Nucleotide binding site
nm	Nanometer
nM	Nanomolar
PDR	Pleiotropic drug resistance
R6G	Rhodamine 6G

TMD	Transmembrane domain
TMH	Transmembrane helix

1. Introduction

1.1 Membrane transport

Biological membranes protect cells from all kind of environmental stress and its integrity is crucial for cell survival (Cocucci et al., 2017; Engelman, 2005). However, they form also a barrier against solutes and molecules that the cell needs in order to survive and to proliferate. Therefore, it is necessary to enable the uptake of these compounds as well as to ensure the efflux of toxic molecules out of the cell. Depending on the chemical and structural characteristics of the molecules, different kinds of transport processes across the membrane can take place (Cocucci et al., 2017; Sugano et al., 2010). In general, membrane transport can occur in two different ways: active or passive. Small nonpolar molecules like oxygen can passively diffuse over the membrane along the concentration gradient, while larger and polar or charged molecules need carrier proteins in order to pass this barrier (Cocucci et al., 2017). Channel proteins interact more weakly with their substrates and therefore are able to transport significantly faster compared to carriers. As depicted in Figure 1, passive transport occurs as diffusion of small nonpolar molecules or as facilitated diffusion by channels or pores as in the case for hydrogen peroxide by aquaporins or various cell metabolites across all organisms (Bienert et al., 2007; Neuhaus and Wagner, 2000). These channels or pores can be voltage-, ligand-gated or mechanosensitive (Armstrong and Hille, 1998; Perozo et al., 2002). Carrier-mediated active membrane transport can be subdivided into secondary and primary active transport. In the case of primary active transport, the carrier or pump utilizes an energy source like ATP or light in order to translocate the substrate across the membrane, which can also occur in an uphill manner, i.e. against the concentration gradient of the substrate. Secondary transporters like antiporters or symporters use co-substrates that are transported unidirectional (symporter) or in opposing directions (antiporter) (Cocucci et al., 2017; Saier, 2000). The largest family of secondary active transporters is the major facilitator superfamily (MFS) consisting of more than 70 subfamilies. They transport a huge variety of different substrates ranging from ions over lipids to peptides (Yan, 2013). One of the most famous families of primary active transporters are the ATP binding cassette (ABC) transporters that energize the substrate transport by binding and hydrolyzing ATP. Like the MFS transporters, ABC

transporters are found in all kingdoms of life (Higgins, 2001). Other transport ATPases like P-type ATPases catalyze the translocation of lipids or cations (Bublitz et al., 2011).

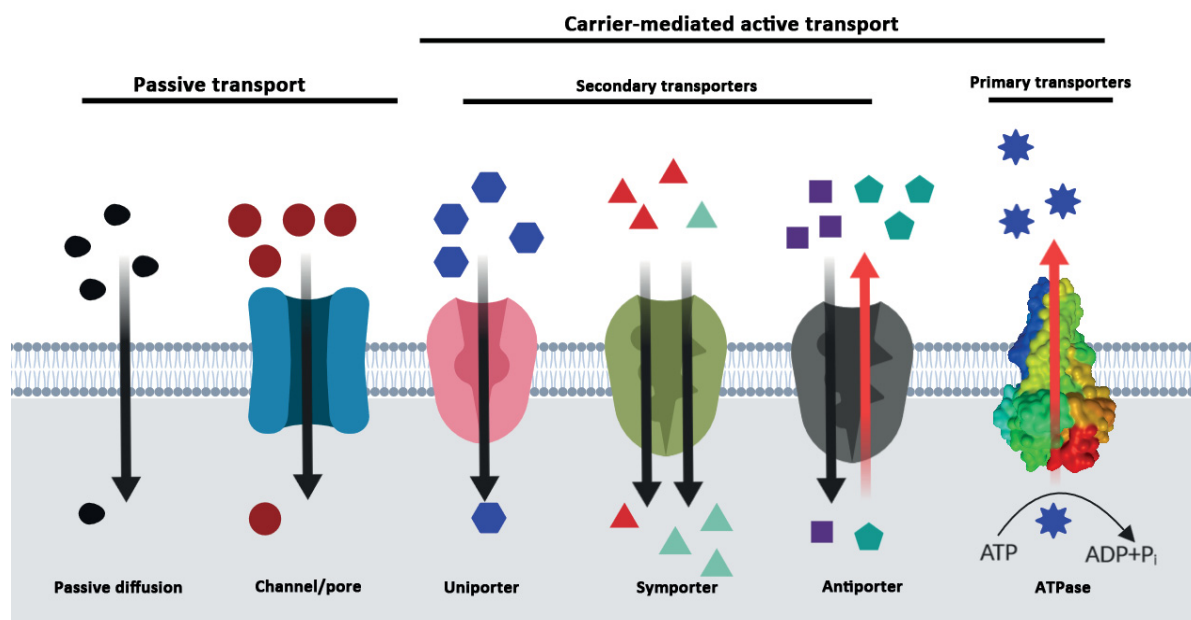


Figure 1 Schematic overview of the membrane transport types. Passive transport occur either by diffusion or facilitated by channel or pore proteins. Carrier-mediated active transport is divided into primary and secondary active transport (based on (Cocucci et al., 2017; Saier, 2000) and created with BioRender).

1.2 Structure of ABC transporters

ABC transporters are ubiquitous integral membrane proteins that serve a variety of physiological roles. Depending on the direction of transport, they are divided in two subclasses: ABC importers and exporters. However, the former are in general only present in prokaryotes while ABC exporters are found in all organisms (Higgins, 2001; Hollenstein et al., 2007; Locher, 2016). Although ABC transporters are highly diverse in their physiological roles, they all share a similar structural blueprint. A functional unit consists of four domains that are either located in one molecule (full-size transporter) or separated in two monomers (half-size transporters): two transmembrane domains (TMDs) and two nucleotide binding domains (NBDs). The latter are the motor-domains of the ABC transporter that bind and hydrolyze ATP and are thought to thereby give the power stroke that is necessary to translocate the substrate across the lipid bilayer (Oswald et al., 2006). These domains share an overall high sequence similarity and consist of

characteristic and conserved sequence motifs that are necessary to bind and hydrolyze the nucleotides: Walker A (consensus sequence GXXGXGKST, where X is any amino acid), C-loop (consensus sequence LSGGQ), Walker B (consensus sequence φ φ φ φ DE, where φ is any hydrophobic amino acid) and additionally the H-loop, Q-loop and D-loop. In the presence of ATP the two NBDs dimerize and form two nucleotide binding sites (NBDs) in which the C-loop of one NBD interacts with the sequence motifs of the second NBD and vice versa (Jones and George, 2013; Oswald et al., 2006).

While there is a high sequence identity within the NBDs throughout the ABC transporter family, the TMDs have low sequence similarity which reflects the substrate diversity of these proteins. The highly hydrophobic TMDs each consist typically of six membrane spanning transmembrane helices (TMHs) although there are examples for 5 up to 11 helices per domain (Biemans-Oldehinkel et al., 2006; Oldham et al., 2008).

Prokaryotic ABC importers consist additionally of a substrate binding protein (SBP) which are located in the periplasmic or extracellular space (see Figure 2) and are necessary for the uptake process as they guide the substrate to the TMDs (Biemans-Oldehinkel et al., 2006).

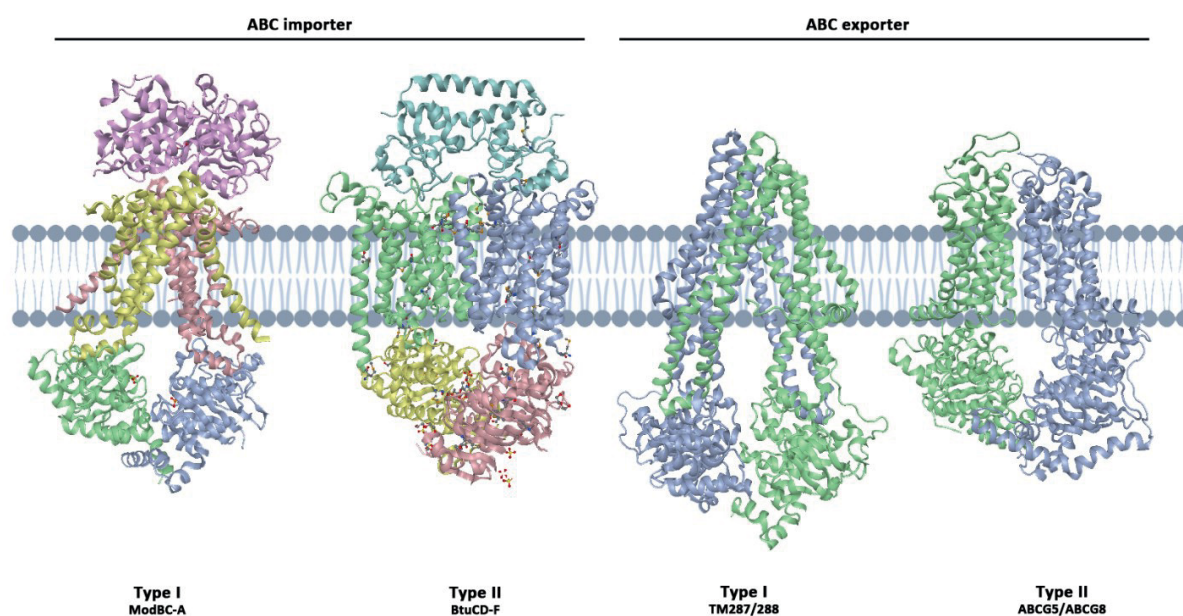


Figure 2 Structures of ABC transporters. Depending on their fold, ABC importers and exporters are subdivided into type I (e.g. ModBC-A, TM287/288) and type II (e.g. BtuCD-F, ABCG5/ABCG8) (created with BioRender based on (Lee et al., 2016)).

Structures of membrane proteins are rare compared to their soluble counterparts. However, especially since the “resolution revolution” in cryo EM began, more and more structures of ABC transporters are solved using this technique (Elmlund et al., 2017). The first structure of an ABC exporter was Sav1866 from *Staphylococcus aureus* (Dawson and Locher, 2006). Since then, it took ten years until it became clear that there are more than one type of exporters similar to the situation of ABC import systems (Figure 2). The structure of the human sterol transporter ABCG5/ABCG8 shows a different fold compared to all other ABC transporters that were determined to that date. Interestingly, it has similarities to type II importers in which coupling helices only interact within one monomer unit, i.e. NBD1 with TMD1 and NBD2 with TMD2 (Lee et al., 2016). The human multidrug transporter ABCG2 has a similar overall fold as ABCG5/ABCG8 which might indicate that exporters of the ABCG subfamily of ABC transporters might share this feature (Paumi et al., 2009; Taylor et al., 2017).

1.3 Models, functions and mechanisms of ABC transporters

ABC transporters fulfill a broad variety of different functions within a cell, ranging from nutrition uptake in bacteria, maintenance of the lipid bilayer asymmetry to efflux of toxic compounds (Locher, 2016; Schmitt and Tampe, 2002). Despite this diversity in function, the known structures of importers and exporters as well as biochemical data proof that the translocation process is coupled to the catalytical process of ATP binding and hydrolysis (Oldham et al., 2008). The mechanism of ATP binding, dimerization of the NBDs and ATP hydrolysis is rather well-understood thanks to structural data of purified NBDs (Oswald et al., 2006). On the other hand, little is known about how the released energy of ATP hydrolysis is transferred to induce the movement of the TMDs or to enable the release of the substrate. Mutational and structural studies point towards several key residues on the transmission interface between the TMDs and NBDs especially of the Q-loops in the NBDs and intracellular loops (ICLs) of the TMDs (Ananthaswamy et al., 2010; Oancea et al., 2009; Sauna et al., 2008). There is an ongoing debate whether the hydrolysis or the binding of ATP to the NBDs is the conformational change inducing step. In the ATP switch model the NBDs dimerize upon ATP binding which induces the conformational change in the TMDs. The subsequent ATP hydrolysis resets the transporter and

leads to the separation of the NBD dimer (Higgins and Linton, 2004). However, the limited amount of structures of ABC pumps in the different conformations that they undergo during a pump cycle makes it difficult to elucidate this question.

Starting from the catalytic ATPase mechanism, over the transmission interface between NBDs and TMDs, there are several models for the translocation mechanism. The importance of understanding the molecular mechanisms of transport results from diverse physiological functions of ABC transporters. Especially diseases caused by pathogenic organisms that are resistant towards drugs by the means of multidrug resistance (MDR) ABC transporters or that are caused by malfunctioning of human ABC transporters that are involved in cellular processes like membrane homeostasis (Borst and Elferink, 2002; Jungwirth and Kuchler, 2006; Prescher et al., 2019). The most prominent model regarding the overall mechanism for ABC transporters is the alternating two-site access model (Jardetzky, 1966). The basis of this model are two major conformations of the membrane protein: the inward-facing conformation and the outward-facing conformation. In the inward-facing conformation, the NBDs of an ABC exporter are monomeric, i.e. no ATP is bound while the high affinity substrate binding pocket is accessible from the cytosol. Upon substrate and ATP binding, the NBDs dimerize and drive a conformational change of the TMDs to the outward-facing conformation that result in the exposure of the substrate to the extracellular space in the low affinity binding pocket. As the ATP switch model proposes, the hydrolysis of ATP leads to the return to monomeric NBDs and therefore the inward-facing conformation (Higgins and Linton, 2004; Hollenstein et al., 2007).

Although this model is widely used to explain the mechanism of ABC transporters, it has its limitations. In the case of lipid transporters for example, it is unlikely that a protein could transport such a highly hydrophobic substrate through a mostly hydrophilic and water filled translocation channel across a membrane. Therefore, it is questionable if these transporters undergo the same conformational changes as proposed by the two-site access model. Another proposed mechanism to explain the translocation of lipids is the credit card mechanism (Pomorski and Menon, 2016). Here, the substrate is not transported through the channel formed by the TMDs, but rather along the transmembrane helices on the surface of the protein and through the membrane bilayer, which prevents unfavorable interactions of the polar head group of the lipid and the hydrophobic interior of the membrane.

1.4 MDR ABC exporters – a special case

Multidrug resistance in cells describes the ability to survive high concentrations of cytotoxic compounds that is caused by different mechanisms. The increasing number of multidrug resistant pathogenic organisms as well as the inefficient chemotherapeutic treatment of cancer caused by multidrug resistance are alarming (Blair et al., 2015; Gottesman et al., 2002).

Multidrug resistance can occur through different mechanisms as for example target modification, decreased uptake, metabolic alterations or increased efflux of the drugs. The latter is caused by MDR transporters that belong to two classes, depending on the energy source: First, secondary active transporters of the multidrug and toxic compound extrusion (MATE) family, the small MDR (SMR) superfamily, the resistance-nodulation-cell division (RND) family and MFS. Second, primary active transporters of the ABC transporter family (Chang, 2003; Lage, 2003; Sa-Correia et al., 2009). MDR ABC transporters have been in the focus of clinical research for years, especially after the discovery of the involvement of human MDR1 (P-glycoprotein (P-gp), ABCB1) in MDR of tumor cells (Kim, 2006). Since then, numerous studies *in vivo* and *in vitro*, including structures of some transporters, have helped to characterize these transporters from human, bacteria or fungi. However, it still is not possible to elucidate how these transport proteins are able to facilitate the efflux of such a wide variety of structurally and chemically unrelated compounds while all other known transporters and enzymes have a high substrate specificity (Chang, 2003; Ernst et al., 2010). The most commonly assumed model for MDR ABC transporters is the ‘drug pump model’, i.e. the transporter actively translocates the substrates across the biological membrane against a concentration gradient. Several studies used liposomal systems or inside-out plasma membrane vesicles to demonstrate substrate transport, although these methods do not provide any proof for uphill transport (Eckford and Sharom, 2008; International Transporter et al., 2010; Kolaczowski et al., 1996; Velamakanni et al., 2008). Another model proposes that these ABC transporters do in fact lower the intracellular drug concentration. However, they do not actively expel the drugs out of the cell through pumping, but through altering the membrane environment. This ‘alternated partitioning model’ describes the ability of ABC transporters to influence the internal pH, membrane potential and lipid environment and thereby lowers the ability of the drugs to pass the membrane (Roepe, 2000). Both models are

able to explain certain aspects of MDR that is mediated by ABC transporters, but none is describing all features of ABC transporters universally and therefore disputed. Most scientific evidence supports the model of direct drug extrusion as the drug resistance conferring mechanism (Ambudkar et al., 1999; Roepe et al., 1996; Sharom, 1997). However, the ability of MDR ABC transporters to mediate ion efflux or uptake was also shown in several studies (Agboh et al., 2018; Hoffman and Roepe, 1997; Milewski et al., 2001; Singh et al., 2016). It is therefore likely that both models interplay and while direct drug extrusion takes place, these membrane proteins alter simultaneously the drug partitioning by changing the membrane environment.

1.5 MDR in yeast – The pleiotropic drug resistance network

Infections with the main pathogenic fungi *Candida albicans* or *Candida glabrata* are primarily treated for decades with antifungals like azoles (Denning and Hope, 2010). Overall, there are only five common drug classes used to treat fungal infections (Kontoyiannis and Lewis, 2002). The general use of this limited number of antifungals has led to the development of isolates that are multidrug resistant, which in yeast is also referred to as pleiotropic drug resistance (PDR) (Alexander and Perfect, 1997; Balzi and Goffeau, 1995). *Saccharomyces cerevisiae* is a model organism for studying PDR in fungi since the genome is fully sequenced and the proteins involved are highly homologues to other fungi like *C. albicans* (Balzi and Moye-Rowley, 2019; Lamping et al., 2010).

The members of the PDR network of *S. cerevisiae* can be divided into 3 major classes: ABC transporters, MFS transporters and transcription factors (Balzi and Goffeau, 1995). As seen exemplary in Figure 3 for PDR1 and PDR3, the regulation of the network is highly complex and involves several transcription factors that interact with each other and have overlapping target genes. Overall there are at least six transcription factors within the PDR network, of which PDR1 and PDR3 with their characteristic Cys₆Zn₂ DNA binding motifs are the most prominent (Balzi and Goffeau, 1995; Kolaczowska and Goffeau, 1999). PDR1 was discovered in 1987 and has since led to important insights into the mechanisms of PDR in yeast (Balzi and Moye-Rowley, 2019). Following the discovery of PDR1, another key player and target gene of PDR1 was discovered three years later.

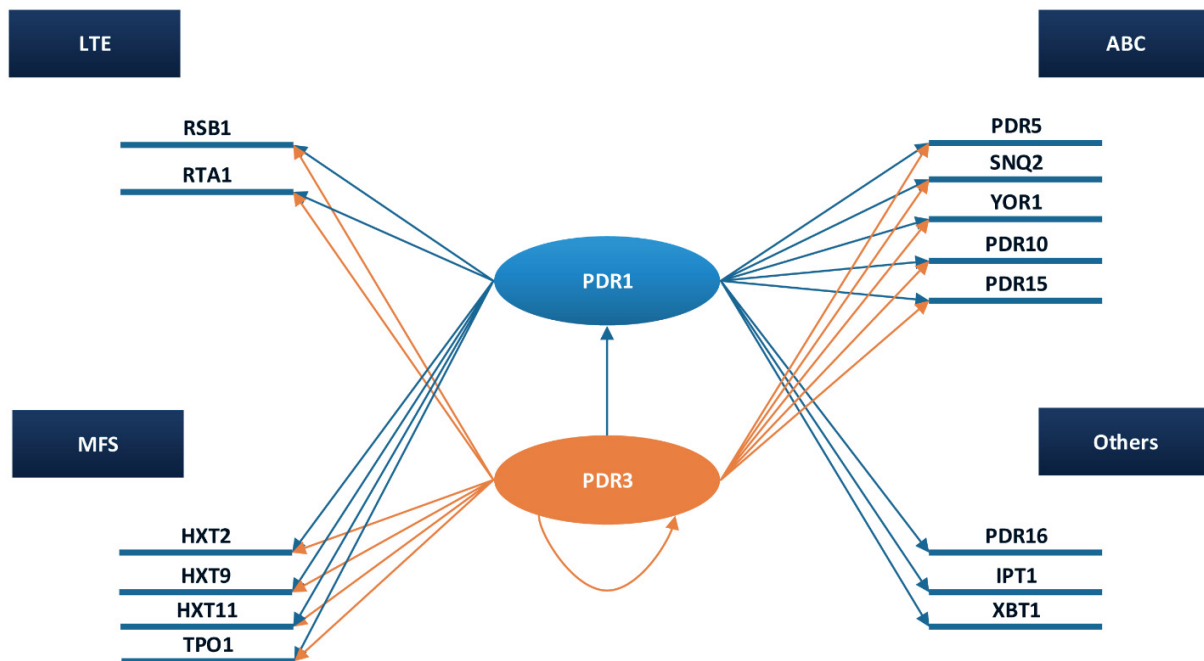


Figure 3 Schematic overview of target genes of the transcription factors PDR1 and PDR3 of the PDR network. LTE: lipid-translocator exporter family, MFS: major facilitator superfamily, ABC: ATP-binding cassette transporter family. Modified based on (Kolaczowska and Goffeau, 1999).

PDR5, a gene that was later found to encode an ABC transporter was found to play a major role in resistance of *S. cerevisiae* towards cycloheximide (Balzi et al., 1994; Leppert et al., 1990). A gain-of-function mutation of PDR1 (PDR1-3) led to overexpression of Pdr5 and thereby to hyper resistance towards cycloheximide (Meyers et al., 1992). In the following years the importance of Pdr1 was further manifested as it was shown that it also regulates the expression of the genes for the PDR ABC transporters SNQ2, which confers resistance towards different xenobiotics, and YOR1 that confers oligomycin resistance (Decottignies et al., 1995; Katzmann et al., 1995; Servos et al., 1993).

Fungal PDR ABC transporters form a first line of defense against a broad range of toxic compounds. They belong to the ABCG subfamily of ABC transporters and like their plant and human homologues, they possess a reverse domain topology of (NBD-TMD) whereas other subfamilies are (TMD-NBD) oriented. In *S. cerevisiae*, except Adp1, all PDR ABC transporter are full-size transporters (Bénédicte et al., 1991; Lamping et al., 2010). An interesting feature of full-size fungal PDR ABC transporter is that they are members of the family of asymmetric ABC

transporters. Although both, N-terminal and C-terminal halves show high similarity as they are likely a product of gene duplication, they have alterations within their NBDs (Lamping et al., 2010). It is important to note, however, that although there are several asymmetric ABC transporters, e.g. CFTR, ABCG5/G8 or MRP1, the degree of asymmetry varies a lot (Lee et al., 2016; Sorum et al., 2017; Yang et al., 2003). It is not well understood yet how the degree of asymmetry within the NBDs influences the overall function of the protein.

1.6 Pdr5 – The key player of the pleiotropic drug resistance

Since the discovery of the PDR5 gene as a cause of cycloheximide resistance in *S. cerevisiae* and that the product of this gene is an ABC transporter, many mutational and biochemical studies provided important insights about fungal drug resistance and ABC transporters in general (Golin and Ambudkar, 2015; Leppert et al., 1990).

Like all members of the PDR ABC full-size transporters family, Pdr5 is an asymmetric ABC transporter. As depicted in Figure 4, the NBS of Pdr5 has amino acid exchanges in all of the key motifs that are necessary to bind and hydrolyze ATP. Compared to other members of this family, e.g. ABCG5/ABCG8 or TM287/288, it has, together with its homologue Cdr1 from *C. albicans*, the highest degree of asymmetry (Banerjee et al., 2019; Gupta et al., 2014; Hohl et al., 2012; Wang et al., 2011). Although the purpose of this degeneration is not known, mutational studies demonstrated that they are crucial for the functionality of the protein as already mutations within the degenerate NBS result in loss of function in ATPase activity, substrate transport or both (Gupta et al., 2014).

A				
	Walker A	C-loop	Walker B	H-loop
Pdr5	GASGAGKTT	VSGGE	LVFLDE	IHQ
Cdr1	GASGAGKTT	CSGGE	LLFLDE	IHQ
ABCG5/G8	GSSGSGKTT	LSGGE	VMLFDE	IHQ
TM287/288	GPTGSGKTT	FSGGQ	ILILDE	AHR
B				
	Walker A	C-loop	Walker B	H-loop
Pdr5	GRPGSGC T	LNVE Q	FQCWD N	I Y Q
Cdr1	GRPGAGC S T	LNVE Q	IQCWD N	I Y Q
ABCG5/G8	GSSGCG R AS	ISTGE	ILILDE	IHQ
TM287/288	GETGSGKST	LSQG Q	VLILDD	T Q K

Figure 4 Sequence alignment of the Walker A, C-loop, Walker B and H-loop motifs of the asymmetric ABC transporters Pdr5, Cdr1, ABCG5/G8 and TM287/288. A: Canonical NBS. B: Degenerate NBS. Residues that are non-canonical are marked red.

Moreover, PDR ABC transporters with their inverse domain topology of (NBD-TMD) belong to the ABCG subfamily of ABC transporters (Paumi et al., 2009). As such, Pdr5 belongs structure wise to the type II exporter that were first identified based on the structure of the human sterol transporter ABCG5/G8 (Lee et al., 2016). A model based on ABCG5/G8 for Pdr5 and its homologue Cdr1 from *C. albicans* indicates differences to known type II structures like ABCG5/G8 and ABCG2 (Tanabe et al., 2019; Taylor et al., 2017). One of the key differences are the larger extracellular loops, a region that is also the target for a known inhibitor FK506 (Kueppers et al., 2013; Tanabe et al., 2019). However, since there is only the computational model of Pdr5 and no structure of fungal ABC transporters has been solved yet, it remains elusive what the exact key features of this efflux pump are.

An interesting feature of Pdr5 is its high basal ATPase activity. Other model MDR ABC transporters as for example MDR1 have a low basal ATPase activity that is stimulated by its substrates and at higher concentrations undergoes substrate inhibition as described by the bell-shaped curves of its substrate dependent ATPase activity curves (Kimura et al., 2007; Muller et al., 1996). MDR1 belongs therefore to the coupled ABC transporters that link directly the ATPase activity to substrate transport. Contrarily, Pdr5 shows no stimulation by any of its substrates but

trans-inhibition at higher concentrations (Decottignies et al., 1994; Ernst et al., 2008). This fact raises several questions:

First, is the high basal ATPase activity in the absence of a substrate a waste of energy and resources for the cell?

Second, if Pdr5 follows the alternating access model that is proposed for all ABC transporters and the ATPase activity is always at the same level, how does substrate selection work for this transporter?

And third, what benefit does the transporter and finally the cell have to keep the efflux pump in an always-on state?

(I) It is argued in literature that the high basal ATPase activity could be an artifact of purification. In fact the maltose ABC importer from *E. coli* displayed high basal activity when solubilized with detergent. However, it was shown that this was indeed a detergent artifact, as the importer did not possess such a high basal ATPase activity upon reconstitution in liposomes and therefore is not an uncoupled transporter (Bao and Duong, 2012; Reich-Slotky et al., 2000). For *S. cerevisiae* it was demonstrated that specific PDR pump inhibitors like FK506 lead to increased intracellular ATP levels (Krasowska et al., 2010). As the study was performed in the absence of any known PDR substrate, it indicates that these ABC transporters are in fact in an always-on state. Moreover, comparison of the overall growth of cells harboring Pdr5 and other PDR ABC transporters and cells lacking these demonstrates that the ATP consumption by the efflux pumps does not inhibit cell proliferation (Krasowska et al., 2010). One has to be aware, however, that the physiological substrate of Pdr5, if there is one, is not known and there is the possibility that a substrate is always present.

(II) The molecular mechanism of substrate recognition and transport of ABC efflux pumps is still unknown. Based on determined structures of ABC transporters together with biochemical data, the alternating access model describes roughly how the underlying mechanism might work. Here, an ABC transporter can adopt two distinct conformations: inward-facing and outward-facing (Jardetzky, 1966). The conformational shift between the two states is driven by ATP binding

and hydrolysis. Some structures, however, show an intermediate state in which the NBDs are dimerized upon ATP binding, but the transporter remains occluded to the extracellular space (Choudhury et al., 2014; Locher, 2016). This indicates that the combination of substrate and ATP binding are necessary to enable the conformational movement from the inward to the outward-facing state. For a coupled ABC transporter like MDR1 this concept seems to make sense as upon substrate binding, the ATPase activity increases in a concentration dependent manner. For an uncoupled system like Pdr5, however, it seems more complicated as the transporter must move always between the inward-facing and occluded conformation. How then does Pdr5 select between substrates, if not the substrate binding induces the shift? One possible explanation is the 'kinetic substrate selection' model. Here, not the affinity of the substrates to the binding pocket of the transporter are the crucial step, but rather the rate of equilibration of the substrate with Pdr5 (Ernst et al., 2010). Interestingly, this model can also explain why trans-inhibition of Pdr5 by its substrates is differently affected depending on which nucleotide is used. For clotrimazole it was shown that at concentrations that inhibit the ATPase activity completely, the GTPase activity remained intact, indicating that the kinetics of NBD dimerization influence the transport activity (Golin et al., 2007).

(III) Assuming that the transporter is in an always-on state and that it is not harming cell proliferation, the question of what the benefits are of a high basal ATPase activity remains. First, in a study on BtuC₂D₂ from *E. coli*, the authors compared the stability as well as the functionality of the ABC transporter *in vitro* coming from an always-on and from an idle state. The always-on state was simulated by repeated additions of ATP to the storage buffer over the time course of several days, while the sample of the idle state lacked ATP. The results proved that BtuC₂D₂ was longer stable and functional if the basal ATPase activity was continuously fueled by ATP additions. Additionally, transport activity did not show any lag phase, which was observed in the idle state sample (Livnat-Levanon et al., 2016). As it was shown *in vivo*, Pdr5 has a long lifetime with more than 80% of the molecules still found after a chase period of 180 min (Decottignies et al., 1999). This fact supports the finding of a high basal ATPase activity as it might stabilize the protein and protect it from degradation. The long lifetime of Pdr5 and the fact that an ABC transporter is more responsive coming from an always-on state make sense for Pdr5 given the fact that this efflux

pump mediates resistance towards such a broad variety of structurally diverse substrates, ranging from azoles over ionophores to steroids and antibiotics (Kolaczkowski et al., 1996; Rogers et al., 2001). Overall, the high basal ATPase activity appears to not be a waste of energy, but rather a mechanism of the yeast cell to ensure the protection towards xenobiotics in the shortest amount of time and thereby cell proliferation.

Although studied over decades, several key characteristics of the PDR ABC transporter Pdr5 are yet to be elucidated. So far, it was not possible to study this transporter in an isolated system that allows for functional and structural characterization in order to understand the molecular mechanisms that underlie substrate binding and translocation. As the model protein of the pleiotropic drug resistance and for asymmetric eukaryotic ABC transporters, it is crucial to establish the necessary tools to study this transporter *in vitro*.

2. Aims

The ABC transporter Pdr5 from *Saccharomyces cerevisiae* is one of the most prominent fungal PDR exporter of great physiological significance that is studied for almost three decades (Golin and Ambudkar, 2015). Since it belongs to the family of asymmetric PDR ABC transporters that confers resistance towards a wide variety of cytotoxic compounds, it is used as a model to study the impact of the degenerated NBS in asymmetric ABC transporters as well as to study multidrug resistance in pathogenic fungi like *Candida albicans* or *Candida gebralta* (Gupta et al., 2014; Prasad et al., 2015; Tanabe et al., 2019; Vermitsky and Edlind, 2004).

Numerous mainly mutational studies on this ABC transporter have been performed, giving insights into possible mechanisms for transport function as well as identifying new substrates and inhibitors. Nonetheless, many open questions remain, especially because it was not possible to purify Pdr5 in an active form and investigate molecular details of this export pump in an isolated system. In order to elucidate the molecular mechanism of substrate transport the first aim of this doctoral thesis was to establish a purification protocol that allows to study Pdr5 in an active and functional state.

Moreover, substrate transport assays have been limited to either *in vivo* or plasma membrane vesicle experiments such as liquid drug assays or fluorescence quenching assays based on rhodamine 6G (Kolaczowski et al., 1996; Rogers et al., 2001). Therefore, a second focus was set on finding new approaches among others using electrophysiological techniques with purified Pdr5 reconstituted into lipid bilayers to further investigate molecular details of the transport process with substrates of varying physicochemical properties.

The degenerate NBS of the asymmetric efflux pump Pdr5 is of fundamental importance (Gupta et al., 2014). However, since there are no structures of fungal ABC transporters, not to mention PDR ABC transporters, it remains unclear what the structural basis for this functionally crucial asymmetry in the motor domains of Pdr5 is. Consequently, the final aim of this thesis was the structure determination of the ABC transporter Pdr5 using single particle cryo-EM that allows in combination with collected biochemical and biophysical data to establish a model for the overall transport mechanism of the ABC transporter Pdr5 on a molecular basis.

3. Publications

3.1 Chapter I

Titel: Transmitting the energy: interdomain cross-talk in Pdr5

Authors: Manuel Wagner, Katja Doehl and Lutz Schmitt

Published in: Biological Chemistry
Impact factor: 3.162

**Proportionate work
on this manuscript:** 60%

Review

Manuel Wagner, Katja Doehl and Lutz Schmitt*

Transmitting the energy: interdomain cross-talk in Pdr5

DOI 10.1515/hsz-2016-0247

Received July 4, 2016; accepted August 16, 2016; previously published online August 20, 2016

Abstract: ABC (ATP-binding cassette) transporters are ubiquitous integral membrane proteins catalyzing the active export or import of structurally and functionally unrelated compounds. In humans, these proteins are clinically and economically important, as their dysfunction is responsible for a number of diseases. In the case of multidrug resistance (MDR) ABC exporters, they particularly confer resistance to a broad spectrum of toxic compounds, placing them in the focus of clinical research. However, ABC-mediated drug resistance is not only restricted to humans. In yeast for example, MDR is called pleiotropic drug resistance (PDR). Important and well-studied members of the PDR subfamily of ABC transporters are Pdr5 from *Saccharomyces cerevisiae* and its homolog Cdr1 from *Candida albicans*. Mutational studies of these two transporters provided many insights into the complexity and conceivable mechanism of the interdomain cross-talk that transmits the energy gained from ATP hydrolysis to the substrate translocation process across the membrane. In this review, we summarize and discuss our current knowledge of the interdomain cross-talk as well as new results obtained for asymmetric ABC transporters and derive possible structural and functional implications for Pdr5.

Keywords: ABC transporter; drug resistance; substrate transport.

Introduction: fungal PDR efflux pumps

Multidrug resistance (MDR) in cancer cells is one of the major challenges, which have to be overcome in order to improve chemotherapy and fight the disease (Gottesman et al., 2002). Several mechanisms of MDR, such as decreased uptake of drugs, alteration of the drugs, increased DNA repair activity and increased efflux of cytotoxic compounds by ATP-binding cassette (ABC) transporters, combine to obstruct an efficient treatment (Gottesman et al., 2002).

Likewise, in pathogenic fungi such as *Candida albicans*, which is the main cause of opportunistic mycosis (Pfaller and Diekema, 2007), MDR against a broad variety of antifungals such as azoles expounds the problem of an efficient treatment (Lamping et al., 2010). The plant and fungal homolog of MDR is called pleiotropic drug resistance (PDR). The PDR network acts as a first line of defense. It consists of several ABC transporters and together with secondary transporters, they are all located in the plasma membrane and regulated by transcription factors such as Pdr1 and Pdr3 (Figure 1), providing a broad spectrum of resistance against a variety of toxic compounds. One of the most well-studied PDR proteins is the ATP-binding cassette (ABC) transporter Pdr5 from *Saccharomyces cerevisiae*, which was first discovered in 1990 (Leppert et al., 1990) as a DNA sequence conferring resistance towards cytotoxic compounds and later classified as an MDR ABC transporter (Balzi et al., 1994; Bissinger and Kuchler, 1994; Hirata et al., 1994). Pdr5 and its homolog from *C. albicans* Cdr1 show unique characteristics that might be transferable to asymmetric, mammalian ABC transporters, which will be specified in detail below.

In general, a functional ABC transporter is composed of two transmembrane domains (TMDs) and two highly conserved nucleotide-binding domains (NBDs) (Biemans-Oldehinkel et al., 2006; Oswald et al., 2006; Oldham et al., 2008). The two NBDs dimerize in the presence of ATP and both NBDs contribute amino acid residues to a catalytic active nucleotide-binding site (NBS). However, there are

*Corresponding author: Lutz Schmitt, Institute of Biochemistry, Heinrich Heine University Düsseldorf, Universitätsstr. 1, D-40225 Düsseldorf, Germany, e-mail: Lutz.Schmitt@hhu.de

Manuel Wagner and Katja Doehl: Institute of Biochemistry, Heinrich Heine University Düsseldorf, Universitätsstr. 1, D-40225 Düsseldorf, Germany

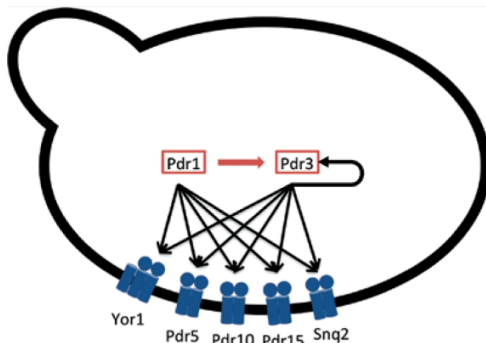


Figure 1: A simplified model of the PDR network in the yeast *Saccharomyces cerevisiae*. The transcriptional regulators Pdr1 and its paralog Pdr3 are responsible for the transcription of several transporters of the ABC and secondary transporter family of the PDR network that are located in the plasma membrane. For further details see also the excellent review of Prasad and Goffeau (2012).

asymmetric or degenerated ABC transporters. Here, one NBS contains catalytically active residues, while these residues are all exchanged against non-active residues in the other NBS (Procko et al., 2006; Golin and Ambudkar, 2015). Examples of such ABC transporters in humans are TAP (transporter associated with antigen processing) (Ernst et al., 2010) or CFTR (cystic fibrosis transmembrane conductance regulator) (Kim Chiaw et al., 2011).

Although extensively studied, the molecular mechanism of transport as well as the energy coupling of ATP binding, hydrolysis and substrate transport and the transmission from the NBS to the transmembrane segments (TMS) remain still elusive. In the following, we will review the current knowledge on the interdomain cross-talk between NBD and TMD and discuss in some detail the effect of substrates on residues that are apparently involved in the communication of these domains in the asymmetric yeast ABC transporter Pdr5.

The cross-talk between NBD and TMD may be substrate dependent

Although the substrate specificity and general physiological function of ABC transporters can be diverse, a fully functional ABC transporter consists of TMDs as well as two NBDs, as briefly described above (Oswald et al., 2006; Hollenstein et al., 2007). These can be either organized in a forward (TMD-NBD)₂ or, in the case of fungal PDR proteins or the human ABCG subfamily, a reverse (NBD-TMD)₂

topology. The conserved NBDs bind and hydrolyze NTPs, particularly ATP (Ernst et al., 2005). Whether the released energy is used to induce directly the transport of substrate across the membrane or whether it is used to reset the exporter into an inward-facing conformation after transport is not fully understood to date. The alternating two-site access model (Jardetzky, 1966), as summarized schematically in Figure 2, describes how binding and hydrolysis of ATP could control the conformational state of an ABC transporter – either in its inward-facing conformation, i.e. its binding pocket is accessible from the cytosol, or in its outward-facing conformation, in which the substrate is released into the extracellular space (Hollenstein et al., 2007). In this model, an ABC transporter, which catalyzes substrate export, switches through binding of ATP and subsequent dimerization of its NBDs from the inward- to the outward-facing conformation. After hydrolysis of ATP, ADP and inorganic phosphate are released and the transporter switches back to the inward-facing orientation.

Generally, TMDs have a higher variation in their sequence, however, they typically consist of at least six transmembrane helices (TMHs) per TMD, which span the membrane and form the so-called core set of the TMDs. They are connected by intra- and extracellular loops (ICL

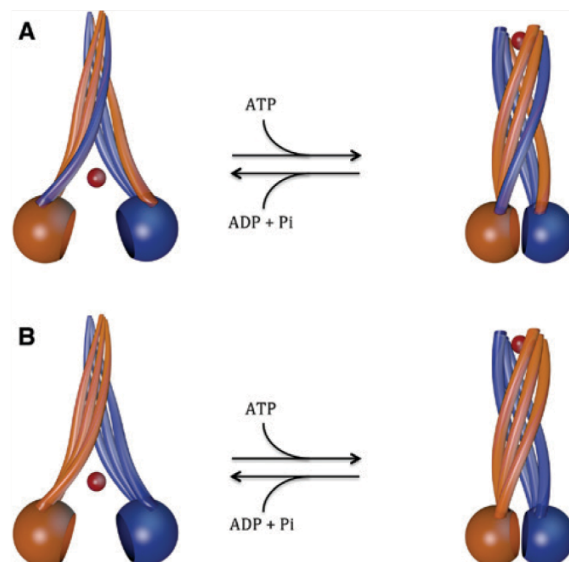


Figure 2: The ‘two-site alternating access’ model of canonical ABC exporters.

NBD1 and TMD1 are colored in orange, NBD2 and TMD2 are colored in blue, and the substrate is colored in red. Each column comprises two TMHs. (A) Alternating access model for type I exporters with interdomain cross-talk between the opposing monomer. (B) Model for type II exporters, where only TMD-NBD interaction within one monomer takes place.

and ECL, respectively) and are presumed to form the substrate binding site and channel through which the substrate is transported (Ernst et al., 2005; Lamping et al., 2010). Even though many details are known about each of the domains, it needs yet to be elucidated how the cross-talk between these two distinct parts of ABC transporters occurs on the molecular level.

Within this context, mutational studies of Pdr5 point towards an important role of TMH2 and ICL1. Sauna et al. (2008) demonstrated that cycloheximide resistance of cells bearing a S558Y mutation in Pdr5 was completely abolished, while ATPase activity of this mutant was comparable to that of the wild-type protein. Furthermore, the authors were able to restore functionality of this mutant by a second mutation located between the Walker A and signature motif of NBD1. Based on the homology model of Rutledge et al. (2011), this second residue, N242, interacts with the intracellular loop 1 (Sauna et al., 2008). Additionally, in a second study investigating mutants that restore functionality of the S558Y mutation, Ananthaswamy et al. (2010) identified nine repressor mutants. Five of these are located close to or within the Q-loop of NBD1, giving evidence that the Q-loop of NBD1 directly interacts with ICL1. Moreover, two mutants that define the Q-loop of the degenerated (E244G) and the canonical (Q951G) NBS were shown to have lower resistance towards cycloheximide and clotrimazole, while the K_m values of ATP hydrolysis did not change significantly. Although asymmetric and symmetric ABC transporters may differ in the functional equivalence of the two NBS, the results of Ananthaswamy et al. demonstrate that both NBS interact with the transmembrane domains, which was also shown for the symmetric ABC transporter P-gp (Urbatsch et al., 2000). Interestingly, a major difference between MDR and PDR ABC transporters is how the Q-loop-ICL interaction takes place. While MDR efflux pumps such as P-gp or non-MDR pumps such as TAP adopt a *trans* conformation (Zolnerciks et al., 2007; Oancea et al., 2009), studies on Pdr5 demonstrated that the interaction of Q-loop and ICL employ a *cis* interface (Ananthaswamy et al., 2010; Furman et al., 2013). This finding is consistent with the newly determined structure of ABCG5/ABCG8 (Lee et al., 2016) as described below. A more recent study by Dou and colleagues showed that two other mutations within TMH2 (E574K and E580K) resulted in hypersensitivity of the cells against several known substrates of Pdr5, comparable to the knock-out mutant, while the ATPase activity was not affected and remained similar to that of wild-type Pdr5. The E570 residue of Cdr1, which is also located within TMH2 also revealed an impaired transport of several drugs (Shah et al., 2015; Dou et al., 2016). Together, these

findings underline the importance of TMH2 for substrate efflux and point towards TMH2 as the main interaction region of NBDs and TMDs. Yet, there are additional mutations showing that the causal relationships are far more complex. For example, a mutation within the H-loop (H1068A) abolished rhodamine 6G transport, while the ATPase activity as well as the resistance towards other substrates of Pdr5 remained identical to the wild-type protein (Ernst et al., 2008). The fact that a single mutation within the NBD abolished transport of a specific set of substrate(s), but does not affect the efflux of other drugs, hints towards a mechanism in which dependent on the substrate of Pdr5, different regions of TMD and NBD might interact. This is also supported by the S1360F mutation leading to a higher resistance against the immunosuppressant FK506 (Egner et al., 1998; Kueppers et al., 2013). S1360 is presumably located in TMH11 near its cytosolic end and thus in a region that might be involved in the interdomain cross-talk of TMDs and NBDs. The exchange of serine to phenylalanine does not change the ATPase activity or drug efflux compared to wild-type Pdr5. However, while the ATPase activity as well as the rhodamine transport is inhibited by FK506 in the wild-type transporter, this effect is significantly less pronounced in the mutant (Kueppers et al., 2013).

In summary, the description of only a minor number of mutants of Pdr5 that have been analyzed in the past provides interesting insights in the complexity of the interdomain cross-talk. Analysis of these mutants raises many questions including whether the substrate, transporter interaction affects conformation and transport.

Substrate selection of fungal PDR proteins

One of the best-characterized human MDR transporters is P-glycoprotein (P-gp, MDR1 or ABCB1). It has been demonstrated that all TMHs are involved in drug transport because of a high number of structure-function studies. Until now it is suggested that P-gp contains at least seven different drug-binding sites (Safa, 2004). More recently, the crystal structure of mouse P-gp in combination with biochemical data identified a large internal binding cavity that is capable of accommodating various, structurally unrelated compounds at the same time (Aller et al., 2009). However, because the transporter-drug interactions of P-gp are believed to be highly dynamic (Ernst et al., 2010), the mechanism of multidrug recognition and selection is still unknown.

Although the substrate spectra of P-gp and Pdr5 are to some extent overlapping, the rules of substrate selection apparently differ. In the case of P-gp, most of the substrates are positively charged and contain aromatic ring systems. Their size spectrum varies from 200 to 1900 Da (Eckford and Sharom, 2009) and it is known that the ability to form hydrogen bonds represents a key factor for efficient recognition by P-gp (Seelig, 1998). For the yeast PDR pump Cdr1, Puri et al. (2010) showed that substrates have specific characteristics such as molecular branching, high aromaticity as well as a so-called atom centered fragment, i.e. (R-CH-R). In the case of Pdr5, Golin and co-workers demonstrated that the molecular volume rather than hydrophobicity is a crucial factor for substrate selection. In this study, tetra-alkylin compounds were used, which are effective Pdr5 substrates, even though they contain neither aromatic nor electron pair donor groups (Golin et al., 2000). Golin et al. were also able to demonstrate that efficient Pdr5 substrates possessed surface volumes of 200–300 Å³. Substrates that are smaller than 90 Å³ are not transported or only with low efficiency. Furthermore, Pdr5 exhibits multiple binding regions (such as P-gp and Cdr1) (Shukla et al., 2003; Safa, 2004) and it was suggested that there are at least three different drug-binding sites (Golin et al., 2003).

But how does drug transport and selection take place? Interestingly, different mutations only affected the

transport of a subset or single substrates of Pdr5. Kueppers et al. (2013) identified the S1360F mutation of Pdr5, which is located in the hydrophilic face of the predicted transmembrane helix 11 (TMH11) (Figure 3), where substrate specificity is altered. Notably, in this mutant, the resistance against the immunosuppressant FK506 was drastically increased. Other kinetic and thermodynamic parameters of the S1360F mutant are similar to those of the wild-type protein in the absence of FK506. These results indicate that the S1360F mutation modulates the ability of NBSs to hydrolyze ATP in the presence of FK506 by interfering with the interdomain cross-talk. A similar effect was shown in the T1351F mutant of Cdr1. Shukla et al. (2004) demonstrated that the mutation of T1351, which is equivalent to S1360 in Pdr5, leads to a downsizing of rhodamine 6G transport. For both proteins, Pdr5 as well as Cdr1, it was shown that the respective residues (S1360 and T1351) are responsible for the synergic effects of immunosuppressant FK506, FK520 and azoles, respectively, which leads to an increased drug susceptibility. Mutation of these residues to phenylalanine eliminated this effect (Egner et al., 1998; Shukla et al., 2004).

For both ABC transporters, P-gp and Pdr5, a phenomenon coined allosteric or trans-inhibition has been described. Here, high concentrations of a subset of drugs cause an inhibition of the ATPase activity of these transporters. Gupta et al. (2011) proposed that efflux pumps,

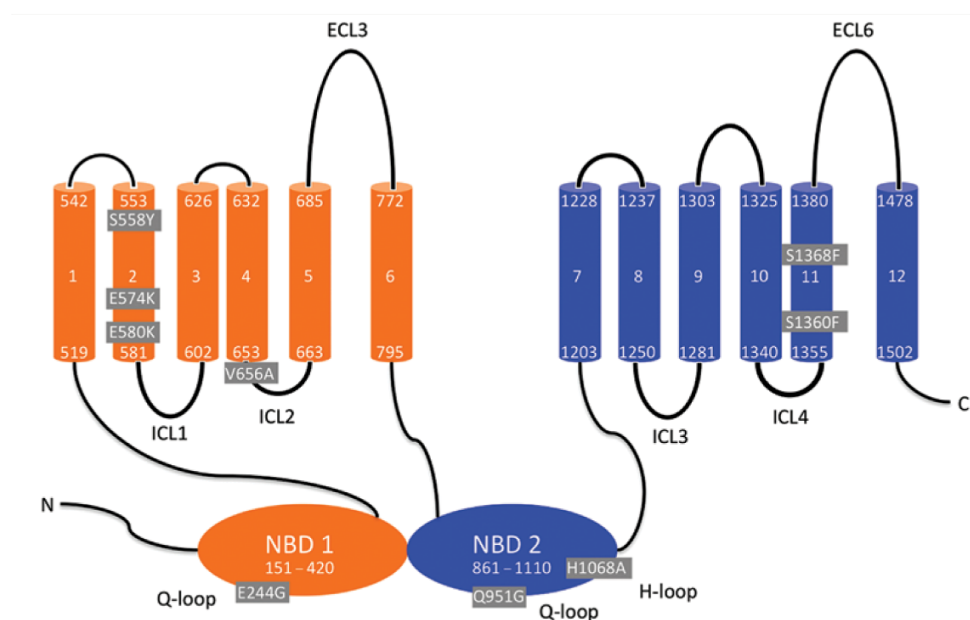


Figure 3: Location of mutations in Pdr5 that are affecting transport or ATPase activity (Ernst et al., 2008; Ananthaswamy et al., 2010; Downes et al., 2013; Kueppers et al., 2013; Mehla et al., 2014; Dou et al., 2016). NBD1 and TMD1 are colored in orange; NBD2 and TMD2 are colored in blue. The mutated amino acids are marked with a gray box.

which fail to release the substrate can not switch back into the inward facing conformation and thereby the bound nucleotide can not be released and finally hinders the substrates from re-entry into the cells.

Many clinically relevant substrates, however, do not inhibit the ATPase activity of P-gp and Pdr5 even at high concentrations (Litman et al., 1997; Golin et al., 2007; Ernst et al., 2008; Downes et al., 2013), which excludes that these molecules act according to the mechanism described above. What prevents these substrates from getting back into the cell at high concentrations? Based on *in silico* studies of P-gp, it was clearly demonstrated that none of the substrates is taken up again although they are apparently not able to inhibit the transporter (Turk et al., 2009). Accordingly, a molecular diode mechanism was proposed by Gupta et al. (2011), who suggested that ABC transporters undergo a re-modeling process after substrate release and ATP hydrolysis. This re-modeling would prevent a re-uptake of the substrate into the cell. Mehla et al. (2014) characterized the S1368A mutant of Pdr5 and provided the first experimental evidence for such a diode mechanism. S1368 is located in transmembrane helix 11 (TMH11) of Pdr5. An atomic model of Pdr5 (Rutledge et al., 2011) places S1368 deep in the proposed drug-binding pocket of Pdr5. Previous work by Egner et al. (1998) demonstrated that mutations in TMH10 (later predicted to be TMH11) affect the substrate specificity of Pdr5. Although drug binding and ATP hydrolysis were similar to the wild-type protein, this mutant showed hypersensitivity to some drugs that are not transported from the same drug-binding site. Furthermore, they developed an assay that directly demonstrated reflux of rhodamine 6G in the S1368A background compared to the wild-type protein. In conclusion they suggested that residue S1368 is central to prevent the reflux of a transported substrates. The best model that fits to their data is that S1368 helps to create a molecular diode or a one-way gate in Pdr5 (Mehla et al., 2014).

Another interesting model for substrate selection in Pdr5 is known as the kinetic substrate selection hypothesis. Here, Ernst et al. (2010) proposed how different substrates are transported with different efficiencies based on the rate of substrate equilibration with Pdr5 and the rate of interconversion of Pdr5 between the inward- and outward-facing state. Thereby, this model provides an explanation of how the dynamics of cross-talk between NBD and TMD can influence the rate of substrate transport. Such a scenario would also explain why mutations remote from the substrate-binding site such as H1068A (Ernst et al., 2008) (Ref) influence the efficiency of substrate translocation (Ernst et al., 2010).

Basal ATPase activity in uncoupled systems – the ‘always-on’ state

Until now, the molecular mechanisms by which ATP is utilized to energize the transport of substrates across membranes by ABC transporters remain unknown. Moreover, the role of ATP hydrolysis for the transport process seems to vary among different transporters. There are many transporters that show strict coupling of ATP hydrolysis and substrate transport such as to name only a single example the bacterial maltose transporter (Davidson et al., 1992). Accordingly, the mammalian multidrug efflux transporter P-gp exhibits only a low basal activity in the absence of substrate, while the ATPase activity is stimulated manifold in presence of substrate (Lerner-Marmarosh et al., 1999; Al-Shawi and Omote, 2005).

Fungal ABC transporters such as Pdr5 from *Saccharomyces cerevisiae* and its homolog Cdr1 from the pathogenic yeast *Candida albicans*, however, show different functional properties. In the absence of substrate, they exhibit a high basal ATPase activity that cannot be stimulated by substrate, or show weak stimulation (1.4-fold) in the case of Cdr1 (Decottignies et al., 1994; Shukla et al., 2006; Ernst et al., 2008). This implies that these transporters are in an ‘always-on’ state. This raises the question why an organism would permanently waste energy in the form of ATP hydrolysis to power an efflux pump even if there is no substrate present. Interestingly, in a recent study of the *E. coli* ABC transporter BtuC₂D₂ that transports vitamin B₁₂ it was observed that the continuous hydrolysis of ATP enables the protein to remain in a stable and functional state for much longer time than a transporter that was in the idle state, e.g. that was kept in buffer without ATP before measurement (Livnat-Levanon et al., 2016). Therefore, it is plausible that cells keep transporters such as Pdr5 or Cdr1 that are crucial for efflux of a high variety of toxic compounds in a permanent active state to reduce response times and increase their efficiency when toxic substrates appear and thus enabling a faster protection.

In a study (Krasowska et al., 2010) investigating the effects of PDR pump inhibitors on the cellular ATP level in *S. cerevisiae* it was demonstrated that the high basal ATPase activity of PDR efflux pumps measured in plasma membranes was not an artifact of purification as it has been demonstrated for the maltose importer from *E. coli* (Reich-Slotky et al., 2000; Krasowska et al., 2010; Bao and Duong, 2012). The fact that PDR pump inhibitors lead to an increased cellular ATP level proves that these pumps are in an ‘always-on’ state *in vivo* even though there is no apparent substrate present. Moreover, comparing the final

A	Walker A	C-loop	Walker B	H-loop
Pdr5	GASGAGKTT	VSGGE	LVFLDE	IHQ
Cdr1	GASGAGKTT	CSGGE	LLFLDE	IHQ
ABCG5	GSSGSKTT		VMLFDE	IHQ
ABCG8		LSGGE		
Consensus	GxSGxGKTT	xSGGE	xxxxDE	IHQ

B	Walker A	C-loop	Walker B	H-loop
Pdr5	GRPGSGCTT	LNVEQ	FQCWDN	IYQ
Cdr1	GRPGAGCST	LNVEQ	IQCWDN	IYQ
ABCG5		ISTGE		
ABCG8	GSSGCGRAS		ILILDE	IHQ
Consensus	GxxGxGxxx	xxxxxx	xxxxDx	IxQ

Figure 4: Alignment of the Walker A, C-loop.

Walker B and H-loop motifs of the asymmetric ABC exporters Pdr5, Cdr1 and human ABCG5/ABCG8. (A) The canonical nucleotide-binding site. (B) The degenerated nucleotide-binding site. Residues that differ from the consensus sequence are highlighted in red.

OD growth values of two yeast strains, one lacking Pdr5, Snq2 and other PDR efflux pumps, and one harboring Pdr5 and other PDR proteins, shows no significant difference in cell proliferation and therefore demonstrates that the ATP consumption by the ABC transporters does not negatively impact cell growth (Krasowska et al., 2010). However, one has to be aware that currently the physiological substrate of Pdr5 is not known, and it could be still possible that the protein is always actively transporting its natural yet unknown substrate.

Another interesting feature of fungal PDR ABC transporter is the presence of a degenerated NBS (Lamping et al., 2010). As seen in Figure 4, several key residues of Pdr5 and Cdr1 that are necessary for hydrolyzing ATP within the Walker A, Walker B and H-loop of NBD1 as well as the ABC signature motif (C-loop) of NBD2 are replaced by non-canonical amino acids (Figure 4B). In the case of the asymmetric human sterol transporter ABCG5/ABCG8, the degeneration is restricted to the C-loop of the ABCG5 molecule and Walker A of the ABCG8 monomer (Wang et al., 2011). This degeneration, however, seems to play an important role in the functionality of these fungal proteins. Gupta et al. showed in a mutational study of Pdr5 that in exchanging these residues with the canonical ones and thereby establishing a symmetrical NBS, Pdr5 loses its ATPase activity completely to background levels and therefore functionality (Gupta et al., 2014). The remaining question is why do PDR transporters contain this degeneration that is essential for their ATPase activity with no apparent other function?

As proposed based on the crystal structure of the asymmetric ABC transporter TM287/288 (Hohl et al., 2012) the degenerated NBS could bind ATP and thereby couple both NBDs permanently and form a rigid connection while

the canonical NBS transmits the motion through binding and hydrolysis of ATP to the transmembrane segment.

Structure of asymmetrical ABC exporters

Until recently, ABC export pumps were believed to share a similar fold and therefore were all classified as type I exporters. The first high-resolution structure of type I exporters, solved in 2006, is the bacterial ABC transporter Sav1866, shown in Figure 5A (Dawson and Locher, 2006), which was believed to represent the basic blueprint for all ABC exporters. This assumption was supported by all structures of ABC exporters determined subsequently. Consequently, the two fungal PDR ABC exporters Cdr1 and Pdr5 were also assumed to adopt the molecular fold of type I exporters. Based on the X-ray structures of Sav1866 (employing only the TMD) and the NBDs of HlyB (Zaitseva et al., 2005), Rutledge and colleagues created a homology model of Pdr5 (Figure 5C) (Rutledge et al., 2011). The model of these type of transporters includes two coupling helices (CH) located within the ICL of each TMD that contacts in the case of the CH1 of ICL1 both NBDs, while the CH2 of ICL2 only reaches to the opposing NBD (Figure 2A). Thereby, the mechanical motion generated in the NBDs by ATP-induced dimerization is transferred to the TMDs energizing substrate efflux by switching from the inward- to the outward-facing conformation (Dawson and Locher, 2006; Oldham et al., 2008). The recently published crystal structure of the asymmetric heterodimer ABCG5/G8 (Figure 5B), however, describes a completely novel fold of ABC exporters, creating a new subfamily of exporters,

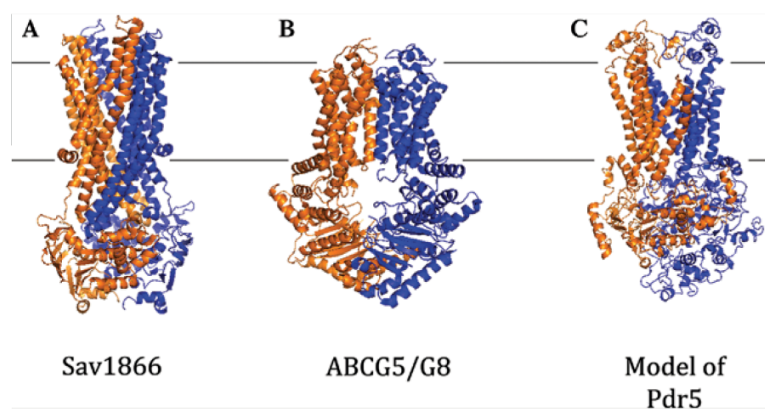


Figure 5: Selected crystal structures of ABC exporter (A and B) and the homology model of Pdr5. In each structure, NBD1 and TMD1 are colored in orange, NBD2 and TMD2 are colored in blue. Lines indicate the approximate position of the lipid bilayer. (A) Structure of the homodimeric bacterial ABC type I exporter Sav1866 (PDB code 2HYD). (B) Structure of the heterodimeric type II ABC exporter ABCG5/G8 (PDB code 5D07). (C) Homology model of Pdr5 based on the structure of Sav1866 (Rutledge et al., 2011).

namely type II (Lee et al., 2016). The authors describe a structure of a transporter in a conformation much like ABC importers with two separated NBDs that interact solely with their respective TMD and not with the TMD of the opposing monomer, as schematically shown in Figure 2B. ABCG5/ABCG8 is a human sterol exporter that in case of mutations within these genes can lead to sitosterolemia (Hubacek et al., 2001). Interestingly, ABCG5/G8 harbors a coupling helix only within ICL1 of each TMD. This coupling helix is, in the case of ABCG5, interacting with the degenerated NBS1 of ABCG5 while the coupling helix of ABCG8 does not interact with the canonical NBS2. Moreover, both TMDs contain a connecting helix that interacts with the respective NBD of the same monomer (Lee et al., 2016). Since PDR ABC transporters are asymmetric with respect to their NBDs and contain an inverse topology (NBD-TMD), they belong to the ABCG subfamily of ABC transporters (Paumi et al., 2009). Obviously, the question arises of what implications of the newly defined type II exporter possesses with respect to the residues involved in interdomain cross-talk in PDR proteins. First, the structure of ABCG5/G8 suggests that the degenerated NBS1, which cannot hydrolyze ATP, works as a rigid connection between TMD and NBD, while the canonical and more flexible NBS2 actually transmits the motion from binding and hydrolysis of ATP to the TMD (Lee et al., 2016). As most mutations influencing the cross-talk between the two distinct domains of Pdr5 are located within either the NBS1 or ICL1, the putative coupling helix, as for example the Q-loop mutants of Pdr5 (Ananthaswamy et al., 2010) or in the case of Cdr1 the I574A and S593A mutants (Shah et al., 2015), it can be assumed that the tight connection of

the two domains is interrupted and therefore functionality is lost. Conversely, mutations near NBS2 or the putative coupling helix of TMD2 in Pdr5, which is in the model of ABCG5/G8 the more flexible region, do not abolish overall drug efflux. The H-loop mutant H1068A for example leads to hypersensitivity towards rhodamine 6G, however, did not influence the transport of other drugs analyzed (Ernst et al., 2008). The importance of the degenerated NBS as indicated by the structure of ABCG5/G8 is underlined by the mutational study of Pdr5, in which the symmetry of both NBS was recovered. It was shown that by eliminating the asymmetry the ABC transporter loses not only its functionality in substrate transport but also its ATPase activity (Gupta et al., 2014).

Conclusion

Although mutational studies help to narrow down the potentially huge amount of possible residues involved in the interdomain cross-talk of Pdr5 and Cdr1, a lot of issues remain elusive and might be only addressed by working in a reconstituted system. These questions include how the series of events of ATP binding, hydrolysis and substrate transport across the membrane takes place. Moreover, the newly published crystal structure of the type II ABC exporter ABCG5/ABCG8, which belongs to the same subfamily as Pdr5 and Cdr1, raises the question if the residues that are thought to be involved in the interdomain cross-talk and were identified based on the homology model of Pdr5 available so far, might play a different role than anticipated so far.

Acknowledgments: We apologize to all our colleagues whose contribution were not referenced appropriately due to space limitations. Furthermore, we thank Dr. Xia, NIH, for kindly providing the coordinates of the homology model of Pdr5. Our research was supported by grants of the DFG, AiF and the EU to L.S.

References

- Al-Shawi, M.K. and Omote, H. (2005). The remarkable transport mechanism of P-glycoprotein: a multidrug transporter. *J. Bioenerg. Biomembr.* 37, 489–496.
- Aller, S.G., Yu, J., Ward, A., Weng, Y., Chittaboina, S., Zhuo, R., Harrell, P.M., Trinh, Y.T., Zhang, Q., Urbatsch, I.L. et al. (2009). Structure of P-glycoprotein reveals a molecular basis for poly-specific drug binding. *Science* 323, 1718–1722.
- Ananthaswamy, N., Rutledge, R., Sauna, Z.E., Ambudkar, S.V., Dine, E., Nelson, E., Xia, D., and Golin, J. (2010). The signaling interface of the yeast multidrug transporter Pdr5 adopts a cis conformation, and there are functional overlap and equivalence of the deviant and canonical Q-loop residues. *Biochemistry* 49, 4440–4449.
- Balzi, E., Wang, M., Leterme, S., Van Dyck, L., and Goffeau, A. (1994). PDR5, a novel yeast multidrug resistance conferring transporter controlled by the transcription regulator PDR1. *J. Biol. Chem.* 269, 2206–2214.
- Bao, H. and Duong, F. (2012). Discovery of an auto-regulation mechanism for the maltose ABC transporter MalFGK2. *PLoS One* 7, e34836.
- Biemans-Oldehinkel, E., Doeven, M.K., and Poolman, B. (2006). ABC transporter architecture and regulatory roles of accessory domains. *FEBS Lett.* 580, 1023–1035.
- Bissinger, P.H. and Kuchler, K. (1994). Molecular cloning and expression of the *Saccharomyces cerevisiae* STS1 gene product. A yeast ABC transporter conferring mycotoxin resistance. *J. Biol. Chem.* 269, 4180–4186.
- Davidson, A.L., Shuman, H.A., and Nikaido, H. (1992). Mechanism of maltose transport in *Escherichia coli*: transmembrane signaling by periplasmic binding proteins. *Proc. Natl. Acad. Sci. USA* 89, 2360–2364.
- Dawson, R.J. and Locher, K.P. (2006). Structure of a bacterial multidrug ABC transporter. *Nature* 443, 180–185.
- Decottignies, A., Kolaczowski, M., Balzi, E., and Goffeau, A. (1994). Solubilization and characterization of the overexpressed PDR5 multidrug resistance nucleotide triphosphatase of yeast. *J. Biol. Chem.* 269, 12797–12803.
- Dou, W., Zhu, J., Wang, T., Wang, W., Li, H., Chen, X., and Guan, W. (2016). Mutations of charged amino acids at the cytoplasmic end of transmembrane helix 2 affect transport activity of the budding yeast multidrug resistance protein Pdr5p. *FEMS Yeast Res.* 16, 1567–1364.
- Downes, M.T., Mehla, J., Ananthaswamy, N., Wakschlag, A., Lamonde, M., Dine, E., Ambudkar, S.V., and Golin, J. (2013). The transmission interface of the *Saccharomyces cerevisiae* multidrug transporter Pdr5: Val-656 located in intracellular loop 2 plays a major role in drug resistance. *Antimicrob. Agents Chemother.* 57, 1025–1034.
- Eckford, P.D. and Sharom, F.J. (2009). ABC efflux pump-based resistance to chemotherapy drugs. *Chem. Rev.* 109, 2989–3011.
- Egner, R., Rosenthal, F.E., Kralli, A., Sanglard, D., and Kuchler, K. (1998). Genetic separation of FK506 susceptibility and drug transport in the yeast Pdr5 ATP-binding cassette multidrug resistance transporter. *Mol. Biol. Cell* 9, 523–543.
- Ernst, R., Klemm, R., Schmitt, L., and Kuchler, K. (2005). Yeast ATP – binding cassette transporters: cellular cleaning pumps. *Methods Enzymol.* 400, 460–484.
- Ernst, R., Kueppers, P., Klein, C.M., Schwarzmüller, T., Kuchler, K., and Schmitt, L. (2008). A mutation of the H-loop selectively affects rhodamine transport by the yeast multidrug ABC transporter Pdr5. *Proc. Natl. Acad. Sci. USA* 105, 5069–5074.
- Ernst, R., Kueppers, P., Stindt, J., Kuchler, K., and Schmitt, L. (2010). Multidrug efflux pumps: substrate selection in ATP-binding cassette multidrug efflux pumps – first come, first served? *FEBS J.* 277, 540–549.
- Furman, C., Mehla, J., Ananthaswamy, N., Arya, N., Kulesh, B., Kovach, I., Ambudkar, S.V., and Golin, J. (2013). The deviant ATP-binding site of the multidrug efflux pump Pdr5 plays an active role in the transport cycle. *J. Biol. Chem.* 288, 30420–30431.
- Golin, J. and Ambudkar, S.V. (2015). The multidrug transporter Pdr5 on the 25th anniversary of its discovery: an important model for the study of asymmetric ABC transporters. *Biochem. J.* 467, 353–363.
- Golin, J., Barkatt, A., Cronin, S., Eng, G., and May, L. (2000). Chemical specificity of the PDR5 multidrug resistance gene product of *Saccharomyces cerevisiae* based on studies with tri-n-alkyltin chlorides. *Antimicrob. Agents Chemother.* 44, 134–138.
- Golin, J., Ambudkar, S.V., Gottesman, M.M., Habib, A.D., Sczepanski, J., Ziccardi, W., and May, L. (2003). Studies with novel Pdr5p substrates demonstrate a strong size dependence for xenobiotic efflux. *J. Biol. Chem.* 278, 5963–5969.
- Golin, J., Kon, Z.N., Wu, C.P., Martello, J., Hanson, L., Supernavage, S., Ambudkar, S.V., and Sauna, Z.E. (2007). Complete inhibition of the Pdr5p multidrug efflux pump ATPase activity by its transport substrate clotrimazole suggests that GTP as well as ATP may be used as an energy source. *Biochemistry* 46, 13109–13119.
- Gottesman, M.M., Fojo, T., and Bates, S.E. (2002). Multidrug resistance in cancer: role of ATP-dependent transporters. *Nat. Rev. Cancer* 2, 48–58.
- Gupta, R.P., Kueppers, P., Schmitt, L., and Ernst, R. (2011). The multidrug transporter Pdr5: a molecular diode? *Biol. Chem.* 392, 53–60.
- Gupta, R.P., Kueppers, P., Hanekop, N., and Schmitt, L. (2014). Generating symmetry in the asymmetric ATP-binding cassette (ABC) transporter Pdr5 from *Saccharomyces cerevisiae*. *J. Biol. Chem.* 289, 15272–15279.
- Hirata, D., Yano, K., Miyahara, K., and Miyakawa, T. (1994). *Saccharomyces cerevisiae* Ydr1, which encodes a member of the ATP-binding cassette (Abc) superfamily, is required for multidrug-resistance. *Curr. Gen.* 26, 285–294.
- Hohl, M., Briand, C., Grutter, M.G., and Seeger, M.A. (2012). Crystal structure of a heterodimeric ABC transporter in its inward-facing conformation. *Nat. Struct. Mol. Biol.* 19, 395–402.

- Hollenstein, K., Dawson, R.J., and Locher, K.P. (2007). Structure and mechanism of ABC transporter proteins. *Curr. Opin. Struct. Biol.* *17*, 412–418.
- Hubacek, J.A., Berge, K.E., Cohen, J.C., and Hobbs, H.H. (2001). Mutations in ATP-cassette binding proteins G5 (ABCG5) and G8 (ABCG8) causing sitosterolemia. *Hum. Mutat.* *18*, 359–360.
- Jardetzky, O. (1966). Simple allosteric model for membrane pumps. *Nature* *211*, 969–970.
- Kim Chiaw, P., Eckford, P.D., and Bear, C.E. (2011). Insights into the mechanisms underlying CFTR channel activity, the molecular basis for cystic fibrosis and strategies for therapy. *Essays Biochem.* *50*, 233–248.
- Krasowska, A., Lukaszewicz, M., Bartosiewicz, D., and Sigler, K. (2010). Cell ATP level of *Saccharomyces cerevisiae* sensitively responds to culture growth and drug-inflicted variations in membrane integrity and PDR pump activity. *Biochem. Biophys. Res. Commun.* *395*, 51–55.
- Kueppers, P., Gupta, R.P., Stindt, J., Smits, S.H., and Schmitt, L. (2013). Functional impact of a single mutation within the transmembrane domain of the multidrug ABC transporter Pdr5. *Biochemistry* *52*, 2184–2195.
- Lamping, E., Baret, P.V., Holmes, A.R., Monk, B.C., Goffeau, A., and Cannon, R.D. (2010). Fungal PDR transporters: phylogeny, topology, motifs and function. *Fungal Genet. Biol.* *47*, 127–142.
- Lee, J.Y., Kinch, L.N., Borek, D.M., Wang, J., Wang, J., Urbatsch, I.L., Xie, X.S., Grishin, N.V., Cohen, J.C., Otwinowski, Z., et al. (2016). Crystal structure of the human sterol transporter ABCG5/ABCG8. *Nature* *533*, 561–564.
- Leppert, G., McDevitt, R., Falco, S.C., Van Dyk, T.K., Ficke, M.B., and Golin, J. (1990). Cloning by gene amplification of two loci conferring multiple drug resistance in *Saccharomyces*. *Genetics* *125*, 13–20.
- Lerner-Marmarosh, N., Gimi, K., Urbatsch, I.L., Gros, P., and Senior, A.E. (1999). Large scale purification of detergent-soluble P-glycoprotein from *Pichia pastoris* cells and characterization of nucleotide binding properties of wild-type, Walker A, and Walker B mutant proteins. *J. Biol. Chem.* *274*, 34711–34718.
- Litman, T., Zeuthen, T., Skovsgaard, T., and Stein, W.D. (1997). Competitive, non-competitive and cooperative interactions between substrates of P-glycoprotein as measured by its ATPase activity. *Biochim. Biophys. Acta* *1361*, 169–176.
- Livnat-Levanon, N., A, I.G., Ben-Tal, N., and Lewinson, O. (2016). The uncoupled ATPase activity of the ABC transporter BtuC2D2 leads to a hysteretic conformational change, conformational memory, and improved activity. *Sci. Rep.* *6*, 21696.
- Mehla, J., Ernst, R., Moore, R., Wakschlag, A., Marquis, M.K., Ambudkar, S.V., and Golin, J. (2014). Evidence for a molecular diode-based mechanism in a multispecific ATP-binding cassette (ABC) exporter: SER-1368 as a gatekeeping residue in the yeast multidrug transporter Pdr5. *J. Biol. Chem.* *289*, 26597–26606.
- Oancea, G., O'Mara, M.L., Bennett, W.F., Tieleman, D.P., Abele, R., and Tampe, R. (2009). Structural arrangement of the transmission interface in the antigen ABC transport complex TAP. *Proc. Natl. Acad. Sci. USA* *106*, 5551–5556.
- Oldham, M.L., Davidson, A.L., and Chen, J. (2008). Structural insights into ABC transporter mechanism. *Curr. Opin. Struct. Biol.* *18*, 726–733.
- Oswald, C., Holland, I.B., and Schmitt, L. (2006). The motor domains of ABC-transporters. What can structures tell us? *Naunyn-Schmiedeberg's Arch. Pharmacol.* *372*, 385–399.
- Paumi, C.M., Chuk, M., Snider, J., Stagljar, I., and Michaelis, S. (2009). ABC transporters in *Saccharomyces cerevisiae* and their interactors: new technology advances the biology of the ABC (MRP) subfamily. *Microbiol. Mol. Biol. Rev.* *73*, 577–593.
- Pfaller, M.A. and Diekema, D.J. (2007). Epidemiology of invasive candidiasis: a persistent public health problem. *Clin. Microbiol. Rev.* *20*, 133–163.
- Prasad, R. and Goffeau, A. (2012). Yeast ATP-binding cassette transporters conferring multidrug resistance. *Annu. Rev. Microbiol.* *66*, 39–63.
- Procko, E., Ferrin-O'Connell, I., Ng, S.L., and Gaudet, R. (2006). Distinct structural and functional properties of the ATPase sites in an asymmetric ABC transporter. *Mol. Cell* *24*, 51–62.
- Puri, N., Prakash, O., Manoharlal, R., Sharma, M., Ghosh, I., and Prasad, R. (2010). Analysis of physico-chemical properties of substrates of ABC and MFS multidrug transporters of pathogenic *Candida albicans*. *Eur. J. Med. Chem.* *45*, 4813–4826.
- Reich-Slotky, R., Panagiotidis, C., Reyes, M., and Shuman, H.A. (2000). The detergent-soluble maltose transporter is activated by maltose binding protein and Verapamil. *J. Bacteriol.* *182*, 993–1000.
- Rutledge, R.M., Esser, L., Ma, J., and Xia, D. (2011). Toward understanding the mechanism of action of the yeast multidrug resistance transporter Pdr5p: a molecular modeling study. *J. Struct. Biol.* *173*, 333–344.
- Safa, A.R. (2004). Identification and characterization of the binding sites of P-glycoprotein for multidrug resistance-related drugs and modulators. *Curr. Med. Chem. Anticancer Agents* *4*, 1–17.
- Sauna, Z.E., Bohn, S.S., Rutledge, R., Dougherty, M.P., Cronin, S., May, L., Xia, D., Ambudkar, S.V., and Golin, J. (2008). Mutations define cross-talk between the N-terminal nucleotide-binding domain and transmembrane helix-2 of the yeast multidrug transporter Pdr5: possible conservation of a signaling interface for coupling ATP hydrolysis to drug transport. *J. Biol. Chem.* *283*, 35010–35022.
- Seelig, A. (1998). A general pattern for substrate recognition by P-glycoprotein. *Eur. J. Biochem.* *251*, 252–261.
- Shah, A.H., Rawal, M.K., Dharmgaye, S., Komath, S.S., Saxena, A.K., and Prasad, R. (2015). Mutational analysis of intracellular loops identify cross talk with nucleotide binding domains of yeast ABC transporter Cdr1p. *Sci. Rep.* *5*, 11211.
- Shukla, S., Saini, P., Smriti, Jha, S., Ambudkar, S.V., and Prasad, R. (2003). Functional characterization of *Candida albicans* ABC transporter Cdr1p. *Eukaryot. Cell* *2*, 1361–1375.
- Shukla, S., Ambudkar, S.V., and Prasad, R. (2004). Substitution of threonine-1351 in the multidrug transporter Cdr1p of *Candida albicans* results in hypersusceptibility to antifungal agents and threonine-1351 is essential for synergic effects of calcineurin inhibitor FK520. *J. Antimicrob. Chemother.* *54*, 38–45.
- Shukla, S., Rai, V., Banerjee, D., and Prasad, R. (2006). Characterization of Cdr1p, a major multidrug efflux protein of *Candida albicans*: purified protein is amenable to intrinsic fluorescence analysis. *Biochemistry* *45*, 2425–2435.
- Turk, D., Hall, M.D., Chu, B.F., Ludwig, J.A., Fales, H.M., Gottesman, M.M., and Szakacs, G. (2009). Identification of compounds selectively killing multidrug-resistant cancer cells. *Cancer Res.* *69*, 8293–8301.

- Urbatsch, I.L., Gimi, K., Wilke-Mounts, S., and Senior, A.E. (2000). Investigation of the role of glutamine-471 and glutamine-1114 in the two catalytic sites of P-glycoprotein. *Biochemistry* 39, 11921–11927.
- Wang, J., Grishin, N., Kinch, L., Cohen, J.C., Hobbs, H.H., and Xie, X.S. (2011). Sequences in the nonconsensus nucleotide-binding domain of ABCG5/ABCG8 required for sterol transport. *J. Biol. Chem.* 286, 7308–7314.
- Zaitseva, J., Jenewein, S., Jumpertz, T., Holland, I.B., and Schmitt, L. (2005). H662 is the linchpin of ATP hydrolysis in the nucleotide-binding domain of the ABC transporter HlyB. *EMBO J.* 24, 1901–1910.
- Zolnerciks, J.K., Wooding, C., and Linton, K.J. (2007). Evidence for a Sav1866-like architecture for the human multidrug transporter P-glycoprotein. *FASEB J.* 21, 3937–3948.

3.2 Chapter II

Titel: *In vitro* NTPase activity of highly purified Pdr5, a major yeast ABC multidrug transporter


Authors: Manuel Wagner, Sander H.J. Smits and Lutz Schmitt

Published in: Scientific Reports
Impact factor: 4.525

**Proportionate work
on this manuscript:** 90%

SCIENTIFIC REPORTS

OPEN *In vitro* NTPase activity of highly purified Pdr5, a major yeast ABC multidrug transporter

Manuel Wagner, Sander H. J. Smits & Lutz Schmitt 

Received: 11 February 2019

Accepted: 15 May 2019

Published online: 23 May 2019

The ABC transporter Pdr5 of *S. cerevisiae* is a key player of the PDR network that works as a first line of defense against a wide range of xenobiotic compounds. As the first discovered member of the family of asymmetric PDR ABC transporters, extensive studies have been carried out to elucidate the molecular mechanism of drug efflux and the details of the catalytic cycle. Pdr5 turned out to be an excellent model system to study functional and structural characteristics of asymmetric, uncoupled ABC transporters. However, to date studies have been limited to *in vivo* or plasma membrane systems, as it was not possible to isolate Pdr5 in a functional state. Here, we describe the solubilization and purification of Pdr5 to homogeneity in a functional state as confirmed by *in vitro* assays. The ATPase deficient Pdr5 E1036Q mutant was used as a control and proves that detergent-purified wild-type Pdr5 is functional resembling in its activity the one in its physiological environment. Finally, we show that the isolated active Pdr5 is monomeric in solution. Taken together, our results described in this study will enable a variety of functional investigations on Pdr5 required to determine molecular mechanism of this asymmetric ABC transporter.

ATP-binding cassette (ABC) transporters are ubiquitous, primary active membrane proteins that are found in all kingdoms of life¹. In general, they can be divided into two classes, depending on the direction of transport: ABC importers (including ECF transporters)² and exporters³. A functional unit of an ABC transporter consists of two nucleotide-binding domains (NBDs) that bind and hydrolyze ATP to energize the transport cycle, and two transmembrane domains (TMDs), which form the translocation pathway across the membrane¹. Overexpression of ABC transporters that export toxic compounds is part of a phenomenon known as multidrug resistance and represents a main obstacle in chemo-therapeutic cancer treatment as well as bacterial infections^{4,5}. In fungi and plants the overexpression of these drug efflux pumps is part of the pleiotropic drug resistance (PDR) network⁶. All PDR ABC transporters are, with the exception of Adp1, full-size transporter and possess a reverse topology of (NBD-TMD)₂^{7,8}. The ABC transporter Pdr5 of *Saccharomyces cerevisiae* has been established as a model for fungal PDR proteins and studied for more than 25 years⁹. It confers resistance towards a broad range of structurally and functionally different substrates including azoles, ionophores, antibiotics and many others^{10,11}. However, the nature of the physiological substrate(s) is not known. The expression of PDR ABC transporters is regulated through a complex regulatory network of transcription factors, of which the zinc finger regulators Pdr1 and Pdr3 are mainly responsible for Pdr5 regulation¹². A mutation in Pdr1 (*pdr1-3*) is used for constitutive overexpression of the transporter¹³, which can also be used to overexpress other ABC transporter using this system¹⁴.

ABC transporters all share conserved motifs within their NBDs, namely the Walker A and B, the signature motif (or C-loop) as well as the D- and H-loop¹⁵. Pdr5, however, features substitutions of key residues in each motif, except of the D-loops, in one of its nucleotide binding sites (NBSs), which renders this NBS ATPase deficient, also known as degenerated. Therefore, Pdr5 belongs to the family of asymmetric ABC transporters amongst CFTR, MRP1, ABCG5/ABCG8 and others¹⁶⁻¹⁸. It remains elusive what the exact physiological function of the degenerated NBS is, but it is obvious that there is an essential function as restoring the canonical motifs leads to inactive Pdr5¹⁹. There are however, indications that the degenerated NBS is involved in the interdomain crosstalk between the NBDs and the TMDs. Single mutations within the deviant NBS did not impact the overall ATPase activity of the transporter while they severely affected the transport functionality^{19,20}. The crystal structure of TM287/288²¹ nicely demonstrated the consequence of one catalytic and one non-canonical site, e. g. only a bound nucleotide (ATP) at the non-canonical site. However, one has to stress that a gradient of asymmetry exists in

Institute of Biochemistry, Heinrich-Heine-Universität Düsseldorf, Universitätsstraße 1, 40225, Düsseldorf, Germany. Correspondence and requests for materials should be addressed to L.S. (email: Lutz.Schmitt@hhu.de)

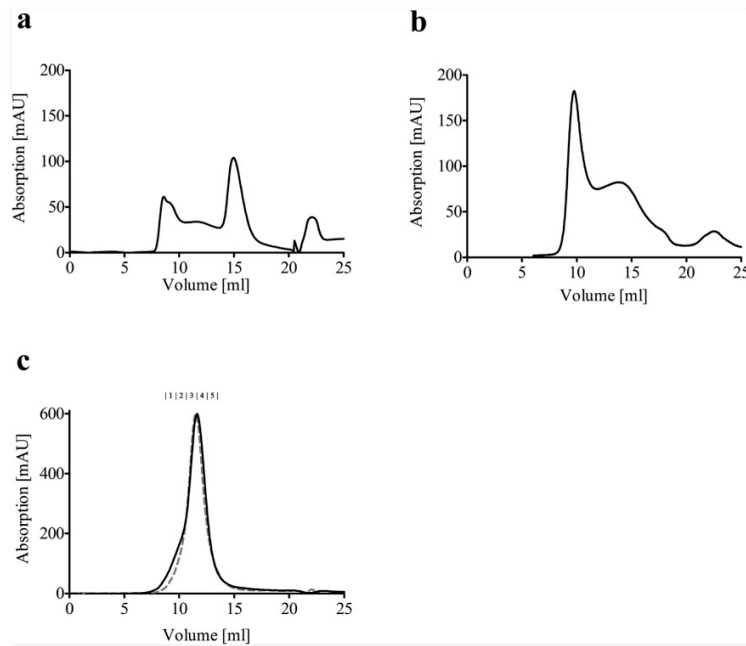


Figure 1. Size exclusion chromatograms of Pdr5 after affinity purification with different detergents. **(a)** SEC of Pdr5 purified with DDM. **(b)** SEC of Pdr5 purified with $C_{12}E_8$. **(c)** SEC of wild-type (black solid line) and E1036Q (gray dashed line) Pdr5 purified with trans-PCC- α -M. SEC was performed in buffer A (50 mM Tris-HCl pH 7.8, 50 mM NaCl, 10% glycerol and 0.05% DDM, 0.01% $C_{12}E_8$ or 0.003% trans-PCC- α -M respectively) on a Superdex 200 10/300 GL column (GE Healthcare). The concentration of Pdr5 was 2 mg/ml. The elution fractions that were analyzed by SDS-PAGE and Western blot (Fig. 2) are indicated above the chromatograms.

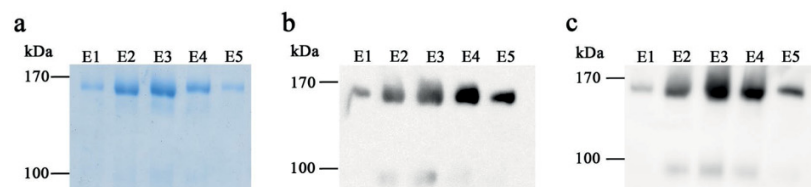


Figure 2. **(a)** Colloidal coomassie stained SDS-PAGE gel showing the elution fractions of the SEC following the affinity purification with trans-PCC- α -M. Western Blot of the elution fractions of the SEC with trans-PCC- α -M detecting **(b)** anti-Penta-His and **(c)** anti-Pdr5 specific antibody. Purified Pdr5 migrates at a molecular weight of approximately 170 kDa. The elution fractions E1-E5 for trans-PCC- α -M purified Pdr5 correspond to the SEC chromatograms in Fig. 1.

asymmetric ABC transporters. The number of mutations in the catalytically relevant motifs resulting in the inactivation of the corresponding nucleotide-binding site ranges from a few (e.g. two mutations in ABCG5/ABCG8¹⁶ or three in CFTR²² and TM287/288²¹) to all motifs forming the NBS (Pdr5 and its homologue in *Candida albicans* Cdr1²³). This obviously raises the questions whether or not a relation between number of disrupted motifs and the molecular mechanism of substrate transport exists.

Pdr5 from *Saccharomyces cerevisiae* was the first identified member of the PDR subfamily of asymmetric ABC transporters⁹. Due to the medical significance of mammalian homologues and the agricultural importance of plant and other fungal homologues, the yeast PDR system serves as a unique model to investigate their molecular mechanisms.

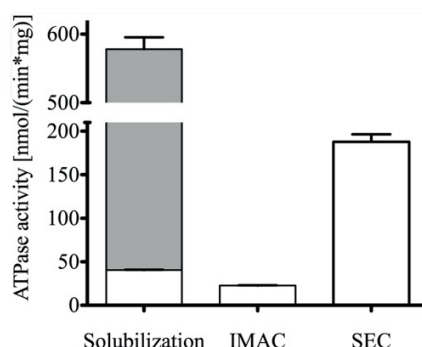


Figure 3. Pdr5-specific ATPase activity after each purification step. After solubilization, oligomycin-sensitive ATPase was measured (grey bar: overall activity, white bars: Pdr5-specific activity). The error bars represent the data of three independent measurements with the standard deviation reported as error.

Moreover, Pdr5 exhibits a high basal ATPase activity that, in contrast to other ABC transporters such as P-gp²⁴, cannot be further stimulated in the presence of its substrates, uncoupling the ATPase activity from drug efflux²⁵. Although there is a long history of studies related to Pdr5, it has not been accomplished to successfully purify the ABC transporter and to study it in detail in an isolated system, which is a prerequisite to fully understand the molecular mechanisms of drug binding and transport.

Results

Isolation and purification of Pdr5 in a functional form. In order to establish the purification of Pdr5 in a functional state at high purity and yield, we screened 20 different detergents for protein solubilization. In the course of these experiments, it turned out that PCC- α -M was the most suitable detergent for solubilization as well as for subsequent affinity purification and size exclusion chromatography. Figure 1 shows three selected examples of size exclusion chromatograms of Pdr5 after affinity purification in the presence of DDM, C₁₂E₈ and trans-PCC- α -M. The protein yield in the case of DDM and the purity after the two-step purification procedure²⁶ was sufficient. However, the inhomogeneity of the sample as evident from the shape of the elution peak (Fig. 1a) shows that DDM does not fulfill the requirements for further, functional analysis of Pdr5. Additionally, when Pdr5 purified with DDM was assayed for ATPase activity, no activity was detected above background levels, although earlier work showed low remaining activity in DDM solubilized membrane fractions²⁷. Therefore, a detergent screen was performed, using the oligomycin sensitive ATPase activity of solubilized plasma membranes containing Pdr5 as an indicator^{25,27,28} (not shown). Besides the initially promising results for DDM, C₁₂E₈ extracts showed rather high ATPase activity. Unfortunately, the following SEC showed again an inhomogeneous elution peak (Fig. 1b), which ruled out further use of this detergent.

We therefore focused on other members of the class of maltosides and an only recently commercially available member of this detergent class, trans-PCC- α -M (*trans*-4-(*trans*-4'-propylcyclohexyl)cyclohexyl- α -D-maltoside)²⁹ was chosen to be tested in all purification steps. Starting with the solubilization, trans-PCC- α -M showed nearly identical results to DDM with respect to the yield after solubilization. The yield of the subsequent affinity purification was even higher as compared to DDM (up to 1 mg of protein per L cell culture compared to 0.3 mg/L cell culture). Figure 1c shows the SEC chromatograms performed with trans-PCC- α -M for wild-type Pdr5 as well as the E1036Q mutant that behaved identically during solubilization and purification. Most importantly and in clear contrast to other tested detergents, the purification protocol using trans-PCC- α -M resulted in a solubilized Pdr5 protein in a highly homogenous state, without aggregates at high purity as evident from the SDS-PAGE shown in Fig. 2a, as well as in the Western blots using anti-Penta-His (Fig. 2b) and polyclonal, anti-Pdr5 antibodies (Fig. 2c). These findings were supported by mass spectrometry (MS) analysis, which demonstrated that more than 90% of peptides observed in the MS spectra were derived from Pdr5 (not shown). Additionally, with trans-PCC- α -M, purified Pdr5 possessed a preserved ATPase active during all steps of the purification (Fig. 3). Thus, with respect to our objectives, trans-PCC- α -M turned out to be the detergent of choice.

Pdr5 is a monomer in solution. Pdr5 is a full-size ABC transporter comprising two NBDs and two TMDs encoded on a single gene¹³. Previously, a low resolution structure (25 Å), obtained by electron microscopy, of Pdr5 in a lipid bilayer showed a square-like arrangement of particles that led to the conclusion that Pdr5 may form a dimer of two full-size transporters²⁶. To assess whether Pdr5 is monomeric or forms higher oligomeric species in solution, multi-angle light scattering in combination with SEC (SEC-MALS) analysis was performed³⁰. As Pdr5 is detergent solubilized, it was necessary to first determine the value of dn/dc as a measure of Pdr5 bound trans-PCC- α -M to be able to distinguish between the mass of the micelle and the protein. The dn/dc value is the specific refractive increment that corresponds to the changes in the refractive index in relation to the change in concentration of the investigated macromolecule and thereby enables to distinguish between the mass of the protein and the bound detergent³⁰. Using a batch method with different detergent concentrations^{30,31} we

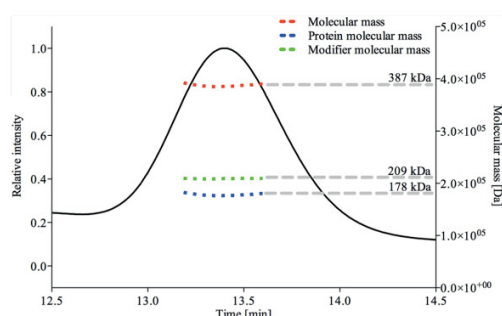


Figure 4. SEC-MALS analysis of purified Pdr5. The dn/dc value for trans-PCC- α -M was calculated in an independent measurement and used for the conjugate analysis. The overall mass of the protein-detergent complex was calculated as 387 kDa (red dashed line), with a protein molecular mass of 178.2 ± 0.2 kDa (blue dashed line). The modifier mass (green dashed line) corresponds to the detergent micelle mass.

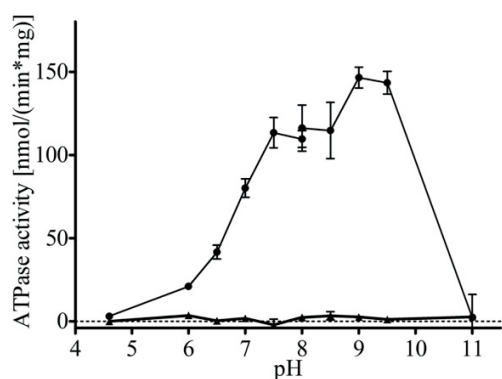


Figure 5. pH dependency of the ATPase activity of purified WT (●) and E1036Q (▲) Pdr5. Release of inorganic phosphate was measured after 20 min incubation with 4 mM ATP. Error bars represent three independent measurements ($n = 3$).

obtained a value of $dn/dc = 0.1392 \pm 0.001$ ml/g. As shown in Fig. 4, this resulted in a calculated protein mass of $M_w = 178.2 \pm 0.2$ kDa, close to the theoretical mass of 173.1 kDa, including the histidine tag and protease cleavage site, demonstrating that Pdr5 is indeed a monomer in solution.

NTPase activity of purified Pdr5. NTPase activity of purified wild type Pdr5 was performed by a colorimetric NTPase activity assay as described in detail by Baykov *et al.*³². The E1036Q Pdr5 mutant, which does not exhibit any significant ATPase activity²⁵, purified by the same protocol, was used as a negative control. Plasma membrane embedded Pdr5 exhibits the highest ATPase activity at pH 9.5²⁵. In order to validate whether this is the case for detergent purified Pdr5, we analyzed the pH dependency of the ATPase activity of Pdr5 in detergent solution. As summarized in Fig. 5, the activity has a broad range with a maximum at pH 9.5. Figure 6 shows the NTPase activity of the WT and E1036Q Pdr5 at different NTP concentrations. At saturating substrate concentrations the measured ATPase activity of WT Pdr5 was 208.5 ± 6.3 nmol/(min*mg) with a K_m of 0.44 ± 0.05 mM while the E1036Q mutant did not exhibit any significant activity above background (see Figure 6a and Table 1). In the context of Golin *et al.*³³, it was of interest to analyze the efficiency of other NTPs as it is suggested that the ABC transporter Pdr5 can utilize other nucleotides to fuel its transport activity. As summarized in Fig. 6 and Table 1, Pdr5 exhibits significant NTPase activity for all nucleotides tested, with the lowest efficiency for UTP and GTP (v_{max}/K_m of 0.0001 L/mg/min) followed by CTP (v_{max}/K_m of 0.0002 L/mg/min), and with the highest efficiency for ATP (v_{max}/K_m of 0.0005 L/mg/min). Although the v_{max} of the CTPase is higher than the ATPase activity, only the latter displays a K_m that is in respect to NTP concentrations within the physiological range (intracellular NTP levels: ATP: 1.51 ± 0.32 mM, GTP: 0.30 ± 0.02 mM, CTP: 0.21 ± 0.03 mM, UTP: 0.33 ± 0.08 mM³⁴) that allows the transporter to work always at saturating levels of nucleotide. The E1036Q mutation in the Walker B motif of NBD2 led to no significant activity in any of the performed assays (Figs 5 and 6), which demonstrates on the one hand that no detectable impurities are present and more importantly that in fact the degenerated NBS is ATPase

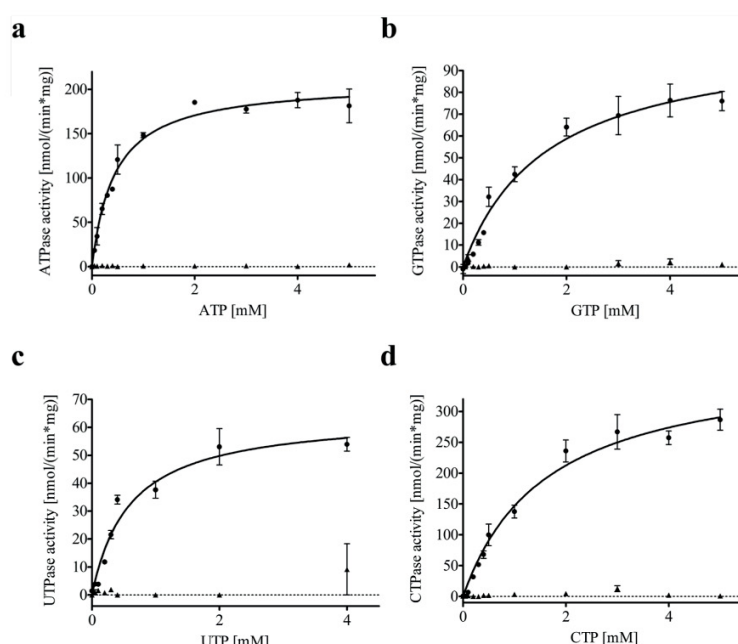


Figure 6. NTPase activity of purified WT (●) and E1036Q (▲) Pdr5. (a) ATPase activity of Pdr5. (b) GTPase activity of Pdr5. (c) UTPase activity of Pdr5. (d) CTPase activity of Pdr5. In all experiments 0–5 mM of NTPs were added and the release of inorganic phosphate was measured after 20 minutes. The error bars represent the data of at least three independent measurements ($n = 3$). Kinetic parameters of the Pdr5 specific NTPase activity can be found in Table 1.

NTP	V_{max} [nmol/mg/min]	K_m [mM]	V_{max}/K_m [L/mg/min]
ATP	208.5 ± 6.3	0.44 ± 0.05	0.0005
GTP	106.0 ± 7.9	1.61 ± 0.30	0.0001
UTP	64.6 ± 4.2	0.59 ± 0.11	0.0001
CTP	384.9 ± 23.2	1.62 ± 0.25	0.0002

Table 1. Kinetic parameters of purified Pdr5 NTPase activity.

deficient as shown earlier²⁵. As proposed by Golin *et al.*³³, we show here that GTP can be used as an energy source for Pdr5. However, with the K_m being above intracellular GTP levels, the significance of this nucleotide for active drug efflux under physiological conditions remains unclear.

Inhibitory effects of substrates and inhibitors on the ATPase activity of purified Pdr5. For plasma membrane vesicles it has been previously shown that Pdr5 is a strictly uncoupled transporter²⁵, as none of the known substrates of Pdr5 were able to stimulate its ATPase activity. However, some substrates as well as inhibitors are able to reduce the ATPase activity up to complete inhibition²⁵. This characteristic allows to validate whether detergent solubilized and purified Pdr5 shows the same or similar characteristics as embedded in its physiological environment, the lipid bilayer. This also opens up a suitable way to compare the functional properties of the transporter in solution with the one embedded in the membrane. We therefore measured the effect of several substrates and inhibitors on its ATPase activity. As shown in Fig. 7, all tested inhibitors and substrates are able to inhibit the purified Pdr5 transporter comparable to what was observed in plasma membranes. The respective K_i of each effector-compound is summarized in Tables 2 and 3, respectively. Interestingly, in solution the concentration necessary to inhibit the ATPase activity of purified Pdr5 by its substrates rhodamine 6G and ketoconazole is roughly 5 times higher than determined for Pdr5 in plasma membrane vesicles (Table 2). Moreover, for inhibitors the corresponding values are even up to 300-fold increased (Table 3). All tested Pdr5 substrates and inhibitors are hydrophobic molecules and have similar partition coefficients to ketoconazole³⁵ (Tables 1 and 2), preferring the hydrophobic nature of a biological membrane. Thus, the local concentrations of the drugs in the

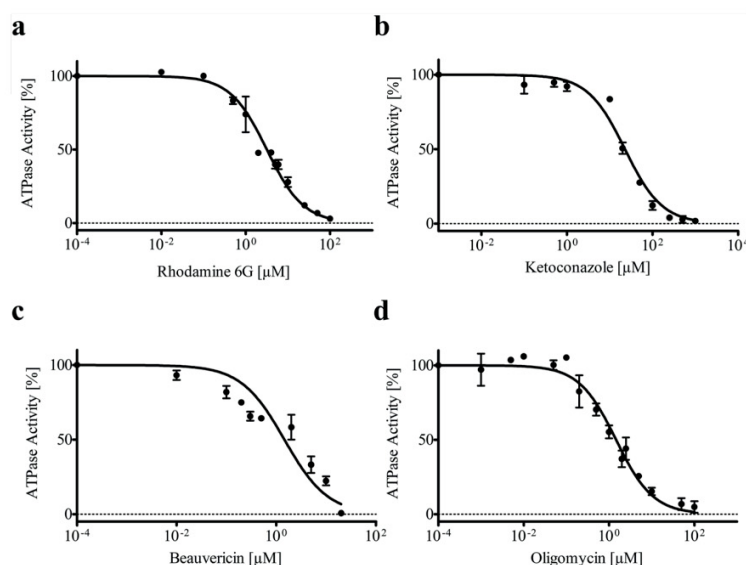


Figure 7. Inhibition of the ATPase activity of purified Pdr5 by its substrates and inhibitors. (a) rhodamine 6 G, (b) ketoconazole, (c) beauvericin, and (d) oligomycin. Error bars represent 3 independent measurements (n = 3).

	Purified Pdr5	Pdr5 in plasma membrane ^a	$K_{i, \text{detergent}}^c$ $K_{i, \text{PM}}$	Partition coefficient
Substrate	K_i [μM]	K_i [μM]		logP
Rhodamin 6G	3.2 ± 0.2	0.6 ± 0.1	5.3	6.52
Ketoconazol	22.73 ± 2.1	5.4 ± 0.8	4.2	4.06

Table 2. Substrate-mediated inhibition of Pdr5 ATPase activity and substrate partition coefficient. ^aTaken from²⁵.

	Purified Pdr5	Pdr5 in plasma membrane	$K_{i, \text{detergent}}^c$ $K_{i, \text{PM}}$	Partition coefficient
Inhibitor	K_i [μM]	K_i [μM]		logP
Oligomycin	1.46 ± 0.13	0.088^b	16.2	6.49
Beauvericin	1.45 ± 0.30	0.004 ± 0.002^c	362.5	9.57

Table 3. Inhibitor-mediated inhibition of Pdr5 ATPase activity and inhibitor partition coefficient. ^bTaken from²⁷ for UTPase activity. ^cTaken from⁴⁴.

membrane are several orders higher than in solution. Therefore, the increase in K_i for purified Pdr5 compared to the membrane system is not surprising. Additionally, these values may reflect the more flexible environment for the protein within a detergent micelle compared to a lipid bilayer. Other tested substrates like cycloheximide did not inhibit the ATPase activity (not shown), similar to what was observed for Pdr5 in plasma membranes²⁵. Together, the results of the Pdr5-ATPase inhibition assay confirm that detergent purified Pdr5 shows comparable properties and characteristics as in plasma membranes.

The asymmetric ABC transporter Pdr5 does not exhibit adenylate kinase activity. We tested whether Pdr5 possesses an adenylate kinase (AK) activity, as it was reported for other asymmetric ABC transporters like CFTR and TmrAB^{36,37}. Therefore, the formation of ADP through the AK catalyzed reaction of $ATP + AMP \rightarrow 2ADP$ was assayed as a function of NADH consumption in the enzyme coupled ATPase assay. In the case of an AK activity, addition of AMP would increase the ADP concentration additionally to the formation

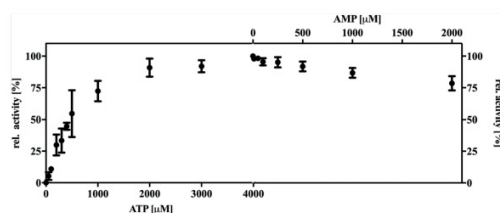


Figure 8. Test for adenylate kinase activity of Pdr5 as described in³⁷. The relative activity in percent corresponds to the formation of ADP as a function of NADH consumption in an enzyme coupled assay. An increasing amount of AMP at saturating ATP concentration (4 mM) was added and in case of adenylate kinase activity, an increase in activity should be observed. Error bars represent 3 independent measurements.

through the ATPase activity of the protein. The method used in this study was first described for CFTR³⁷. Since Pdr5 exhibits a high basal ATPase activity that is not further stimulated by its substrates, as described in this study, other methods of assaying AK activity are in our opinion unsuitable. However, as seen in Fig. 8, the addition of AMP to the reaction did not increase the formation of ADP. Conversely, it led to a slight decrease in NADH consumption, which indicates a minor inhibition of the ATPase activity of Pdr5 with a maximum inhibition of about 20% at 2 mM AMP. We therefore can rule out that Pdr5 exhibits an adenylate kinase activity that was shown for other ABC transporter³⁶.

Discussion

Pdr5 is the major ABC protein in the PDR network of *S. cerevisiae*^{9,38} conferring resistance to many unrelated exogenous drugs or xenobiotics¹². Although extensively studied for more than 25 years⁹, the molecular mechanism of the efflux pump remains mostly elusive, as it was not possible to investigate it in an isolated and functional state. This is most certainly due to the fact that mainly the detergent solubilization process causes an inactivation of the protein, leading to inactive protein after purification, as demonstrated in our present study. Previously, numerous mutational studies have provided important insights in residues involved in drug binding, interdomain crosstalk as well as the molecular diode function^{38–43} of the unidirectional substrate transport of Pdr5. However in order to disclose at a molecular level how these mutations affect the different steps in the pump cycle, it is necessary to isolate the ABC transporter for these mechanistic studies in a functional state and, as a final goal, to determine the 3D-structure.

In plasma membranes vesicles, it was shown that Pdr5 exhibits a high basal ATPase activity over a broad pH range with a maximum at pH 9.5 that could not be further stimulated in the presence of substrates. However, some of its substrates inhibit the ATPase activity at high concentration, possibly due to non-competitive inhibition^{25,27,33}. We tested whether purified Pdr5 shows similar behavior towards the well-studied substrates ketoconazole and rhodamine 6G and two inhibitors (oligomycin¹¹ and beauvericin⁴⁴) and could demonstrate that, indeed, the substrates and inhibitors affect the ATPase activity in the same way as it was shown for Pdr5 in plasma membranes. The measured K_i s however differed in magnitudes, especially for the inhibitors. This finding however is not surprising, given the hydrophobic nature of the substances tested, which show a high preference for partitioning into the membrane as highlighted by the partition coefficients of these compounds. For beauvericin it was shown that only nanomolar concentrations are required to inhibit the ATPase and transport activity in plasma membranes, while in whole cell assays the concentration necessary to observe an impact on the Pdr5-mediated drug efflux was within the micromolar range⁴⁴. This indicates that the drug cannot freely partition in the membrane presumably due to polar groups on the cell surface and/or the cell wall, which are not present in isolated plasma membranes. Therefore, higher concentrations were required to obtain inhibitory effects on Pdr5 compared to isolated plasma membranes. A similar effect is likely observed in our detergent-solubilized system, where such an increased drug accumulation within the protein-detergent micelle does not occur. Moreover, oligomycin is a known inhibitor of the Pdr5 ATPase activity¹¹ as well as of ATP synthase. Here, it binds to the membrane embedded F_0 subunit, which was shown by cryo-EM structure analysis⁴⁵. Additionally, this effect is not specific to Pdr5. It was shown for the well-studied ABC transporter P-gp that EC_{50} values for some hydrophobic compounds like verapamil with a logP value of 4.55 are well-above 300 times higher in a detergent system compared to P-gp embedded in a lipid bilayer⁴⁶.

Pdr5 exhibits significant NTPase activity for all NTPs as shown in this study. Although ATP shows the highest efficiency with a K_m below physiological ATP concentrations, we cannot rule out that the transporter might utilize other NTPs. In the light of the work of Golin *et al.*³³, in which it was shown that substrate inhibition for GTP fueled transport takes place at higher concentrations compared to ATP mediated efflux and the 'kinetic substrate selection model' proposed by Ernst *et al.*⁴⁷ it can be speculated that the NTPs are utilized depending on the present substrate and its concentration as they exhibit different kinetic parameters. Additionally, it was shown for the multidrug transporter PatA/PatB that GTP is actually the preferred nucleotide to energize the translocation of its substrates compared to ATP⁴⁸. This indicates that the choice of nucleotide might depend on several factors and it is not necessarily ATP inducing NBD dimerization and being hydrolyzed to energize the substrate efflux of ABC transporters, as it was also proposed in a study of a NBD from *Methanocaldococcus jannaschii*⁴⁹. It is worth mentioning that the reported basal ATPase activity of Pdr5 in plasma membranes is in some cases up to 2 μ mol/

min/mg²⁵. However, it is important to note that the catalytic efficiency (v_{\max}/K_m) of Pdr5 for ATP in detergent is 0.0005 and in the case of plasma membrane bound Pdr5 0.0008 L/mg/min (values taken from¹⁹) which is a factor of 1.6, as the v_{\max} and K_m are both lower compared to plasma membrane preparations. This reflects a v_{\max}/K_m compensation. Additionally, the reported activity of Pdr5 in plasma membranes varies a lot as Golin *et al.* report an activity of about 150 nmol/mg/min³³, which is within the range of activity reported in this study. The above described findings need further support from studies in a reconstituted system. However, it was not possible so far for us to reproducibly measure rhodamine 6G transport in Pdr5 containing proteoliposomes.

The low resolution structure of Pdr5 suggested that Pdr5 might function as a dimer in the membrane²⁶. As Pdr5 is a full-size ABC transporter consisting of two NBDs and two TMDs within a single molecule⁸, these findings were quite surprising. However, as the author state in their study, dimerization was only observed upon detergent removal and no activity of the purified or reconstituted protein was reported²⁶. It was shown for other ABC transporters like ABCA1 as well as the peroxisomal ABC transporters ABCD1 and ABCD2 that these proteins can actually form higher oligomeric functional units^{50,51}. Nevertheless, for Pdr5 it is assumed that the functional unit is a monomer as shown for other full-size ABC transporters⁵². In our experiments, we used SEC-MALS analysis³⁰ of the purified functional Pdr5 in trans-PCC- α -M micelles to gain information of the oligomeric state of the protein in solution. Size-exclusion chromatography, coupled with multiangle light scattering, is a most widely used technique for determining the absolute molecular weight distribution and averaged molecular weights of proteins and natural polymers⁵³. Here, we show with *in vitro* assays that we purified Pdr5 in a functional state and by SEC-MALS analysis that the functional, purified Pdr5 is monomeric in solution.

In summary, the above described purification protocol for Pdr5 in a monomeric physiological competent, high active form will allow further detailed functional and structural investigations on the molecular steps during the transport cycles of Pdr5. Additionally, the presented data and purification approach could be extended to the Pdr5 homolog Cdr1 of the clinically important pathogen *C. albicans*. Initial studies on Cdr1 purified with Triton X-100 resulted in rather low activity and might be improved using our protocol⁵⁴.

Methods

Growth media and chemicals. Yeast strains were cultured in YPD medium (20 g/l tryptone/peptone, 10 g/l yeast extract and 20 g/l glucose). All chemicals, if not stated otherwise, were obtained from Carl Roth or Sigma-Aldrich. trans-PCC- α -M was purchased from Glycon Biochemicals. anti-Pdr5 antibody was purchased from Davids Biotechnology, anti-Penta-His antibody was obtained from Qiagen.

Yeast strains. In this study we used the *S. cerevisiae* strain YRE1001 (*MATa ura3-52 trp1-1 leu2-3,112 his3-11,15 ade2-1 pdr1-3 pdr5pdr5promΔ::TRP1*). For more detailed information on the strain construction see²⁵.

Total membrane isolation and solubilization. Cells were grown at 30 °C in YPD medium. The nitrogen source was refreshed at an OD₆₀₀ of 1.5 by addition of 10% (v/v) 5x YP (100 g/l tryptone/peptone, 50 g/l yeast extract). At an OD₆₀₀ of 3.5 the cells were harvested at 5000 × g for 15 min (4 °C).

All steps of the membrane isolation were performed at 4 °C. Cells were resuspended in 50 mM Tris-HCl pH 8.0, 5 mM EDTA and two protease inhibitor tablets (EDTA-free, ROCHE). Lysis of the cells was performed with glass beads. The suspension was centrifuged twice at 1000 × g for 5 min (4 °C) and once at 3000 × g for 5 min (4 °C) to remove cell debris and the supernatant was centrifuged at 20,000 × g for 40 min (4 °C). The resulting pellet was resuspended in buffer A (50 mM Tris-HCl pH 7.8, 50 mM NaCl, 10% (w/v) glycerol) and adjusted to 10 mg/ml overall protein concentration. Solubilization of the membrane proteins was carried out with 1% (w/v) trans-PCC- α -M for 1 h under gentle stirring at 4 °C.

Affinity purification and size exclusion chromatography. The immobilized metal ion affinity chromatography (IMAC) of N-terminal 14x histidine tagged Pdr5 was performed as described in¹⁴. In short, solubilized proteins were separated from the non-solubilized fraction by ultracentrifugation at 170,000 × g for 45 min at 4 °C. A 1 ml HiTrap Chelating column loaded with Zn²⁺ ions was equilibrated using low histidine buffer (50 mM Tris-HCl pH 7.8, 500 mM NaCl, 10% glycerol, 2.5 mM L-histidine, 0.003% (w/v) trans-PCC- α -M). Subsequently, the sample was loaded on the column, washing and elution was performed by a step gradient using low and high histidine buffer (50 mM Tris-HCl pH 7.8, 500 mM NaCl, 10% glycerol, 100 mM L-histidine, 0.003% (w/v) trans-PCC- α -M).

For size exclusion chromatography, the elution fractions were pooled and concentrated using a Vivaspin 6 (Sartorius) centrifugal concentrator (100 kDa MWCO). The size exclusion chromatography was performed on a Superdex 200 10/300 GL column (GE Healthcare) equilibrated with buffer A containing 0.003% (w/v) trans-PCC- α -M. Both purification steps were carried out on the Äkta protein purification systems (GE Healthcare).

SEC-MALS analysis. To investigate the oligomeric state of purified Pdr5, multi-angle light scattering in combination with size exclusion chromatography (SEC-MALS) analysis was performed on an Agilent 1260 HPLC System. A triple-angle light scatter detector in combination with a differential refractive index detector (miniDAWN TREOS and Optilab rEX, respectively (Wyatt Technology Europe) were used and data analyzed with Astra 4 Software (Wyatt Technology Europe).

NTPase activity assay. Purified Pdr5 (1 μ g per well) was incubated with 10 mM MgCl₂, 300 mM Tris-glycine buffer pH 9.5, 0.004% (w/v) trans-PCC- α -M and 0–5 mM NTP in a reaction volume of 25 μ l.

pH dependency of the Pdr5 ATPase activity was measured as described in²⁵. In short, 1 μ g Pdr5 was incubated with 4 mM ATP, 10 mM MgCl₂ and 0.004% (w/v) trans-PCC- α -M in 300 mM MES-Tris (pH 4.6–8.0) or 300 mM

Tris-glycine (pH 8.0–11.0) buffer. After incubation for 20 min at 30 °C, the reaction was stopped by adding 175 µl of ice-cold 40 mM H₂SO₄.³²

Oligomycin (OM) sensitive ATPase activity of solubilized plasma membrane proteins was performed as described in^{25,27,28}.

Released inorganic phosphate was determined by a colorimetric assay using Na₂HPO₄ as a standard⁵⁵.

ATPase inhibition assay. The inhibition assays were performed as the NTPase activity assays described above. The compounds were dissolved in an appropriate solvent (water, methanol or DMSO) and mixed with 750 mM Tris-glycine buffer to reach the desired stock concentrations. Purified Pdr5 was incubated with each substance for 5 min before the reaction was started by addition of 4 mM ATP. Detection of released inorganic phosphate was performed as described for the NTPase activity assay. The non-inhibited ATPase activity was set to 100%. The K_i was determined using Equation (1) as described in²⁵.

$$v = 100 * \frac{1 - [drug]}{K_i + [drug]} \quad (1)$$

Here, v corresponds to the relative ATPase activity, K_i to the inhibitory constant in mol/L constant and [drug] to the drug concentration in mol/L.

logP values of the tested compounds were calculated with the Chem3D program (Perkin Elmer) based on Molecular Networks' cheminformatics platform MOSES (<https://www.mn-am.com/moses>).

Adenylate kinase activity assay. Adenylate kinase activity assay was performed as described in³⁷. In brief, an enzyme coupled ATPase assay was performed in a 96-well plate at 30 °C and measured in a Tecan Infinite 200 PRO reader (Tecan). The reaction volume of 200 µl was composed of 300 mM Tris-glycine buffer pH 8, 0.004% (w/v) trans-PCC-α-M, 5 mM MgCl₂, 4 mM PEP, 0.6 mM NADH, 3.5 µl pyruvate kinase/lactic dehydrogenase (PK/LDH) (Sigma-Aldrich). The reaction was started by the addition of 0–4 mM ATP. For detection of adenylate kinase activity, 0–2 mM AMP were added at saturating concentrations of ATP (4 mM). The absorbance of NADH was detected at 340 nm for 20 minutes. The decrease in NADH absorbance is proportional to the increase in ADP.

References

- Locher, K. P. Mechanistic diversity in ATP-binding cassette (ABC) transporters. *Nat Struct Mol Biol* **23**, 487–493, <https://doi.org/10.1038/nsmb.3216> (2016).
- Rice, A. J., Park, A. & Pinkett, H. W. Diversity in ABC transporters: type I, II and III importers. *Crit Rev Biochem Mol Biol* **49**, 426–437, <https://doi.org/10.3109/10409238.2014.953626> (2014).
- Oswald, C., Holland, I. B. & Schmitt, L. The motor domains of ABC-transporters. What can structures tell us? *Naunyn Schmiedeberg Arch Pharmacol* **372**, 385–399, <https://doi.org/10.1007/s00210-005-0031-4> (2006).
- Gottesman, M. M., Fojo, T. & Bates, S. E. Multidrug resistance in cancer: role of ATP-dependent transporters. *Nat Rev Cancer* **2**, 48–58, <https://doi.org/10.1038/nrc706> (2002).
- Lage, H. ABC-transporters: implications on drug resistance from microorganisms to human cancers. *Int J Antimicrob Agents* **22**, 188–199, [https://doi.org/10.1016/s0924-8579\(03\)00203-6](https://doi.org/10.1016/s0924-8579(03)00203-6) (2003).
- Ernst, R., Klemm, R., Schmitt, L. & Kuchler, K. Yeast ATP-Binding Cassette Transporters: Cellular Cleaning Pumps. *Methods Enzymol* **400**, 460–484, [https://doi.org/10.1016/s0076-6879\(05\)00026-1](https://doi.org/10.1016/s0076-6879(05)00026-1) (2005).
- Purnelle, B., Skala, J. & Goffeau, A. The product of the YCR105 gene located on the chromosome III from *Saccharomyces cerevisiae* presents homologies to ATP-dependent permeases. *Yeast* **7**, 867–872, <https://doi.org/10.1002/yea.320070813> (1991).
- Lamping, E. *et al.* Fungal PDR transporters: Phylogeny, topology, motifs and function. *Fungal Genet Biol* **47**, 127–142, <https://doi.org/10.1016/j.fgb.2009.10.007> (2010).
- Golin, J. & Ambudkar, S. V. The multidrug transporter Pdr5 on the 25th anniversary of its discovery: an important model for the study of asymmetric ABC transporters. *Biochem J* **467**, 353–363, <https://doi.org/10.1042/BJ20150042> (2015).
- Rogers, B. *et al.* The pleiotropic drug ABC transporters from *Saccharomyces cerevisiae*. *J Mol Microb Biotech* **3**, 207–214 (2001).
- Kolaczowski, M. *et al.* Anticancer Drugs, Ionophoric Peptides, and Steroids as Substrates of the Yeast Multidrug Transporter Pdr5p. *J Biol Chem* **271**, 31543–31548, <https://doi.org/10.1074/jbc.271.49.31543> (1996).
- Jungwirth, H. & Kuchler, K. Yeast ABC transporters—a tale of sex, stress, drugs and aging. *FEBS Lett* **580**, 1131–1138, <https://doi.org/10.1016/j.febslet.2005.12.050> (2006).
- Balzi, E., Wang, M., Leterme, S., Van Dyck, L. & Goffeau, A. PDR5, a novel yeast multidrug resistance conferring transporter controlled by the transcription regulator PDRI. *J Biol Chem* **269**, 2206–2214 (1994).
- Gupta, R. P., Kueppers, P. & Schmitt, L. New examples of membrane protein expression and purification using the yeast based Pdr1-3 expression strategy. *J Biotechnol* **191**, 158–164, <https://doi.org/10.1016/j.jbiotec.2014.07.010> (2014).
- Schmitt, L. & Tampe, R. Structure and mechanism of ABC transporters. *Curr Opin Struct Biol* **12**, 754–760 (2002).
- Lee, J. Y. *et al.* Crystal structure of the human sterol transporter ABCG5/ABCG8. *Nature* **533**, 561–564, <https://doi.org/10.1038/nature17666> (2016).
- Sorum, B., Torocsik, B. & Csanady, L. Asymmetry of movements in CFTR's two ATP sites during pore opening serves their distinct functions. *Elife* **6**, <https://doi.org/10.7554/eLife.29013> (2017).
- Yang, R., Cui, L., Hou, Y.-x., Riordan, J. R. & Chang, X.-b. ATP Binding to the First Nucleotide Binding Domain of Multidrug Resistance-associated Protein Plays a Regulatory Role at Low Nucleotide Concentration, whereas ATP Hydrolysis at the Second Plays a Dominant Role in ATP-dependent Leukotriene C₄ Transport. *J Biol Chem* **278**, 30764–30771, <https://doi.org/10.1074/jbc.M304118200> (2003).
- Gupta, R. P., Kueppers, P., Hanekop, N. & Schmitt, L. Generating symmetry in the asymmetric ATP-binding cassette (ABC) transporter Pdr5 from *Saccharomyces cerevisiae*. *J Biol Chem* **289**, 15272–15279, <https://doi.org/10.1074/jbc.M114.553065> (2014).
- Furman, C. *et al.* The deviant ATP-binding site of the multidrug efflux pump Pdr5 plays an active role in the transport cycle. *J Biol Chem* **288**, 30420–30431, <https://doi.org/10.1074/jbc.M113.494682> (2013).
- Hohl, M., Briand, C., Grutter, M. G. & Seeger, M. A. Crystal structure of a heterodimeric ABC transporter in its inward-facing conformation. *Nat Struct Mol Biol* **19**, 395–402, <https://doi.org/10.1038/nsmb.2267> (2012).
- Basso, C., Vergani, P., Nairn, A. C. & Gadsby, D. C. Prolonged nonhydrolytic interaction of nucleotide with CFTR's NH₂-terminal nucleotide binding domain and its role in channel gating. *J Gen Physiol* **122**, 333–348, <https://doi.org/10.1085/jgp.200308798> (2003).
- Prasad, R., Banerjee, A., Khandelwal, N. K. & Dharmgaye, S. The ABCs of *Candida albicans* Multidrug Transporter Cdr1. *Eukaryot Cell* **14**, 1154–1164, <https://doi.org/10.1128/EC.00137-15> (2015).

24. Aller, S. G. *et al.* Structure of P-glycoprotein reveals a molecular basis for poly-specific drug binding. *Science* **323**, 1718–1722, <https://doi.org/10.1126/science.1168750> (2009).
25. Ernst, R. *et al.* A mutation of the H-loop selectively affects rhodamine transport by the yeast multidrug ABC transporter Pdr5. *Proc Natl Acad Sci USA* **105**, 5069–5074, <https://doi.org/10.1073/pnas.0800191105> (2008).
26. Ferreira-Pereira, A. *et al.* Three-dimensional reconstruction of the Saccharomyces cerevisiae multidrug resistance protein Pdr5p. *J Biol Chem* **278**, 11995–11999, <https://doi.org/10.1074/jbc.M212198200> (2003).
27. Decottignies, A., Kolaczowski, M., Balzi, E. & Goffeau, A. Solubilization and characterization of the overexpressed PDR5 multidrug resistance nucleotide triphosphatase of yeast. *J Biol Chem* **269**, 12797–12803 (1994).
28. Goffeau, A. & Dufour, J.-P. In *Meth Enzymol* Vol. Volume 157 528–533 (Academic Press, 1988).
29. Hovers, J. *et al.* A class of mild surfactants that keep integral membrane proteins water-soluble for functional studies and crystallization. *Mol Membr Biol* **28**, 171–181, <https://doi.org/10.3109/09687688.2011.552440> (2011).
30. Slotboom, D. J., Duurkens, R. H., Olleman, K. & Erkens, G. B. Static light scattering to characterize membrane proteins in detergent solution. *Methods* **46**, 73–82, <https://doi.org/10.1016/j.ymeth.2008.06.012> (2008).
31. Strop, P. & Brunger, A. T. Refractive index-based determination of detergent concentration and its application to the study of membrane proteins. *Protein Sci* **14**, 2207–2211, <https://doi.org/10.1110/ps.051543805> (2005).
32. Baykov, A. A., Evtushenko, O. A. & Avaeva, S. M. A malachite green procedure for orthophosphate determination and its use in alkaline phosphatase-based enzyme immunoassay. *Anal Biochem* **171**, 266–270, [https://doi.org/10.1016/0003-2697\(88\)90484-8](https://doi.org/10.1016/0003-2697(88)90484-8) (1988).
33. Golin, J. *et al.* Complete inhibition of the Pdr5p multidrug efflux pump ATPase activity by its transport substrate clotrimazole suggests that GTP as well as ATP may be used as an energy source. *Biochemistry* **46**, 13109–13119, <https://doi.org/10.1021/bi701414f> (2007).
34. Osorio, H. *et al.* H₂O₂, but not menadione, provokes a decrease in the ATP and an increase in the inosine levels in Saccharomyces cerevisiae. An experimental and theoretical approach. *Eur J Biochem* **270**, 1578–1589, <https://doi.org/10.1046/j.1432-1033.2003.03529.x> (2003).
35. Pyka, A., Babuska, M. & Zachariasz, M. A comparison of theoretical methods of calculation of partition coefficients for selected drugs. *Acta Pol Pharm* **63**, 159–167 (2006).
36. Kaur, H. *et al.* Coupled ATPase-adenylate kinase activity in ABC transporters. *Nat Commun* **7**, 13864, <https://doi.org/10.1038/ncomms13864> (2016).
37. Randak, C. *et al.* A recombinant polypeptide model of the second nucleotide-binding fold of the cystic fibrosis transmembrane conductance regulator functions as an active ATPase, GTPase and adenylylase kinase. *FEBS Letters* **410**, 180–186, [https://doi.org/10.1016/s0014-5793\(97\)00574-7](https://doi.org/10.1016/s0014-5793(97)00574-7) (1997).
38. Downes, M. T. *et al.* The transmission interface of the Saccharomyces cerevisiae multidrug transporter Pdr5: Val-656 located in intracellular loop 2 plays a major role in drug resistance. *Antimicrob Agents Chemother* **57**, 1025–1034, <https://doi.org/10.1128/AAC.02133-12> (2013).
39. Wagner, M., Doehl, K. & Schmitt, L. Transmitting the energy: interdomain cross-talk in Pdr5. *Biol Chem* **398**, 145–154, <https://doi.org/10.1515/hsz-2016-0247> (2017).
40. Ananthaswamy, N. *et al.* The signaling interface of the yeast multidrug transporter Pdr5 adopts a cis conformation, and there are functional overlap and equivalence of the deviant and canonical Q-loop residues. *Biochemistry* **49**, 4440–4449, <https://doi.org/10.1021/bi100394j> (2010).
41. Sauna, Z. E. *et al.* Mutations define cross-talk between the N-terminal nucleotide-binding domain and transmembrane helix-2 of the yeast multidrug transporter Pdr5: possible conservation of a signaling interface for coupling ATP hydrolysis to drug transport. *J Biol Chem* **283**, 35010–35022, <https://doi.org/10.1074/jbc.M806446200> (2008).
42. Dou, W. *et al.* Mutations of charged amino acids at the cytoplasmic end of transmembrane helix 2 affect transport activity of the budding yeast multidrug resistance protein Pdr5p. *FEMS Yeast Research*, 1567–1364, <https://doi.org/10.1093/femsyr/fow031> (2016).
43. Mehla, J. *et al.* Evidence for a molecular diode-based mechanism in a multispecific ATP-binding cassette (ABC) exporter: SER-1368 as a gatekeeping residue in the yeast multidrug transporter Pdr5. *J Biol Chem* **289**, 26597–26606, <https://doi.org/10.1074/jbc.M114.586032> (2014).
44. Shekhar-Guturja, T. *et al.* Dual action antifungal small molecule modulates multidrug efflux and TOR signaling. *Nat Chem Biol* **12**, 867–875, <https://doi.org/10.1038/nchembio.2165> (2016).
45. Srivastava, A. P. *et al.* High-resolution cryo-EM analysis of the yeast ATP synthase in a lipid membrane. *Science* **360**, <https://doi.org/10.1126/science.aas9699> (2018).
46. Shukla, S., Abel, B., Chufan, E. E. & Ambudkar, S. V. Effects of a detergent micelle environment on P-glycoprotein (ABCB1)-ligand interactions. *J Biol Chem* **292**, 7066–7076, <https://doi.org/10.1074/jbc.M116.771634> (2017).
47. Ernst, R., Kueppers, P., Stindt, J., Kuchler, K. & Schmitt, L. Multidrug efflux pumps: substrate selection in ATP-binding cassette multidrug efflux pumps—first come, first served? *FEBS J* **277**, 540–549, <https://doi.org/10.1111/j.1742-4658.2009.07485.x> (2010).
48. Orelle, C. *et al.* A multidrug ABC transporter with a taste for GTP. *Sci Rep* **8**, 2309, <https://doi.org/10.1038/s41598-018-20558-z> (2018).
49. Fendley, G. A., Urbatsch, I. L., Sutton, R. B., Zoghbi, M. E. & Altenberg, G. A. Nucleotide dependence of the dimerization of ATP binding cassette nucleotide binding domains. *Biochem Biophys Res Commun* **480**, 268–272, <https://doi.org/10.1016/j.bbrc.2016.10.046> (2016).
50. Tromprier, D. *et al.* Transition from dimers to higher oligomeric forms occurs during the ATPase cycle of the ABCA1 transporter. *J Biol Chem* **281**, 20283–20290, <https://doi.org/10.1074/jbc.M601072200> (2006).
51. Geillon, F. *et al.* Peroxisomal ATP-binding cassette transporters form mainly tetramers. *J Biol Chem* **292**, 6965–6977, <https://doi.org/10.1074/jbc.M116.772806> (2017).
52. Hollenstein, K., Dawson, R. J. & Locher, K. P. Structure and mechanism of ABC transporter proteins. *Curr Opin Struct Biol* **17**, 412–418, <https://doi.org/10.1016/j.sbi.2007.07.003> (2007).
53. Hong, P., Koza, S. & Bouvier, E. S. A review size-exclusion chromatography for the analysis of protein biotherapeutics and their aggregates. *J Liquid Chrom & Rel Technol* **35**, 2923–2950 (2012).
54. Shukla, S. *et al.* Candida drug resistance protein 1, a major multidrug ATP binding cassette transporter of Candida albicans, translocates fluorescent phospholipids in a reconstituted system. *Biochemistry* **46**, 12081–12090, <https://doi.org/10.1021/bi700453e> (2007).
55. Zaitseva, J., Holland, I. B. & Schmitt, L. The role of CAPS buffer in expanding the crystallization space of the nucleotide-binding domain of the ABC transporter haemolysin B from Escherichia coli. *Acta Crystallogr D Biol Crystallogr* **60**, 1076–1084, <https://doi.org/10.1107/S0907444904007437> (2004).

Acknowledgements

We thank Nikolaus Pfanner, University of Freiburg, Germany, who brought trans-PCC- α -M to our attention. We thank all members of the Institute of Biochemistry for stimulating discussions. We thank Michael Lenders and Sven Reimann for their support during SEC-MALS analysis experiments.

Author Contributions

M.W. performed the measurements presented in this manuscript and wrote the manuscript. All authors reviewed the manuscript.

Additional Information

Competing Interests: The authors declare no competing interests.

Publisher's note: Springer Nature remains neutral with regard to jurisdictional claims in published maps and institutional affiliations.



Open Access This article is licensed under a Creative Commons Attribution 4.0 International License, which permits use, sharing, adaptation, distribution and reproduction in any medium or format, as long as you give appropriate credit to the original author(s) and the source, provide a link to the Creative Commons license, and indicate if changes were made. The images or other third party material in this article are included in the article's Creative Commons license, unless indicated otherwise in a credit line to the material. If material is not included in the article's Creative Commons license and your intended use is not permitted by statutory regulation or exceeds the permitted use, you will need to obtain permission directly from the copyright holder. To view a copy of this license, visit <http://creativecommons.org/licenses/by/4.0/>.

© The Author(s) 2019

3.3 Chapter III

Titel: An A666G mutation in transmembrane-helix 5 of the yeast multidrug transporter Pdr5 increases drug efflux by enhancing cooperativity between transport sites

Authors: Nidhi Arya, Hadiar Rahman, Andrew Rudrow, Manuel Wagner, Lutz Schmitt, Suresh V. Ambudkar, and John Golin

Published in: Molecular Microbiology
Impact factor: 3.816

Proportionate work on this manuscript: 10%

An A666G mutation in transmembrane helix 5 of the yeast multidrug transporter Pdr5 increases drug efflux by enhancing cooperativity between transport sites

Nidhi Arya,^{1,†} Hadiar Rahman,^{1,†} Andrew Rudrow,¹ Manuel Wagner,² Lutz Schmitt,² Suresh V. Ambudkar³ and John Golin^{1*}

¹The Department of Biology, Catholic University of America, Washington, DC 20064, USA.

²Institute of Biochemistry, Heinrich-Heine-Universität Düsseldorf, Düsseldorf, Germany.

³The Laboratory of Cell Biology, Center for Cancer Research, NCI, NIH, Bethesda, MD 20892, USA.

Summary

Resistance to antimicrobial and chemotherapeutic agents is a significant clinical problem. Overexpression of multidrug efflux pumps often creates broad-spectrum resistance in cancers and pathogens. We describe a mutation, A666G, in the yeast ABC transporter Pdr5 that shows greater resistance to most of the tested compounds than does an isogenic wild-type strain. This mutant exhibited enhanced resistance without increasing either the amount of protein in the plasma membrane or the ATPase activity. In fluorescence quenching transport assays with rhodamine 6G in purified plasma membrane vesicles, the initial rates of rhodamine 6G fluorescence quenching of both the wild type and mutant showed a strong dependence on the ATP concentration, but were about twice as high in the latter. Plots of the initial rate of fluorescence quenching versus ATP concentration exhibited strong cooperativity that was further enhanced in the A666G mutant. Resistance to imazalil sulfate was about 3–4x as great in the A666G mutant strain as in the wild type. When this transport substrate was used to inhibit the rhodamine 6G transport, the A666G mutant inhibition curves also showed greater cooperativity than the wild-type strain. Our results

suggest a novel and important mechanism: under selection, Pdr5 mutants can increase drug resistance by improving cooperative interactions between drug transport sites.

Introduction

Broad-spectrum resistance to antibiotics in pathogens and chemotherapeutic agents in tumor cells remains a major clinical problem. Multiple mechanisms are responsible for this, with genetic alterations in ATP-binding cassette (ABC) multidrug transporters playing a major role. Often, multidrug resistance results from the overexpression of these proteins in fungal pathogens and cancers (Konotylannis and Lewis, 2002; Gottesman *et al.*, 2002; Lage, 2003; Pfaller, 2012; Prasad *et al.*, 2014; Kathawala *et al.*, 2015). It seemed plausible that additional mechanisms for increased multidrug resistance existed and were worth identifying.

Multidrug transporters of the ABC superfamily are polytopic proteins. They bind and hydrolyze nucleotides in the nucleotide-binding domains (NBDs). The energy from binding and hydrolysis is used to affect conformational changes in the transmembrane domains (TMDs), where drugs bind to many sites in a large drug-binding pocket. These changes allow the transporter to cycle from an inward-facing, drug-binding conformation to an outward-facing, drug-releasing structure (Seeger *et al.*, 2015). Activities at these separate domains are coordinated through a transmission interface that has been well characterized in the yeast Pdr5 multidrug transporter, the founding member of the large Pdr fungal subfamily of ABC proteins (Gbelska *et al.*, 2006). Typically, loss-of-function mutations in the transmission interface exhibit reduced ATPase and GTPase activities, increased drug hypersensitivity to xenobiotic agents and increased resistance to noncompetitive inhibition of the ATPase activity (Sauna *et al.*, 2008; Downes *et al.*, 2013; reviewed in Golin and Ambukar, 2015).

The Pdr subfamily of fungal transporters is closely related to the ABCG family found in plants and animals

Accepted 7 July, 2019. *For correspondence: E-mail golin@cua.edu; Tel. 240-643-3968; Fax 202-319-5722. †Drs. Arya and Rahman are considered joint first authors.

© 2019 John Wiley & Sons Ltd

(Lamping *et al.*, 2010). Both subfamilies have a reverse orientation of NBDs and TMDs, high basal ATPase activities, a cis orientation of the signaling interface and short intracellular loops.

As is the case with other multidrug transporters, overexpression of Pdr5 leads to hyperresistance (Meyers *et al.*, 1992). Furthermore, these high levels of Pdr5 are stably maintained even under conditions of nutrient stress (Rahman *et al.*, 2018). Recently, however, Downes *et al.* (2013) demonstrated that multidrug-resistant yeast cells that were already overexpressing the Pdr5 transporter achieved even greater levels of drug resistance because of gain-of-function mutations in the transmission interface. In particular, they showed that a V656L substitution in the intracellular loop-2 (ICL-2) of Pdr5 was responsible for approximately doubling the resistance. Remarkably, there was no further increase in either the amount of Pdr5 in the plasma membrane (PM) or the level of ATPase activity. Molecular modeling of this region suggests that ICL-2 is too short to make direct contact with an ATP binding site. Nevertheless, it appears to play a significant role in the intradomain crosstalk. A V656A mutant exhibited significant levels of ATPase activity, but had almost no transport. Furthermore, the hypersensitive E244G Q-loop mutation was suppressed by the V656L mutation. The Q-loop is known to play a critical role in the intradomain crosstalk of ABC transporters, including Pdr5 (Urbatsch *et al.*, 2000; Dalmás *et al.*, 2005; Ananthaswamy *et al.*, 2010). Kolaczowski *et al.* (2013) characterized a series of hyperresistant mutants in the CaCdr1 transporter of the pathogenic fungus *C. albicans* in an important study. This ABC efflux pump has 56% amino acid identity to Pdr5. The mutations lie in the signal transmission interface and these investigators analyzed both single mutant and multiple mutant combinations with respect to drug resistance and ATPase activity in the presence of transport substrates. Several mutants were similar phenotypically to ours, but the mechanism responsible for the increased resistance in these mutants was not elucidated.

In this report, we probe the mechanism responsible for Pdr5-mediated hyperresistance with a more robust mutant: an A666G alteration located near Val-656 that appeared in two screens for mutants that increased the cycloheximide resistance (Downes *et al.*, 2013).

ABC transporters are known to have multiple drug binding sites (Bruggemann *et al.*, 1989; Golin *et al.*, 2003; Shukla *et al.*, 2003) with simultaneous binding of more than one molecule (Loo *et al.*, 2003; Lugo and Sharom, 2005). An early study demonstrated that mammalian multidrug transporter P-glycoprotein (P-gp) binds azidopine in two places (Martin *et al.*, 2000). It is now clear that both regions are part of the large, drug-binding pocket. Our results suggest that transport efficiency and resistance are enhanced by the A666G

mutation, which establishes significant cooperativity between transport sites.

Results

Isolation of the A666G mutation

The A666G mutation appeared in two separate genetic screens. In the first screen, it was isolated as a suppressor of a Q-loop region mutant N242K, which resulted in increased hypersensitivity to Pdr5 transport substrates (Sauna *et al.*, 2008). In the second screen, yeast cells already overexpressing Pdr5 were plated on a lethal concentration of cycloheximide (Downes *et al.*, 2013). The A666G substitution arose here as well. We recreated this mutation on the integrating plasmid pSS607, which was placed in the Δ Pdr5 strain R-1. We confirmed that the resulting strains were hyperresistant to cycloheximide. We performed all of the work in this study with the recreated mutation. We made two additional substitutions: A666V and A666L. The former was phenotypically identical to the A666G mutant. Western blotting demonstrated that the latter failed to localize the PM (data not shown).

The evolutionary relationships between fungal ABC transporters were the subject of a detailed study (Gbelska *et al.*, 2006). The Pdr subfamily was initially described as one of the eight clusters found in fungi. It was further subdivided into four groups of ABC transporters, each resembling Pdr5, Snq2, Pdr12 or Pdr11. A more recent study divided the Pdr subfamily into nine distinct clusters (Lamping *et al.*, 2010). Among transporters of this subfamily, Ala-666 shows 97% conservation (Lamping *et al.*, 2010).

The steady-state level of Pdr5 was not increased in A666G mutant PM vesicles

To determine whether the steady-state level of Pdr5 in PM vesicles could account for the large increase in drug resistance, we performed a Western blot analysis with three sets of purified PM vesicles from the A666G strain with WT and Δ Pdr5 preparations as controls. We obtained a Pdr5/Pma1 ratio for each of the samples in each blot where Pdr5 could be detected. We then compared these values from the WT and the A666G mutant preparations. The A666G had 1.03 ± 0.26 the amount of Pdr5 as the WT. A t-test indicated no significant difference between the two sets of preparations. The results, therefore, demonstrate that steady-state levels of Pdr5 in vesicles prepared from the WT and A666G strains do not differ (Fig. 1A). During the course of this study, we switched to a vastly improved method for purifying vesicles. This ensured preparations of much higher enzyme and transport activity. Coomassie Blue-stained samples of

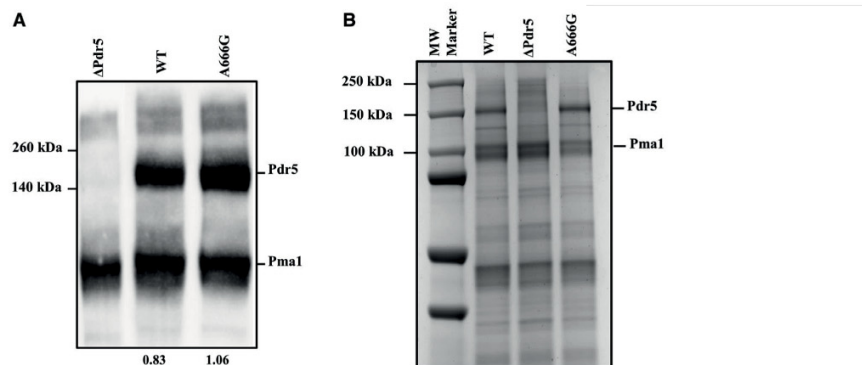


Fig. 1. The steady-state level of Pdr5 in PM vesicles is unaltered in the A666G mutant.

A. We performed Western blotting as described in the Experimental Procedures with 10 μg of purified PM vesicle protein solubilized for 30 min at 37°C in SDS-PAGE. All lanes are from the same gel, but a lane with a blot of another strain was cropped and is not shown. The ratio of Pdr5/ Pma1 is shown below the WT and A666G lanes.
 B. We performed gel electrophoresis with 10 μg samples of solubilized PM vesicle protein prepared according to Kolaczowski *et al.* (1996) as modified by Ernst *et al.* (2008). The following electrophoresis as described in the Experimental Procedures, the gel was stained in SimplyBlue SafeStain solution for one hour and destained in reverse osmosis water overnight. A different set of molecular weight markers was used in each panel.

WT, A666G and ΔPdr5 preparations are shown in Fig. 1B. The Pdr5 band, which was absent in the ΔPdr5 sample, was estimated to make up roughly 10% of the total PM vesicle protein. We also determined that the ΔPdr5 vesicles consistently had more Pma1 in PM vesicles than either the WT or A666G mutant preparations.

The ATPase activities of the WT and A666G PM vesicle preparations are similar

We routinely measured the ATPase activity of all of our PM vesicle preparations with 3 mM ATP at 35°C. We saw no difference in the activity between the PM vesicles (data not shown). We also tested the ATPase activity as a function of ATP concentration at 35°C in four independent sets of PM vesicle preparations from both strains, with the same HEPES transport buffer (pH 7.0) employed in fluorescence quenching studies described below. We made each pair, consisting of PM vesicles from the WT and mutant, on the same day or on successive days. Under these conditions we noted little difference in the ATPase activities of the WT and mutant preparations (Fig. 2A). Therefore, the increased resistance of the A666G mutant cannot be attributed to increased ATPase activity. Similarly, the K_m values were not significantly different (Fig. 2B).

These vesicles have a large amount of Pma1, which retains the significant activity at a pH of 7.0. This results in significant background, especially at ATP concentrations that are 3 mM or greater. We, therefore, probably underestimated the Pdr5-specific ATPase; however, we saw no difference between the strains.

The Pdr5 ATPase activity has a broad pH range (Ernst *et al.*, 2008). When Tris-glycine (pH 9.5) served as the assay buffer to measure the activities in two sets of PM vesicles (Fig. 2C), the background observed in the negative control was considerably reduced. In this particular experiment, the V_{max} of the WT ATPase activity was $\sim 1.5 \mu\text{mol min}^{-1} \text{mg}^{-1}$ and the K_m was $\sim 1.1 \text{ mM}$. The corresponding values for the A666G mutant were $1.9 \mu\text{mol min}^{-1} \text{mg}^{-1}$ and 0.7 mM .

The A666G mutant increased resistance to many Pdr5 transport substrates

We compared the resistance of the WT and A666G strains to the six Pdr5 transport substrates as shown in Fig. 3. Five additional plots are found in the Supporting Information (Fig. S1). The entire collection encompassed compounds that are distinct in the structure and mechanism of action (tamoxifen, two trialkyltin chlorides, cycloheximide and cerulenin) and a set of structurally similar compounds (bifonazole, clotrimazole, imazalil sulfate (IMZ) and cyproconazole) that inhibit ergosterol (and therefore membrane) biosynthesis. Thus, we tested 11 Pdr5 transport substrates. These varied considerably in hydrophobicity and size. Cycloheximide was the most polar ($\log p = 0.56$); tripen-tyl-tin chloride was the most hydrophobic ($\log p = 5.84$) and largest. Cerulenin was the smallest of the Pdr5 substrates tested.

The A666G mutation created robust resistance to 10 of the 11 tested compounds. Depending on the compound,

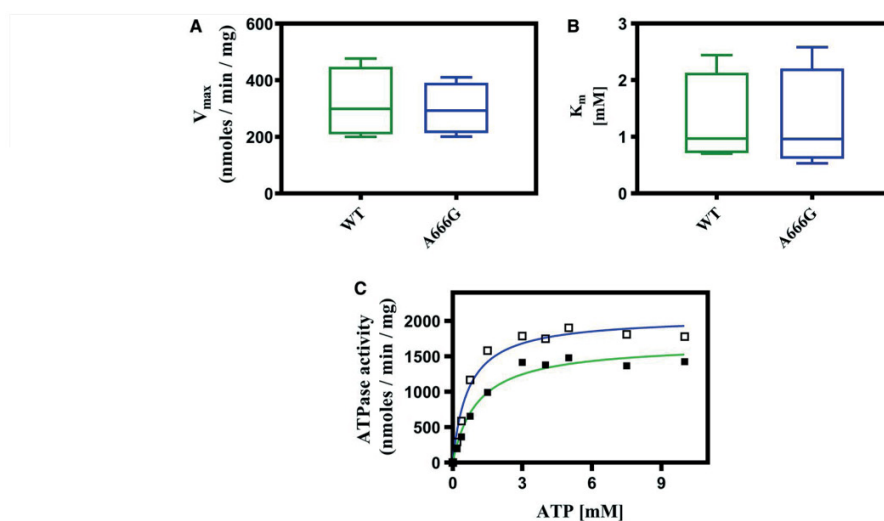


Fig. 2. The WT and mutant PM vesicle preparations have indistinguishable ATPase activities. V_{max} (A) and K_m (B) values from assays of four PM vesicles preparations from WT (green box) and A666G (blue box) mutant strains. The assays were performed in HEPES buffer (pH 7.0) as described in the Experimental Procedures. The horizontal bars indicate the median values. (C) The ATPase activity was also assayed in Tris-glycine buffer (pH 9.5). No other parameters of the assay were altered. In this panel: green line (■) = WT and blue line (□) = A666G mutant.

the resistance to these substrates in the A666G mutant strain was roughly 2–4x higher than in the WT. The mutant did not exhibit enhanced clotrimazole resistance. In two-way ANOVA tests, only the plots for clotrimazole showed no significant difference between the WT and A666G strains.

Identification of substrates whose transport is not enhanced by the A666G mutation may have bearing on the mechanism of resistance. The clotrimazole data are complicated by the fact that this transport substrate is a potent inhibitor of Pdr5 ATPase *in vitro*, which might limit any additional resistance above the WT level *in vivo*. In the Supporting Information, we identify coumarin 6 as a strong Pdr5 substrate whose transport was not enhanced further by the A666G mutant (Fig. S2) and did not inhibit the Pdr5-specific ATPase activity.

The A666G mutant had increased R6G transport in whole cells

We also compared the whole cell R6G transport capability of the WT, A666G and G312A mutant strains with 5 μ M (Fig. 4A) and 10 μ M R6G (Fig. 4B). The G312A null mutant and the isogenic Δ Pdr5 strain served as negative controls. In an assay with 5 μ M R6G, the WT strain accumulated a median value of 94.4 arbitrary fluorescence units (a.u.); the Δ Pdr5 strain retained 1920 a.u. Cells treated with 50 mM 2-deoxyglucose to deplete ATP

levels retained levels of fluorescence that were comparable to the negative control. Fluorescence was 6x as great in the WT as in the A666G strain (15.7 a.u.). A similar result appeared in a transport assay conducted with 10 μ M R6G. In this case, the differential between the A666G and WT strains was about 5x (Fig. 4B).

Whole cell transport experiments and measurements of drug resistance were carried out at 30°C and various *in vitro* assays were performed at 35°C. We, therefore, performed one set of whole cell transport experiments at a higher temperature to determine whether the relative difference between the strains was maintained (Fig. 4B). However, transport was reduced overall, the WT still accumulated about 5x as much R6G as the A666G mutant strain. We concluded that the A666G mutant was not temperature sensitive and that the results obtained at the two temperatures were comparable.

Imazalil sulfate inhibits R6G transport in whole cells

In a previous study, IMZ exhibited the concentration-dependent inhibition of R6G whole cell transport (Mehla *et al.*, 2014). IMZ was also useful because it did not inhibit the Pdr5 ATPase activity at the concentrations used in our transport assays (Downes *et al.*, 2013). When 5 μ M R6G was the substrate, IMZ caused concentration-dependent inhibition with levels of retained fluorescence reaching that of the Δ Pdr5 control (Fig. 5A). The IC_{50} of IMZ in the WT strain

© 2019 John Wiley & Sons Ltd, *Molecular Microbiology*, 0, 1–14

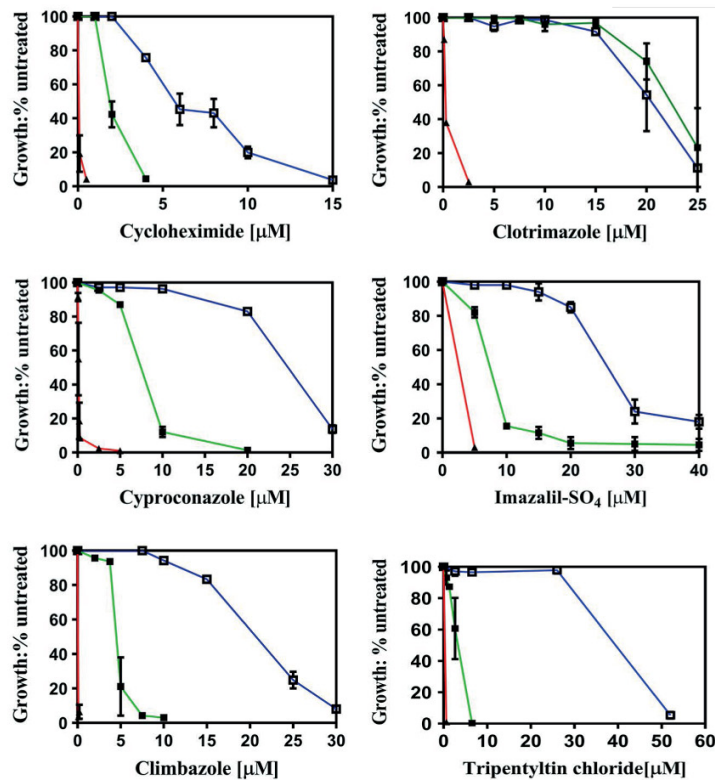


Fig. 3. The A666G mutant exhibits strong hyperresistance to multiple Pdr5 substrates. Cells were cultured in YPD broth at 30°C for 48 h in the presence of drugs as described in the Experimental Procedures. YPD cultures of each strain that contained no drug served as an untreated control for growth comparisons. Cell concentration was determined at 600 nm. In this figure: ■, green, WT; ▲, red, Δ Pdr5 and □, blue, A666G ($n = 3$).

was ~ 60–70 μ M. The A666G mutant, however, behaved differently. It took a larger concentration of IMZ to begin to see the inhibition. At higher concentrations, however, the mutant curve increased sharply so that the IC_{50} (about 100 μ M) was similar to that of the WT. When we used a nonlinear transformation to make plots of the log of the IMZ concentration versus the fluorescence (Fig. 5B), the WT curve had a Hill (h) coefficient of 0.9, but the mutant value was 2.4, suggesting cooperativity between transport sites.

The concentrations of IMZ used to inhibit R6G transport also inhibited growth in the culture. However, the gating profiles of IMZ-treated cells obtained during fluorescence cell sorting were similar to the untreated controls and gave no evidence of increased cellular damage or death during the relatively short incubation period, caution is required in interpreting these results. Studies carried out by Siegel and Ragsdale (1978) demonstrated the effects of imazalil on ergosterol precursor pools as early as 30 min. Therefore, it was important to perform the *in vitro* studies described below.

© 2019 John Wiley & Sons Ltd, *Molecular Microbiology*, 0, 1–14

The A666G mutant enhanced R6G fluorescence quenching in purified PM vesicles

We developed a fluorescence quenching assay suitable for measuring the R6G transport for Pdr5 (Kolaczowski *et al.*, 1996) and have used it to analyze the transport capability of several mutants (Ernst *et al.*, 2008; Furman *et al.*, 2013). However, R6G is a known inhibitor of Pdr5 ATPase. It was, therefore, important to establish whether the WT and A666G mutant enzyme activities were inhibited to the same degree. If, for example, the A666G mutant enzyme was more sensitive to inhibition than the WT, the initial rate (IR) of fluorescence quenching would be underestimated in the mutant. In the Supporting Information (Fig. S3, panel A), we present the data indicating that the IC_{50} of the A666G ATPase was only modestly lower than that of the WT when assayed in HEPES (pH 7.0) buffer with relatively high concentrations of R6G (5–35 μ M). At the concentration of R6G used in most of our quenching experiments

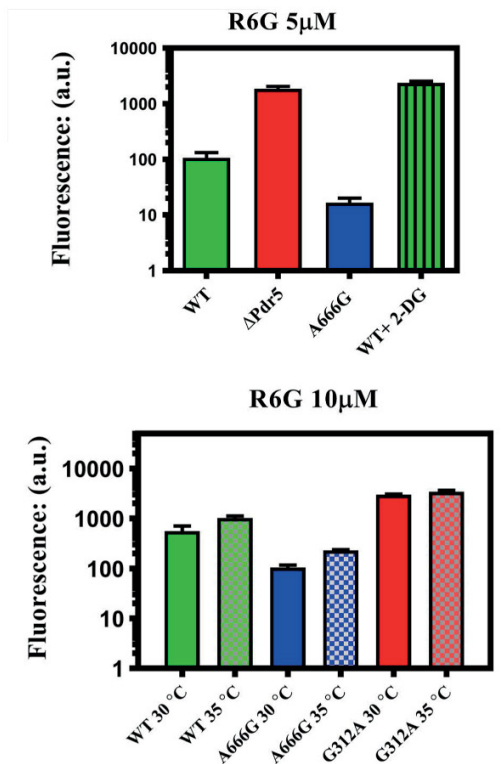


Fig. 4. The A666G mutant enhances the R6G transport in whole cells. Transport of 5 μ M (A) or 10 μ M (B) R6G against a concentration gradient was performed as described in the Experimental Procedures at 30°C for 90 min. The median fluorescence (a.u.) obtained from sorting 10,000 cells per sample is shown ($n = 3$). We also compared the transport at 30°C and 35°C in the same strains (B). Each independent culture ($n = 3$) was split into two portions and the transport was monitored at the two temperatures with the whole cell transport protocol described in the Experimental Procedures.

(100 nM), the WT enzyme retained 90% of the activity found in untreated samples; the A666G mutant retained 80% (Fig. S3, panel B).

We initially assayed a single preparation of PM vesicles from the WT and A666G strains (Fig. 6A). We performed reactions with 3 mM ATP, a concentration thought to be physiological for *Saccharomyces* (Ozalp *et al.*, 2010). As expected, the kinetics of R6G quenching in the WT and A666G strains were first order (R^2 values = 0.9926 and 0.9965 respectively) when we performed a linear regression on a plot of the natural logarithm (ln) of the fluorescence a.u. versus time (Fig. 6B). PM vesicles from the isogenic Δ Pdr5 served as a negative control and showed no quenching. The plot from this preparation yielded a slope that was not significantly different from zero. We

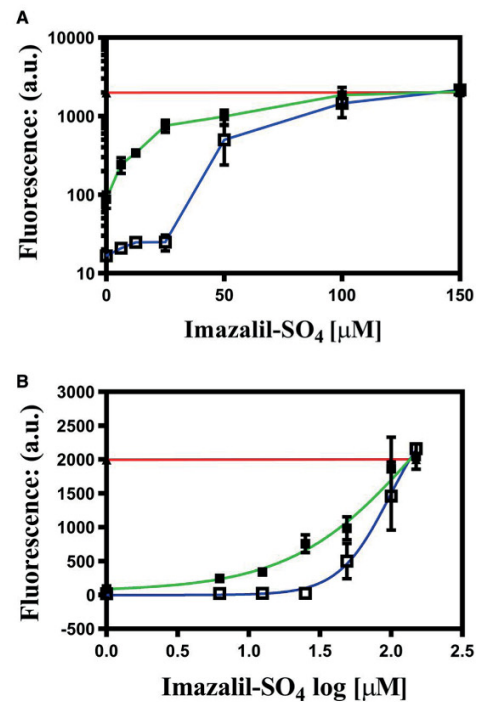


Fig. 5. Imazalil sulfate inhibition of the R6G transport is concentration dependent. A. Inhibition of 5 μ M R6G transport was performed in the presence of IMZ. The assay was the same as the one used throughout the whole cell transport studies except that during inhibition assays, IMZ was added at the same time as R6G and remained throughout the entire incubation period. The red line indicates the level of fluorescence in the Δ Pdr5 control strain. In these experiments, $n = 6$ for WT (green line) and $n = 4$ for the A666G mutant (blue line). B. A logarithmic plot was constructed from the same data.

obtained a similar result when we omitted ATP from a reaction containing either WT or A666G (data not shown). Because the ATPase activities of the WT and A666G PM vesicles used in this experiment were similar, thus we concluded that the IR of fluorescence quenching was about twice as fast in the mutant.

ATPase activities varied somewhat from one PM vesicle preparation to another; furthermore, we switched to a much improved method of PM vesicle preparation that yielded significantly higher ATPase activities. We used this method to prepare the PM vesicles used exclusively in the experiments described in Figs 8 and 9. Therefore, it was important to determine whether IRs of R6G fluorescence quenching and ATPase activity were proportional. Results presented in the Supporting Information (section S2 and Fig. S4) demonstrate that this was the case.

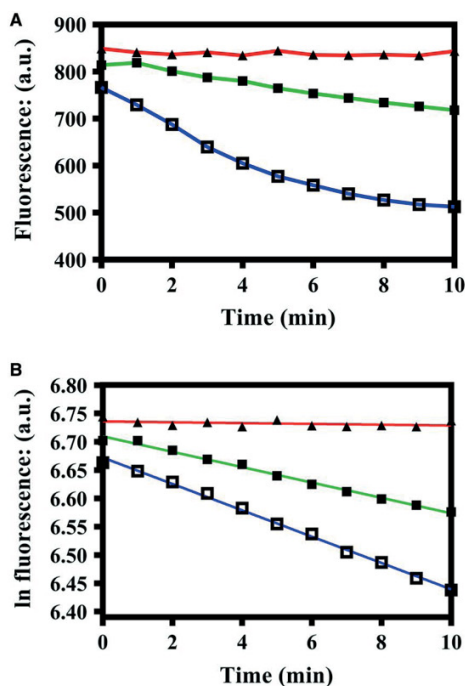


Fig. 6. Pdr5-mediated R6G transport is enhanced in PM vesicles prepared from A666G cells. In these experiments: \blacksquare , green, WT; \blacktriangle , red, Δ Pdr5 and \square , blue, A666G. Fluorescence quenching was carried out as described in the Experimental Procedures at 35°C with 30 μ g PM vesicle protein suspended in transport buffer containing 100 nM R6G and 3 mM ATP in a final volume of 2 ml, as described by Furman *et al.* (2013). A. Quenching was carried out with PM vesicles prepared from WT, Δ Pdr5 and the A666G mutant strains as described in the Experimental Procedures. The plot shows the fluorescence in a.u. at 1 min intervals. B. A linear regression was performed on the same data shown in Fig. 7A by plotting the ln fluorescence (a.u.) against the time using GraphPad software. C. Fluorescence quenching experiments used independent PM preparations from the WT and A666G mutant strains. Initial quenching rates were determined by linear regression performed on each plot as shown in panel B. We plotted the rates against the ATPase activity determined in HEPES transport buffer with 3mM ATP, with the assay described in the Experimental Procedures.

No large changes occurred in the IRs of fluorescence quenching over an 8x range of R6G concentrations

We looked at the IRs of fluorescence quenching over an 8x range in R6G concentration in the preparations of WT and the A666G mutant (12.5 nM–100 nM). We observed no consistent change in the quenching rates over this range of concentrations (Fig. 7). If anything, the mutant rates decreased very slightly with increased concentrations of R6G.

© 2019 John Wiley & Sons Ltd, *Molecular Microbiology*, 0, 1–14

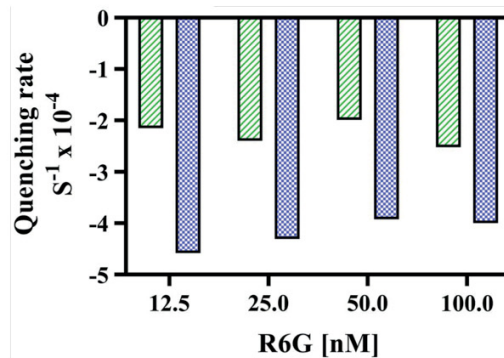


Fig. 7. IRs of fluorescence quenching measured over a range of R6G concentrations. Fluorescence quenching experiments with WT (green bar) and A666G (blue bar) PM vesicles were performed as described in the Experimental Procedures with different concentrations of R6G (12.5–100 nM).

The enhanced fluorescence quenching observed in the A666G PM vesicles is attributable to increased cooperativity between transport sites

To evaluate whether the A666G phenotype is attributable to altered kinetics of the drug transport cycle, we initially compared the IRs of fluorescence quenching of the WT and mutant PM vesicles with similar preparation dates and ATPase activities over a range of ATP concentrations (1.5–10 mM).

With the improved method of purifying PM vesicles, we obtained preparations of much higher ATPase activity and fluorescence quenching capability. We observed that at higher IRs of R6G fluorescence quenching, the curves became nonlinear with increasing time in both WT and A666G vesicles. By carrying out linear regression on the entire data set (20 min) would have resulted in an underestimation of the IRs of fluorescence quenching once we performed a linear transformation (and the R^2 values in some cases would have been less). Therefore, we determined the IRs of R6G fluorescence quenching for these from the linear portion of the curves, with linear regression. Representative plots of the ln fluorescence versus time are found in the Supporting Information (Fig. S5) from assays with 1.5, 3.0 and 5.0 mM ATP. The linear portions used to determine rates are indicated. The R^2 values for the linear portions were all ≥ 0.99 .

When we plotted the rates versus ATP concentration (Fig. 8A), several features were readily apparent. The curves for both the mutant and the WT fit a nonlinear transformation that used an allosteric sigmoid equation. The R^2 values for the WT and A666G plots were 0.9776 and 0.9921, respectively, indicating a reasonably strong fit. The $K_{m(ATP)}$ s necessary to reach half the V_{max} of fluorescence quenching were similar: 3.5 mM for the WT and 3.4 mM

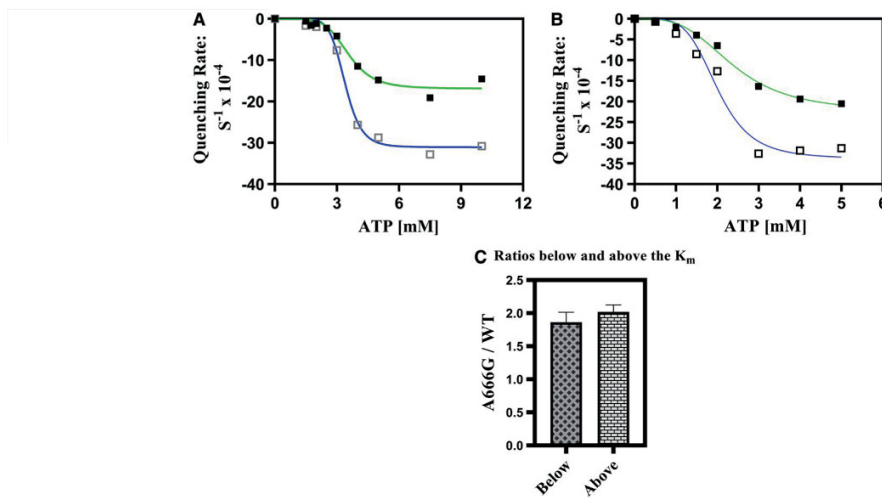


Fig. 8. The A666G mutant enhances cooperativity between transport sites. Fluorescence quenching was performed with 100 mM R6G at 35°C for 20 min as described in the Experimental Procedures except that 60 μ g of purified PM vesicles were used in each reaction with the first set of PM vesicles tested (A) and 30 μ g were used with a second set of WT and mutant PM vesicles (B). In each panel: ■, green line = WT and □, blue line = the A666G mutant. The ratio of the A666G mutant and WT IRs is compared above and below the K_m (C).

for the A666G mutant (Table 1). There was a remarkable increase in the IRs of fluorescence quenching between 3 and 4 mM ATP in both cases. This largely accounts for the high h coefficients of 5.9 for the WT and 8.6 for the mutant. This cooperativity represents interactions between the drug transport sites rather than the ATP hydrolysis sites. The Pdr5-mediated ATPase activity is well studied, follows strict Michaelis–Menten kinetics and therefore exhibits no cooperativity (Golin *et al.*, 2007; see also Fig. 2C).

The higher h coefficient observed in the plot from the A666G mutant was potentially important because it suggested a mechanism by which resistance could be enhanced. For this reason, we prepared a new set of WT and A666G PM vesicles and again tested the effect of varying ATP concentrations on the IRs of fluorescence quenching. In this experiment, however, we also measured the IRs of R6G fluorescence quenching at the lower ATP concentrations of 0.5 and 1.0 mM. The results in the two experiments were qualitatively similar (Fig. 8B). The pertinent kinetic data for the experiments shown in Fig. 8 are averaged and are presented in Table 1.

The Supporting Information presents the results from a set of WT and A666G mutant preparations that were made and tested independently of each other (Fig. S6A and B). In addition, an earlier experiment used a pair of WT and A666G PM vesicles prepared with the original purification method and therefore lower ATPase and quenching activity (Fig. S6C). In all of these, the h coefficient was noticeably higher for the mutant than the WT.

We compared the enhancement of quenching in the A666G PM vesicles at each of the ATP concentrations that we tested (Fig. 8C). Overall, we saw no significant difference in the enhancement at concentrations that were above or below the K_m values. However, in both experiments, the ATP concentration directly above the K_m resulted in the largest enhancement.

The inhibition of R6G fluorescence quenching by IMZ in A666G PM vesicles also exhibited enhanced cooperativity

We also observed enhanced cooperativity in the A666G mutant PM vesicles when we used IMZ to inhibit R6G fluorescence quenching. We compared the inhibition of R6G fluorescence quenching with 50, 75 and 100 nM R6G in new pairs of PM vesicles prepared from the WT and A666G strains (Fig. 9A–C). The lowest concentration of IMZ used (0.5 μ M) resulted in 0%–15% inhibition relative to the untreated control depending on the strain and R6G concentration. The mutant curves exhibited greater cooperativity than the WT ones at all three concentrations. The data are summarized in Table 2, where they are compared to the values obtained from experiments in which we monitored the IR of R6G fluorescence quenching as a function of ATP concentration. The h coefficients for both WT and mutant were higher in the experiments where ATP was varied than in those in which we used IMZ as an inhibitor.

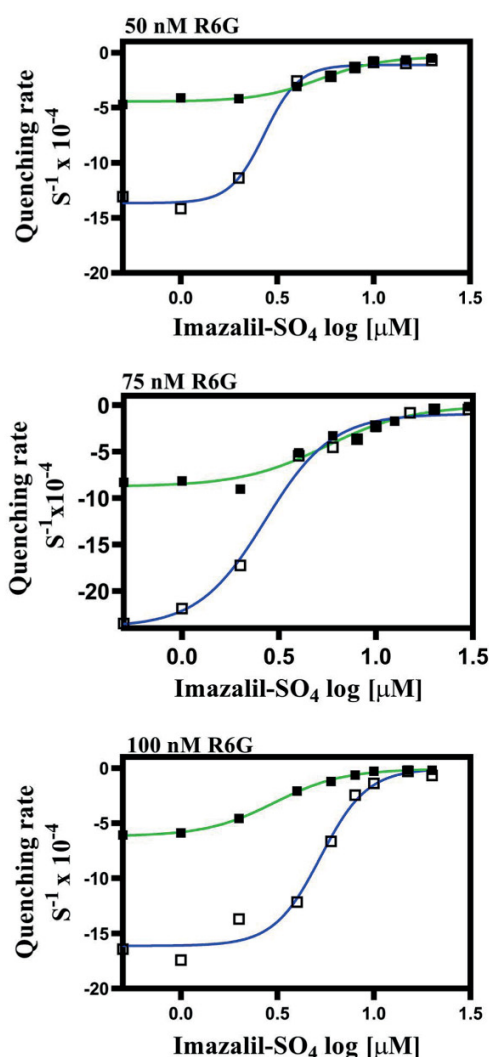


Fig. 9. Inhibition of R6G fluorescence quenching by IMZ mirrors the results with whole cell transport studies. Fluorescence quenching experiments were performed with 25 μg of purified PM vesicle protein for 20 min at 35°C as described in the Experimental Procedures. A different pair of PM vesicles was used to monitor fluorescence quenching at 75 nM R6G. Inhibition studies were performed with IMZ with (A) 50 nM, (B) 75 nM and (C) 100 nM R6G with various concentrations of IMZ (0.5–30 μM). The IRs were determined using Graph Pad software through the same linear transformation that was applied to the tamoxifen data. The resulting curves were fitted by a nonlinear transformation (IR versus log [inhibitor], variable slope with four parameters). In all panels: WT = ■, green line and A666G = □, blue line.

Discussion

Traditionally, cancers and pathogenic organisms are screened for the overexpression of these efflux pumps.

© 2019 John Wiley & Sons Ltd, *Molecular Microbiology*, 0, 1–14

Table 1. IR of fluorescence quenching versus ATP concentration: kinetic parameters^a

Kinetic parameters	WT	A666G
V_{max} quenching ($\text{S}^{-1} \times 10^{-4}$)	−19 (3.5)	−33 (1.4)
K_{m} quenching (mM)	2.9 (0.9)	2.2 (0.4)
Hill values (h)	4.7 (1.8)	6.8 (2.6)
V_{max} ATPase ($\mu\text{mol min}^{-1} \text{mg}^{-1}$) ^b	1.4 (0.2)	1.4 (0.7)
K_{m} ATPase (mM)	2.1 (1.3)	2.1 (0.9)

^aThe kinetic parameters are the average values for the experiments shown in Fig. 8A and B. The kinetic parameters were determined using GraphPad Prism 8.0 software. The standard deviations are included in parentheses. Each point on a curve is the average IR of R6G fluorescence quenching for two quenching reactions. One of these (2 mM ATP, A666G) was recognized as an outlier by the GraphPad software and removed.

^bThe ATPase activity was measured in Tris-glycine buffer (pH 9.5).

In this report, we describe the phenotypic features of a novel mutation: A666G, which exhibited robust enhancement in drug resistance. This mutant acquired under selection generally had IC_{50} values that were 2.5–4x as high as the WT depending on the substrate. When we measured the R6G efflux in whole cells, the WT retained ~ 3.4–6x as much fluorescence as the mutant. Significantly, these enhancements occurred, however, no further increase in the ATPase activity or the steady-state level in the PM.

These observations have major implications for the therapeutic treatment of cancers and fungal pathogens. They suggest that further robust resistance mediated by ABC transporters may be obtained without overexpression. The transport of clotrimazole and coumarin 6, however, was not enhanced by this alteration. We observed no difference in clotrimazole resistance or coumarin-6 transport capability between the WT and A666G mutant strains. Understanding the mechanism behind the increased resistance that defines the A666G mutant phenotype might offer improved treatment of fungal resistance and drug-resistant cancer. It may help identify therapeutic compounds that are more effective because mutants similar to A666G are unable to enhance their transport.

Our observations suggest a novel mechanism for the resistance exhibited by the A666G mutant. Conservation of this residue in numerous clinically relevant fungal transporters and the similar phenotype of the A666G substitution in CaCdr1 suggests that this could be a significant way to increase the multidrug resistance.

Both whole cell transport and fluorescence quenching assays in the presence and absence of competing transport substrates indicate that this mutant makes the efflux process more efficient by increasing the cooperativity between transport sites. It is important to note that the cooperativity between drug binding sites in P-gp has been known for some time (Shapiro and Ling, 1997). However, genetic modification can result in greater resistance

Table 2. Summary of h values from various experiments

Strain	Conditions	Mean h value	n	SD
WT (JG2015)	Varying the ATP concentration	4.1	3 ^a	1.6
WT (JG2015)	Imazalil sulfate inhibition	2.3	3	0.5
A666G	Varying the ATP concentration	6.6	3 ^a	1.8
A666G	Imazalil sulfate inhibition	3.7	3	1.1

The h values were determined for two different types of experiments. One set of experiments determined the IRs as a function of ATP concentration. A second set of experiments compared the inhibition of R6G fluorescence quenching in WT and A666G PM vesicles by imazalil sulfate.

^aThese calculations include an experiment performed with an additional PM preparation of WT and A666G PM vesicles made and tested separately. The additional plots are found in the Supporting Information (Fig. S6A and B).

because of increased cooperativity, a novel and important observation. However, there are numerous examples of multidrug transporter overexpression leading to hyperresistance, the mechanism behind mutants such as A666G remained unknown. When the IRs of R6G fluorescence quenching were plotted as a function of ATP concentration, both mutant and WT preparations showed cooperativity. However, it was greater in the mutant. We observed a similar phenomenon with IMZ inhibition of R6G fluorescence quenching. It should be noted, however, that small changes in the IRs of R6G fluorescence quenching can result in relatively large changes in h coefficients. Therefore, a single experiment is probably not definitive. For instance, in the plot shown in Fig. 8A, the 95% confidence interval for the WT gives a range for the h coefficient of 4.2–8.6. For the A666G mutant, the range is 6.7–11. When we included all of the data including that found in the Supporting Information, the difference in h coefficients between WT and mutant was significant according to the *t*-test ($p = 0.036$). Furthermore, in all of the experiments in which we determined the h coefficient, the mutant value was always higher than the corresponding WT coefficient obtained at the same time. Thus, the evidence that the A666G mutant enhances resistance by increasing cooperativity between transport sites is striking.

Interestingly, when we compared the kinetics of IMZ inhibition of R6G transport to ATP-dependent R6G fluorescence quenching, the former exhibited less cooperativity in both the mutant and WT preparations. The WT differential was statistically significant ($p = 0.022$). This observation suggested that though Pdr5 ATPase is unstimulated by its substrates, they affect the interaction between transport sites. Consistent with this idea is the observation that IMZ is a weaker substrate than R6G. For instance, the Δ Pdr5 strain was only 10 times as sensitive to IMZ as the WT (Downes *et al.*, 2013). In contrast, the strain lacking Pdr5 retained 20 times as much R6G fluorescence as the WT strain. Furthermore, it took micromolar amounts of IMZ to completely inhibit nanomolar amounts of R6G quenching.

We considered the possibility that the cooperativity we observed could be accounted for the kinetic drug

selection model first proposed by Ernst *et al.* (2008) to explain the behavior of a substrate-specific H-loop mutation of Pdr5. This model proposes that the time spent in each conformational state during the transport cycle is subjected to genetic control. Therefore, a mutation could lead to a longer period spent in the inward-facing, drug-binding structure. This might also result in a longer period for a substrate to interact with Pdr5 and perhaps allow increased cooperativity. This model may very well explain some of the interesting FK506 hyperresistant mutants in Cdr1 and Pdr5 (Tanabe *et al.*, 2019). However, we have no concrete kinetic evidence that it explains the behavior of the A666G mutant, some observations from this study lend support to this model. The kinetic drug selection model predicts that when the IRs of the quenching reaction are below the K_m (which is ~ 2.0 – 3.5 mM ATP), the differential between the mutant and WT should be reduced or perhaps even eliminated because the ATP is rate limiting. Under such conditions, the entire transport cycle would be moving relatively slow and the substrate (R6G) would, therefore, have more time to interact with the WT transporter. It is not clear how far below the K_m the ATP concentration would need to observe such an effect. However, we saw no significant difference when we compared the quenching enhancement above and below the K_m , the difference at the 0.5 mM ATP concentration was lower (1.5x faster in the mutant preparations) than that observed directly above the K_m (2.3x faster in the mutant preparations). Furthermore, the lack of enhancement in coumarin-6 transport (Supporting Information) in the A666G strain makes us cautious about discarding the kinetic substrate selection as the explanation for this mutant's behavior. One prediction of this model is that strong Pdr5 substrates (for instance, those that equilibrate rapidly) might interact so quickly with Pdr5 that the time spent in the drug-binding conformation is not rate limiting. The transport of such compounds would therefore not enhance further by increasing the proportion of time spent in the drug-binding (inward-facing) conformation.

The recently reported cryo-EM structure of ABCG2 (Manolaridis *et al.*, 2018) suggests that substrates bind to an inner pocket containing drug binding sites. During the

ATP-driven conformational switch, drug molecules pass through a gate to an outer binding pocket before release. It is possible that Pdr5 has an analogous structure. Pdr5 has a gating function and Ser-1368 is critical (Mehla *et al.*, 2014). An alignment of ABCG2 and Pdr5 places Ser-1368 quite close to Leu-554 and Leu-555, which make up part of the gate in the former efflux pump. It is possible that the A666G mutant fosters even greater cooperativity between two pockets during this two-step exit process.

Experimental procedures

Yeast strains and plasmids

All the *Saccharomyces cerevisiae* strains (Table 3) we used were isogenic and derived from R-1, which lacks all PM ABC transporters and contains a *PDR1-3* mutation, which causes overexpression of *PDR5*. Thus, the Pdr5 efflux pump mediates virtually all drug resistance to the particular compounds that we tested. This strain offers numerous other advantages for genetic and biochemical analyses, which are described in detail elsewhere (Sauna *et al.*, 2008; Ananthaswamy *et al.*, 2010). It served as a negative control for most of the experiments in this research. We also used a phenotypically null mutation, G312A, as a negative control. We cultured the strains at 30°C in the yeast extract peptone dextrose (YPD) medium. We used the pSS607-integrating plasmid for site-directed mutagenesis, as previously described (Golin *et al.*, 2007). This plasmid has a WT *PDR5* gene under the transcriptional control of its own upstream region, as well as a *URA3* selectable marker. We initially used isogenic strains containing two copies of either WT or an A666G mutant gene to make purified PM vesicles for ATPase, fluorescence quenching and vesicle transport assays. Double-copy strains were also used for the whole cell transport assays with [³H]-clotrimazole. In general, we cultured cells in the yeast extract peptone dextrose (YPD) medium at 30°C. Cultures used to perform whole cell transport assays were grown in synthetic dextrose, yeast nitrogen base medium (SD) supplemented with uracil and histidine. Later in this study, when we switched to a better method for purifying PM vesicles that yielded preparations of much higher ATPase activity, we used the single-copy WT (JG2015) and A666G strains for the biochemical assays.

Chemicals and media

We purchased most of our chemicals from Sigma Aldrich. Five-fluoroorotic acid and G-418 were purchased from Research Products International and we purchased climbazole, cerulenin, cyproconazole, tebuconazole and IMZ from LKT laboratories and from Sigma Aldrich. We purchased tributyltin chloride from Alfa Aesar. All chemicals were dissolved in DMSO except for 5-fluoroorotic acid and G-418, which were dissolved in the sterilized YPD medium and cycloheximide, which was dissolved in sterile, MilliQ water. [³H]-coumarin 6 (20 Ci mmol⁻¹) was purchased from American Radiolabeled Chemicals.

Measurement of relative resistance of strains

To measure the relative resistance of each strain to all the compounds except for R6G, we inoculated yeast strains in 5 ml of YPD broth and grew them overnight at 30°C in an incubator shaker overnight at 110 rpm. The next day, we placed 2 ml of sterile YPD broth into sterile glass tubes. We introduced the desired concentration of drug into each tube. We measured the absorption of overnight culture with a spectrophotometer at ABS600 and used the value to calculate the cell concentration; we added 0.5×10^5 cells (typically 2–5 μ l). We incubated cultures at 30°C for 48 h at 110 rpm in a shaking incubator. We measured absorbance at 600 nm (A_{600}). We used isogenic WT and Δ *pdr5* strains to compare the susceptibility of the mutants to the drugs. For each strain, an untreated culture served as a growth control.

Site-directed mutagenesis

We introduced the Ala-666 substitutions into pSS607 using a QuikChange Lightning site-directed mutagenesis kit (Agilent Technologies). We designed mutant primers with a genomics program provided by Agilent Technologies (www.genomics.agilent.com). The mutant plasmids were introduced into XL-Gold *E. coli* by transformation, as described in the QuikChange instruction manual. We extracted plasmid DNA from the transformants with an IBI miniprep kit (Midwest Scientific) and had it sequenced commercially to confirm the presence of the mutation in the plasmid (SeqWright). We introduced the

Table 3. Yeast strains used in this study^a

Strain number	Genotype	Reference
R-1	<i>MATα his1, ura3, PDR1-3, pdr5::KanMX4, snq2, yor1, pdr3, pdr10, ycf1</i>	Sauna <i>et al.</i> (2008)
JG2015	Isogenic to R-1, but contains an insertion of pSS607 that has a WT <i>PDR5</i> gene in addition to the <i>pdr5::KanMX4</i> cassette	Golin <i>et al.</i> (2007)
JG2063	Isogenic to JG2015 but containing a G312A mutation in the insertion plasmid pSS607 instead of the WT allele	Furman <i>et al.</i> (2013)
JG2133	Isogenic to JG2015, but containing an A666G mutation in the insertion plasmid pSS607 instead of the WT allele	This study
JG2004	Isogenic to JG2015, but the <i>pdr5::KanMX4</i> cassette was replaced with a second copy of <i>PDR5</i>	Sauna <i>et al.</i> (2008)
JG2153	Isogenic to JG2133, but the strain contains two copies of the A666G mutation	This study

^aAll of the yeast strains used in this study are derivatives of the R-1 strain.

mutant plasmid DNA into R-1 with a Sigma Aldrich yeast transformation kit. Genetic testing described elsewhere (Ananthaswamy *et al.*, 2010) confirmed that the construct was correctly inserted.

Preparation of purified PM vesicles

We initially prepared purified PM vesicles essentially as described by Shukla *et al.* (2003), with minor modifications. We determined the protein concentration of PM vesicle protein with a bicinchoninic acid kit. However, this protocol gave satisfactory results, the proportion of Pdr5 in PM vesicles and therefore the ATPase activity varied significantly from preparation to preparation. Midway through this study, we adopted the procedure of Kolaczowski *et al.* (1996) as modified by Ernst *et al.* (2008), which significantly reduces the amount of contaminating mitochondrial membrane and gives consistently higher ATPase activity.

Gel electrophoresis of PM vesicle proteins

To check the quality of PM vesicle proteins, we solubilized samples containing 5 and 10 μg PM vesicle protein in SDS-PAGE buffer for 30 min at 37°C. We separated the proteins on NU PAGE 7% Tris-acetate gels (125–150 V for ~ 80 min; Life Technologies) before staining them for one hour in SimplyBlue (Coomassie G-250) SafeStain (Thermo Fisher) and destaining for 24–36 hours in MilliQ water.

Western blots of Pdr5 in PM vesicles

We conducted Western blotting with 10 μg PM vesicle protein as previously described (Downes *et al.*, 2013). We performed the transfer from the gel to the nitrocellulose membrane (400 mAmp, 60 min) with an X Cell II minicell apparatus (Invitrogen). We purchased all the antibodies from Santa Cruz Biotechnology. We diluted the polyclonal goat anti-Pdr5 (yC18) and anti-Pma1 (yN-20) antibodies 1:1000 and 1:250 respectively. We blocked the nitrocellulose membranes for 30 min with 5% nonfat milk in PBS containing 1% Tween 20. Following this, we incubated the filters with both the Pdr5 and Pma1 primary antibodies overnight at 4°C. We washed three times for 15 min before adding a 1:5000 dilution of secondary antibody (donkey, antigoat IgG horseradish peroxidase; SC2033) and incubating at a room temperature for 2 h. We developed blots with a Novex ECL horseradish peroxidase chemiluminescent substrate reagent kit (ThermoFisher). The relative amount of Pdr5 protein was compared with the Pdr5/Pma1 ratio as previously described (Downes *et al.*, 2013).

Assay of ATPase activity

We initially measured the Pdr5-specific ATPase activity for 8 min at 35°C with 16 μg purified PM vesicle protein in a final volume of 100 μl as previously described (Golin *et al.*, 2007), except that we assayed activity for 8 min at 35°C in the same HEPES transport buffer used to measure Pdr5-mediated

coumarin 6 and R6G quenching (50mM HEPES, pH 7.0 and 5 mM MgCl_2). After we switched to the PM vesicle preparation method of Kolaczowski *et al.* (1996), we reduced the amount of protein/assay to 5.0 μg . To measure the ATPase activity of the PM vesicles purified with the Kolaczowski method, we used 300mM Tris-glycine buffer (pH 9.5) in a final volume of 100 μl for 8 min at 35°C. To reduce the background, we added 0.2 mM ammonium molybdate, 50mM KNO_3 and 10mM NaN_3 respectively (Goffeau and Dufour, 1988). The non-Pdr5 activity observed in ΔPdr5 negative control PM vesicles was subtracted from the background before the calculating activity.

Assay of [^3H]-coumarin-6 transport in whole cells

To measure [^3H]-coumarin-6 transport against a concentration gradient (Supporting Information), 3×10^6 cells in the exponential phase of growth were pelleted in sterile Eppendorf tubes. We removed the supernatant and resuspended the pellets in 500 μl of 0.02 M HEPES, 1 mM glucose (pH 7.0) containing [^3H]-coumarin 6 made up to 20 μM with nonradioactive compound. We incubated the cells at 30°C in a circulating water bath for 90 min, pelleted them and washed them twice with 1 ml of cold 0.02M HEPES buffer (pH 7.0) without glucose. The pellets were resuspended in 500 μl of the same buffer and analyzed with a Triathler liquid scintillation counter (Lab Logic).

R6G transport in whole cells

We measured the R6G transport against a 10 μM concentration gradient. We placed 3×10^6 cells in 500 μl of 0.02 M HEPES, 1 mM glucose (pH 7.0) and 10 μM R6G and incubated them at 30°C for 90 min. The cells were pelleted and washed with 1 ml of cold 0.02M HEPES buffer (pH 7.0) without glucose. The pellets were resuspended in 500 μl of the same buffer and analyzed with a FACSort with an excitation wavelength of 529 nm and an emission wavelength of 553 nm. For each determination, the median retained fluorescence was obtained from sorting 10,000 cells. We analyzed the data with a CellQuest program. We expressed retained fluorescence in a.u. When IMZ was used to inhibit R6G transport, it was present throughout the assay.

R6G and coumarin-6 transport in purified PM vesicles

We performed assays of R6G quenching in purified PM vesicles as described by Kolaczowski *et al.* (1996) with the same buffer conditions at 35°C and a few minor modifications (Furman *et al.*, 2013). We compared activities in preparations that were made within a few days of each other, with identical buffers and reagents. Unless otherwise indicated, each reaction contained 30 μg of purified PM vesicle protein. We used a Varian Cary Eclipse fluorimeter (Agilent Technologies). The excitation wavelength was 529 nm and the emission wavelength was 553 nm. We used 12.5–100 nM R6G for the quenching reactions. We mixed multiple reactions' worth of components in a 15 ml tube to ensure uniformity across a set of assays. Following this, we split the mixture and placed 2 ml of portions in cuvettes. We added a fixed concentration of

ATP to one tube and immediately placed it in the fluorimeter at 35°C; we monitored quenching for 8–20 min, depending on the experiment. Our kinetic analysis of quenching used Varian Cary Eclipse kinetics software (Agilent Technologies). Fluorescence was expressed as a.u. In inhibition studies with IMZ, the antagonist was present for the duration of the reaction. The same fluorescence quenching assay was adapted for the use with coumarin 6 (Supporting Information). We used coumarin 6 concentrations of 100–300 nM. The excitation was 460 nm and the emission wavelength was 500 nm.

Statistical and kinetic analyses

We performed statistical and kinetic analyses using Prism GraphPad 8 software. Error bars in the figures or a \pm designation in the text indicates the standard error of the mean.

Acknowledgements

This work was supported by NSF grant MCB1048838 and NIH grant GM07721 to J.G. SVA's work is supported by the Intramural Health, National Cancer Institute, Center for Cancer Research. We thank Dante Nicotera and William Braungart for help with the fluorescence quenching assays and Ekaterina Nestorovich for help with the analysis of fluorescence quenching plots.

Author contributions

The work was conceived and designed by J.G., L.S. and S.V.A. N.A. and H.R. did the majority of the experiments. A.R. performed experiments. M.W. helped with the preparation of PM vesicles. All of the authors helped write and edit the manuscript.

Conflict of interest

The authors declare no conflict of interest with the contents of this article. The content is solely the responsibility of the authors and does not necessarily represent the official views of the National Institutes of Health.

References

- Ananthaswamy, N., Rutledge, R., Sauna, Z.E., Ambudkar, S.V., Dine, E., Nelson, E., *et al.* (2010) The signaling interface of the yeast multidrug transporter Pdr5 adopts a cis configuration and there are functional overlap and equivalence of the deviant and canonical Q-loop residues. *Biochemistry*, **49**, 4440–4449.
- Bruggemann, E.P., Germann, U.A., Gottesman, M.M. and Pastan, I. (1989) Two different regions of P-glycoprotein are photoaffinity labeled by azidopine. *Journal of Biological Chemistry*, **264**, 15483–15488.
- Dalmas, O., Orelle, C., Foucher, A.E., Geourjon, C., Crouzy, S., Pietro, A.D. and Jault, J.M. (2005) The Q-loop disengages from the first intracellular loop during the catalytic cycle of the multidrug ABC transporter BmrA. *Journal of Biological Chemistry*, **280**, 36857–36864.
- Downes, M.T., Mehla, J., Ananthaswamy, N., Wakschlag, A., LaMonde, M., Dine, E., *et al.* (2013) The transmembrane interface of the *Saccharomyces cerevisiae* multidrug transporter Pdr5: Val-656 located in intracellular-loop 2 plays a major role in drug resistance. *Antimicrobial Agents and Chemotherapy*, **57**, 1025–1034.
- Ernst, R., Kueppers, P., Klein, C.H., Schwarzmueller, T., Kuchler, K. and Schmitt, L. (2008) A mutation of the H-loop selectively affects rhodamine transport by the yeast ABC transporter Pdr5. *Proceedings of the National Academy of Sciences*, **105**, 5069–5074.
- Furman, C., Mehla, J., Ananthaswamy, N., Arya, N., Kulesh, B., Kovach, I. and Golin, J. (2013) The deviant ATP-binding site of the multidrug efflux pump Pdr5 plays an active role in the transport cycle. *Journal of Biological Chemistry*, **288**, 30420–30431.
- Gbelska, Y., Krjger, J.-J. and Breunig, K.D. (2006) Evolution of gene families: the multidrug transporter genes in five related yeast species. *FEMS Yeast Research*, **6**, 345–355.
- Goffeau, A. and Dufour, J.P. (1988) Plasma membrane ATPase from the yeast *Saccharomyces cerevisiae*. *Methods in Enzymology*, **157**, 528–533.
- Golin, J. and Ambukar, S.V. (2015) The multidrug transporter Pdr5 on the 25th anniversary of its discovery: an important model for the study of asymmetric ABC transporters. *Biochemical Journal*, **467**, 353–363.
- Golin, J., Ambudkar, S.V., Gottesman, M.M., Habib, A., Szczepanski, J., Ziccardi, W., *et al.* (2003) Studies with novel Pdr5p substrates demonstrate a strong size dependence for xenobiotic efflux. *Journal of Biological Chemistry*, **278**, 5963–5969.
- Golin, J., Kon, Z.N., Wu, C.P., Martello, J., Hanson, L., Supernavage, S., *et al.* (2007) Complete inhibition of the Pdr5 multidrug efflux pump ATPase activity by its transport substrate clotrimazole suggests GTP as well as ATP may be used as an energy source. *Biochemistry*, **46**, 13109–13119.
- Gottesman, M.M., Fojo, T. and Bates, S.E. (2002) Multidrug resistance in cancer: role of ATP-dependent transporters. *Nature Review of Cancer*, **2**, 46–58.
- Kathawala, R.J., Gupta, P., Ashley, C.R. and Chen, Z.-S. (2015) The modulation of ABC transporter-mediated multidrug resistance in cancer: a review of the past decade. *Drug Resistance Updates*, **18**, 1–17.
- Kolaczowski, M., van der Rest, M., Cybularz-Kolaczowski, A., Soumillion, J.P., Konigs, W.N., *et al.* (1996) Anticancer drugs, ionophoric peptides, and steroids as substrates of the yeast multidrug transporter Pdr5. *Journal of Biological Chemistry*, **271**, 31543–31548.
- Kolaczowski, M., Sroda-Pomianek, K., Kolaczowski, A. and Hichalak, K. (2013) A conserved interdomain communication pathway of pseudosymmetrically distributed residues affects the substrate specificity of fungal multidrug transporter Cdr1. *BBA Biomembranes*, **1828**, 479–490.
- Konotylannis, D. and Lewis, R.E. (2002) Antifungal drug resistance of pathogenic fungi. *Lancet*, **355**, 1135–1144.
- Lage, H. (2003) ABC transporters: implication on drug resistance from microorganisms to human cancers. *International Journal of Antimicrobial Agents*, **22**, 188–199.

- Lamping, E., Baret, P.V., Holmes, A.R., Monk, B.C., Goffeau, A. and Cannon, R.D. (2010) Fungal PDR transporters: phylogeny, topology, motifs, and function. *Fungal Genetics and Biology*, **47**(2), 127–142.
- Loo, T.W., Bartlett, M.C. and Clarke, D.M. (2003) Simultaneous binding of two drugs in the binding pocket of human multidrug resistance protein P-glycoprotein. *Journal of Biological Chemistry*, **278**, 39706–39710.
- Lugo, M. and Sharom, F.J. (2005) Interactions of LDS-751 and rhodamine 123 with P-glycoprotein. Evidence for simultaneous binding of both drugs. *Biochemistry*, **44**, 14020–14029.
- Manolaridis, I., Jackson, S.M., Taylor, N.M.I., Korval, J., Stahlberg, H. and Locker, K.P. (2018) Cryo-EM structures of a human ABCG2 mutant trapped in ATP-bound and substrate bound states. *Nature*, **563**, 426–430.
- Martin, C., Berridge, C., Higgins, C.F., Mistry, P., Charlton, P. and Callaghan, R. (2000) Communication between multiple drug-binding sites on P-glycoprotein. *Molecular Pharmacology*, **56**, 624–632.
- Mehla, J., Ernst, R., Moore, R., Wakschlag, A., Marquis, M.K., Ambudkar, S.V. and Golin, J. (2014) Evidence for a diode-based mechanism in a multispecific ATP-binding cassette (ABC) transporter Pdr5. *Journal of Biological Chemistry*, **289**, 26597–26606.
- Meyers, S., Schauer, W., Balzi, E., Wagner, M., Goffeau, A. and Golin, J. (1992) Interaction of the pleiotropic drug resistance genes *PDR1* and *PDR5*. *Current Genetics*, **21**, 431–436.
- Ozalp, V.C., Pedersen, T.R., Nielsen, L.J. and Olsen, L.F. (2010) Time-resolved measurements of intracellular ATP in the yeast, *Saccharomyces cerevisiae* using a new type of nanosensor. *Journal of Biological Chemistry*, **285**, 37579–37588.
- Pfaller, M.A. (2012) Antifungal drug resistance: mechanisms, epidemiology, and consequences for treatment. *The American Journal of Medicine*, **125**, S3–S13.
- Prasad, R., Banerjee, A., Khandewal, N.K. and Dhamagaye, S. (2014) The ABCs of *Candida albicans* multidrug transporter Cdr1p. *Eukaryotic Cell*, **14**, 1154–1164.
- Rahman, H., Carneglia, I., Lausten, M., Robertello, M., Choy, J. and Golin, J. (2018) Robust, pleiotropic drug resistance 5 (Pdr5)-mediated drug resistance is vigorously maintained in *Saccharomyces cerevisiae* during glucose and nitrogen limitation. *FEMS Yeast Research*, **18**, foy029.
- Sauna, Z.E., Bohn, S.S., Rutledge, R., Dougherty, M.P., Cronin, S., May, L., et al. (2008) Mutations define cross-talk between the N-terminal transporter Pdr5: possible conservation of a signaling interface for coupling ATP hydrolysis to drug transport. *Journal of Biological Chemistry*, **283**, 35010–35023.
- Seeger, M.A., Bordignon, E. and Hohl, M. (2015) ABC exporters from a structural perspective. In: George, A.M. (Ed.) *ABC Transporters: Forty Years*. Cham: Springer, pp. 65–84.
- Shapiro, A. and Ling, V. (1997) Positively cooperative sites for drug transport by P-glycoprotein with distinct drug specificities. *European Journal of Biochemistry*, **250**, 130–137.
- Shukla, S., Saini, P., Jha, S., Ambudkar, S.V. and Prasad, R. (2003) Functional Characterization of *C. albicans* ABC transporter Cdr1. *Eukaryotic Cell*, **2**, 1361–1375.
- Siegel, M. and Ragsdale, N. (1978) Antifungal mode of action of imazalil. *Plant Biochemistry and Physiology*, **9**, 48–56.
- Tanabe, K., Bonus, M., Tomryama, S., Miyoshi, K., Nagi, M., Nimi, K., et al. (2019) FK506 resistance of *S. cerevisiae* Pdr5 and *C. Albicans* Cdr1 involves mutants in transmembrane domains and extracellular loops. *Antimicrobial Agents and Chemotherapy*, **63**(1), e01146-18. Available at doi:<https://doi.org/10.1128/AAC.01146-18>.
- Urbatsch, I.L., Gimi, K., Wilke-Mounts, S. and Senior, A.E. (2000) Investigation of the role of glutamine-471 and glutamine-1114 in the catalytic sites of P-glycoprotein. *Biochemistry*, **39**, 11921–11927.

Supporting information

Additional supporting information may be found online in the Supporting information section at the end of the article.

SUPPORTING INFORMATION**An A666G mutation in transmembrane-helix 5 of the yeast multidrug transporter Pdr5 increases drug efflux by enhancing cooperativity between transport sites**

Nidhi Arya, Hadiar Rahman, Andrew Rudrow, Manuel Wagner, Lutz Schmitt, Suresh V. Ambudkar, and John Golin

CONTENTS:

Results	
S1.	Coumarin 6 transport was not increased in the A666G mutant
S2.	Fluorescence quenching was directionally proportional to ATPase activity
Figures	
Fig. S1.	The A666G mutant increases resistance to transport substrates
Fig. S2.	Coumarin 6 transport is not enhanced by the A666G mutant.
Fig. S3.	The A666G mutant ATPase exhibits a modest hypersensitivity to R6G inhibition.
Fig. S4.	The initial rates of fluorescence quenching are directly proportional to ATPase activity.
Fig. S5.	Representative plots of fluorescence quenching performed with 1.5, 3.0, and 5.0 mM ATP
Fig. S6.	The A666G mutant exhibits increased cooperativity between transport sites

Results***S1. Coumarin 6 transport was not increased in the A666G mutant***

The A666G mutant failed to enhance clotrimazole resistance or transport. This suggested that the A666G phenotype could be substrate-specific. Such an observation would have important bearing on mechanistic explanations for the otherwise robust enhancement of drug resistance observed in this mutant. Previous work demonstrated, however, that clotrimazole is a potent, non-competitive inhibitor of Pdr5 ATPase activity with an IC_{50} of ~ 2.0 - $2.5 \mu M$ when WT PM vesicles were used in the reaction (10).

This inhibition might therefore impose limits on the ability of the A666G mutant to enhance transport of this substrate. We discovered, however, that coumarin 6 transport was also not enhanced by the A666G mutant.

As part of an attempt to identify additional fluorescent substrates of Pdr5 beside R6G, we tested the fluorescence quenching capability of coumarin 6. This compound that appeared to have the features of a strong Pdr5 substrate particularly because its molecular volume ($267.1 \text{ cm}^3 / \text{Mol}$) is between two strong substrates: climbazole ($248.4 \text{ cm}^3 / \text{Mol}$) and clotrimazole ($302.0 \text{ cm}^3 / \text{Mol}$). It also did not inhibit Pdr5-specific ATPase activity in either WT or A666G PM vesicle preparations even at high concentrations. (Fig. S2A). When we tested the fluorescence quenching capability of the compound with WT PM vesicles, we observed that it was concentration-dependent (Fig. S2 B). The observed initial rate (IR) in a reaction containing 300nM coumarin 6 was $8.3 \times 10^{-4} \text{ S}^{-1}$. Control experiments demonstrated that quenching was both nucleotide and Pdr5-dependent. However, when we tried to use a 500 nM concentration, there was strong, nucleotide- independent autoquenching of coumarin 6; an observation made by others using micromolar concentrations (Li *et al.* 2005).

We compared the coumarin 6 quenching capability of PM vesicles made from WT and A666G strains (Fig. S2 C). These preparations had similar ATPase activities and representative plots are shown ($n=3$). In this set of plots, the observed IRs of coumarin 6 fluorescence quenching ($-6.6 \times 10^{-4} \text{ S}^{-1}$ and $-6.4 \times 10^{-4} \text{ S}^{-1}$) were not significantly different once the rates were normalized to ATPase activity. The same result was also observed with two other sets of WT and A666G PM vesicle preparations (Fig.S2 D).

Coumarin 6 is not toxic to yeast cells. However, we were able to measure [^3H]-coumarin 6 transport in whole cells (Fig. S2 E). Transport was clearly Pdr5-dependent. The WT strain accumulated about 4x less coumarin 6 than the ΔPdr5 control. There was, however, no significant difference in the transport capability of the WT and A666G strains.

S2. Fluorescence quenching was directionally proportional to ATPase activity

We evaluated the relationship between fluorescence quenching and ATPase activities, which we measured in the Hepes buffer (pH 7.0) using the same (3 mM) concentration of ATP (Fig. S4). We did this for six preparations of A666G mutant and eight preparations of WT vesicles. The data demonstrate that although ATPase activities can vary considerably, the IRs of fluorescence quenching in the A666G mutant (blue line) were roughly 2x faster than the WT (green line) regardless of enzyme activity. Thus, a linear regression was performed and yielded slopes of -0.0092 and -0.0209 for the WT and A666G mutant respectively. This indicated that the IRs of fluorescence quenching of the A666G mutant are about 2.3x faster than the WT. The R-squared values were 0.7888 and 0.8558 respectively indicating acceptable fits.

To determine whether the slopes of the lines were different, a t-test was performed. We obtained a t-value of 0.0106 indicating a very high probability that the lines were different (0.9918).

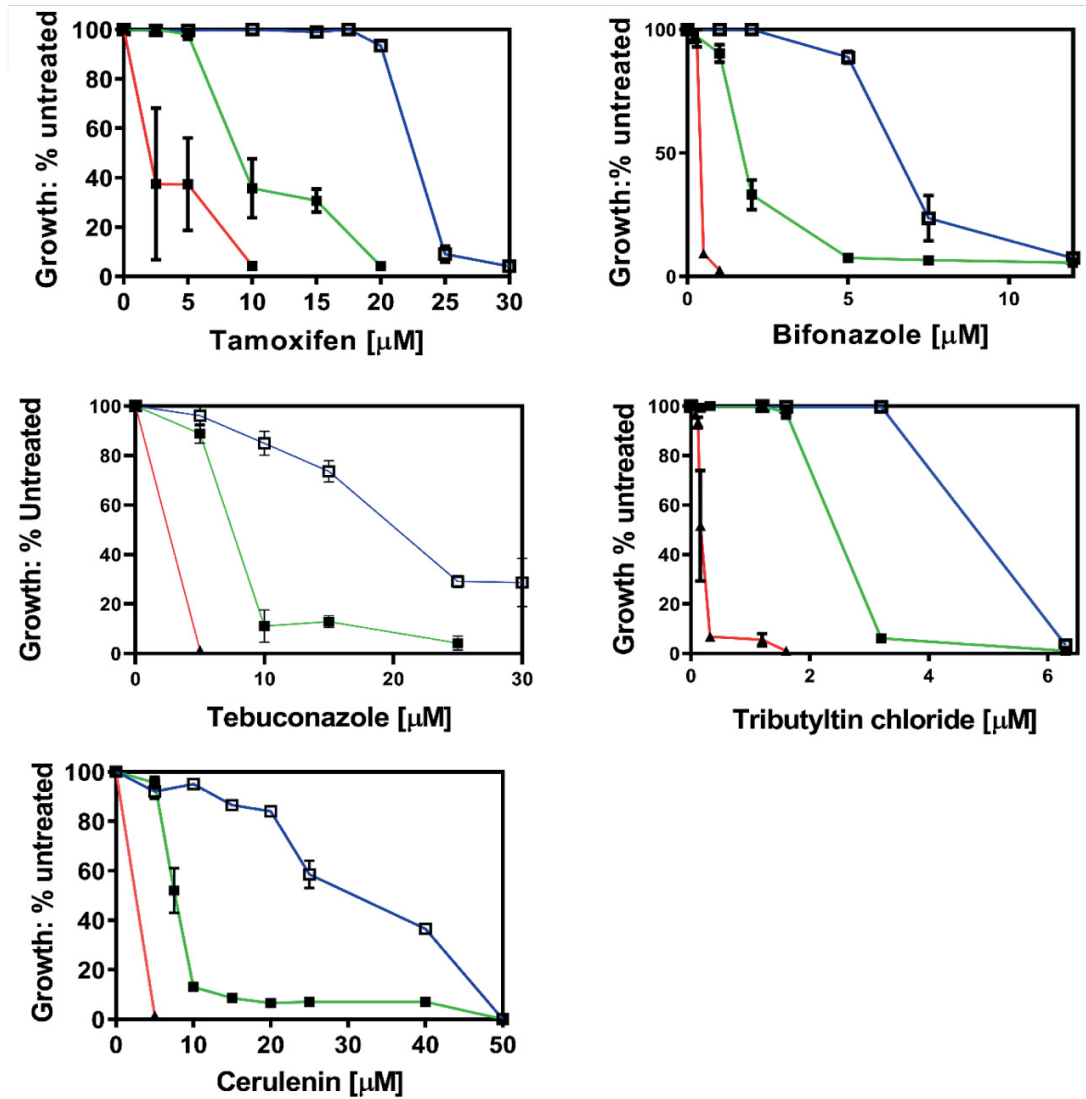


Fig. S1. The A666G mutant increases resistance to transport substrates. Cells were cultured in YPD broth at 30 °C for 48 h in the presence of drugs as described in the Experimental Procedures. YPD cultures of each strain that contained no drug served as an untreated control for growth comparisons. Cell concentration was determined at 600 nm. In this figure: ■, green WT; ▲, red, $\Delta Pdr5$; and □, blue, A666G (n = 3).

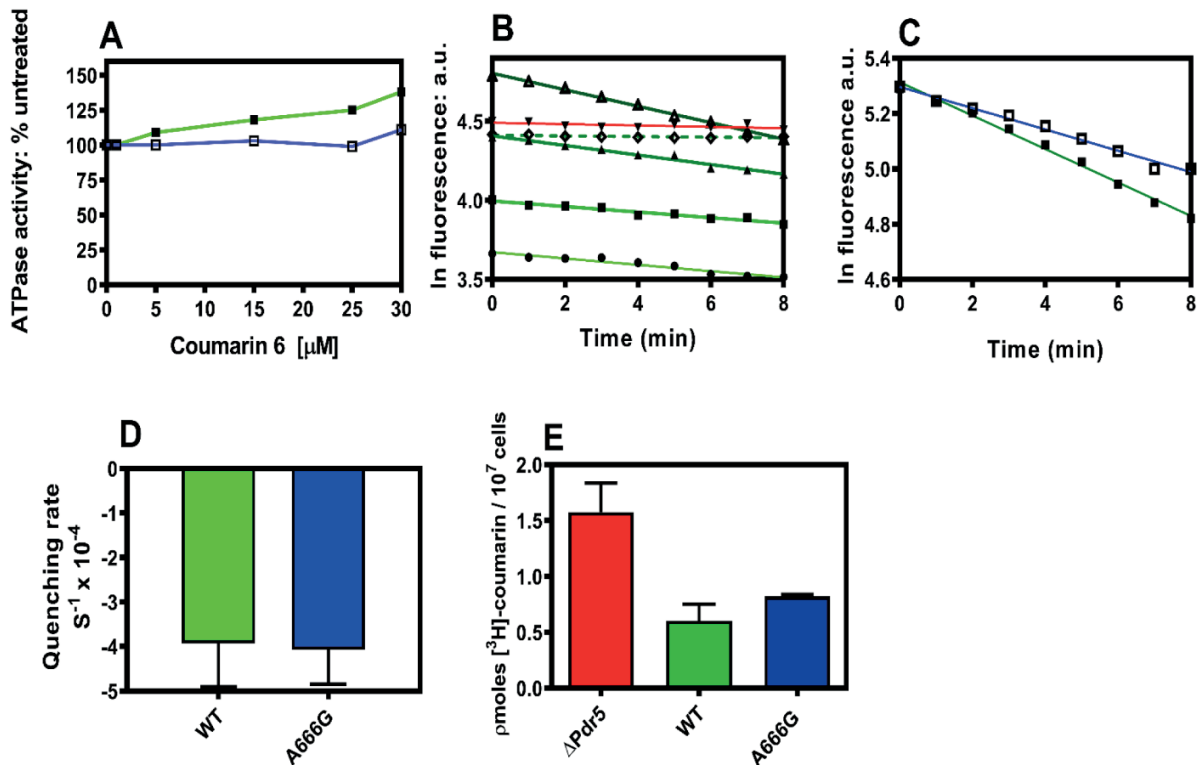


Fig. S2. Coumarin 6 transport is not enhanced by the A666G mutant. In panels (A) and (C), ■, green WT; ▲, red, ΔPdr5 ; and □, blue, A666G. (A) ATPase activity was monitored as described in the Experimental Procedures. Reactions were made up in HEPES transport buffer and included 16 μg purified PM vesicle protein, 3mM ATP \pm coumarin 6 in a final volume of 100 μl . Incubations were performed for 8 min at 30 $^\circ\text{C}$. (B) Coumarin 6 fluorescence quenching was performed as described in the Experimental Procedures. In these experiments, each sample was made up in HEPES transport buffer and contained 30 μg of purified PM vesicles, 3 mM ATP, and coumarin 6 concentrations of: ●, 100 nM; ■, 150 nM; ▲, 250 nM, and Δ , 300nM. The dashed green line represents a sample in which ATP was omitted, although 250 nM coumarin 6 was present. (C) Coumarin 6 fluorescence quenching was performed with PM vesicles prepared from the WT, ΔPdr5 , and A666G strains using 300 nM coumarin 6 and the same set of conditions described in panel B. Representative plots are shown ($n=3$). (D) The initial rates from three independent preparations of WT and A666G PM vesicles are shown. (E) [^3H]-coumarin 6 transport in whole cells was measured as described in the Experimental Procedures. Reactions contained 3×10^6 cells in a final volume of 500 μl 0.2M HEPES buffer containing 100 mM glucose and 20 μM [^3H]-coumarin 6. In these experiments, $n=6$.

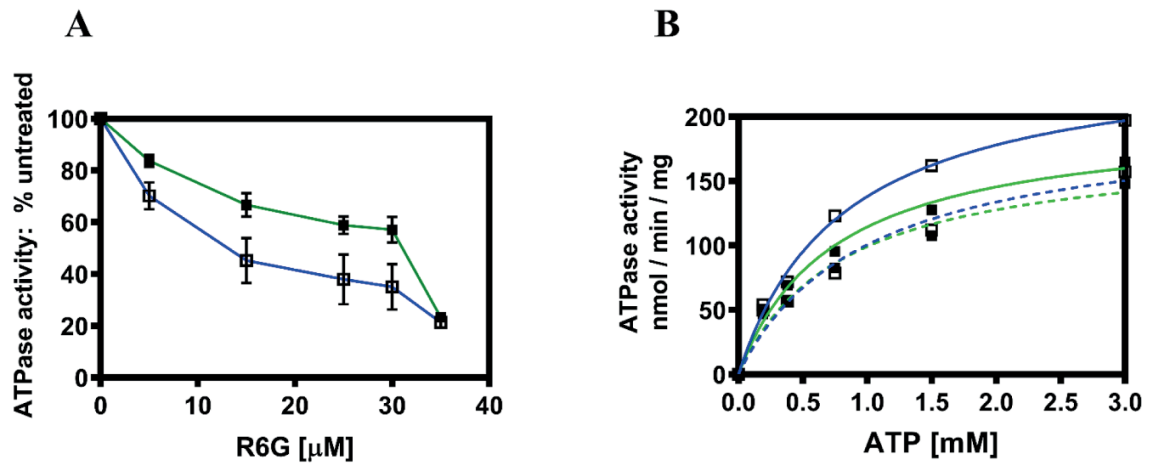


Fig. S3. The A666G mutant ATPase exhibits a modest hypersensitivity to R6G inhibition.

(A) ATPase activity was measured in Hepes (pH 7.0) buffer as described in the Experimental Procedures in the presence of R6G (0-35 μM) which was added five minutes prior to initiating hydrolysis with the addition of 3 mM ATP. In this figure: WT activity = green line, A666G activity = blue line. (B) ATPase activity was measured at various ATP concentrations in the presence of 100 nM R6G (dashed green line = WT activity; dashed blue line = A666G mutant activity). These activities were compared to corresponding reactions containing no R6G (solid green line = WT; solid blue line = A666G mutant).

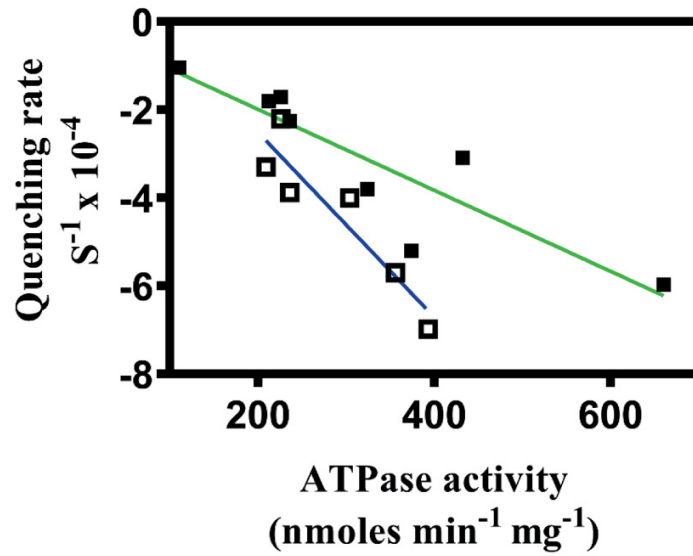


Fig. S4. The initial rates of fluorescence quenching are directly proportional to ATPase activity.

Fluorescence quenching experiments were performed with independent PM preparations of the WT and A666G mutant. Initial quenching rates were determined by linear regression performed on each plot shown in panel B of fig S2. The rates were plotted versus ATPase activity determined in HEPES transport buffer with 3mM ATP using the assay described in the Experimental Procedures.

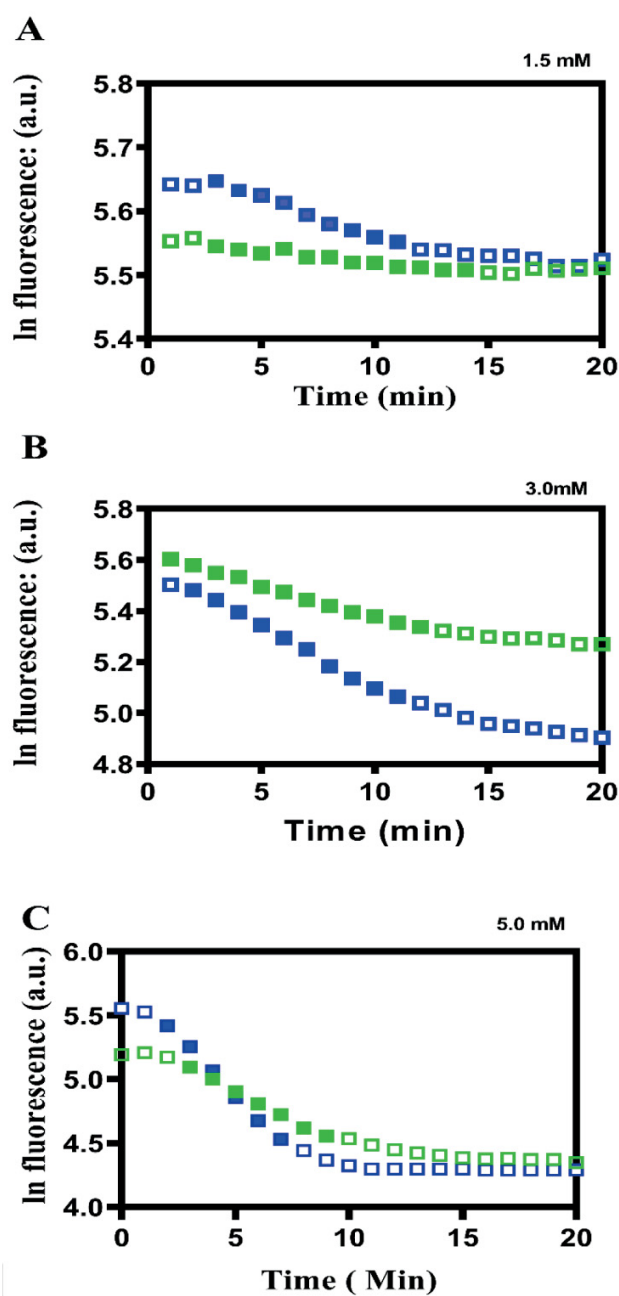


Fig. S5. Representative plots of fluorescence quenching performed with 1.5, 3.0, and 5.0 mM ATP. Fluorescence quenching experiments were performed as described in the Experimental Procedures. We plotted the ln of the fluorescence values taken at one-minute intervals. WT: green; A666G: blue. The linear portions of the curves used to determine the IRs have solid symbols.

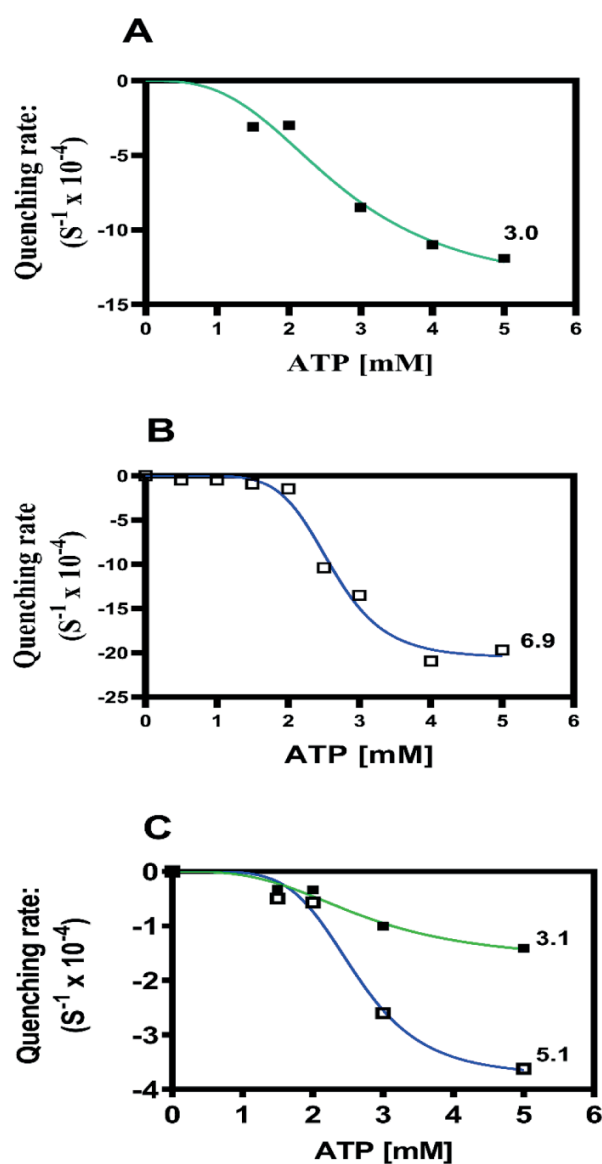


Fig. S6. The A666G mutant exhibits increased cooperativity between transport sites. The experiments shown in this figure are analogous to those illustrated in Fig. 8. The quenching reaction was performed as described in the Experimental Procedures. In addition to the data found in Fig. 8, we did the analogous experiment with (A) an additional WT and (B) A666G mutant preparations that were made and assayed independently of each other. (C) We also performed the same assay with PM vesicles that were made using the older protocol and were therefore were not as active. The number at the bottom of each curve is the Hill coefficient. In this figure: ■, green WT; and □, blue, A666G.

3.4 Chapter IV

Title: Pdr5: An ABC Drug/Proton Symporter
Authors: Manuel Wagner, Daniel Blum, Sander H.J. Smits, Richard Wagner,
and Lutz Schmitt
Published in: (submitted)
**Proportionate work
on this manuscript:** 50%

The yeast ABC transporter Pdr5 belongs to a new class of ATP-dependent drug/proton symporters

Pdr5: An ABC Drug/Proton Symporter

Manuel Wagner^{1,†}, Daniel Blum^{2,†}, Sander H. J. Smits¹, Richard Wagner^{2,*}, Lutz Schmitt^{1,*}

¹ Institute of Biochemistry, Heinrich-Heine-Universität Düsseldorf, Universitätsstraße 1, 40225, Düsseldorf, Germany.

² Department of Life Sciences and Chemistry, Jacobs University Bremen, 28719 Bremen, Germany

* Corresponding authors. Email: ri.wagner@jacobs-university.de or Lutz.Schmitt@hhu.de

† These authors contributed equally to this work

Abstract

Pdr5 from *Saccharomyces cerevisiae* is a prominent member of eukaryotic ATP binding cassette (ABC) transporters that are involved in multidrug resistance (MDR) and thus a broadly used model system. Although studied for decades, the underlying molecular mechanisms of drug transport and substrate specificity remain elusive. Here, we provide electrophysiological data on the reconstituted ABC transporter Pdr5 demonstrating that Pdr5 can transport K⁺ and Cl⁻ ions at high rates across the membrane. Strikingly, in the presence of Mg²⁺-ATP and substrates, Pdr5 generates a proton motive force across the membrane by acting as a proton/drug symporter. It is important to emphasize that similar observations have not been shown for any MDR efflux pump previously. We conclude from these findings that the mechanism of MDR conferred by Pdr5 and most probably other transporters is more complex than the sole extrusion of cytotoxic compounds and involves secondary coupled mechanisms of action.

Introduction

The phenomenon of multidrug resistance (MDR) exists in all cells ranging from prokaryotes to higher eukaryotes and describes the ability to abolish the effectiveness of a wide range of functionally and structurally different cytotoxic compounds. One of the major mechanisms that confers MDR is the overexpression of certain efflux pumps that expel these toxic compounds into the extracellular space (Gottesman et al., 2002). Two classes of transporters are involved: ATP binding cassette (ABC) transporters that utilize the binding and hydrolysis of ATP to transport their substrates as well as secondary transporters of the major facilitator superfamily (MFS), the RND and the MATE family that use an electrochemical gradient across the membrane in order to export the compounds (Kumar et al., 2016; Quistgaard et al., 2016; Sa-Correia et al., 2009; Schmitt and Tampe, 2002). Although studied for decades, the molecular mechanisms underlying the resistance conferred by these membrane proteins often remain elusive (Chang, 2003).

In general, membrane transporters and channels reveal a high specificity towards their substrates. Therefore, the large variety of substrates of individual MDR transporters raises the question whether these MDR transporters directly transport such a broad variety of structurally unrelated compounds or whether their physiological role within the cellular membrane leads to an indirect protection against the cytotoxic compounds (Roepe, 2000; Sa-Correia et al., 2009). For the well-characterized human MDR ABC transporter P-gp (MDR1 or ABCB1), it was shown that cells expressing this protein have an altered cytosolic pH and membrane potential compared to cells not harboring MDR1. Therefore, two models were proposed: the ‘drug pumping’ and the ‘altered partitioning’ model (Ambudkar et al., 1999; Hoffman and Roepe, 1997; Roepe, 2000). While the first model claims the direct extrusion of drugs, the latter refers to a decreased uptake of compounds due to a changed cytosolic pH and membrane potential. Similar to the ABC transporter MDR1, several studies reported alterations of the membrane environment through altered ion gradients by MDR efflux pumps. For the bacterial multidrug transporter LmrA from *Lactococcus lactis*, electrophysiological measurements indicated that the efflux of ethidium is coupled to an ion translocation in an antiport fashion (Agboh et al., 2018). Earlier, *in vivo* studies demonstrated that Cdr1, a major MDR ABC transporter from pathogenic *Candida albicans* and a close homologue to *S. cerevisiae* Pdr5, alters the extracellular pH (Milewski et al., 2001).

Pdr5 is a long-studied member of the MDR ABC transporter and the major player of the pleiotropic drug resistance (PDR) network of *S. cerevisiae* (Balzi et al., 1994; Ernst et al., 2008; Golin and Ambudkar, 2015; Kolaczowski et al., 1996; Rogers et al., 2001). Like other MDR ABC efflux pumps, *in vivo* and *in vitro* studies with plasma membrane vesicles reported that Pdr5 confers resistance towards a wide variety of hydrophobic compounds that are structurally unrelated, as well as metabolites (Kolaczowski et al., 1996; Mamnun et al., 2004; Rogers et al., 2001). Only recently it was possible to isolate this transporter and purify it in an active state and thereby paving the way to study the underlying molecular mechanisms of drug efflux *in vitro* (Wagner et al., 2019).

Here, we used purified Pdr5 reconstituted into planar lipid bilayers and provide *in vitro* data for this MDR ABC transporter demonstrating that Pdr5 can act as an ATP and substrate dependent drug/H⁺ symporter. Not only do we demonstrate that for Pdr5 both, the ‘drug efflux’ and the ‘altered partitioning’ model apply and are actually interconnected, but we also provide important insights into the molecular mechanisms of MDR ABC transporters. Moreover, we demonstrate the power and the informative value of single molecule electrophysiological measurements for the *in vitro* investigation of the molecular mechanisms of ABC transporters.

Results

Pdr5 shows voltage dependent ion channel activity

In order to verify whether wild-type Pdr5 (Pdr5_{WT}) can facilitate voltage dependent ionic currents of small cations or anions across a membrane, purified Pdr5 was reconstituted into planar lipid bilayer (DOPC/DOPE lipids) and voltage dependent currents across the bilayer were monitored.

The slope conductance of the control (“empty”) bilayer was $G_{sl} = 2 \text{ pS}$ (Fig. 1A) when a voltage ramp from $V_h = -150 \text{ mV}$ to $+150 \text{ mV}$ was applied. After addition of detergent solubilized Pdr5_{WT} to the cis-compartment of the bilayer (symmetrical cis/trans 250 mM KCl, 10 mM HEPES pH 7.0 buffer) and applying a voltage ramp starting at a holding potential of $V_h = 0 \text{ mV}$ small ion currents were observed (Fig. 1B, $G_{sl} = 140 \text{ pS}$). Starting the same voltage ramp at a holding potential of $V_h = +100 \text{ mV}$, a significant increase of the Pdr5_{WT} mediated membrane current was observed ($G_{sl} = 5.7 \text{ nS}$, Fig. 1C). This demonstrates that Pdr5_{WT} spontaneously incorporates into the planar bilayer and conducts voltage dependent K^+ and Cl^- ions at high rates across the membrane. Moreover, as demonstrated by the rectifying current-voltage relation Pdr5 incorporation into the membrane occurred unidirectional with the nucleotide binding site at the cis compartment. With prolonged exposure of Pdr5_{WT} to higher positive stationary holding potentials $V_h \geq +100 \text{ mV}$ appear to induce an ion conducting conformation of membrane integrated Pdr5_{WT}. Thus, Pdr5_{WT} when reconstituted into a planar bilayer displays voltage activated ion-channel activity. This ion conducting state of Pdr5_{WT} appears to be transiently induced by high positive membrane potentials ($V_h \geq 100 \text{ mV}$).

Pdr5 possesses three main conductance states

The observation of voltage activation was confirmed by results shown in Fig. 2, displaying currents induced by voltage gates from $V_h = \pm 80 \text{ mV}$ to $V_h = \pm 140 \text{ mV}$. Voltage gates of 10 seconds duration at the indicated V_h were used to gain information on the single channel conductance of Pdr5_{WT}. Fig. 2A shows a current recording from a bilayer containing a single active Pdr5_{WT} channel where above $V_h = +100 \text{ mV}$ flickering current gating events from closed to open states were observed.

A closer inspection of the current recordings at $V_h = \pm 140 \text{ mV}$ (Fig. 2B-G) demonstrates that channel gating occurred with different open channel amplitudes. Due to the very short durations of the channel opening at positive V_m and the small open current amplitudes only a log-plot of the all point current histogram allows detection of the different open channel amplitudes (Fig. 2D). Nevertheless, in the all point current histogram individual open channel current peak are hardly resolved, except the peak of the bilayer leak current (Fig. 2D).

However, the histogram in combination with a mean variance analysis of the current recording at $V_h = 140 \text{ mV}$ was helpful in resolving the amplitudes of the channel openings (Patlak, 1993). The mean variance plot (Fig. 2E) displays the current transitions of each channel-gating event in Fig. 2A ($V_h = \pm 140 \text{ mV}$). Furthermore, by combining the current and mean-variance histograms (see Fig. S3 for details) we were able to disclose that the voltage activated open Pdr5_{WT} channel current displayed three different main open channel amplitudes, corresponding to the mean current values in the mean variance histogram. From the analysis of current recordings at higher membrane potentials ($V_h = \pm 120 \text{ mV}, V_h = \pm 130 \text{ mV}, V_h = \pm 140 \text{ mV}$ (see Fig. 2A)) the following main mean conductance states of Pdr5_{WT} were obtained: $G_1 \cong 25 \pm 3.6 \text{ pS}$, $G_2 \cong 134 \pm 16 \text{ pS}$, $G_3 \cong 250 \pm 78 \text{ pS}$. From these results the question arises whether these different conductance states belong to a single Pdr5_{WT} transporter or whether the particular channel open states reveal inhomogeneous open channel amplitudes with simultaneous channel opening or closing. Closer inspection of the time-course of gating events (see Fig. 2B, C and Fig. S3) clearly demonstrates that one single Pdr5_{WT} transporter displayed multiple open channel states (for more details see SI).

Thus, the mean variance analysis demonstrates that voltage activated Pdr5_{WT} displays at least three distinct main subconductance states. Remarkably, the mean open state G_2 was nearly exclusively occupied at membrane potentials above 100 mV (see SI for more details). Considering the most frequent conductance state of $G_2 \cong 134 \text{ pS}$ at 250 mM ionic strength and using the simplified model of a cylindrical restriction channel zone (Hille, 1968; Smart et al., 1997) with a length of 1 nm, we can calculate the pore diameter of the restriction zone to be $d_{\text{restriction}} \cong 6.4 \text{ \AA}$.

Ion selectivity of Pdr5

At higher positive membrane potentials, Pdr5_{WT} mediated current increased exponentially indicating that either rectification occurred or opening of additional Pdr5_{WT} channels took place (Fig. S1A). Additionally, in asymmetric buffer conditions (590 mM KCl (cis)/250 mM KCl (trans)) we observed a reversal potential of $V_{rev} = 9$ mV (Fig. S1B). Using the commonly applied macroscopic GHK approach (Goldman, 1943) (see SI for more details) this value corresponds to a slight cation over anion selectivity of $P_{K^+} : P_{Cl^-} = 2.5:1$ of reconstituted Pdr5_{WT}.

Modulation of Pdr5 mediated ion conductance by its substrates

We also tested the effect of Pdr5 substrates such as rhodamine 6G (R6G), ketoconazole (KA) and cycloheximide (CHX) on voltage-induced ion channel activity of Pdr5_{WT}. Fig. 3A shows a voltage ramp from a bilayer containing a single active copy of reconstituted and activated Pdr5_{WT}. The activation was performed by exposing Pdr5_{WT} containing bilayer to $V_h = +150$ mV for 30s followed by a voltage ramp from $V_h = -150$ mV to $V_h = +150$ mV as shown in the right part of Fig. 3A. As obvious, ion conducting activity with channel gating was observed (see enlarged panel for details). The linear slope conductance (indicated by the black lines in Fig. 3A) reveal values of $G_1 = 14 \pm 0.14$ pS and $G_2 = 129 \pm 0.2$ pS. These values are very close to the mean values of the three Pdr5_{WT} conductance states deduced from channel gating (see above). Therefore, the current-voltage ramp can be attributed to a single activated Pdr5_{WT} unit. After addition of 2 mM Mg²⁺-ATP (cis/trans) and 330 nM R6G to the cis compartment of the same bilayer, no further voltage dependent channel gating could be observed. The current was drastically reduced while the shape of the current-voltage ramp changed to an exponential form no matter whether the command voltage was run from $+V_h$ to $-V_h$ or vice versa (Fig. 3A and B). In addition, the zero current potential (V_{rev}) changed completely and unexpectedly to $V_{rev} = -46$ mV. This effect was reproducibly observed in seven different bilayer experiments with $V_{rev} = -43.8 \pm 4.8$ mV, $n = 7$ no matter whether the bilayer contained single activated or multiple activated copies of Pdr5_{WT}. In this context, it is particularly important to mention that this R6G-induced shift of V_{rev} was strictly dependent on the presence of Mg²⁺-ATP in the cis compartment. Addition of AMP (cis) ($n = 3$) did not show this effect.

In order to explain the observed shift of V_{rev} we can use the macroscopic GHK approach to calculate the expected reversal potentials from the GHK current equation based on the ion₆₇

composition of the bilayer cis and trans compartments (the detailed calculation can be found in SI). The ion concentrations in the cis/trans compartments were held completely symmetrical (250 mM KCl, 10 mM HEPES pH 7.0, 2 mM Mg^{2+} -ATP) before the addition of 330 nM R6G to the cis compartment and corresponding to this we observed $V_{rev} = 0 \pm 1.5 \text{ mV}$, $n = 7$. The calculation of the reversal potential by the GHK current equations (see SI for details) at the given ionic concentrations in cis/trans before and after addition of charged R6G ($n=+1$) clearly shows that this ion concentration across the Pdr5_{WT} containing membrane can by no means produce a current voltage-relation with a zero current crossing at $V_{rev} = -43.8 \pm 4.8 \text{ mV}$ (see Fig. S2). Therefore, we can conclude that R6G induced a Pdr5_{WT} mediated active ion transport of one of the anions or cations present in solution. With symmetrical cis/trans 250 mM KCl either Cl^- ion have to be transported from trans to cis to final concentrations of $c_{trans}^{Cl^-} = 75 \text{ mM}$ and $c_{cis}^{Cl^-} = 425 \text{ mM}$, or in the case of K^+ the ions would be transported from cis to trans to the final concentrations of $c_{cis}^{K^+} = 75 \text{ mM}$ and $c_{trans}^{K^+} = 425 \text{ mM}$ (for details see SI). This massive ion pumping of one of the two ion species would in both cases reduce and increase the bulk conductance in either bilayer compartments, which in fact was not observed. Consequently, H^+ – ions are the remaining candidates to build up an ion gradient across the Pdr5_{WT} containing bilayer yielding a zero current potential of $V_{rev} = -47.2 \pm 5.4 \text{ mV}$ (mean value of $n=12$). Introducing H^+ as an additional ion in the GHK current equations (see Fig. S6 for details), we finally conclude that starting with pH 7 symmetrically H^+ ions are transported from cis to trans to a final concentrations of $c_{cis}^{H^+} = 7.94 \text{ nM}$ (pH 8.1) and $c_{trans}^{H^+} = 0.9 \mu\text{M}$ (pH 6.03).

As it is obvious from the calculated current voltage relation (Fig. S2), R6G addition to the cis compartment in Pdr5_{WT} containing bilayer induced apparently active (active means: H^+ permeability $P_{H^+} \rightarrow \infty$) H^+ transport from the cis to the trans compartment. Using a high resolution setup we discovered during the course of our experiments that even without voltage activation incorporation of Pdr5_{WT} into the bilayer induced a small but characteristic increase of bilayer currents when applying voltage ramps (Fig. 4A, B). We therefore performed the same experiment as described above, however without activating Pdr5_{WT} higher conductance channel activity by application of a membrane potential of $V_m = +150 \text{ mV}$ for 30s. Fig. 4 shows a series of experiments on a single identical bilayer with the current-voltage ramp of a control bilayer and Fig. 4B the same bilayer after addition of Pdr5_{WT} to the cis compartment. While the control bilayer displays a linear current voltage relation with a slope conductance of $G_{sl} = 2.0 \text{ pS}$, the current after addition of Pdr5_{WT} displayed a rectifying shape and increased significantly.

Addition of Mg^{2+} -ATP increased the current slightly further (Fig. 4C), while addition of R6G changed the reversal potential to $V_{rev} = -58 \text{ mV}$, which matches a ΔpH shift of ~ 2.3 units (cis: pH 8.1 vs trans: pH 5.85) (see above). Again, this effect was only observed when Mg^{2+} -ATP and R6G were present. Therefore, also non-activated Pdr5_{WT} in the presence of Mg^{2+} -ATP and R6G seemingly pumps H^+ actively from cis to the trans compartment. When the bilayer leak conductance of the control is subtracted from Pdr5_{WT} mediated currents and Pdr5_{WT} currents in the presence of Mg^{2+} -ATP and R6G the situation becomes even more prominent (see Table S1 and Fig. S5).

At negative membrane potentials flow of small cation currents only from trans to cis are observed with $V_{rev} = 0 \text{ mV}$, while in the presence of Mg^{2+} -ATP/R6G an additional cationic current from cis to trans with zero current crossing of $V_{rev} = -57 \text{ mV}$ is observed.

In similar experiments we tested whether the non-charged KA, another well-known substrate of Pdr5_{WT}, also modulates the activity of reconstituted Pdr5_{WT} in planar bilayer. In a series of four different experiments, we observed a Mg^{2+} -ATP/KA induced shift of the zero current potential of $V_{rev} = -64 \pm 8 \text{ mV}$ ($n = 4$) (see Fig. S4).

Based on these results, we conclude analogously that also KA in the presence of Mg^{2+} -ATP induces active Pdr5_{WT} mediated H^+ transport from the cis to the trans compartment. Interestingly, with CHX as a potential substrate, we did in contrast to R6G and KA, not observe a significant modulation of Pdr5_{WT}-mediated currents.

Proton gradient is ATPase dependent

In order to verify the significance of the observed modulation of Pdr5_{WT} activity by its substrates, we performed the same set of experiments as describe above except that we used the ATPase deficient E1036Q mutant (Pdr5_{EQ}) instead of the Pdr5_{WT}.

Fig. 5A and B demonstrate that Pdr5_{EQ} also incorporates into the planar bilayer membrane and can form a voltage dependent ion channel. However, Pdr5_{EQ} mediated currents were observed already at membrane potentials above 20 mV. In more than 90% of the attempts in voltage ramps rather large currents were observed (Fig. 5C) and correspondingly also in voltage gates (Fig. 5D). These results indicate that a high number of ion conducting Pdr5_{EQ} have been incorporated into the bilayer. It is worth noting that in the case of Pdr5_{EQ} channel gating was rarely observed and the channels remained almost exclusively in the open states. The conductance values of the

Pdr5_{EQ} was in the same range as observed for Pdr5_{WT} with $G_2 \cong 121.7 \pm 19 \text{ pS}$, $G_3 \cong 365 \pm 57 \text{ pS}$ ($n \geq 4$). This also holds for the ion selectivity of the Pdr5_{EQ} mutant determined to be $P_{K^+}/P_{Cl^-} = 3.5:1$ (see SI for details). We also tested whether channel currents of Pdr5_{EQ} could be modulated by the substrates R6G and KA in a similar set of experiments as described above for Pdr5_{WT}. We observed in none of the 15 attempts with both substrates any modulation of Pdr5_{EQ} mediated currents showing that ATPase activity and transport of the substrate is an absolute requirement for substrate induced H⁺ symport currents.

Beauvericin locks Pdr5 in an open state

Beauvericin (BEA) is known as a potent inhibitor of Pdr5 (Shekhar-Guturja et al., 2016) and in addition it can mediate ion transport across the membrane most likely in a carrier like mode (Benz, 1978). We therefore first investigated membrane currents after addition of 3.3 μM and 9.9 μM BEA on the cis side (Fig. 6B and C). The conductance values of these measurements are listed in Table S2. Next we addressed the question whether BEA might suppress the substrate induced H⁺ symport of Pdr5_{WT}. Fig. 6 shows a representative series of experiments with an identical bilayer. Graphs 6G and E demonstrate that Pdr5_{WT} was incorporated in the membrane in the non-activated form and after addition of R6G to the cis compartment a shift of $V_{rev} = -51 \text{ mV}$ is observed. Remarkably, after addition of 1.7 μM BEA the overall current increased drastically and the shift of the reversal potential disappeared completely (Fig. 6D). These recordings show clearly that BEA can act as a carrier, but most importantly act as a Pdr5 inhibitor that locks Pdr5 in an open conformation. The conductance values of the different measurements in Fig. 6 are listed in Table S3.

Discussion

MDR ABC transporters have a broad and diverse range of substrates that are highly diverse in terms of structure and physico-chemical properties. There has been a long debate on how these membrane proteins confer resistance, i.e. how the transporters reduce the drug concentration within a cell. There are numerous studies that support the ‘drug pump model’, in which ABC transporters actively expel the compounds out of the cell (Ambudkar et al., 1999; Sharom, 1997). On the other side, studies including human MDR1 and Cdr1 from the pathogenic fungi *C. albicans*, as well as the bacterial MDR ABC transporter LmrA have demonstrated that these proteins effect intracellular pH and are able to conduct ions across the membrane, giving evidence towards the ‘altered partitioning model’ (Agboh et al., 2018; Hoffman and Roepe, 1997; Milewski et al., 2001; Roepe, 2000). After all, the question arises whether all of the known substrates of MDR transporters are actually real substrates in a sense that they are indeed actively transported out of the cell against the concentration gradient, or if they mediate a decreased influx of the drugs by altering the membrane properties, or whether both mechanisms are actually used by MDR ABC transporters.

Although studies performed on MsbA and LmrA indicate that ion gradients benefit the activity of the respective ABC transporter (Agboh et al., 2018; Singh et al., 2016), there are to our knowledge up to now no in-depth electrophysiological characterizations of MDR ABC transporters *in vitro*. We were able to work with the functionally purified, reconstituted Pdr5 and a well-studied ATPase deficient mutant as a control as well as known substrates of Pdr5 (R6G, KA and CHX (Ernst et al., 2008; Kolaczowski et al., 1996; Rogers et al., 2001; Wagner et al., 2019)) and the potent Pdr5-specific inhibitor BEA that enabled an extensive electrophysiological *in vitro* characterization.

An interesting feature of the ABC transporter Pdr5 is that it can be voltage activated and allows high current fluxes across the membrane even in the absence of Mg^{2+} -ATP or substrates and conducts K^+ and Cl^- ions with a slight cation selectivity. Cation selectivity is not surprising at all as all known charged substrates of Pdr5, like for most MDR ABC transporters, are cationic (Ambudkar et al., 1999; Kolaczowski et al., 1996; Rogers et al., 2001). We were also able to show that Pdr5 switches between at least three major conformations as apparent from the three distinct conductance states with mean subconductance values of $G_1 \cong 20 \text{ pS}$, $G_2 \cong 134 \text{ pS}$, $G_3 \cong 250 \text{ pS}$;₁

Moreover, the rather broad distribution of open channel states indicates that Pdr5 has a rather flexible membrane part responsible for the membrane translocation of its substrates. Additional experiments with the Pdr5 inhibitor BEA demonstrated that it locks Pdr5 in an open conformation as indicated by the measured high conductance.

Most importantly, we were able to demonstrate in our setup that Pdr5 in the presence of Mg^{2+} -ATP and substrate can generate a membrane potential that, under the given conditions, can only be a result of the generation of a proton gradient (ΔpH) across the membrane. We therefore conclude that the MDR ABC transporter Pdr5 is an ATP-dependent drug/ H^+ symporter that actively translocates substrates, while it simultaneously influences the trans-membrane proton gradient and thereby the membrane potential. It was speculated before from *in vivo* experiments that MDR1 as well as the Pdr5 homologue Cdr1 may transport protons from the intra- to the extracellular space and thereby alkalize the cytoplasm (Hoffman and Roepe, 1997; Milewski et al., 2001). However, the complexity of the cell environment of *in vivo* experiments did not allow to unambiguously pinpoint observations to a single protein level nor for the experimenter to control all relevant critical cellular parameters. For Cdr1 it was hypothesized that the ABC transporter creates an additional proton motive force when it was expressed in *S. cerevisiae*. It is important to note that in our experiments, the proton gradient does only occur in an Mg^{2+} -ATP and strictly substrate dependent manner. This means that in the absence of a substrate, Pdr5 does not participate in pH homeostasis of the membrane even if ATPase activity is present.

Interestingly, the H^+ gradient occurs independently of the charge of the substrate. Both, the cationic R6G as well as the neutral KA are transported in a drug/ H^+ symporter fashion. Our electrophysiological measurements with a charged and neutral substrate also allow to prove that Pdr5 actively transports the substrate across the bilayer and does not solely follow the 'altered partitioning model' by pumping ions. The zero current potentials of $V_{rev} = -64 \pm 8$ mV for KA and $V_{rev} = -47.2 \pm 5.3$ mV for R6G clearly show that R6G is transported from cis to trans since the putative $V_{rev} = +13.6$ mV (see Fig. S2) of the $R6G^+$ -ions contributes to the overall V_{rev} , which is reduced in comparison with the non-charged substrate KA (Fig. S6A, B). This conclusion assumes a nearly identical stoichiometry of drug/ H^+ translocation for both substrates. Another tested substrate, CHX, however, did not induce any proton gradient or change in conductance. CHX does not, opposed to the majority of known Pdr5 substrates, influence the ATPase activity of Pdr5 and is hydrophilic (Ernst et al., 2008; Wagner et al., 2019). One can speculate that either a different transport mechanism for this hydrophilic substrate exists, or that CHX is not a substrate at all and

the observed resistance conferred by Pdr5 is due to intracellular alkalization caused by Pdr5 mediated proton pumping as CHX undergoes degradation at basic pH (Garrett and Notari, 1965). Further evidence that the observed proton gradient is strictly Mg^{2+} -ATP and substrate dependent is given by the fact that the ATPase deficient E1036Q mutant (Pdr5_{EQ}) was not affected in its ion conducting properties when tested under the same conditions as the wild type protein

Since we used R6G, which is a cationic substrate as well as the uncharged KA, we conclude that the measured gradient cannot be an artifact of the efflux of a protonated or cationic substrate and instead is a real H^+ gradient created by Pdr5 in an Mg^{2+} -ATP- and substrate-dependent manner. The acidification of the trans compartment of our setup reflects an acidic external pH in an *in vivo* setting, which compares well with the results that were obtained previously for Cdr1 and MDR1 *in vivo* (Hoffman and Roepe, 1997; Milewski et al., 2001).

The phenomenon of drug extrusion in a proton-dependent manner is known for MFS proteins. However, all so far characterized MDR MFS transporter in yeast are drug/ H^+ antiporters (Sa-Correia et al., 2009; Saier and Paulsen, 2001). With the exception of MsbA that was shown to operate in a drug/proton antiport fashion (Singh et al., 2016), ABC transporters are not known to couple substrate with proton transport. Pdr5 is therefore the first member of a new class of MDR transporter, an ATP-dependent drug/proton symporter. Since Pdr5 belongs to the large family of MDR as well as to the family of asymmetric ABC transporters that share common motifs and characteristics, our here presented findings are presumably of significant relevance for other efflux pumps. Moreover, the here described electrophysiological approach can provide powerful tools to get insight into the molecular mechanisms that underlie substrate transport as well as binding of potential inhibitors and might help to further characterize other ABC transporters *in vitro*.

Materials and Methods

Pdr5 Expression and Purification

Pdr5 was expressed and purified as described in (Wagner et al., 2019). Briefly, *S. cerevisiae* YRE1001 (Ernst et al., 2008) cells were grown at 30 °C to a final OD₆₀₀ of 3.5. Cells of 4 L YPD media were harvested and disrupted using glass beads. Total membranes were collected adjusted to 10 mg/ml total protein concentration with buffer A (50 mM Tris-HCl, pH 7.8, 50 mM NaCl, 10% (w/v) glycerol) and solubilized for 1 h 1% (w/v) trans-PCC- α -M under gentle stirring at 4 °C. Immobilized metal ion affinity chromatography of the His-tagged Pdr5 was performed with a Zn²⁺ loaded 1 ml HiTrap Chelating column (GE Healthcare) and elution was carried with a step gradient using low and high histidine buffers (50 mM Tris-HCl pH 7.8, 500 mM NaCl, 10 % (w/v) glycerol, 0.003% (w/v) trans-PCC- α -M and 2.5 mM or 100 mM l-histidine). The elution fractions were collected, pooled and concentrated in a ultrafiltration unit (100 kDa MWCO). The size exclusion chromatography was performed on a Superdex 200 10/300 GL column (GE Healthcare) with buffer A containing 0.003 % (w/v) trans-PCC- α -M. All chromatography steps were performed on the Äkta protein purification systems (GE Healthcare).

Single Channel Recordings from Planar Lipid Bilayers and Data Analysis

Planar lipid bilayer measurements using the Compact bilayer platform (Ionovation GmbH) were performed as described in detail previously (Bartsch et al., 2013). In brief: if not explicitly stated otherwise, symmetric conditions (250 mM KCl, 10 mM HEPES, pH 7.0) were used in cis and trans compartments. The denomination cis and trans corresponds to the half-chambers of the bilayer unit. Reported membrane potentials are always referred to the trans compartment. Bilayer fabrication was performed on PTFE film at a 100 μ m preapertured (1 % hexadecane in n-hexane) aperture with a Phosphatidylcholine (18:1) (PC) / Phosphatidylethanolamine (18:1) (PE) (7:3 ratio) lipid mixture (both lipids were purchased from Avanti Polar Lipids) in n-pentane using the “thinning method” (Bartsch et al., 2013).

Ion channel currents were recorded using an EPC 10 USB amplifier (HEKA Elektronik GmbH) in combination with the Patchmaster data acquisition software (HEKA Elektronik GmbH). For data acquisition a sampling rate of 5kHz (voltage ramps) and 10 kHz (continuous recording) was used and the data were further analyzed using the Origin package (Origin Lab) and the MATLAB₇₄

(MathWorks) based Ion-channel-Master software developed in our laboratory (Bartsch et al., 2013). After addition of Pdr5 to the cis compartment, channel insertion into the bilayer occurred unidirectional as deduced from the rectification characteristics of the current-voltage ramps. Gating transition amplitudes were analyzed and subsequently filtered for dwell times exceeding five times the sampling interval to exclude incompletely resolved gating transitions from the analysis (McManus et al., 1987). When required and applicable, currents traces with amplitudes well below 10pA were filtered by a Savitzky-Golay filter (Gorry, 1990; Savitzky and Golay, 1964) to enhance the S/N ratio. Single channel analysis was performed essentially as described in detail (Harsman et al., 2011). In brief, we used the robust mean variance approach (Patlak, 1988, 1993) that allows rigorous unbiased analysis of single channel recordings. For this, we had developed a Matlab-based program that allows the automatic current-amplitude and channel state dwell time analysis of single channel recordings (Bartsch et al., 2013) (see also SI).

H2: Supplementary Materials

Fig. S1. Ion selectivity of the activated Pdr5_{WT} channel.

Fig. S2. Current-voltage relations calculated by the GHK current equations using experimental ionic conditions for 3 cases.

Fig. S3. Mean variance analysis.

Fig. S4. Effects of KA on Pdr5 mediated ion conductance.

Fig. S5. Current-voltage ramps of non-activated Pdr5_{WT} after bilayer leak subtraction.

Fig. S6. Comparison of experimental and calculated fits for the reversal potentials.

Table 1. Conductance parameter of non-activated Pdr5_{WT} (Fig. 4A-D) after subtraction of the bilayer leak conductance (see Fig. S3).

Table 2. BEA induced conductivity across an empty bilayer (Fig. 6A-C).

Table 3. Conductance parameters of Pdr5_{WT} in the presence of Mg²⁺-ATP, R6G and BEA

Data analysis S1. Determination of the conductance states of the voltage activated Pdr5 channel.

Data analysis S2. Determination of the substrate induced reversal potential shift with the reconstituted non activated Pdr5.

References

Agboh, K., Lau, C.H.F., Khoo, Y.S.K., Singh, H., Raturi, S., Nair, A.V., Howard, J., Chiapello, M., Feret, R., Deery, M.J., *et al.* (2018). Powering the ABC multidrug exporter LmrA: How nucleotides embrace the ion-motive force. *Science advances* 4.

Ambudkar, S.V., Dey, S., Hrycyna, C.A., Ramachandra, M., Pastan, I., and Gottesman, M.M. (1999). Biochemical, cellular, and pharmacological aspects of the multidrug transporter. *Annual review of pharmacology and toxicology* 39, 361-398.

Balzi, E., Wang, M., Leterme, S., Van Dyck, L., and Goffeau, A. (1994). PDR5, a novel yeast multidrug resistance conferring transporter controlled by the transcription regulator PDR1. *J Biol Chem* 269, 2206-2214.

Bartsch, P., Harsman, A., and Wagner, R. (2013). Single channel analysis of membrane proteins in artificial bilayer membranes. *Methods Mol Biol* 1033, 345-361.

Benz, R. (1978). Alkali ion transport through lipid bilayer membranes mediated by enniatin A and B and beauvericin. *J Membr Biol* 43, 367-394.

Chang, G. (2003). Multidrug resistance ABC transporters. *FEBS Lett* 555, 102-105.

Corry, B., Kuyucak, S., and Chung, S.-H. (2000). Tests of continuum theories as models of ion channels. II. Poisson–Nernst–Planck theory versus Brownian dynamics. *Biophys J* 78, 2364-2381.

Ernst, R., Kueppers, P., Klein, C.M., Schwarzmüller, T., Kuchler, K., and Schmitt, L. (2008). A mutation of the H-loop selectively affects rhodamine transport by the yeast multidrug ABC transporter Pdr5. *Proc Natl Acad Sci U S A* 105, 5069-5074.

Garrett, E.R., and Notari, R.E. (1965). Cycloheximide Transformations. II. Kinetics and Stability in a Pharmaceutically Useful Ph Range. *J Pharm Sci* 54, 209-215.

Goldman, E. (1943). Potentials impedance, and rectification in membranes. *J Gen Physiol* 27, 37-60.

Golin, J., and Ambudkar, S.V. (2015). The multidrug transporter Pdr5 on the 25th anniversary of its discovery: an important model for the study of asymmetric ABC transporters. *Biochem J* 467, 353-363.

Gorry, P.A. (1990). General least-squares smoothing and differentiation by the convolution (Savitzky-Golay) method. *Anal Chem* 62, 570-573.

Gottesman, M.M., Fojo, T., and Bates, S.E. (2002). Multidrug resistance in cancer: role of ATP-dependent transporters. *Nat Rev Cancer* 2, 48-58.

Harsman, A., Bartsch, P., Hemmis, B., Kruger, V., and Wagner, R. (2011). Exploring protein import pores of cellular organelles at the single molecule level using the planar lipid bilayer technique. *Eur J Cell Biol* 90, 721-730.

Hille, B. (1968). Pharmacological modifications of the sodium channels of frog nerve. *J Gen Physiol* 51, 199-219.

Hille, B. (2001). *Ionic Channels of Excitable Membranes, Vol 3* (Sunderland, Ma 01375: Sinauer Ass. Inc.).

Hodgkin, A.L., and Katz, B. (1949). The effect of sodium ions on the electrical activity of giant axon of the squid. *J Physiol* 108, 37-77.

Hoffman, M.M., and Roepe, P.D. (1997). Analysis of ion transport perturbations caused by hu MDR 1 protein overexpression. *Biochemistry* 36, 11153-11168.

Kolaczowski, M., van der Rest, M., Cybularz-Kolaczowska, A., Soumillion, J.P., Konings, W.N., and Goffeau, A. (1996). Anticancer drugs, ionophoric peptides, and steroids as substrates of the yeast multidrug transporter Pdr5p. *J Biol Chem* 271, 31543-31548.

Kumar, S., He, G., Kakarla, P., Shrestha, U., Kc, R., Ranaweera, I., Mark Willmon, T., R. Barr, S., J. Hernandez, A., and F. Varela, M. (2016). Bacterial Multidrug Efflux Pumps of the Major Facilitator Superfamily as Targets for Modulation. *Infect Disord Drug Targets* 16, 28-43.

Mamnun, Y.M., Schuller, C., and Kuchler, K. (2004). Expression regulation of the yeast PDR5 ATP-binding cassette (ABC) transporter suggests a role in cellular detoxification during the exponential growth phase. *FEBS Lett* 559, 111-117.

McManus, O.B., Blatz, A.L., and Magleby, K.L. (1987). Sampling, log binning, fitting, and plotting durations of open and shut intervals from single channels and the effects of noise. *Pflugers Archiv : European journal of physiology* 410, 530-553.

Milewski, S., Mignini, F., Prasad, R., and Borowski, E. (2001). Unusual susceptibility of a multidrug-resistant yeast strain to peptidic antifungals. *Antimicrob Agents Chemother* 45, 223-228.

Moy, G., Corry, B., Kuyucak, S., and Chung, S.-H. (2000). Tests of continuum theories as models of ion channels. I. Poisson– Boltzmann theory versus Brownian dynamics. *Biophys J* 78, 2349-2363.

Patlak, J.B. (1988). Sodium channel subconductance levels measured with a new variance-mean analysis. *J Gen Physiol* 92, 413-430.

Patlak, J.B. (1993). Measuring kinetics of complex single ion channel data using mean-variance histograms. *Biophys J* 65, 29-42.

Quistgaard, E.M., Low, C., Guettou, F., and Nordlund, P. (2016). Understanding transport by the major facilitator superfamily (MFS): structures pave the way. *Nature reviews Molecular cell biology* 17, 123-132.

Roepe, P. (2000). What is the Precise Role of Human MDR 1 Protein in Chemotherapeutic Drug Resistance. *Curr Pharm Des* 6, 241-260.

Rogers, B., Decottignies, A., Kolaczowski, M., Carvajal, E., Balzi, E., and Goffeau, A. (2001). The pleiotropic drug ABC transporters from *Saccharomyces cerevisiae*. *J Mol Microbiol Biotechnol* 3, 207-214.

Sa-Correia, I., dos Santos, S.C., Teixeira, M.C., Cabrito, T.R., and Mira, N.P. (2009). Drug:H⁺ antiporters in chemical stress response in yeast. *Trends in microbiology* 17, 22-31.

Saier, M.H., Jr., and Paulsen, I.T. (2001). Phylogeny of multidrug transporters. *Seminars in cell & developmental biology* 12, 205-213.

Savitzky, A., and Golay, M.J. (1964). Smoothing and differentiation of data by simplified least squares procedures. *Anal Chem* 36, 1627-1639.

Schmitt, L., and Tampe, R. (2002). Structure and mechanism of ABC transporters. *Curr Opin Struct Biol* 12, 754-760.

Sharom, F.J. (1997). The P-Glycoprotein Efflux Pump: How Does it Transport Drugs? *J Membr Biol* 160, 161-175.

Shekhar-Guturja, T., Gunaherath, G.M., Wijeratne, E.M., Lambert, J.P., Averette, A.F., Lee, S.C., Kim, T., Bahn, Y.S., Tripodi, F., Ammar, R., *et al.* (2016). Dual action antifungal small molecule modulates multidrug efflux and TOR signaling. *Nat Chem Biol* 12, 867-875.

Singh, H., Velamakanni, S., Deery, M.J., Howard, J., Wei, S.L., and van Veen, H.W. (2016). ATP-dependent substrate transport by the ABC transporter MsbA is proton-coupled. *Nat Commun* 7, 12387.

Smart, O.S., Breed, J., Smith, G.R., and Sansom, M.S. (1997). A novel method for structure-based prediction of ion channel conductance properties. *Biophysical journal* 72, 1109-1126.

Syganow, A., and von Kitzing, E. (1999). (In)validity of the constant field and constant currents assumptions in theories of ion transport. *Biophys J* 76, 768-781.

Wagner, M., Smits, S.H.J., and Schmitt, L. (2019). In vitro NTPase activity of highly purified Pdr5, a major yeast ABC multidrug transporter. *Scientific reports* 9, 7761.

Acknowledgments

General: We thank Prof. Oliver Ebenhöf (Heinrich Heine University Düsseldorf), Stefanie Raschka and all members of the Institute of Biochemistry for stimulating discussions.

We thank Prof. Mathias Winterhalter (Jacobs University Bremen) for support.

Author contributions: M.W., D.B. and R.W performed the experiments and evaluated the data.

All authors wrote the manuscript.

Competing interests: The authors declare no competing interests.

Figures and Tables

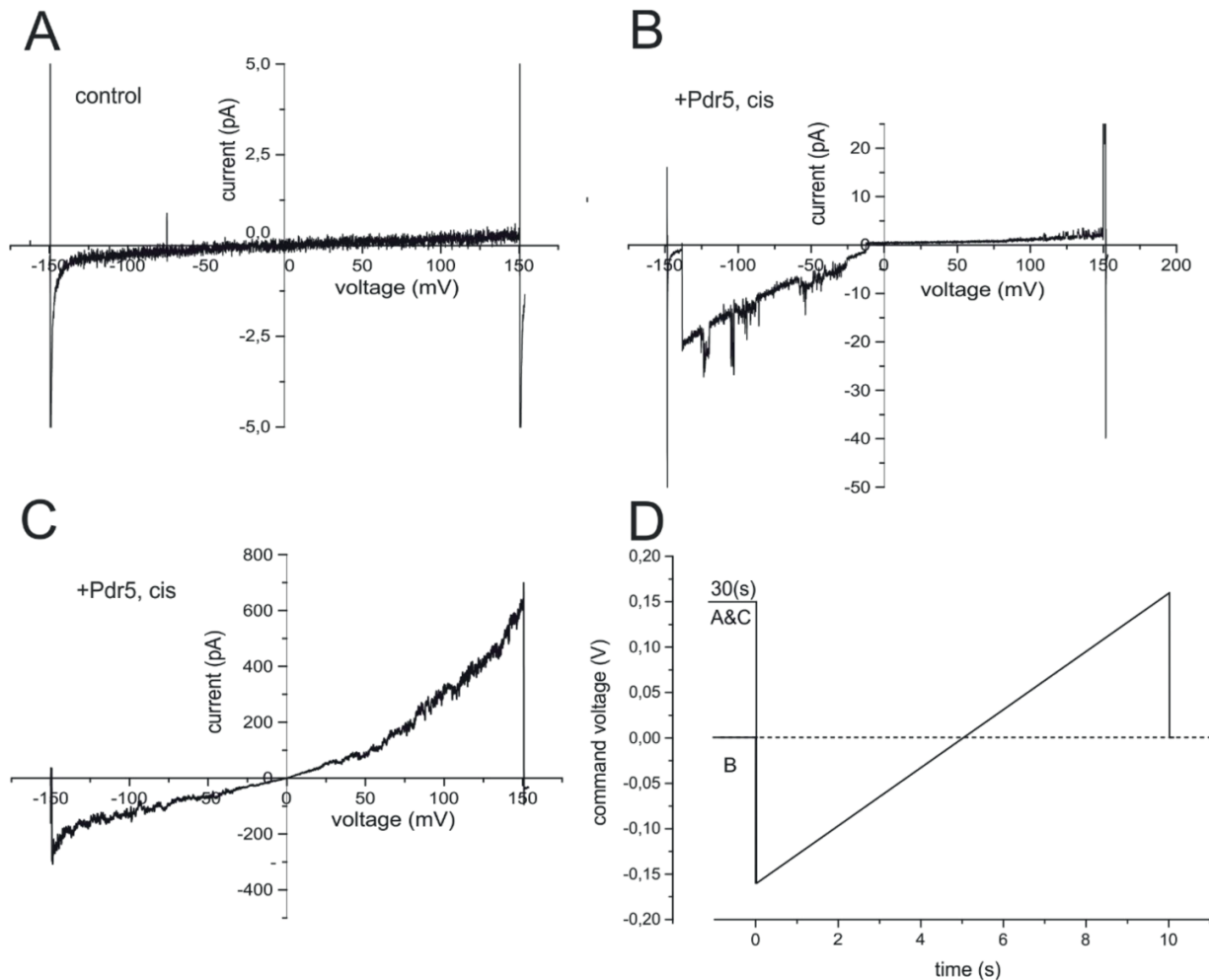


Fig. 1. Current recordings from a planar lipid bilayer. (A) Current-voltage ramp measurement with a DOPE/DOPC (7:3) bilayer in symmetrical cis/trans buffer conditions (control). (B) Current recording of the same bilayer as in (A), but after insertion of detergent purified Pdr5_{WT} from the cis compartment. (C) Voltage ramp of the same bilayer as in (B), but Pdr5_{WT} activated for 30s at +150 mV. (D) Time course and amplitude of the command voltage in the measurements in (A-C).

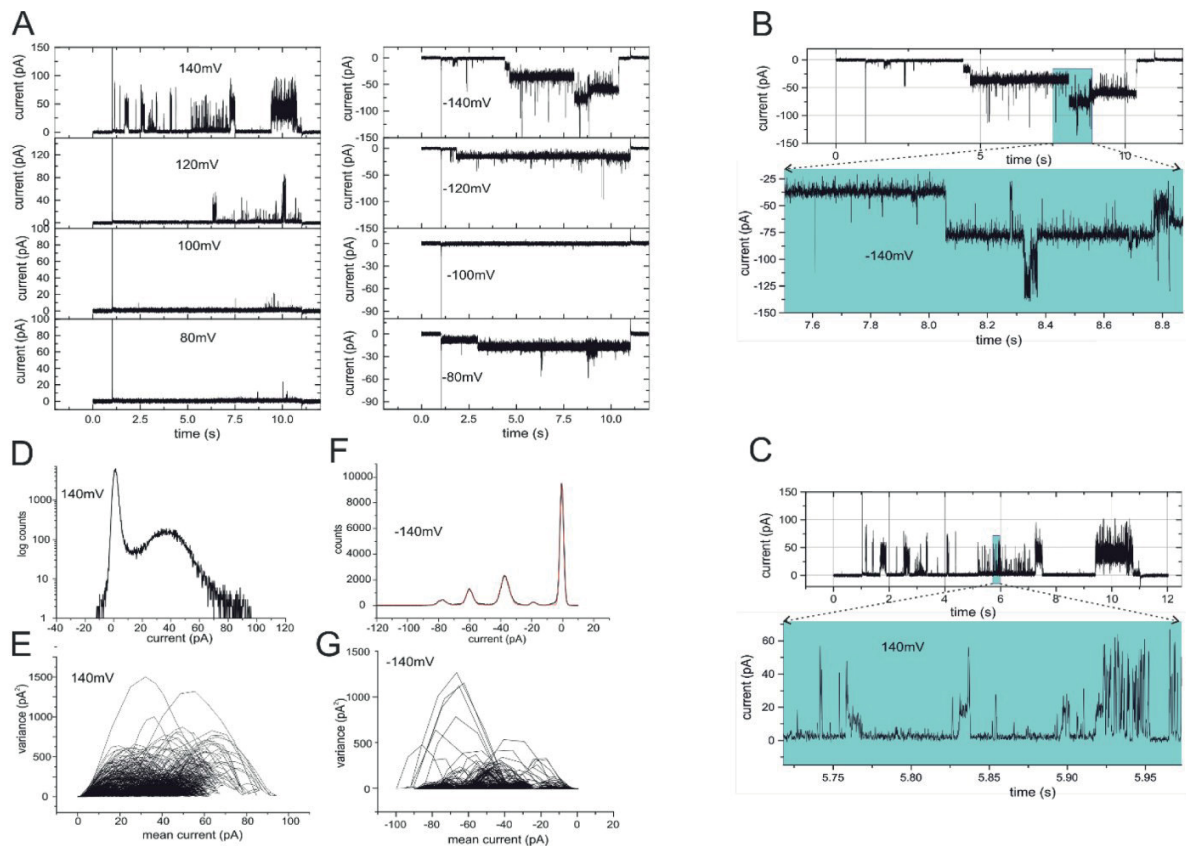


Fig. 2. Single channel analysis of Pdr5^{WT}. (A) Current recordings in response to voltage gates with the indicated amplitudes. (B) Extension plot of the current recording at V_h = -140 mV. (C) Extension plot of the current recording at V_h = +140 mV. (D) All point current histogram at V_h = +140 mV (log scale). (E) Mean variance plot of the current recording at V_h = +140 mV. (F) All point current histogram at V_h = -140 mV. (G) Mean variance plot of the current recording at V_h = -140 mV.

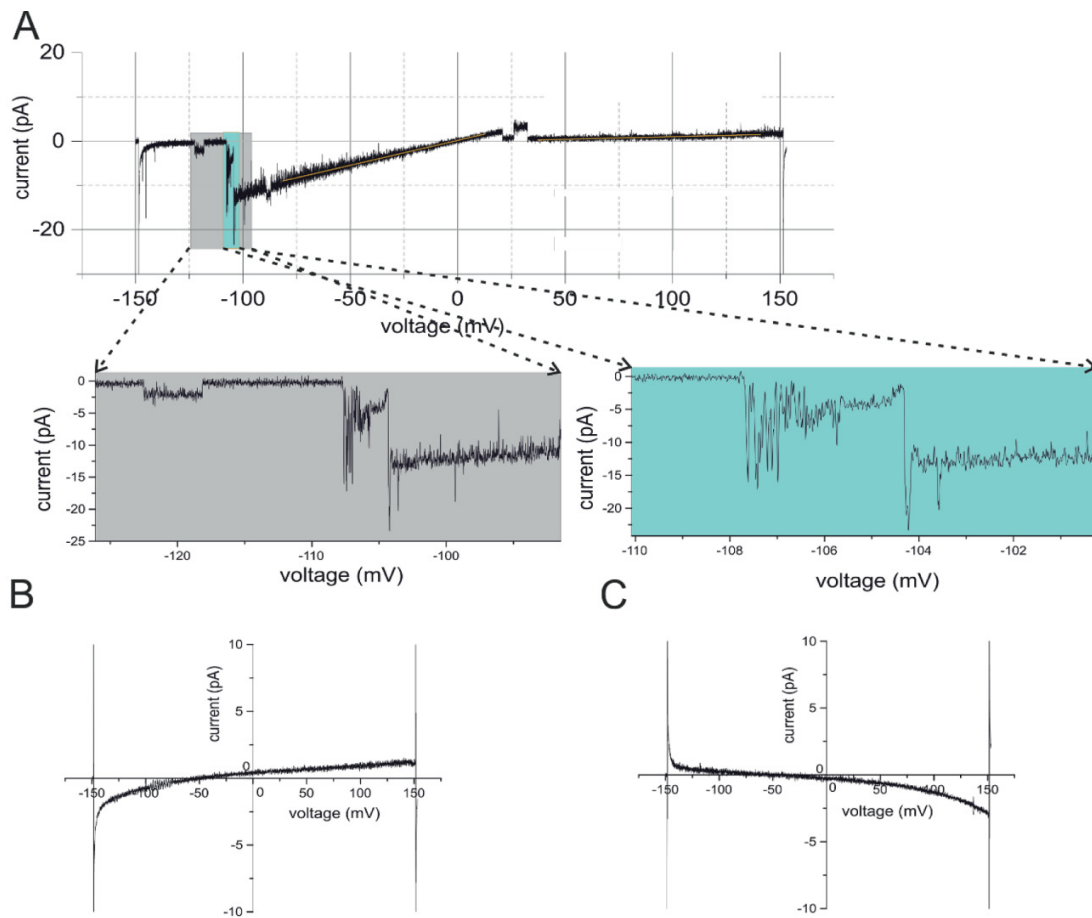


Fig. 3. Voltage ramps of voltage activated Pdr5_{WT} containing bilayer. Voltage ramp with 2 mM Mg²⁺-ATP cis/trans in the absence (A) or presence (B and C) of 330 nM rhodamine 6G (cis). (B) Voltage ramp starts at V_h = -150 mV. (C) Ramp starts at V_h = +150 mV.

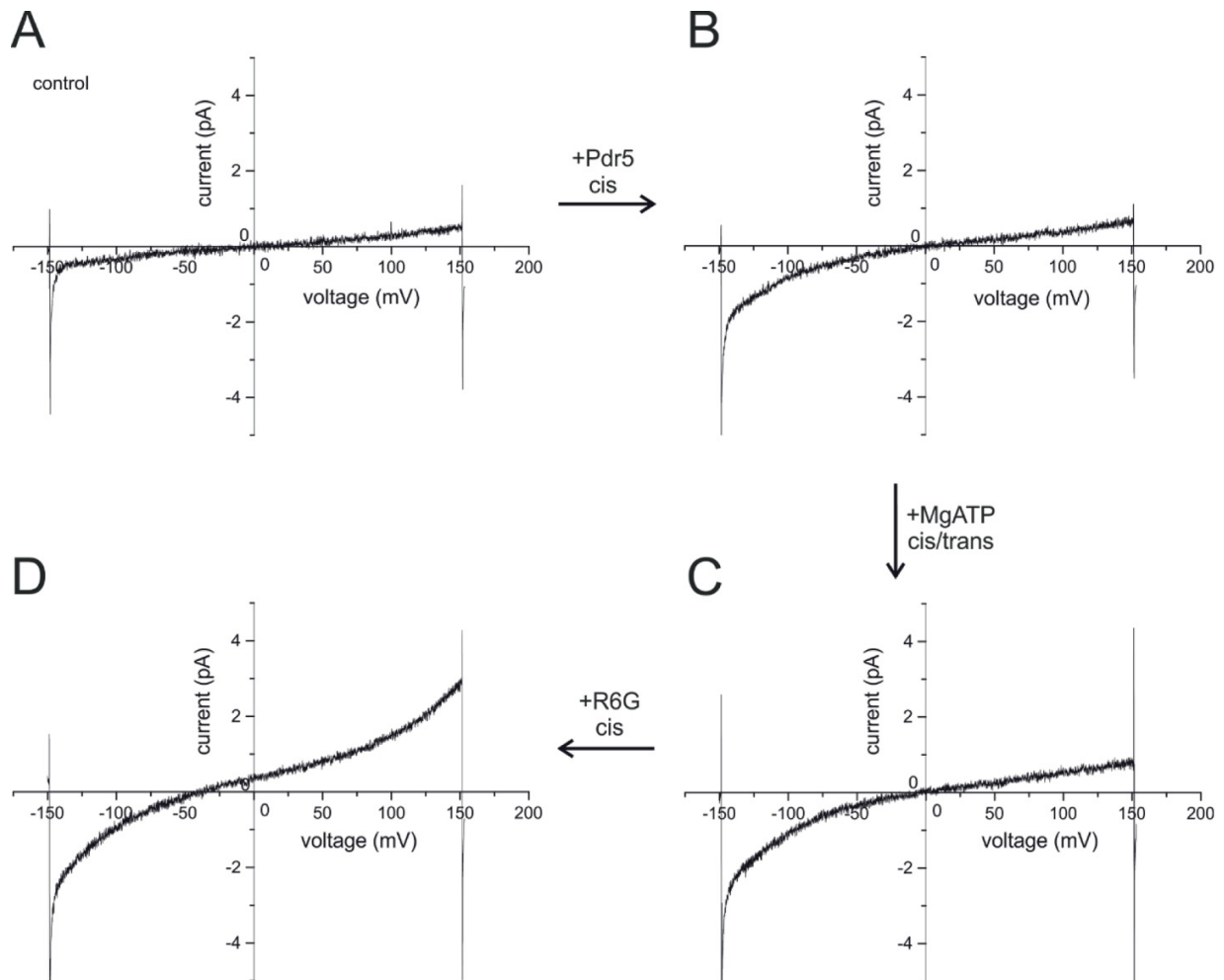


Fig. 4. R6G and ATP dependent shift of the reversal potential in a Pdr5_{WT} containing bilayer. (A) Control bilayer. (B) Non-activated Pdr5_{WT} containing bilayer in the absence of ATP and R6G. (C) The same bilayer as in B in the presence of Mg²⁺-ATP (cis/trans). (D) Addition of R6G to (C) induces reversal potential that is caused by a proton gradient. Current recordings (A) to (C) were performed sequentially on the same bilayer.

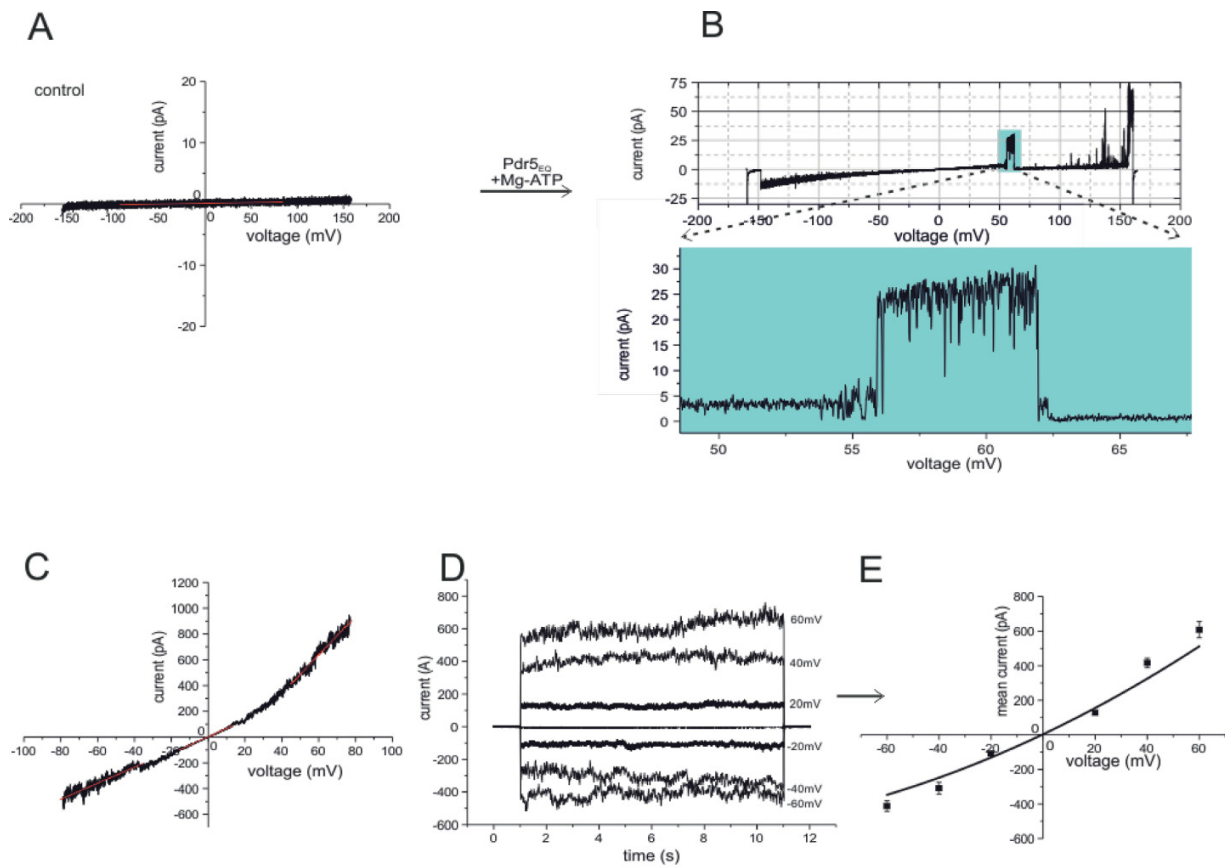


Fig. 5. Current-voltage measurements of the ATPase-deficient Pdr5_{EQ} mutant. (A) Control bilayer. **(B)** the same bilayer as in **(A)** after addition of Pdr5_{EQ} and Mg²⁺-ATP to the cis compartment. **(C)** current-voltage ramp from a bilayer containing multiple active copies of Pdr5_{EQ}. **(D)** current-voltage gates of the same bilayer as in **(C)**. **(E)** Current-voltage relation obtained from the mean currents in **(D)**.

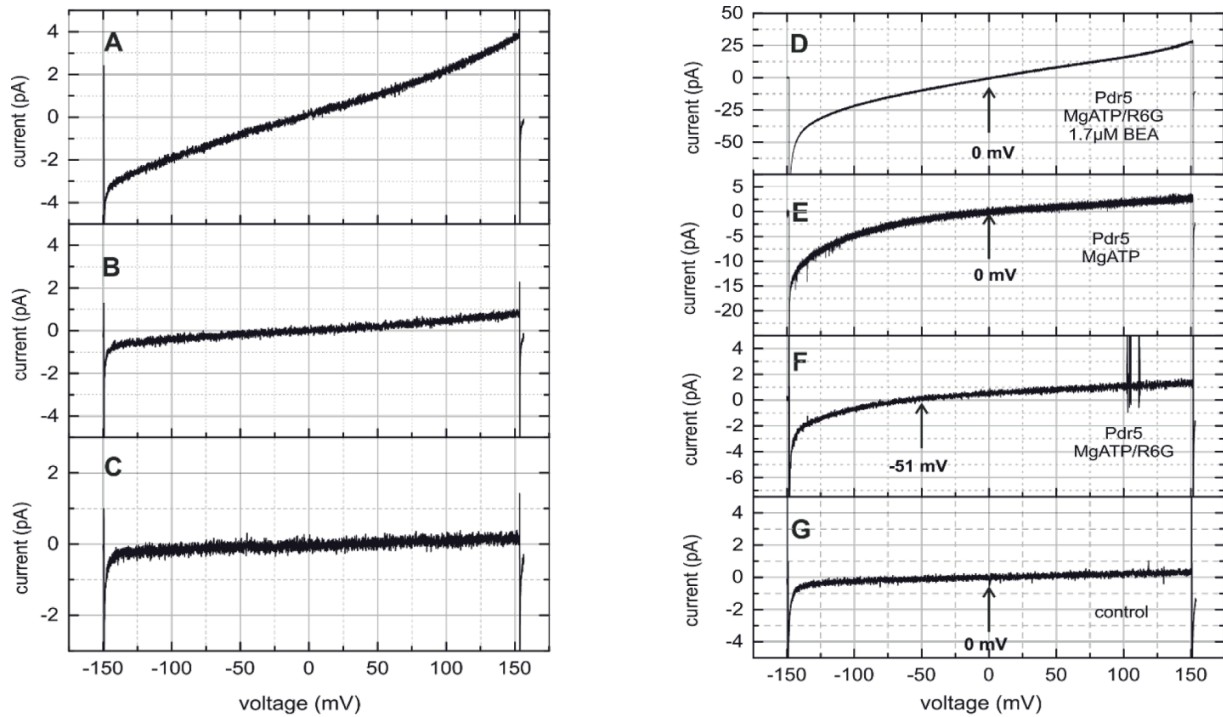


Fig. 6. Current-Voltage recording in the presence of BEA in the cis compartment. (A-C) Current-voltage ramps with bilayer in the presence of 9.9 (A), 3.3 (B) and 0 μM (C) BEA. (D-G) series of current voltage ramps from the same bilayer: (G): empty bilayer, (F) Pdr5_{WT} incorporated, (E) is (F) in the presence of Mg²⁺-ATP/R6G and (D) is (E) after addition of BEA. The reversal potentials are indicated with an arrow.

Supplementary Materials

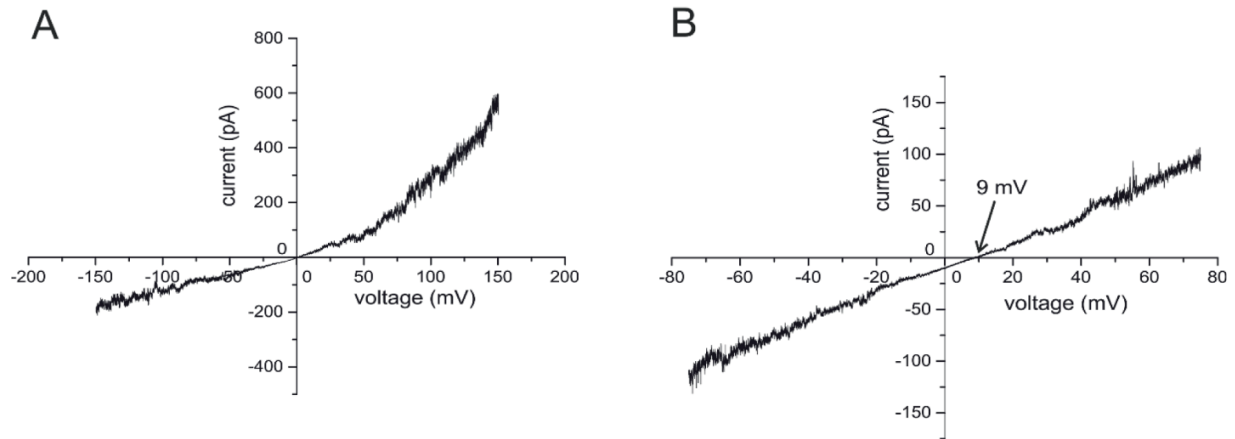


Fig. S1. Ion selectivity of the activated Pdr5_{WT} channel. (A) Current recording from a bilayer containing multiple active copies of the reconstituted voltage activated Pdr5_{WT} in response to a voltage ramp from -150 mV to +150 mV in symmetrical cis/trans (250 mM KCl, 10 mM HEPES, pH 7.0) buffer. Pdr5_{WT} always displayed a rectifying current voltage relation with significant higher currents at positive V_h . (B) Asymmetric buffer conditions (590 mM/250 mM KCl (cis/trans)) led to V_{rev} of +9 mV.

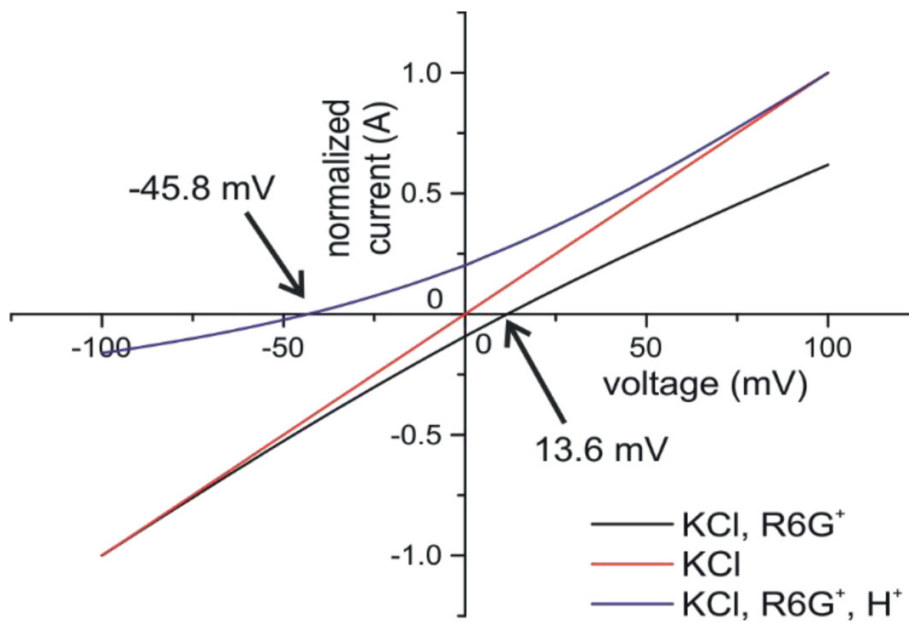


Fig. S2. Current-voltage relations calculated by the GHK current equations using experimental ionic conditions for 3 cases. Red: KCl (only permeation of K^+ and Cl^- ions), Black: KCl-R6G (permeation of K^+ and Cl^- ions and active transport of $R6G^+$ ions), Blue: KCl-R6G- H^+ (permeation of K^+ and Cl^- ions and active symport of $R6G^+$ and H^+ ions). Currents were normalized to i_{max} . (for more details see Methods section and SI).

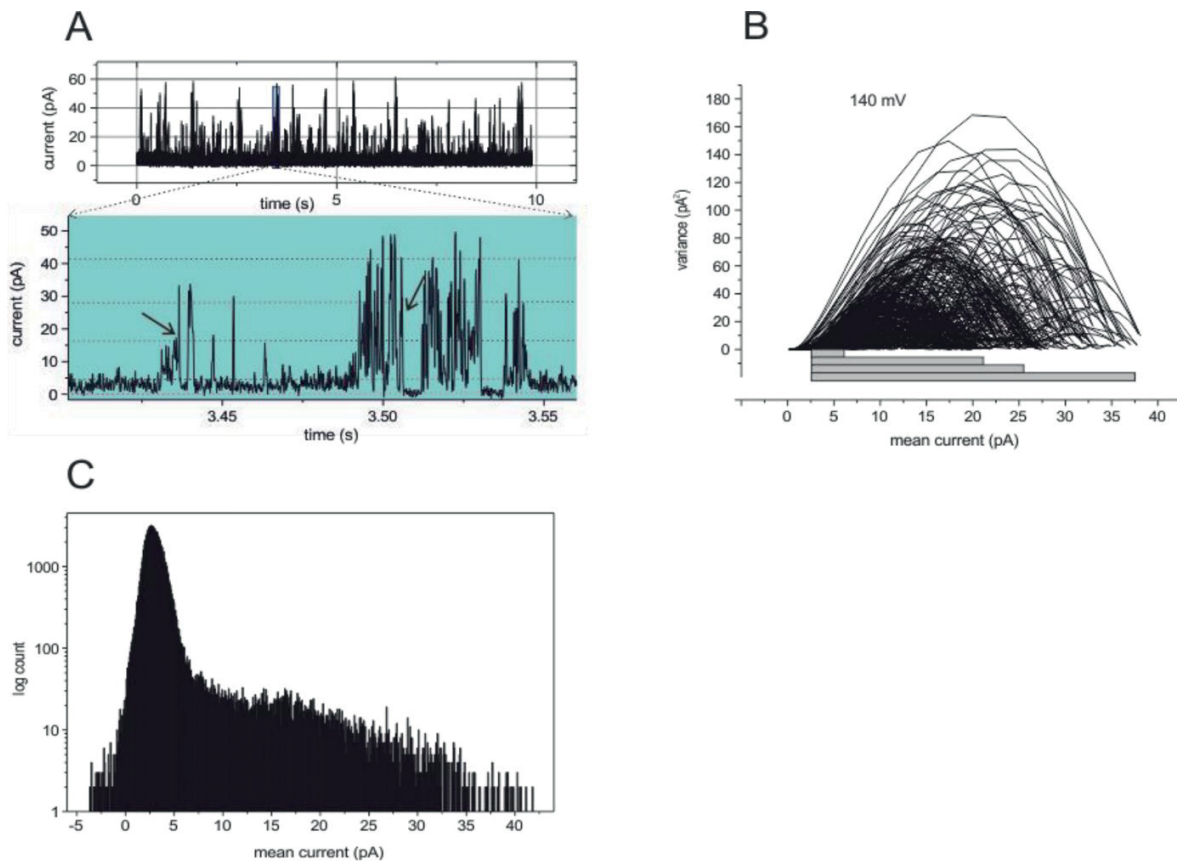


Fig. S3. Mean variance analysis. (A) Single channel recording from a bilayer containing a single active copy of the reconstituted voltage activated Pdr5 at $V_h = +140\text{mV}$. (B) Mean variance plot of the data from (A). (C) Histogram of the mean currents of the data in (B).

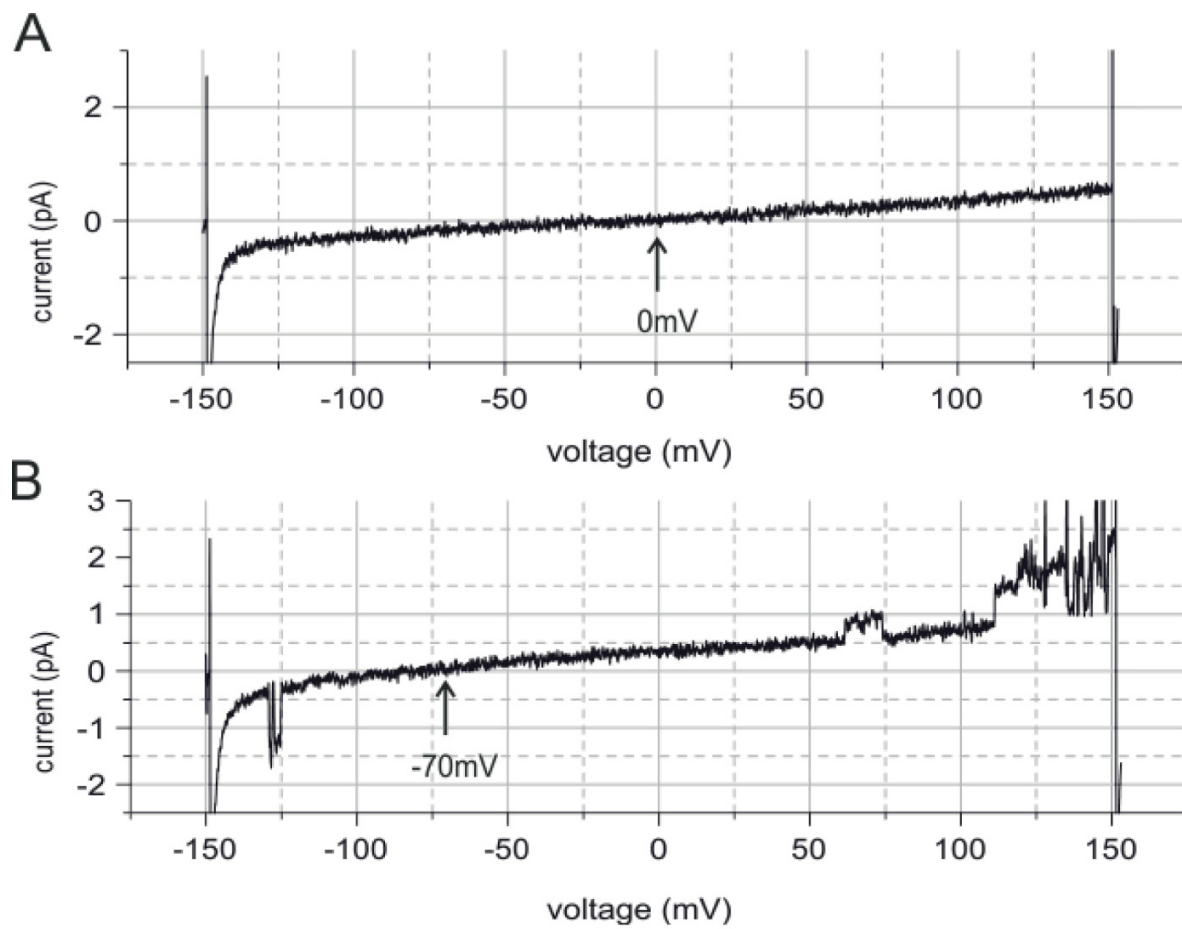


Fig. S4. Effects of KA on Pdr5 mediated ion conductance. (A) Control bilayer after reconstitution of Pdr5. **(B)** Same bilayer as in **(A)** but after addition of 330 nM KA to the cis compartment.

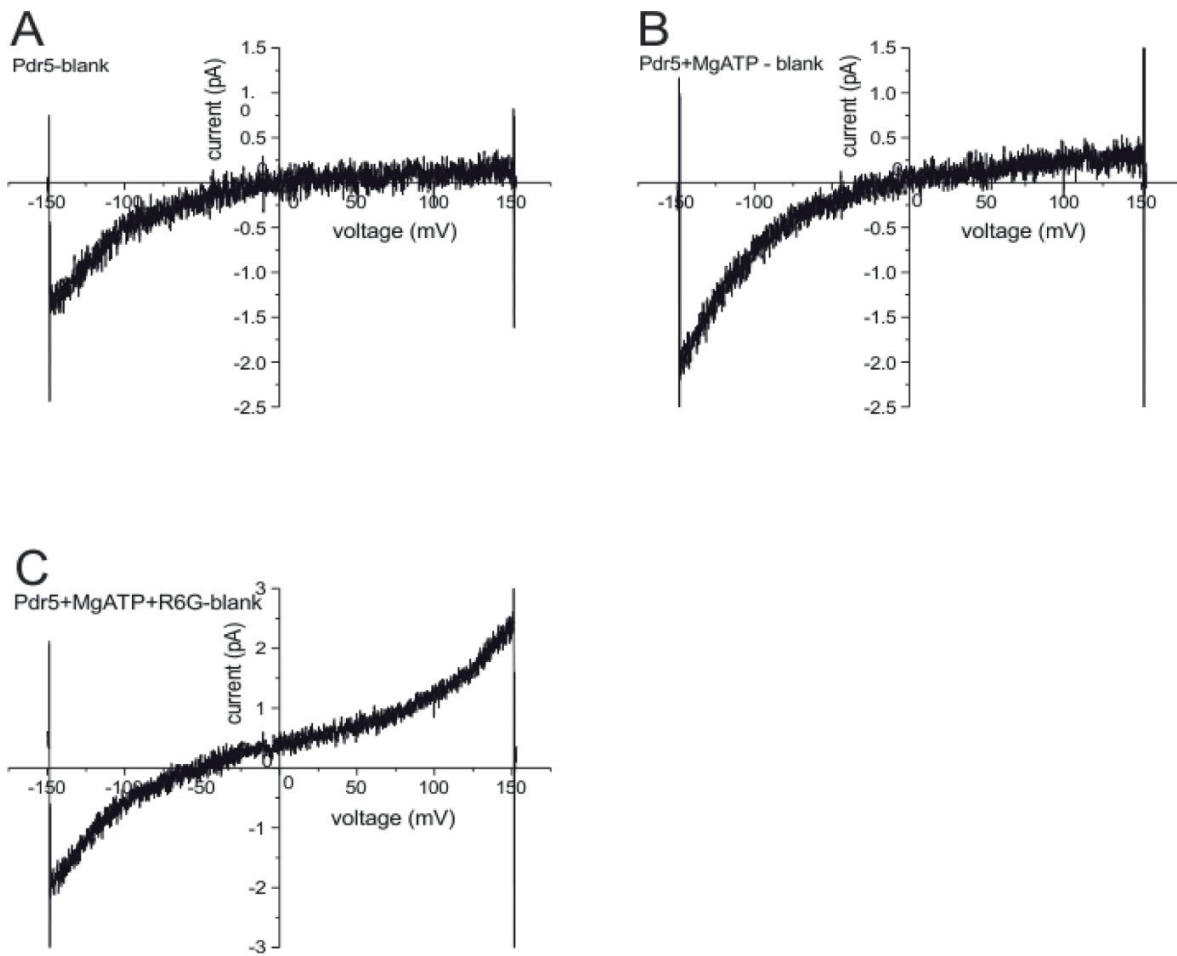


Fig. S5. Current-voltage ramps of non-activated Pdr5_{WT} after bilayer leak subtraction. (A) Current voltage ramp of reconstituted Pdr5_{WT}. **(B)** Same bilayer as **(A)** but in the presence of 2 mM Mg²⁺-ATP cis/trans. **(C)** Same bilayer as **(B)** but in the presence of 330nM R6G cis.

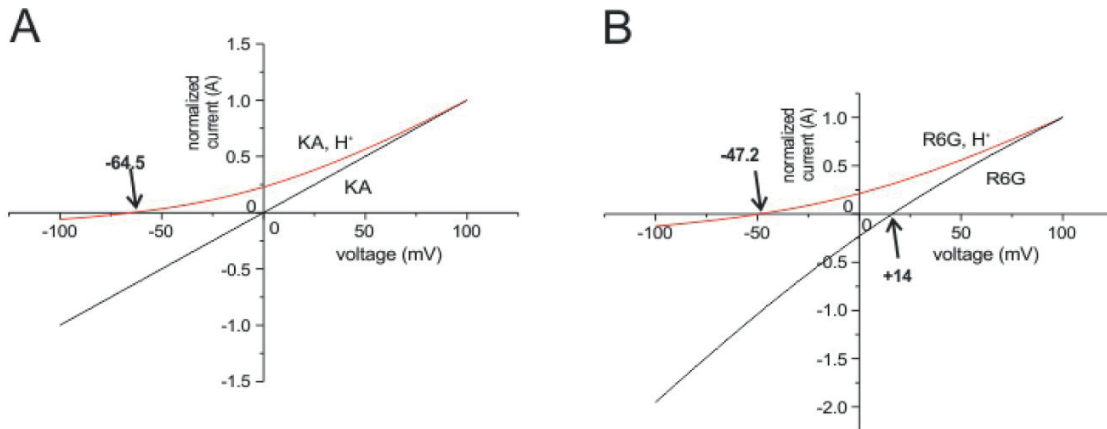


Fig. S6. Comparison of experimental and calculated fits for the reversal potentials. Fit of the experimental reversal potentials (red) and comparison to the calculated fit of the reversal potentials if no protons are symported (black) for KA (**A**) and R6G (**B**).

Table S1. Conductance parameter of non-activated Pdr5_{WT} (Fig. 4A-D) after subtraction of the bilayer leak conductance (see Fig. S3).

	Pdr5_{WT}	Pdr5_{WT} -ATP	Pdr5_{WT} -ATP-R6G
G_{sl} (pS) (+V_h)	0.72	1.8	6.7 (19.2)
G_{sl} (pS) (-V_h)	19.2	21,4	31
V_{rev} (mV)	0	0	-58
Rectification	26.7	11.9	4.6 (1.6)

Table S2. BEA induced conductivity across an empty bilayer (Fig. 6A-C).

	Control	BEA (3.3μM)	BEA (9.9μM)
G_{sl} (pS)	1.3 (Fig. 6C)	4.2 (Fig. 6B)	20.8 (Fig. 6A)
V_{rev} (mV)	0	0	0

Table S3. Conductance parameters of Pdr5_{WT} in the presence of Mg²⁺-ATP, R6G and BEA

	Blank	Pdr5-Mg²⁺-ATP	Pdr5-Mg²⁺-ATP/R6G	Pdr5-MgATP/R6G-BEA (1.7μM)
G_{sl} (pS)	1.2	2.4 (Fig. 6F)	7.7 (Fig. 6E)	175 (Fig. 6D)
V_{rev} (mV)	0	0	-51	0

Data analysis S1. Determination of the ion selectivity and conductance states of the voltage activated Pdr5 channel.

After voltage activation, reconstituted Pdr5_{WT} always displayed a rectifying current voltage relation with significant higher currents at positive membrane voltages no matter whether single active channels or multiple active channel currents were detected. Under asymmetric buffer conditions (590 mM/250 mM KCl (cis/trans)) a reversal potential of $V_{rev} = +9 \text{ mV} \pm 2.8$ (n=3) was observed for the Pdr5_{WT}, while for the Pdr5_{EQ} mutant we obtained $V_{rev} = +13 \text{ mV} \pm 2.2$ (n=3) with the same gradient (details not shown). Using the GHK approach the corresponding relative permeability for the Pdr5_{WT} and the Pdr5_{EQ} mutant are $P_{K^+}/P_{Cl^-} = 2.5:1$ and $P_{K^+}/P_{Cl^-} = 3.5:1$ respectively.

After voltage activation, reconstituted Pdr5_{WT} displayed membrane potentials above ± 100 mV and complex, fast channel gating (Fig. S3). We analyzed the single channel recordings using the mean variance analysis, which allows an unbiased determination of ion-channel conductance states (Patlak, 1988, 1993). For this we applied the Matlab based Ion-Channel-Master program (Bartsch et al., 2013).

The Pdr5_{WT} channel displayed fast flickering gating transitions from the closed to the open state with different open channel amplitudes (see expansion plot in the lower part of Fig. S3A). The time-course of the gating events (see marked events) clearly indicates that the observed complex gating to different open states cannot be due to the presence of two or more active channels with simultaneous gating. The probability of to observe 2 simultaneous gating transitions within the sampling window of 100 μs is: $W = (\tau_s)^2 = 1 \cdot 10^{-8} \text{ s}$. Thus in 3 years and 21 days measuring time, the probability (W) of a simultaneous gating in this time window would be $W=1$. The mean variance plot in Fig. S3B depicts directly each of the resolved gating transition with variable amplitude in Fig. S3A. The bars below the mean variance plot indicate the amplitudes of the four most frequent gating transitions deduced from the histogram in Fig. S3C. The dashed lines in the lower part of the expansion plot in Fig. S3A also mark the same most frequent current amplitudes. In Fig. S3A the following main current transitions were observed: $\Delta i_1 = 3.8 \text{ pA}$, $\Delta i_2 = 18.5 \text{ pA}$, $\Delta i_3 = 25 \text{ pA}$, $\Delta i_4 = 35 \text{ pA}$. We collected similar set off data (n \geq 10) from recordings with $V_h = \pm 120$ to $V_h = \pm 140$ mV. It turned out that the gating transitions could be grouped into three different Pdr5 conductance states: $G_1 \cong 25 \pm 3.6 \text{ pS}$, $G_2 \cong 134 \pm 26 \text{ pS}$, $G_3 \cong 250 \pm 78 \text{ pS}$.

Data analysis S2. Determination of the substrate induced reversal potential shift with the reconstituted non activated Pdr5.

After reconstitution into a planar bilayer, Pdr5_{WT} induced small ion currents and we tested whether the substrates Ketoconazole (KA) and Rhodamine 6G (R6G) in the presence of Mg²⁺-ATP induces shifts in a similar way as with the voltage activated Pdr5.

In these measurement, addition of KA to the cis compartment induced a drastic shift of the reversal potential of $V_{rev} = -70\text{mV}$. In four different bilayer experiments we obtained an average of $\Delta V_{rev} = -64 \pm 8\text{ mV}$ ($n = 4$).

Similar experiments were conducted with R6G as a substrate. Starting with the control bilayer (Fig. 6A), we added Pdr5_{WT} to the cis compartment of the same bilayer and observed spontaneous insertion of Pdr5_{WT} into the bilayer without applying prolonged high voltage by small rectifying current (Fig. 1B). After subsequent addition of Mg²⁺-ATP to cis/trans (Fig. 6C) and 300nM R6G we observed again a significant shift in the reversal potential (Fig. 6D). Subtraction of the bilayer leak conductance (Fig. 6A) discloses that Pdr5_{WT} behaves as an almost complete rectifier since it allowed nearly exclusively transport of K^+ ions from trans to cis (Fig. S5A, B), while in the presence of R6G an additional cation current from cis to trans with $\Delta V_{rev} = -57\text{ mV}$ was observed (Fig. S5C). In different bilayer experiments with R6G as a substrate we observed a shift of the reversal potential of $V_{rev} = -47.2 \pm 5.3\text{mV}$ ($n = 12$).

Data analysis S3. Electrophysiological permeation assay (GHK approach).

The Goldman-Hodgkin-Katz approach is by far the most commonly used framework to describe ion permeability and selectivity of membranes (Goldman, 1943; Hodgkin and Katz, 1949). Beside the principal difficulties underlying the macroscopic GHK constant field theory, which assumes independent movement of the ions through membrane pores (see references (Corry et al., 2000; Moy et al., 2000; Syganow and von Kitzing, 1999) for a detailed discussion) it has been demonstrated that the methodology can be used to obtain reliable semi-quantitative measures for permeation of charged drugs through membranes (Hille, 2001).

We were interested in obtaining information on the selectivity of the membrane transport mediated by the ABC transporter Pdr5_{WT}. For this, we used high-resolution electrophysiological recordings from planar bilayer containing the reconstituted Pdr5_{WT}. In practice, this method can be used to measure ion currents across the membrane up to a maximum resolution of 100 fA with

a maximal bandwidth of 1 kHz. In the case of ion channels, for example, a channel with a conductance of $G = 100\text{pS}$ the current through the open channel at $V_h = 100\text{mV}$ is $i = 10\text{pA}$ corresponding to a turnover of $n = 6.2 \cdot 10^7 \text{ions/s}$. Therefore, by this method the current through a single ion channel molecule can be measured. The situation with Pdr5_{WT} is different: from the ATP turnover of approx. 6 ATP / s (Ernst et al., 2008) which in the worst case is connected to the same turnover (stoichiometry 1: 1) of a charged molecule across the membrane, we obtain a conductance of $G = 10 \text{fS}$ and a current $i = 0.001 \text{fA}$. It is therefore clear that even under the most optimal conditions, the ion currents across the membrane mediated by individual ABC transporters cannot be resolved. On the contrary, in the case of such electrophysiological measurements, it is necessary to rely on the largest possible number of transporters being active. A planar bilayer with a radius of $100\mu\text{m}$ has an area of approx. $F = 3 \cdot 10^{-4} \text{cm}^2$, which implies that the bilayer with 300 active Pdr5_{WT} (see above) would have a specific conductivity of roughly $G_m = 10\mu\text{S}/\text{cm}^2$. When applying a voltage of $V_m = +100\text{mV}$ this results in a total flux of about $n = 6.2 \cdot 10^7 \text{ions/s}$ to adjust the new membrane equilibrium. Moreover, from the specific resistance and specific capacity of the planar bilayer one can calculate that the new equilibrium states are realized with an exponential time constant of about 1ms. In other words, at small membrane currents the measurement of zero current potentials is an excellent opportunity to study the properties of the ion fluxes mediated by transporters with low turnover rates across the membrane.

During the electrophysiological experiments with Pdr5_{WT} reconstituted into planar bilayer, however, it turned out that Pdr5_{WT} can be transferred by exposure to higher voltages ($V_m \geq \pm 100\text{mV}$) to an ion channel like state capable to conduct ions at high rates with a main conductance state of $G_2 \cong 134\text{pS}$ and subconductance states of $G_1 \cong 25\text{pS}$, and $G_3 \cong 250\text{pS}$. Moreover, we observed that BEA opened concentration dependent activated Pdr5_{WT} channels in a saturating fashion allowing a rough estimate of the total number of Pdr5_{WT} incorporated into the bilayer. On the other hand, we also detected very small membrane currents after incorporation of Pdr5_{WT} into the planar bilayer without voltage activation (see Fig. 6). These small currents revealed in asymmetric buffer (590 mM KCl (cis)/250 mM KCl (trans)) a reversal potential of $V_{rev} = 11\text{mV}$ (details not shown) a similar value as obtained for the high conductance form of Pdr5_{WT} (see Fig. 3B). This shows that the currents are likewise carried by K^+ and Cl^- ions with almost the same permeability ratio of $\frac{P_{K^+}}{P_{Cl^-}} = 3.3$ as in the Pdr5_{WT} high conductance states. One

interesting estimate concerning the turnover for cations through Pdr5_{WT} can be deduced from measurements with the activated form (details not shown) and a BEA titration of bilayer yielding a maximal slope conductance of 106 nS. Considering the mean conductance of $G_2=134$ pS, this means that the bilayer contained ~ 800 copies of the active Pdr5_{WT}. With the slope conductance of $G_{sl}(pS) \cdot (-V_h)=19$ pS (Table 1) we obtain a "native" conductance of Pdr5_{WT} $G \cong 20$ fS for K^+ -ions.

To characterize the ion fluxes mediated by the activated and non-activated Pdr5_{WT} we employed the following experimental conditions for bilayer containing an unknown number for Pdr5_{WT}.

Permeability Pdr5_{WT}: $P_{K^+} = 2.5$; $P_{Cl^-} = 1$; $P_{R6G^+} = \text{variable}$; $P_{H^+} = \text{variable}$

Cation: $z_{K^+} = 1$; $c_{K^+ cis} = 250$ mM; $c_{K^+ trans} = 250$ mM

Anion: $z_{Cl^-} = -1.0$; $c_{Cl^- cis} = 250$ mM; $c_{Cl^- trans} = 250$ mM

Substrate KA: $z_{KA} = 0$; $c_{AB^- cis} = 330$ nM; $c_{KA-trans} = 00$ mM

Zero current potential KA: $V_{rev} = -64.5$ mV (experimental value $n = 4$)

Protons: $z_{H^+} = 1$; $c_{H^+ cis} = 8 \cdot 10^{-9}$ M (pH 8.1); $c_{H^+ trans} = 1.04 \cdot 10^{-6}$ M (pH 5.98)

Substrate R6G: $z_{R6G^+} = 1$; $c_{AB^- cis} = 330$ nM; $c_{KA-trans} = 00$ mM

Protons: $z_{H^+} = 1$; $c_{H^+ cis} = 7.94 \cdot 10^{-9}$ M (pH 8.1); $c_{H^+ trans} = 9.3 \cdot 10^{-7}$ M (pH 6.03)

Zero current potential R6G: $V_{rev} = -47.2$ mV (experimental value ($n = 12$))

Assuming electrical recording from a bilayer with the above concentrations in the cis and trans compartment and considering that the assumptions of the GHK-theory are valid we can calculate the expected current voltage relation for the above bilayer membrane containing an unknown number of active Pdr5_{WT} channels for the particularly given combination of ion concentration on both sides of the membrane.

GHK-current equations

1. $I_{K^+}(V) = I(V, P_{K^+}, Z_{K^+}, c_{K^+}^{cis}, c_{K^+}^{trans}),$
2. $I_{Cl^-}(V) = I(V, P_{Cl^-}, Z_{Cl^-}, c_{Cl^-}^{cis}, c_{Cl^-}^{trans})$
3. $I_{R6G^+}(V) = I(V, P_{R6G^+}, Z_{R6G^+}, c_{R6G^+}^{cis}, c_{R6G^+}^{trans})$
4. $I_{H^+}(V) = I(V, P_{H^+}, Z_{H^+}, c_{H^+}^{cis}, c_{H^+}^{trans})$
5. $\Sigma I(V) = I_{K^+}(V) + I_{Cl^-}(V) + I_{R6G^+}(V) + I_{H^+}(V)$

Using equation 1-5 we calculated for the ionic conditions given above the corresponding current-voltage relations using a Mathcad (PTC-Software) based routine. Starting with ketaconazole addition to the cis compartment in the presence of MgATP however we have to propose that the reconstituted Pdr5_{WT} initiates active substrate and Mg²⁺-ATP driven transport of H⁺-ions from cis to the trans compartment (H⁺-Symport) to explain the observed $V_{rev} = -64.5 \text{ mV}$ (Fig. S3A). Active transport means that the permeability (P) approaches in the GHK formalism towards infinity. Starting for KA at pH 7 (cis/trans) we obtained by generating a pH gradient through iteration the “new” equilibrium concentration of H⁺-ions in the cis and trans compartment after initiation of transport with the corresponding value of P_{H^+} ($P = 10^6 \text{ cm}^3/\text{s}$) and with the now fixed ΔpH we obtain the value for P_{R6G^+} ($P = 2 \cdot 10^5 \text{ cm}^3/\text{s}$). Since KA induced H⁺-pumping by Pdr5 is expected to be in the same order of magnitude as for R6G it appeared justified to use the values ($P_{H^+}, c_{H^+}^{cis} = 8 \cdot 10^{-9} \text{ M (pH 8.1)}; c_{H^+}^{trans} = 1.04 \cdot 10^{-6} \text{ M (pH 5.98)}$) obtained for KA to fit the observed reversal potential obtained with R6G as substrate. Provided Mg²⁺-ATP driven R6G transport would occur without H⁺ pumping at the given ionic conditions (cis/trans) we should have observed $V_{rev} \cong +14 \text{ mV}$ (Fig. S4B) which was not the case. However our calculations show that R6G⁺ and H⁺ ions are symported at a relative permeability of $P_{H^+}/P_{R6G^+} \cong 5$.

3.5 Chapter V

Titel: Structure of the fungal asymmetric ABC transporter Pdr5

Authors: Manuel Wagner, Dijun Du, Andrzej Szewczak-Harris, Arthur Neuberger, Sander H. J. Smits, Holger Gohlke, Ben F. Luisi, Lutz Schmitt

Published in: to be submitted

Proportionate work on this manuscript: 50%

Structure of the fungal asymmetric ABC transporter Pdr5

Pdr5: An ABC transporter with a twist

Manuel Wagner¹, Dijun Du^{2,3}, Andrzej Szewczak-Harris², Arthur Neuberger², Sander H. J. Smits¹, Holger Gohlke⁴, Ben F. Luisi^{2,#}, Lutz Schmitt^{1,#}

¹ Institute of Biochemistry, Heinrich-Heine-Universität Düsseldorf, Universitätsstraße 1, 40225, Düsseldorf, Germany.

² Department of Biochemistry, University of Cambridge, Tennis Court Road, Cambridge CB2 1GA, UK.

³ School of Life Science and Technology, ShanghaiTech University, Shanghai, 201210, China.

⁴ Institute for Pharmaceutical and Medicinal Chemistry, Heinrich-Heine-Universität Düsseldorf, Universitätsstraße 1, 40225, Düsseldorf, Germany.

Corresponding authors. Email: Lutz.Schmitt@hhu.de, bfl20@cam.ac.uk

Abstract

The overexpression of ATP-binding cassette (ABC) transporters is one of the main mechanisms that confer multidrug resistance (MDR) to all living organisms. Several structures of MDR ABC transporters in bacteria and humans have been solved over the recent years, especially since the advances in single particle cryo-electron microscopy (cryo-EM). However, there are no known structures of any ABC transporters from fungi or plants to this date. Here, we present the structure of *Saccharomyces cerevisiae* ABC transporter Pdr5 obtained through single particle cryo-EM and additional density maps of the occluded ATP-bound state. Our results suggest a new mechanism for this asymmetric ABC transporter, in which the nucleotide binding domains (NBDs) stay in constant contact without any ATP molecule present. Moreover, comparison of the apo and occluded state demonstrates that the transmembrane region of Pdr5 moves in a twist-like fashion and possibly does not follow the classical ‘alternating access model’.

Introduction

ABC transporters are ubiquitous integral membrane proteins that exist in all prokaryotes as well as eukaryotes that facilitate the transport of a broad range of structurally and chemically diverse substrates across biological membranes in an ATP dependent manner (Higgins, 2001; Rees et al., 2009). A functional unit of an ABC transporter consists of two highly conserved NBDs that represents the motor domains of the pump by binding and hydrolysis of ATP and two transmembrane domains (TMDs) that form the translocation channel through the membrane (Locher, 2016; Oswald et al., 2006; Schmitt and Tampe, 2002). Depending on the direction of transport, ABC transporters are subdivided into exporters and importers. While in prokaryotes both classes exist, eukaryotes in general only possess ABC exporters that fulfill a variety of cellular functions (Rees et al., 2009). One growing concern in bacterial and fungal infections as well as cancer treatment is the raise of MDR as known therapeutics fail to succeed in the treatment of the disease. The mechanisms that cause the resistance towards the xenobiotics are often based on the overexpression of ABC transporters (Lage, 2003). The phenomenon of MDR in pathogenic fungi like *Candida albicans* correlates with the overexpression of pleiotropic drug resistance (PDR) ABC transporters (Lamping et al., 2010; Prasad et al., 2015). In *S. cerevisiae*, the most prominent member of this protein family is Pdr5, which was first discovered as a gene conferring resistance towards the antifungal cycloheximide (Golin and Ambudkar, 2015; Leppert et al., 1990). Since then, numerous biochemical and mutational studies have been performed that helped to understand many aspects of the molecular mechanisms of this transporter (Ananthaswamy et al., 2010; Ernst et al., 2008; Golin and Ambudkar, 2015; Golin et al., 2007; Gupta et al., 2014; Kolaczowski et al., 1996; Kueppers et al., 2013; Sauna et al., 2008; Wagner et al., 2019). Pdr5 belongs like all PDR ABC transporter to the ABCG subfamily of eukaryotic ABC transporters that feature an inverse topology of (NBD-TMD)₂ and adopt a type II exporter fold (Lamping et al., 2010; Paumi et al., 2009; Tanabe et al., 2019). A key feature of Pdr5 is the asymmetry of its NBDs, also referred to the canonical and the degenerate NBD. It was demonstrated that this asymmetry is crucial for the functionality of the protein (Gupta et al., 2014). Although there are other asymmetrical ABC transporters, like ABCG5/ABCG8, TM287/288 or CFTR (Hohl et al., 2012; Sorum et al., 2017; Wang et al., 2011), the degree of degeneration with mutations of residues in five NBD

motifs is the highest within this class of fungal transporters. To date, the mechanistic and structural implications of this degeneration remain elusive.

Recent advances in single particle cryo-EM led to the ‘resolution revolution’ and to the determination of a constantly increasing number of structures of membrane proteins (Cheng, 2018; Lee and Rosenbaum, 2017; Locher, 2016; Subramaniam et al., 2016; Taylor et al., 2017). However, to date no structures resolved of fungal membrane proteins nor structures of PDR ABC transporters have been determined. Here, we present the first 3-D structure of the fungal ABC transporter Pdr5 in different conformations providing important molecular insights into this class of membrane proteins. We provide first structural evidence for the significance of the asymmetry of the NBDs of Pdr5 and propose a new ‘twist model’ for substrate transport that differs from the classic ‘alternating access model’ (Jardetzky, 1966).

Material and Methods

Protein purification

Pdr5_{WT} and Pdr5_{EQ} were expressed and purified as described in (Wagner et al., 2019). In short, *S. cerevisiae* YRE1001 (Ernst et al., 2008) cells were grown to an OD₆₀₀ of 3.5 at 30 °C. For one purification procedure, cells of 4 L YPD liquid media were harvested and disrupted using glass beads. Total membranes were solubilized in buffer A (50 mM Tris-HCl, pH 7.8, 50 mM NaCl, 10% (w/v) glycerol) for 1 h with 1% (w/v) trans-PCC- α -M under gentle stirring at 4 °C. Next, a two-step purification was performed with an immobilized metal ion affinity chromatography of the His-tagged Pdr5 followed by a size exclusion chromatography on a Superdex 200 10/300 GL column (GE Healthcare) with buffer A containing 0.003 % (w/v) trans-PCC- α -M. All chromatography steps were performed on the Äkta protein purification systems (GE Healthcare).

In order to force the ABC transporter into the occluded state, purified Pdr5_{WT}, Pdr5_{EQ} or the Pdr5-peptidase complex was incubated with 200 μ M ortho-vanadate, 2 mM Mg²⁺-ATP in the presence or absence of 100 μ M rhodamine 6G, ketoconazole or beauvericin and incubated for 5 min at 30 °C.

Cryo-EM specimen preparation, data collection and processing

Cryo-EM specimen preparation as well as data collection and processing were in general performed as described in (Du et al., 2014; Wang et al., 2017).

Homology modelling, model docking and optimization

Homology modelling, model docking and optimization were essentially performed as described in (Du et al., 2014; Tanabe et al., 2019; Wang et al., 2017).

Results***Sample preparation and reconstitution into peptidisc***

For a structural analysis of Pdr5, active and functional wildtype Pdr5 as well as the ATPase deficient E1036Q mutant were purified as described in (Wagner et al., 2019). Further details are described in the Materials and Methods section. The main elution fraction with a concentration between 1.3-1.7 mg/ml was collected and directly blotted onto grids for cryo-EM screenings. Additionally, in order to improve the particle number and stabilize the protein in solution, detergent solubilized Pdr5 was reconstituted into peptidisc. Peptidisc consists of a small amphipathic bi-helical peptide called nanodisc scaffold protein (NSP_r) that wraps in multiple copies around the membrane protein and, opposed to classical nanodisc, does not need any lipid addition (Bayburt and Sligar, 2010; Carlson et al., 2018). Pdr5_{WT} was purified with the detergent trans-PCC- α -M and concentrated to a final concentration of 4 mg/ml. For reconstitution, Pdr5_{WT} was mixed with NSP_r in a 1:1 (wt/wt) ratio resulting in a molar ratio of 1:39 for Pdr5_{WT}:NSP_r. The subsequent size exclusion chromatography was performed with buffer lacking detergent (50 mM Tris-HCl pH 7.8, 50 mM NaCl) and is depicted in Figure 1A. Reconstituted Pdr5_{WT} eluted similar to the detergent solubilized protein at approximately 10 ml. An additional elution peak at 14 ml indicated excess NSP_r molecules that did not reconstitute with Pdr5_{WT}. In order to verify the reconstitution as well as the stability of the Pdr5_{WT}-peptidisc complex, two additional injections of the main elution peaks were performed (see Figure 1A and B). As obvious from Figure 1, Pdr5_{WT} remains stable in buffer without detergent, which indicates the successful reconstitution into

peptidisc. The resulting reconstituted Pdr5_{WT} was incubated with different additives (see Table 1) and grids for a cryo-EM screening were prepared as described in Materials and Methods section.

Unfortunately, the initial screenings of the grids showed that the Pdr5_{WT}-peptidisc complex resulted in a preferred orientation of the particles that limited the angular information drastically and thereby led only to low resolution three-dimensional maps (not shown). In order to overcome this obstacle, new samples were prepared, to which the detergent CHAPSO was added, right before blotting the grid. This technique has been shown before to eliminate the problem of preferred orientation in cryo-EM for the bacterial RNA polymerase (Chen et al., 2019).

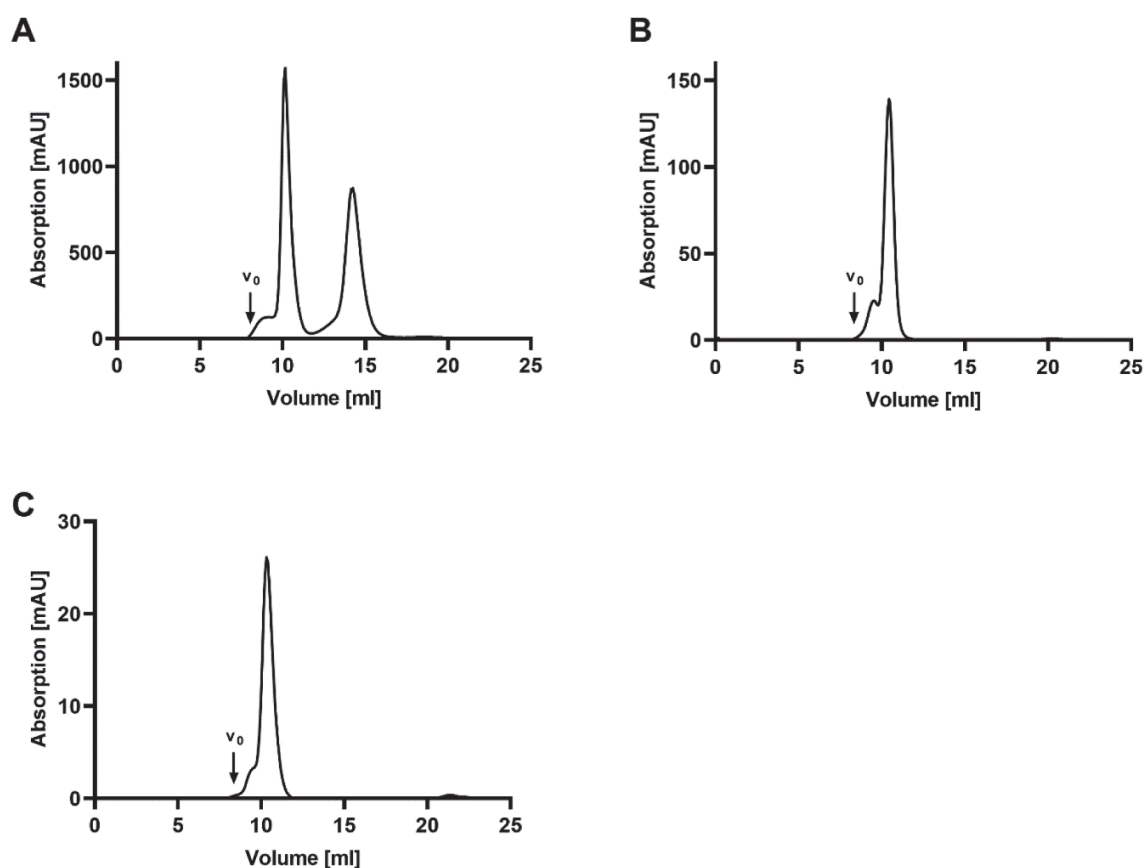


Figure 1 SEC chromatograms of reconstituted Pdr5_{WT} in peptidisc. A: First injection after mixing Pdr5_{WT}:NSP_r at a 1:39 molar ratio. **B:** Reinjection injection of the main elution peak of **A**. **C:** Reinjection of the elution peak in of **B**. All SEC experiments were performed with detergent-free buffer (50 mM Tris-HCl pH 7.8, 50 mM NaCl). V_0 indicates the void volume of the column.

Cryo-EM density maps of Pdr5

The resulting density maps (resolution ~ 3.8 Å) of detergent purified Pdr5_{WT} as well as the reconstituted Pdr5_{WT}-peptidisc complex after the addition of CHAPSO to the sample are shown in Figure 2. When compared to the electron density map of apo Pdr5_{WT} solubilized with trans-PCC- α -M (Figure 2A), the sample of the Pdr5_{WT}-peptidisc complex (Figure 2B) resulted in an identical density map as seen in the superposition of both densities (Figure 2C). This indicates that the detergent does not drastically alter the conformation or fold of the protein and thus allows to investigate the structure of the protein in detergent solution.

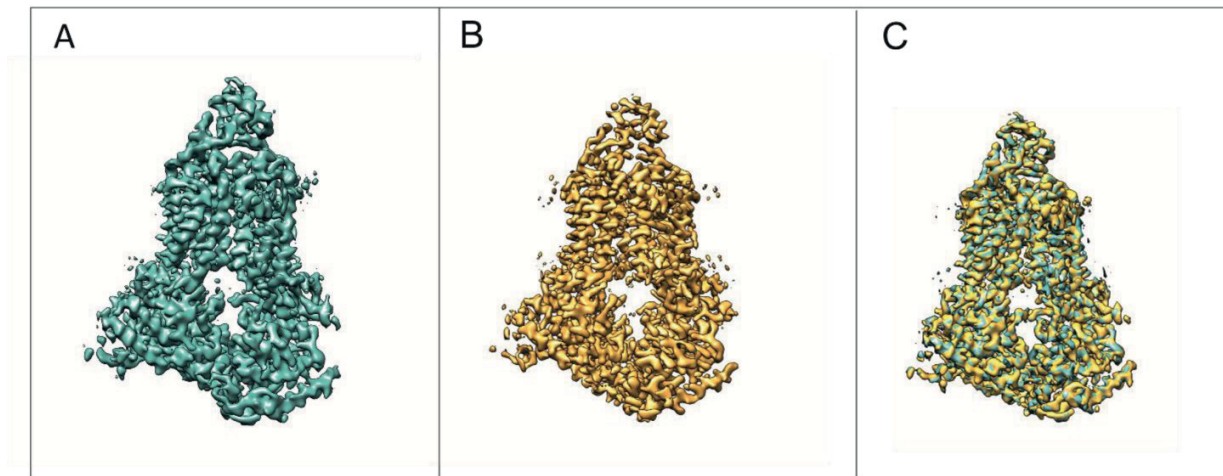


Figure 2 Density maps of Pdr5_{WT}. **A:** Electron density map of apo Pdr5_{WT} solubilized with trans-PCC- α -M. **B:** Electron density map of apo Pdr5_{WT} reconstituted into peptidisc. **C:** Superposition of the electron density maps shown in **A** and **B**.

The obtained resolution of 3.8 Å allows to identify single helical structures in the transmembrane region as well as the NBDs and demonstrate that the protein adopts the inward facing conformation in both density maps. Furthermore, the detergent solubilized E1036Q mutant incubated with Mg²⁺-ATP was prepared in order to force Pdr5 to adopt the outward facing conformation. Unfortunately, no difference was apparent in the electron densities and resulted in an identical map as for the wild-type samples (not shown).

Only the N-terminal TMD moves

Next, we were interested in the conformational shift that might take place upon ATP binding, i.e. how the dimerization of the NBDs affect the conformation of the TMDs. Therefore, Pdr5_{WT} solubilized with trans-PCC- α -M was incubated with ortho-vanadate and ATP in order to trap the protein in the dimerized NBD state. Interestingly, cryo-EM screenings demonstrated that the ABC transporter was not trapped in one distinct state, but shows a variety of transient conformations that resulted in rather low particle numbers of each of these classes. However, it was possible to isolate two classes with roughly 5000 particles that resulted in the density maps seen in Figure 3A and Figure 3C.

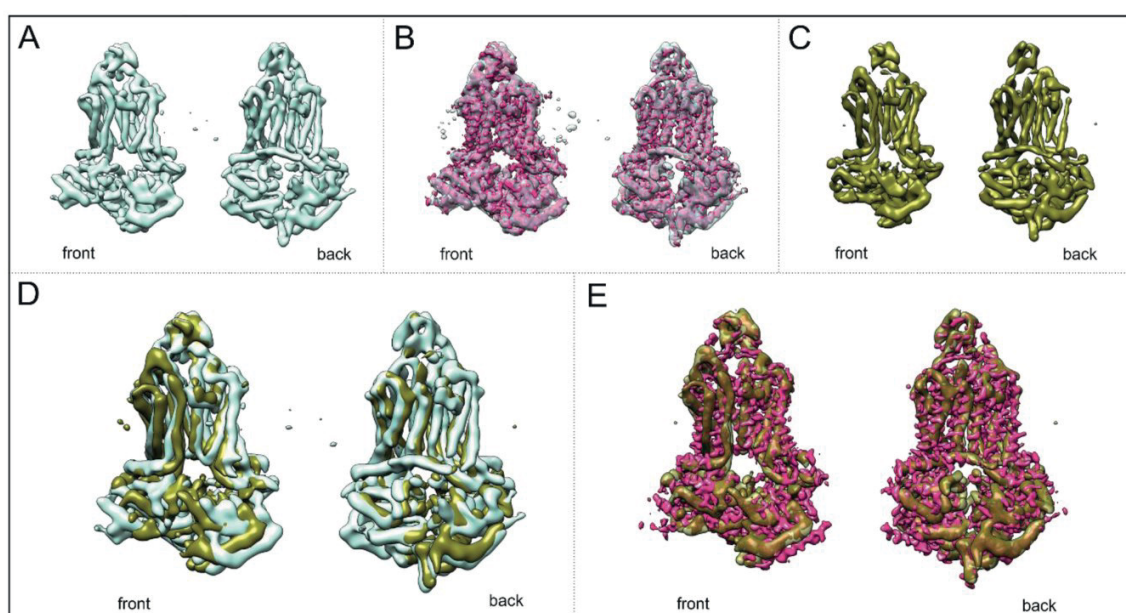


Figure 3 Cryo-EM densities from the two main classes of the ‘V_i trapped state’. **A:** Front and back view of the first class resembling the apo state. **B:** Superposition of A with the density map of the apo state seen in **Figure 2A**. **C:** Front and back view of the second class that belongs to the occluded state. **D:** Superposition of the two classes found in the ‘V_i trapped state’ (**A** and **C**). **E:** Superposition of the apo with the occluded state with the density maps of **Figure 2A** and **C**.

As obvious from the density maps, the first of the two classes (Figure 3A) identified belongs to the apo state that we observed in the absence of any ATP and vanadate as shown in Figure 2. Although the resolution is low due to the low particle number, Figure 3B demonstrates clearly the

overlapping densities and therefore demonstrates that although ATP and vanadate are present, the protein still adopted the apo state, i.e. the inward facing conformation. The second class, however, shows a different conformation as highlighted in Figure 3D and E. In this conformation, the electron density of the NBDs indicates that they dimerized compared to the apo state. Particularly the front view shows a movement of the NBDs towards each other, while the back view of the superposition indicates only minor movement of the TMDs and degenerate NBS. Moreover, the main displacement in the TM region is observed in the coupling helix of the N-terminal TMD (left side of the respective front views) that is shifted inside while the C-terminal TMD does not move significantly compared to the apo form.

The model of Pdr5

Based on the crystal structure of ABCG5/ABCG8 (Lee et al., 2016) a homology model for the three dimensional structure of Pdr5 was created as shown in Figure 4. Since the electron density allows only for a map to a resolution up to 3.8 Å, we were not able to create a complete model for Pdr5. The missing parts are highlighted by the dashed lines within the model. These areas include the extracellular loops (ECL) as well as the N-terminal extension that precedes the first NBD of the ABC transporter. Especially the N-terminal extension is predicted to be highly disordered (not shown) which could be the reason of the low electron density of this region. Overall the generated model resembles well the structure of the type II ABC exporters ABCG5/ABCG8 as well as ABCG2 (Taylor et al., 2017). Characteristic for type II exporters is the absence of transmembrane coupling helices interacting with the NBD of the opposing NBD, i.e. the N-terminal NBD is only interacting with the N-terminal TMD and *vice versa*. Strikingly, the extracellular loops of Pdr5 are significantly larger compared to its human homologs.

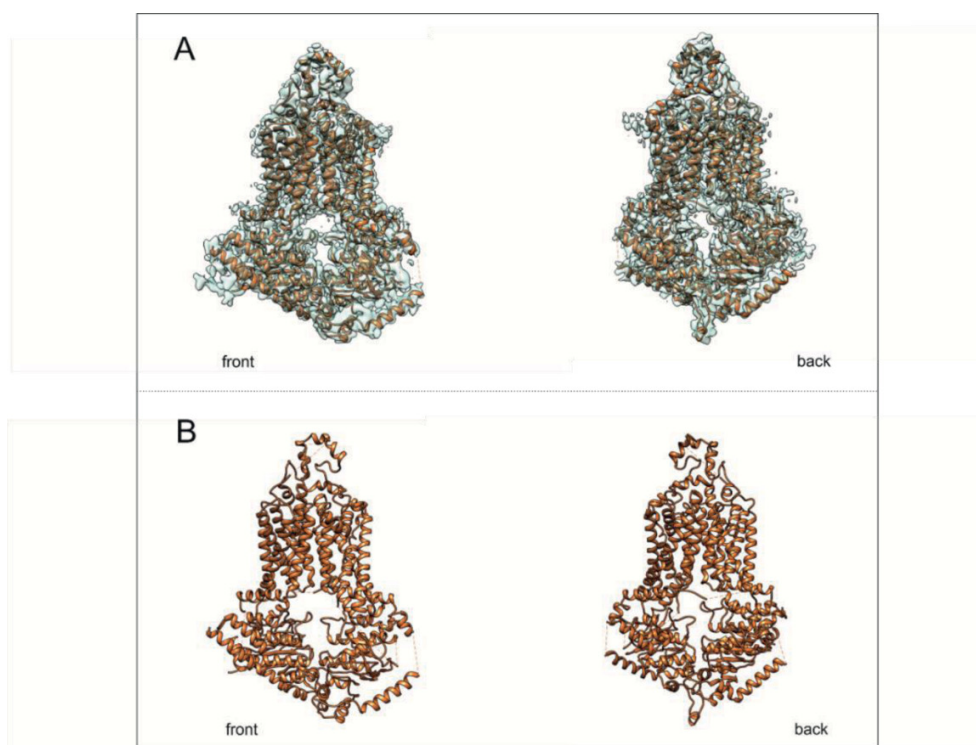


Figure 4 Initial model of Pdr5 based on the obtained density maps using the structure of ABCG5/ABCG8 as templates.

A: Fit of the model into the electron density of Pdr5_{WT} as shown in **Figure 2A**. **B:** Front and back view of the Pdr5 model alone.

The deviant nucleotide binding site – the foundation for the constant contact model

As an asymmetric ABC transporter, Pdr5 possesses a degenerate NBS that is unable to hydrolyze ATP. Mutational studies demonstrated that this degeneration is crucial for the functionality of this ABC transporter (Gupta et al., 2014). Based on our structural model, a closer look and comparison of the two NBSs could explain why this degeneration could be fundamental for ATPase and transport functionality. A zoom-in in both NBS (Figure 5) reveals that the canonical NBS is separated as the distance between the ATP binding motifs are 12.7 Å apart, which is expected for the apo state. In clear contrast, the degenerate site remains in close contact. The measured distance of 3.4 Å between residue R194 of the Walker A motif in NBD1 and E1013 of the C-loop of NBD2 is within hydrogen bond distance (Jeffrey, 1997), or can form a salt bridge (Walker and Causgrove, 2009) and indicates that NBS1 could form the basis for a ‘constant contact’ model of Pdr5, in which only NBS2 is binding and hydrolyzing ATP. This is further

supported by the density map of the occluded state (Figure 3). In comparison to the apo state, only the N-terminal TMD and coupling helix show significant movements, whereas the C-terminal site slightly shifts from the apo to the occluded state. Further, the back view of the electron density maps (Figure 3D and E) demonstrates no movement of the degenerate NBS even if ATP and V_i are present.

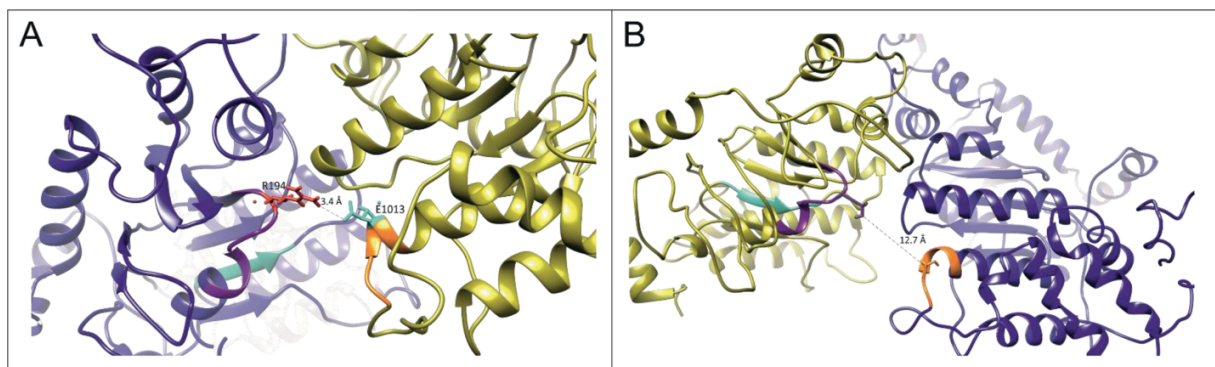


Figure 5 Focus view on the NBS of Pdr5^{wt}. **A:** The degenerate nucleotide binding site with the indicated distance between key residues of Walker A of NBD1 and the C-loop of NBD2. **B:** The canonical NBS with the closest distance indicated between the Walker A of NBD2 and the C-loop of NBD1. The color coding is as follows: NBD1: blue, NBD2: yellow, Walker A motif: purple, Walker B motif: light green, C-loop: orange, R194: red, E1013: cyan.

Discussion

The determined structure of Pdr5 represents the first high resolution 3D structure of an ABC transporter from fungi in general and in particular the class of PDR ABC transporter that exists in plants and fungi. Since Pdr5 belongs to the ABCG subfamily of ABC transporters (Paumi et al., 2009), it is not surprising that the overall fold of the protein resembles that of type II exporters such as the MDR exporter ABCG2 and the sterol transporter ABCG5/ABCG8, respectively (Lee et al., 2016; Taylor et al., 2017). However, our structural models, based on the different electron density maps, revealed certain key features that were not observed in other structures of ABC exporters. Compared to ABCG2 as well as ABCG5/ABCG8, the extracellular loops (ECLs) of Pdr5 are significantly larger. In a mutational study of Cdr1 and Pdr5, it was demonstrated that the ECLs play a critical role in drug release and therefore in the conferred resistance by the transporter (Tanabe et al., 2019). The observed movement of the coupling helix of the N-terminal half of Pdr5 between the apo and occluded state indicates how the transmission interface between the NBDs and TMDs take place in this transporter. Interestingly, only the N-terminal half shows a shift of transmembrane helices while the C-terminal part is rigid. This observation could indicate that the transporter is not undergoing the classical ‘alternating access model’ (Jardetzky, 1966) movement, but the movement represents rather a twisting of the transmembrane domain without an actual drug release through the extracellular loops. This ‘twist model’ could also explain, how the drug efflux takes place. The substrates of Pdr5 are – with a few exceptions – all hydrophobic (Kolaczowski et al., 1996; Rogers et al., 2001) and will freely partition into the membrane. It is to assume that Pdr5 takes up the drugs from the inner leaflet of the membrane in order to expel them. The hydrophobic nature of these compounds makes it energetically disadvantageous to transport the drug through a water filled cavity into the extracellular space. Therefore, it is tempting to speculate that the actual transport process rather takes place at the membrane/protein interface from the inner to the outer leaflet of the membrane, which does not require an opening of the extracellular loops but instead a twist of the transmembrane helices. To further elucidate the possible molecular mechanism of ATP binding, hydrolysis and drug efflux, we have to look closer into the degenerated NBS of Pdr5. In the literature, two models exist that describe how the NBDs dimerize upon ATP binding and dissociate (or do not dissociate)

upon ATP hydrolysis. The first one is called the ‘switch model’ and proposes that the NBDs of an ABC transporter form a symmetrical dimer with two ATP molecules bound, which dissociate to two monomers after ATP hydrolysis (Higgins and Linton, 2004). A second model, the ‘constant contact model’, however, describes a mechanism in which the hydrolysis of ATP takes place in an alternating fashion in each of the NBS and thereby the NBD stay in constant contact throughout the catalytic cycle (Jones and George, 2013). However, in the case of Pdr5 and probably other asymmetric ABC transporters, a different mechanism than these described by the two models has to be operational for the individual molecular steps during transport. The fact that the degenerated NBS lacks key residues in each of the NBD motifs renders this site incapable to hydrolyze ATP (Gupta et al., 2014). Moreover, the distance shown here in our model of 3.4 Å between the arginine of the Walker A motif in NBD1 and the glutamine of the C-loop in NBD2 is too small to allow binding of an ATP molecule ($R_{SE} = 7 \text{ \AA}$ (Azarashvili et al., 2011)), but is close enough for a hydrogen bond or salt bridge (Jeffrey, 1997; Walker and Causgrove, 2009). Therefore, we can propose an alteration of the ‘constant contact model’ in which, based on their asymmetry, the NBDs are indeed always dimerized, even in the absence of ATP. Only the canonical NBS induces the movement of the TMDs through binding and hydrolysis of ATP.

In summary, the here presented structure and electron densities of the asymmetric ABC transporter Pdr5 in the apo and occluded state provides important insights into the molecular mechanism of this class of membrane proteins. Existing models like the ‘switch model’ and ‘constant contact model’ are not sufficient to describe the molecular mechanism that underlies the energy transmission between the NBDs and TMDs of Pdr5. This might hold as well for other asymmetric export pumps. Additionally, the electron density of the occluded state points to a transport mechanism that differs from the ‘alternating access model’ as it appears that the transmembrane helices undergo a twist movement that might enable the transport from the inner to the outer leaflet.

References

- Ananthaswamy, N., Rutledge, R., Sauna, Z.E., Ambudkar, S.V., Dine, E., Nelson, E., Xia, D., and Golin, J. (2010). The signaling interface of the yeast multidrug transporter Pdr5 adopts a cis conformation, and there are functional overlap and equivalence of the deviant and canonical Q-loop residues. *Biochemistry* 49, 4440-4449.
- Azarashvili, T.S., Odinkova, I.V., Krestinina, O.V., Baburina, Y.L., Grachev, D.E., Teplova, V.V., and Holmuhamedov, E.L. (2011). Role of phosphorylation of porin (VDAC) in regulation of mitochondrial outer membrane under normal conditions and alcohol intoxication. *Biochemistry (Moscow) Supplement Series A: Membrane and Cell Biology* 5, 11-20.
- Bayburt, T.H., and Sligar, S.G. (2010). Membrane protein assembly into Nanodiscs. *FEBS Lett* 584, 1721-1727.
- Carlson, M.L., Young, J.W., Zhao, Z., Fabre, L., Jun, D., Li, J., Li, J., Dhupar, H.S., Wason, I., Mills, A.T., *et al.* (2018). The Peptidisc, a simple method for stabilizing membrane proteins in detergent-free solution. *Elife* 7.
- Chen, J., Noble, A.J., Kang, J.Y., and Darst, S.A. (2019). Eliminating effects of particle adsorption to the air/water interface in single-particle cryo-electron microscopy: Bacterial RNA polymerase and CHAPSO. *Journal of Structural Biology: X* 1, 100005.
- Cheng, Y.F. (2018). Single-particle cryo-EM-How did it get here and where will it go. *Science* 361, 876-+.
- Du, D., Wang, Z., James, N.R., Voss, J.E., Klimont, E., Ohene-Agyei, T., Venter, H., Chiu, W., and Luisi, B.F. (2014). Structure of the AcrAB-TolC multidrug efflux pump. *Nature* 509, 512-515.
- Ernst, R., Kueppers, P., Klein, C.M., Schwarzmüller, T., Kuchler, K., and Schmitt, L. (2008). A mutation of the H-loop selectively affects rhodamine transport by the yeast multidrug ABC transporter Pdr5. *Proc Natl Acad Sci U S A* 105, 5069-5074.

Golin, J., and Ambudkar, S.V. (2015). The multidrug transporter Pdr5 on the 25th anniversary of its discovery: an important model for the study of asymmetric ABC transporters. *Biochem J* **467**, 353-363.

Golin, J., Kon, Z.N., Wu, C.P., Martello, J., Hanson, L., Supernavage, S., Ambudkar, S.V., and Sauna, Z.E. (2007). Complete inhibition of the Pdr5p multidrug efflux pump ATPase activity by its transport substrate clotrimazole suggests that GTP as well as ATP may be used as an energy source. *Biochemistry* **46**, 13109-13119.

Gupta, R.P., Kueppers, P., Hanekop, N., and Schmitt, L. (2014). Generating symmetry in the asymmetric ATP-binding cassette (ABC) transporter Pdr5 from *Saccharomyces cerevisiae*. *J Biol Chem* **289**, 15272-15279.

Higgins, C.F. (2001). ABC transporters: physiology, structure and mechanism--an overview. *Research in microbiology* **152**, 205-210.

Higgins, C.F., and Linton, K.J. (2004). The ATP switch model for ABC transporters. *Nat Struct Mol Biol* **11**, 918-926.

Hohl, M., Briand, C., Grutter, M.G., and Seeger, M.A. (2012). Crystal structure of a heterodimeric ABC transporter in its inward-facing conformation. *Nat Struct Mol Biol* **19**, 395-402.

Jardetzky, O. (1966). Simple allosteric model for membrane pumps. *Nature* **211**, 969-970.

Jeffrey, G.A. (1997). *An Introduction to Hydrogen Bonding* (Oxford University Press).

Jones, P.M., and George, A.M. (2013). Mechanism of the ABC transporter ATPase domains: catalytic models and the biochemical and biophysical record. *Crit Rev Biochem Mol Biol* **48**, 39-50.

Kolaczowski, M., Michel, v.d.R., Cybularz-Kolaczowska, A., Soumillion, J.P., Konings, W.N., and Andre, G. (1996). Anticancer Drugs, Ionophoric Peptides, and Steroids as Substrates of the Yeast Multidrug Transporter Pdr5p. *Journal of Biological Chemistry* **271**, 31543-31548.

Kueppers, P., Gupta, R.P., Stindt, J., Smits, S.H., and Schmitt, L. (2013). Functional impact of a single mutation within the transmembrane domain of the multidrug ABC transporter Pdr5. *Biochemistry* 52, 2184-2195.

Lage, H. (2003). ABC-transporters: implications on drug resistance from microorganisms to human cancers. *Int J Antimicrob Agents* 22, 188-199.

Lamping, E., Baret, P.V., Holmes, A.R., Monk, B.C., Goffeau, A., and Cannon, R.D. (2010). Fungal PDR transporters: Phylogeny, topology, motifs and function. *Fungal Genet Biol* 47, 127-142.

Lee, J.Y., Kinch, L.N., Borek, D.M., Wang, J., Wang, J., Urbatsch, I.L., Xie, X.S., Grishin, N.V., Cohen, J.C., Otwinowski, Z., *et al.* (2016). Crystal structure of the human sterol transporter ABCG5/ABCG8. *Nature* 533, 561-564.

Lee, J.Y., and Rosenbaum, D.M. (2017). Transporters Revealed. *Cell* 168, 951-953.

Leppert, G., McDevitt, R., Falco, S.C., Van Dyk, T.K., Ficke, M.B., and Golin, J. (1990). Cloning by gene amplification of two loci conferring multiple drug resistance in *Saccharomyces*. *Genetics* 125, 13-20.

Locher, K.P. (2016). Mechanistic diversity in ATP-binding cassette (ABC) transporters. *Nat Struct Mol Biol* 23, 487-493.

Oswald, C., Holland, I.B., and Schmitt, L. (2006). The motor domains of ABC-transporters. What can structures tell us? *Naunyn Schmiedebergs Arch Pharmacol* 372, 385-399.

Paumi, C.M., Chuk, M., Snider, J., Stagljar, I., and Michaelis, S. (2009). ABC transporters in *Saccharomyces cerevisiae* and their interactors: new technology advances the biology of the ABCC (MRP) subfamily. *Microbiology and molecular biology reviews : MMBR* 73, 577-593.

Prasad, R., Banerjee, A., Khandelwal, N.K., and Dhamgaye, S. (2015). The ABCs of *Candida albicans* Multidrug Transporter Cdr1. *Eukaryot Cell* 14, 1154-1164.

Rees, D.C., Johnson, E., and Lewinson, O. (2009). ABC transporters: the power to change. *Nature reviews Molecular cell biology* 10, 218-227.

Rogers, B., Decottignies, A., Kolaczowski, M., Carvajal, E., Balzi, E., and Goffeau, A. (2001). The pleiotropic drug ABC transporters from *Saccharomyces cerevisiae*. *J Mol Microb Biotech* 3, 207-214.

Sauna, Z.E., Bohn, S.S., Rutledge, R., Dougherty, M.P., Cronin, S., May, L., Xia, D., Ambudkar, S.V., and Golin, J. (2008). Mutations define cross-talk between the N-terminal nucleotide-binding domain and transmembrane helix-2 of the yeast multidrug transporter Pdr5: possible conservation of a signaling interface for coupling ATP hydrolysis to drug transport. *J Biol Chem* 283, 35010-35022.

Schmitt, L., and Tampe, R. (2002). Structure and mechanism of ABC transporters. *Curr Opin Struct Biol* 12, 754-760.

Sorum, B., Torocsik, B., and Csanady, L. (2017). Asymmetry of movements in CFTR's two ATP sites during pore opening serves their distinct functions. *Elife* 6.

Subramaniam, S., Earl, L.A., Falconieri, V., Milne, J.L., and Egelman, E.H. (2016). Resolution advances in cryo-EM enable application to drug discovery. *Curr Opin Struct Biol* 41, 194-202.

Tanabe, K., Bonus, M., Tomiyama, S., Miyoshi, K., Nagi, M., Niimi, K., Chindamporn, A., Gohlke, H., Schmitt, L., Cannon, R.D., *et al.* (2019). FK506 Resistance of *Saccharomyces cerevisiae* Pdr5 and *Candida albicans* Cdr1 Involves Mutations in the Transmembrane Domains and Extracellular Loops. *Antimicrob Agents Chemother* 63.

Taylor, N.M.I., Manolaridis, I., Jackson, S.M., Kowal, J., Stahlberg, H., and Locher, K.P. (2017). Structure of the human multidrug transporter ABCG2. *Nature* 546, 504-509.

Wagner, M., Smits, S.H.J., and Schmitt, L. (2019). In vitro NTPase activity of highly purified Pdr5, a major yeast ABC multidrug transporter. *Scientific reports* 9, 7761.

Walker, K.D., and Causgrove, T.P. (2009). Contribution of arginine-glutamate salt bridges to helix stability. *Journal of molecular modeling* 15, 1213-1219.

Wang, J., Grishin, N., Kinch, L., Cohen, J.C., Hobbs, H.H., and Xie, X.S. (2011). Sequences in the nonconsensus nucleotide-binding domain of ABCG5/ABCG8 required for sterol transport. *J Biol Chem* 286, 7308-7314.

Wang, Z., Fan, G., Hryc, C.F., Blaza, J.N., Serysheva, I.I., Schmid, M.F., Chiu, W., Luisi, B.F., and Du, D. (2017). An allosteric transport mechanism for the AcrAB-TolC multidrug efflux pump. *eLife* 6, e24905.

4. Discussion

This thesis focusses on elucidating the molecular mechanism of substrate transport of the asymmetric ABC transporter Pdr5 from *S. cerevisiae*. In a first step and in order to perform biochemical, functional and structural analysis *in vitro*, it was necessary to establish an isolation and purification protocol for the protein in an active and functional state. Initial studies performed by Decottignies *et al.* indicated that n-Dodecyl- β -D-maltoside (DDM) as a detergent might retain the ATPase activity of Pdr5 (Decottignies *et al.*, 1994). So far, we have not been able to reproduce these results and instead had to experience that Pdr5 does not retain any significant ATPase activity in DDM. Extensive detergent screens and optimization of the purification protocol led to functional and homogenous Pdr5 as described in detail in Chapter II. The key to the final success was the use of the detergent trans-4-(trans-4'-propylcyclohexyl)cyclohexyl- α -D-maltoside (trans-PCC- α -M) (Hovers *et al.*, 2011). Only this detergent allowed to purify Pdr5 in a two-step procedure (immobilized metal ion chromatography (IMAC) (loaded with Zn²⁺ ions) in combination with size exclusion chromatography (SEC)) to homogeneity while retaining its ATPase activity (see Chapter II, Figures 1-3).

Although it remains elusive why certain detergents retain the activity of a membrane protein while others, even structurally similar detergents inactivate the protein, we can speculate that some features of trans-PCC- α -M are beneficial to maintain Pdr5 functionality. Trans-PCC- α -M is a mild, non-ionic detergent of the class of maltosides that are widely used in the field of membrane protein purification (Seddon *et al.*, 2004). Comparing the structures of one of the most prominent member of the class of maltosides DDM and trans-PCC- α -M (Figure 5) it becomes apparent that the more bulky di-cyclohexyl moiety of trans-PCC- α -M gives a more rigid hydrophobic structure compared to the alkyl chain of DDM. One might therefore speculate that exactly this rigidity is the cause for the mildness of the detergent as there will be fewer interactions with the hydrophobic transmembrane parts of the protein and less tightly bound lipids will be displaced by the detergent (Hovers *et al.*, 2011)

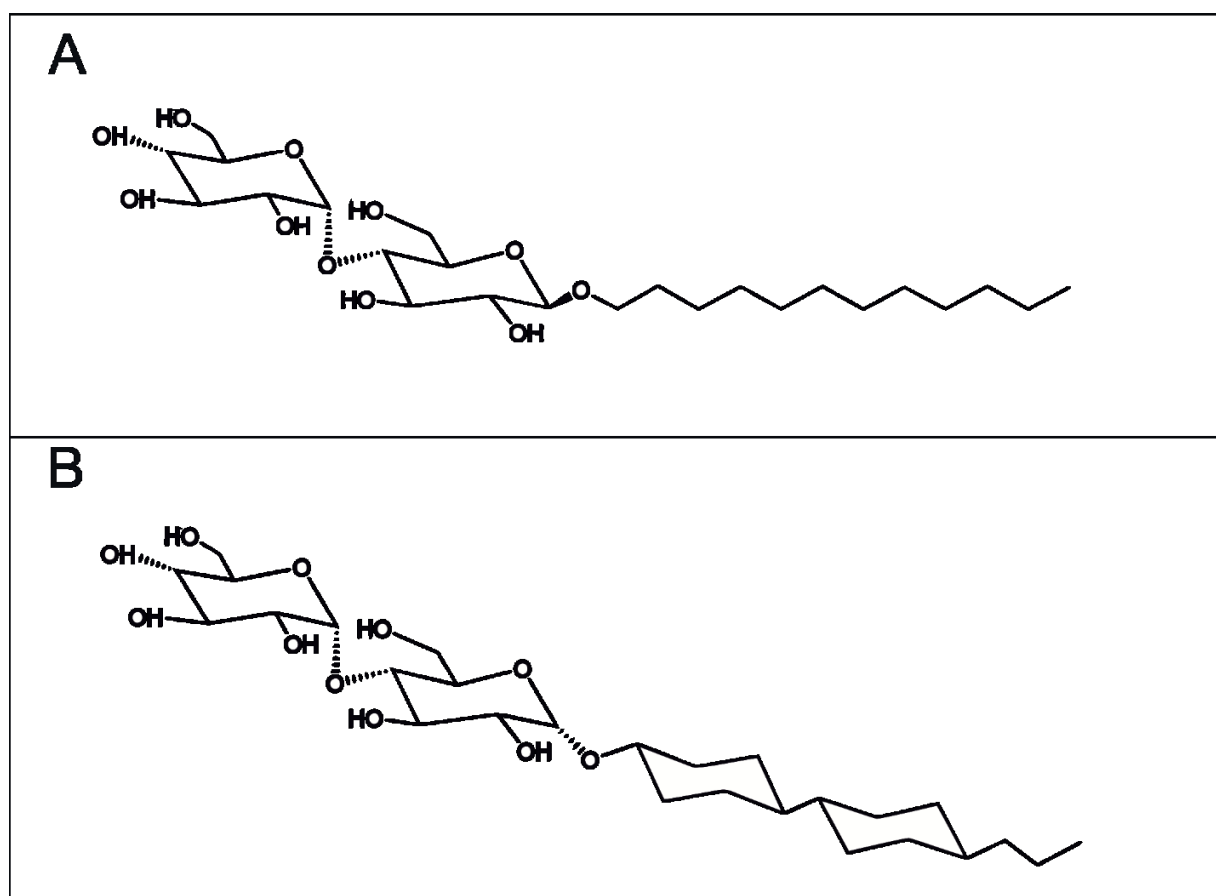


Figure 5 Structural comparison of two maltosides. A: n-Dodecyl- β -D-maltoside (DDM). **B:** trans-4-(trans-4'-propylcyclohexyl)cyclohexyl- α -D-maltoside (trans-PCC- α -M).

After this basic task was fulfilled, biochemical, biophysical and structural analysis of this efflux pump could be performed. During these investigations, the following four discoveries on the molecular basics of the Pdr5 activity were obtained:

First, Pdr5 has a high basal NTPase activity in solution that cannot further stimulated by its substrates but at high concentrations undergoes trans-inhibition.

Second, Pdr5 functions as an H^+ /drug symporter and therefore represents a new class of ABC transporters.

Third, the NBDs of Pdr5 are always dimerized even in the absence of ATP, which is based on the degenerated NBS.

Fourth, Pdr5 might not follow the 'alternating access model' with two distinct inward and outward facing conformations but rather function in a twist-like fashion that allows substrate transport at the membrane-protein interface from the inner to the outer leaflet of the membrane.

4.1 Pdr5 is an uncoupled transporter

Since its discovery, it was always controversial discussed whether the high basal ATPase activity of Pdr5 in plasma membrane preparations is artificial, if it's due to the 'real' substrate being present or whether this ABC transporter is in fact an uncoupled transporter that hydrolyzes ATP at high rates even in the absence of a substrate that cannot be further stimulated (Decottignies et al., 1994; Ernst et al., 2008; Golin and Ambudkar, 2015). Other MDR ABC transporters like P-gp are strictly coupled transporters with a rather low basal ATPase activity that can be stimulated by its substrates which was shown for membrane vesicles as well as in detergent purified preparations (Shukla et al., 2017). The data presented in Chapter II of isolated, detergent purified Pdr5 wildtype in comparison to the ATPase deficient E1036Q mutant proves that the ATPase activity is indeed uncoupled from transport activity. Similar to plasma membrane preparations the ATPase activity cannot be stimulated beyond the basal level, but Pdr5 undergoes allosteric or trans-inhibition at high substrate concentrations (see Chapter II, Figure 7) (Ernst et al., 2008). This on the first sight futile ATPase activity in the absence of substrate makes sense if one considers the broad substrate specificity of Pdr5 (Kolaczkowski et al., 1996; Rogers et al., 2001). As stated by *Ernst et al.*, it is difficult to imagine for MDR ABC transporters how the binding of hundreds of structurally and physicochemical diverse substrates can lead to the same response of the transporter in upregulating its ATPase activity (Ernst et al., 2008). Moreover, given the importance of the efflux pump Pdr5 for cell survivability in the presence of xenobiotics, the response time to toxic compounds should be as short as possible while the lifetime of the transporter should be considerable high. As shown for the ABC transporter BtuC₂D₂, the protein remains stable over a longer period with a shorter response time towards the addition of substrate if ATP is continuously added compared to the same protein under starving conditions (Livnat-Levanon et al., 2016).

The fact that isolated, detergent-purified Pdr5 exhibits a high basal ATPase activity supports the finding that this ABC transporter works in fact uncoupled. From a physiological perspective, basal ATPase activity is necessary for MDR ABC efflux pumps as they need to be able to respond fast upon presence of xenobiotic compounds in order to protect the cell.

4.2 Pdr5 as a proton pump and its implications

The most common model to explain the drug resistance conferred by ABC transporters is the 'pump model'. In this model, the MDR ABC transporter actively expel the drugs from the cell into the extracellular space against a concentration gradient (Gottesman and Pastan, 1988). Although most biochemical studies support this model some key features of MDR pumps are not explained by it. Therefore, the 'altered partitioning model' challenges the 'pump model' as it assumes MDR ABC transporter do not actively transport their substrates but rather change the membrane environment by ion transport which leads to lowered drug accumulation within the cells (Roepe, 2000; Roepe et al., 1996). This model was mainly discussed in the field of MDR1 and supported by data demonstrating elevated intracellular pH of MDR1 containing cell lines and changed ion concentrations as well as the argument of lack of MDR1 substrate specificity (Hoffman and Roepe, 1997). Nonetheless, these findings are not sufficient to account for the magnitude of fold increase in resistance of MDR cell lines (Ambudkar et al., 1999).

Interestingly, during our biochemical and biophysical characterization of Pdr5, we discovered that not the 'pump model' nor the 'altered partitioning model' are sufficient to describe the mechanism of Pdr5 conferred drug resistance. *In vivo* studies on MDR1 and the Pdr5 homologue Cdr1 from *Candida albicans* indicated altered intracellular pH compared to null-mutant cells, supporting the 'altered partitioning model' (Hoffman and Roepe, 1997; Milewski et al., 2001). Unfortunately, the complexity of the cell environment renders *in vivo* studies unsuitable to draw exact direct conclusions from the multitude of altered cellular parameters. Therefore, we reconstituted purified functional Pdr5 into planar lipid bilayers and performed electrophysiological measurements in the absence and presence of substrates and inhibitors (see Chapter III). The electrophysiological data on the reconstituted Pdr5 demonstrate that Pdr5 can facilitate permeation of K⁺ and Cl⁻ ions at high rates across the membrane. Moreover, in the

presence of Mg^{2+} -ATP and substrates, Pdr5 can generate a proton motive force (ΔpH) across the membrane by acting as a proton/drug symporter (see Chapter IV). At the same time, the measured difference of the reversal potentials between the neutral ketoconazole and charged rhodamine 6G (R6G) proves that not only a proton gradient is established, but also the R6G substrate is actively transported across the bilayer. Although in a study of the ABC transporter LmrA and MsbA indications of ion transport and effects of ions on the translocation activity were shown, these studies did not provide direct evidence of a generated proton gradient nor active substrate transport (Agboh et al., 2018; Singh et al., 2016). Remarkably, in the yeast *S. cerevisiae* only two classes of MDR efflux pumps are known so far: MDR ABC transporter and major facilitator superfamily (MFS) transporter that all function as drug/ H^+ antiporters. Pdr5 is therefore the first representative of a new type of drug/ H^+ ABC symporter. Similar transporters have not been identified yet. Since no other ABC transporter so far was systematically examined by electrophysiological means, it remains unclear (i) whether this is a general mechanism of MDR ABC transporters, or (ii) whether it is a feature of asymmetric ABC transporters, or (iii) solely a unique characteristic of Pdr5, which, given the observations of *in vivo* studies performed on MDR1 and Cdr1, seems rather unlikely.

4.3 On the proposed R6G transport mechanism mediated by Pdr5

One of the most commonly used biochemical assays for Pdr5 is the R6G transport assay in isolated inside-out plasma membrane vesicles ((Ernst et al., 2008; Kolaczowski et al., 1996; Kueppers et al., 2013)). In these vesicles, the NBDs of the transporter are situated outside of the vesicles, which enables the substrate transport into the vesicle lumen (see Figure 6). Since its first appearance, it was described as a concentration-dependent quenching assay in which R6G molecules undergo self-quenching by forming non-fluorescent excimers (Figure 6A) (Ernst et al., 2008; Furman et al., 2013; Kolaczowski et al., 1996).

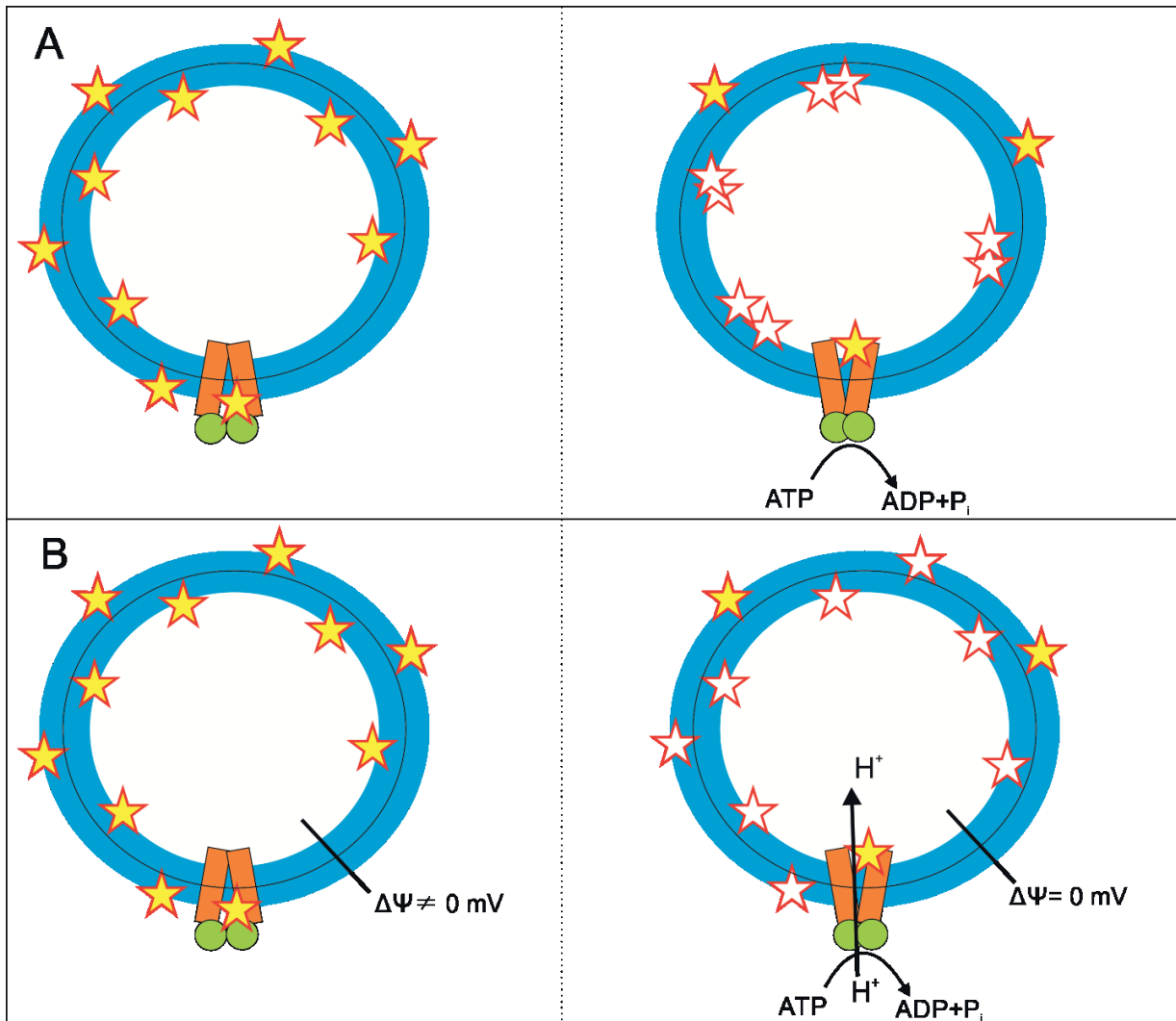


Figure 6 Schematic overview of the R6G transport assay mediated by Pdr5. **A:** R6G transport assay with fluorescence quenching based on concentration dependent non-fluorescent excimer formation upon transport initiation by ATP addition. Left panel: Pdr5 is inside-out oriented in the vesicle membrane and R6G molecules are evenly distributed between the two leaflets. Right panel: ATP addition initiates the Pdr5-mediated transport of R6G from the outer to the inner leaflet where concentration dependent self-quenching of R6G excimers takes place. **B:** R6G fluorescence quenching based on depolarization of the vesicle membrane. Left panel: as in **A**, Pdr5 is inside-out oriented. The R6G molecules are evenly distributed and highly fluorescent as an intact membrane potential ($\Delta\Psi \neq 0$ mV) is given. Right panel: upon ATP addition, Pdr5 actively transports R6G and H^+ which leads to the depolarization of the membrane ($\Delta\Psi = 0$ mV) which causes quenching of the R6G fluorescence. Note that although R6G is transported in **B**, it remains evenly distributed across the membrane as it freely diffuses between the membrane leaflets. Pdr5 is depicted with its TMDs in orange, the NBDs in green; the vesicle membrane is shown in blue; fluorescent R6G molecules as yellow stars, quenched R6G molecules as white stars.

Without doubt, we can confirm that following published protocols a Pdr5 and Mg²⁺-ATP-dependent fluorescence quenching is observed. However, it is to question whether it is concentration-dependent or if there might be other reasons causing the quenching of R6G fluorescence. In R6G transport assays with Pdr5 containing plasma membrane vesicles, a R6G concentration between 75 – 600 nM is commonly used, although R6G causes trans-inhibition with a $K_i = 600$ nM (Ernst et al., 2008; Furman et al., 2013; Kolaczkowski et al., 1996; Kueppers et al., 2013). Now, if we consider the partition coefficient of R6G of $\log P = 6.52$ (see Chapter II, Table 2), virtually all R6G molecules will be located in the membrane, roughly equally distributed between the inner and outer leaflet. Next, if an initial concentration of 300 nM is used, the concentration at start within one leaflet is approximately 150 nM and at the end of the transport assay - assuming 100% transport rate - 300 nM in the inner leaflet, causing complete quenching of the R6G fluorescence (see Figure 6A). Now, if a start concentration for R6G of 600 nM is chosen instead, the concentration in both membrane leaflets will be 300 nM at the beginning of the experiment. This is the concentration that arguably led to the complete quenching of R6G in the experiment with an initial concentration of 300 nM. We would expect a complete self-quenching at the beginning of the experiment with a start concentration for R6G of 600 nM. Instead, the fluorescence increases and only after addition of ATP a decrease in fluorescence is observed. Moreover, complete fluorescence self-quenching of R6G is not to be expected at concentrations below 40 μ M, which is probably not reached in experiments with concentrations far below 1 μ M as it is usually the case in Pdr5 transport assays (Bavali et al., 2015).

Another explanation for the observed fluorescence decrease can be derived from the use of R6G as a mitochondrial marker, as it passes the outer mitochondrial membrane and accumulates at the inner mitochondrial membrane that carries an electronegative potential of about $V_m = -180$ mV (Scaduto and Grotyohann, 1999; Trounce and Wallace, 1996; Ziegler and Davidson, 1981). In a study with R6G as a probe for membrane potential in bovine aortic endothelial cells, it was shown that R6G is strongly responsive to the membrane potential as it is highly fluorescent if an intact membrane potential exists, while it can be completely quenched if the membrane is depolarized (Mandala et al., 1999). Now, taking this into consideration for the transport assay in combination with the fact that Pdr5 is a drug/H⁺ symporter, we can come to the conclusion that the reason for the fluorescence decrease is very likely the result of a

depolarization of the membrane by Pdr5-mediated proton transport (see Figure 6B). It is important to note that the R6G transport assay is only established for plasma membrane vesicles in which numerous other pumps and ion channels like the proton pump Pma1 are present. So far, we were not able to perform the R6G transport assay with isolated Pdr5 reconstituted into liposomes, which is possibly caused by the missing initial polarization of the membrane generated by other electrogenic pumps present in plasma membrane vesicles.

4.4 The structure of Pdr5

So far, only structures of bacterial type I and type II importers, e.g. ModBC-A and BtuCD-F and type I exporters like Sav1866 as well as mammalian type I (e.g. MDR1) and type II exporters (ABCG5/G8 and ABCG2) have been determined (Dawson and Locher, 2006; Lee et al., 2016; Taylor et al., 2017). However, structures of plant and fungal ABC transporter have not been reported to date.

In Chapter IV, we present the first structure of the ABC transporter Pdr5, which at the same time is the first structure of a fungal ABC transporter in general. As infectious diseases with fungal pathogens is a growing risk (Pfaller and Diekema, 2007), it is important to develop new strategies and treatments as the limiting number of clinically used antifungals leads to rising multidrug resistance (Cannon et al., 2009). The presented structure of Pdr5 provides new insights into the molecular mechanisms of fungal MDR ABC transporters and can open new avenues to determine new drug target sites in pathogenic homologues such as Cdr1 from *C. albicans*.

4.5 Asymmetry of the NBDs – A new constant contact model

The ‘switch model’ is the most prominent model for describing the process of energizing the substrate transport of ABC efflux pumps (Higgins and Linton, 2004). Here, the NBDs of a transporter switch between two main conformations: a closed dimer that forms upon ATP binding in both NBS and an open conformation in which the dimer opens up after ATP hydrolysis. The switch between the two conformations drives the conformational change of the TMDs to translocate the substrate. A second model is the ‘constant contact model’ (Jones and George,

2013). The basic steps of ATP binding and hydrolysis driving the overall energization of the catalytic cycle are the same. However, the main difference is that while in the 'switch model' the C-loop (signature motif) and Walker A motif separate completely in both NBS after ATP hydrolysis, the constant contact model assumes that ATP hydrolysis takes place in one NBS at a time and thereby the NBDs always remain as a dimer. It is long ongoing debate with both models having biochemical and structural evidence (Higgins, 2007; Janas et al., 2003; Jones and George, 2009). Based on the complexity and versatility of the huge family of ABC transporters one wonders whether only one of the two, neither or both models can explain the actual mechanism of the catalytic cycle. Especially since, although the NBDs of ABC transporters are highly conserved in sequence and structure compared to their TMDs, variations occur as for example in the case of asymmetric ABC transporters like ABCG5/ABCG8, TM287/288, CFTR or Pdr5 that all have alterations within key motifs of their NBDs (Basso et al., 2003; Furman et al., 2013; Hohl et al., 2012; Wang et al., 2011). As shown in Figure 6A of Chapter IV, the structure of the yeast ABC transporter Pdr5 leads to a different and so far not described model as a basis for the conformational changes. Based on this structure, a constant contact model can be assumed that differs from the model described in literature in two major aspects: ATP hydrolysis does not occur alternatingly in both NBS but only in the canonical NBS while the degenerate site stays in constant contact speculatively by a hydrogen bond between R194 of the N-terminal NBD Walker A and E1013 of the C-terminal NBD C-loop.

The duality in literature between the 'constant contact model' and the 'switch model' does not account for the complexity of the ABC transporter superfamily. The presented structural data in Chapter IV indicates that another mechanism exists that forms the basis for the conformational shifts during the transport cycle. At the same time, it allows for a variation of the well-established 'alternating access model' (Jardetzky, 1966) as only one NBS induces a movement of the TMDs.

4.6 Pdr5 – An ABC transporter with a twist

Based on the electron density maps in the presence and absence of ATP-V_i, i.e. the apo and occluded state of Pdr5 (see Chapter IV, Figure 3D and E), it is apparent that the extracellular

loops of Pdr5 do not open up during the dimerization of the canonical NBD and the induced movement of the coupling helix of the N-terminal TMD. The classical 'alternating access model' describes the switch between two distinct states: the inward- and the outward-facing conformation, facilitated by the association and dissociation of the NBD dimer (Higgins, 2001; Jardetzky, 1966). Several structures of ABC transporters in the presence of nucleotides with or without substrate suggest that the mechanism follows a transport mechanism as depicted in Figure 7A. In the inward-facing conformation, the substrate can bind to the high affinity binding pocket. Upon ATP binding, the NBDs dimerize and the overall conformation switches to the outward-facing conformation that opens up the translocation pathway with the low affinity binding pocket accessible towards the extracellular space and the substrate can exit the efflux pump. Structures of type I exporters like MsbA, BtuC₂D₂, P-gp and TmrAB all support this translocation pathway and mechanism with the ECLs opening towards the extracellular space to release the substrate (Hofmann et al., 2019; Locher et al., 2002; Rosenberg et al., 2003; Ward et al., 2007).

Since Pdr5 belongs to the ABCG subfamily of ABC transporters (Paumi et al., 2009) and as obvious from its structure, it follows the type II exporter fold that was first described for the human sterol transporter ABCG5/ABCG8 (Lee et al., 2016). Two of the key features of the type II exporter fold are that there is no NBD-TMD interdomain crosstalk between the N-terminal and C-terminal half, as described in Chapter I and that in the apo state the NBDs are not as far separated as seen in structures of type I exporters like MDR1. It could be tempting to assume that proteins of the same class with similar structure and type follow the same mechanism. However, as the structure of the human type II MDR ABC transporter ABCG2 suggests, the translocation process for this pump follows the same principle as described in the model in Figure 7A in which the ECLs separate and thereby open the translocation pathway towards the extracellular space to release the substrate. (Manolaridis et al., 2018).

Nonetheless, some open questions remained concerning the transport mechanism regarding structures of ABCG2 in the inward- and outward-facing state, especially in light of its substrate estrone-3-sulfate (E₁S) that was identified in the structure. E₁S is a lipophilic compound with a partition coefficient of logP = 2.36 (Steingold et al., 1986). Therefore, it is likely that this substrate locates within the lipid bilayer and avoids the water-filled pore that forms the

translocation channel. However, the structure and model described in the study suggests that the substrate is released upon opening of the gate that is formed by the ECLs (Manolaridis et al., 2018).

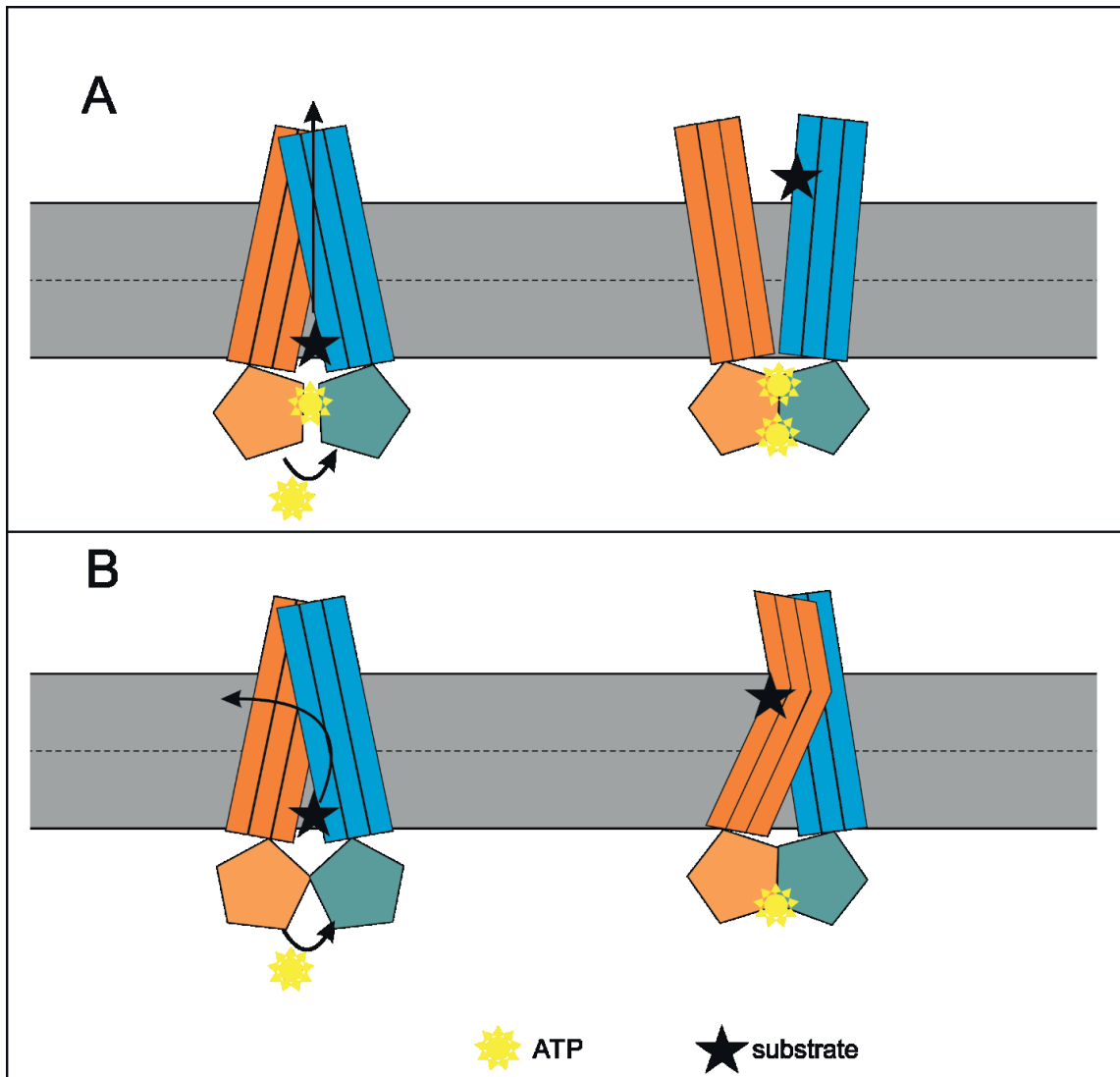


Figure 7 Simplified schematic representation of possible transport mechanisms. A: Alternating access model that shifts between the inward- and the outward-facing conformation. Left panel: the substrate can bind to the high affinity binding pocket that is accessible from the intracellular space. ATP binding leads to the dimerization of the NBDs, which induces the conformational shift of the TMDs. Right panel: the NBDs are dimerized and the low affinity binding pocket is accessible from the extracellular space. B: Twist model based on the constant contact model for Pdr5. Left panel: the substrate binds on the membrane protein interface (inner leaflet) to the high affinity binding pocket. The NBDs are dimerized by the degenerate NBS. ATP binding induces the closure of the canonical NBS that induces the twist-like movement of the N-terminal TMD. Right panel: the substrate diffuses from the accessible low affinity binding pocket into the outer leaflet of the lipid bilayer. The ECLs do not open as the translocation pathway lays within the membrane.

Similar to ABCG2, Pdr5 substrates are – with a few exceptions – hydrophobic with high partition coefficients (see also Chapter II) (Kolaczowski et al., 1996; Rogers et al., 2001). Consequently, these substrates will be concentrated within the membrane and not in solution (intra- or extracellular) where they can be taken up by Pdr5 from the inner leaflet. Our transport model for Pdr5 as depicted in Figure 7B is based on the electron density that was obtained from ATP- V_i trapping, suggests that the translocation process is as follows: Starting in the inward-facing conformation, the substrate is taken up from the inner leaflet of the lipid bilayer into the high affinity binding pocket by Pdr5. Following, the canonical NBS dimerizes upon ATP binding which induces a twist-like shift in the N-terminal TMD. This makes the low affinity binding pocket at the outer-leaflet-protein interface accessible from which the substrate subsequently diffuses into the outer leaflet. During this process the hydrophobic compound does not interact with the water-filled pore and the ECLs do not open towards the extracellular loop.

4.7 Cycloheximide – Transport or degradation?

Pdr5 was first discovered as a gene product in *S. cerevisiae* that confers resistance towards cycloheximide (CYH) (Leppert et al., 1990). CYH is a naturally occurring fungicide that is produced by *Streptomyces griseus* and acts as protein synthesis inhibitor (Müller et al., 2011). Since the discovery of Pdr5, numerous mutational studies on this MDR ABC transporter were conducted. Thereby, the resistance towards CYH was used as a read out in liquid drug or similar microbiological assays to validate whether and how the mutation impacts the transport functionality (Ananthaswamy et al., 2010; Dou et al., 2016; Downes et al., 2013; Golin et al., 2000; Gupta et al., 2014).

Interestingly, CYH is a hydrophilic molecule ($\log P = 0.55$ (Hansch et al., 1995)), which is quite different to all other known Pdr5 substrates. If the proposed ‘twist-model’ holds true (Figure 7B), it is rather unlikely that CYH is taken up by Pdr5 at the membrane-protein interface and in the same way unlikely to exit the transporter towards the membrane. Additionally, CYH does not lead to allosteric or trans-inhibition during the measurement of the Pdr5 ATPase activity like other tested substrates in plasma membrane vesicles (Ernst et al., 2008) or purified in solution (Chapter II). Moreover, when tested as a substrate for electrophysiological measurements with Pdr5 (see

Chapter III), CYH did not cause a Pdr5 induced proton gradient across the membrane like ketoconazole and rhodamine 6G did, which means that it was not transported in symport with protons.

In conclusion, the above described findings could be explained in either of two ways: First, cycloheximide is transported in a different fashion than its hydrophobic counterparts such as ketoconazole or rhodamine 6g. The latter two freely partition into the membrane and are able to enter and exit the transporter at the protein-membrane interface and both are transported together unidirectional with protons (see Chapter III). CYH could be transported through the water-filled pore of the translocation channel as shown in Figure 7A without the co-translocation of protons. The second possibility is that CYH is not a substrate of Pdr5. The fact that it behaves completely different from all other tested substrates and that it is hydrophilic opens up the question, if the effects seen in *in vivo* experiments are directly attributed to Pdr5 or whether indirect effects cause the resistance. CYH is stable at neutral and acidic pH, but rapidly degrades at basal pH (Müller et al., 2011). Assuming Pdr5 is active and transports lipids, steroids or other cellular compounds as suggested (Decottignies et al., 1998; Mahe et al., 1996), it will influence the intracellular pH by pumping protons outwards, leading to a basic cytosolic pH_i. Since CYH degrades at basic pH, the Pdr5-mediated, observed resistance towards this fungicide could be an indirect effect instead of an active extrusion which would eventually mean that CYH is not a real substrate of Pdr5.

5. References

Agboh, K., Lau, C.H.F., Khoo, Y.S.K., Singh, H., Raturi, S., Nair, A.V., Howard, J., Chiapello, M., Feret, R., Deery, M.J., *et al.* (2018). Powering the ABC multidrug exporter LmrA: How nucleotides embrace the ion-motive force. *Science advances* 4, eaas9365.

Alexander, B.D., and Perfect, J.R. (1997). Antifungal resistance trends towards the year 2000. Implications for therapy and new approaches. *Drugs* 54, 657-678.

Ambudkar, S.V., Dey, S., Hrycyna, C.A., Ramachandra, M., Pastan, I., and Gottesman, M.M. (1999). Biochemical, cellular, and pharmacological aspects of the multidrug transporter. *Annual review of pharmacology and toxicology* 39, 361-398.

Ananthaswamy, N., Rutledge, R., Sauna, Z.E., Ambudkar, S.V., Dine, E., Nelson, E., Xia, D., and Golin, J. (2010). The signaling interface of the yeast multidrug transporter Pdr5 adopts a cis conformation, and there are functional overlap and equivalence of the deviant and canonical Q-loop residues. *Biochemistry* 49, 4440-4449.

Armstrong, C.M., and Hille, B. (1998). Voltage-gated ion channels and electrical excitability. *Neuron* 20, 371-380.

Balzi, E., and Goffeau, A. (1995). Yeast multidrug resistance: the PDR network. *J Bioenerg Biomembr* 27, 71-76.

Balzi, E., and Moye-Rowley, W.S. (2019). Unveiling the transcriptional control of pleiotropic drug resistance in *Saccharomyces cerevisiae*: Contributions of Andre Goffeau and his group. *Yeast* 36, 195-200.

Balzi, E., Wang, M., Leterme, S., Van Dyck, L., and Goffeau, A. (1994). PDR5, a novel yeast multidrug resistance conferring transporter controlled by the transcription regulator PDR1. *J Biol Chem* 269, 2206-2214.

Banerjee, A., Vishwakarma, P., Kumar, A., Lynn, A.M., and Prasad, R. (2019). Information theoretic measures and mutagenesis identify a novel linchpin residue involved in substrate selection within the nucleotide-binding domain of an ABCG family exporter Cdr1p. *Archives of biochemistry and biophysics* 663, 143-150.

Bao, H., and Duong, F. (2012). Discovery of an auto-regulation mechanism for the maltose ABC transporter MalFGK2. *PloS one* 7, e34836.

- Basso, C., Vergani, P., Nairn, A.C., and Gadsby, D.C. (2003). Prolonged nonhydrolytic interaction of nucleotide with CFTR's NH₂-terminal nucleotide binding domain and its role in channel gating. *J Gen Physiol* 122, 333-348.
- Bavali, A., Parvin, P., Mortazavi, S.Z., and Nourazar, S.S. (2015). Laser induced fluorescence spectroscopy of various carbon nanostructures (GO, G and nanodiamond) in Rd6G solution. *Biomedical optics express* 6, 1679-1693.
- Bénédicte, P., Jacek, S., and André, G. (1991). The product of the YCR105 gene located on the chromosome III from *Saccharomyces cerevisiae* presents homologies to ATP-dependent permeases. *Yeast* 7, 867-872.
- Biemans-Oldehinkel, E., Doeven, M.K., and Poolman, B. (2006). ABC transporter architecture and regulatory roles of accessory domains. *FEBS Lett* 580, 1023-1035.
- Bienert, G.P., Moller, A.L., Kristiansen, K.A., Schulz, A., Moller, I.M., Schjoerring, J.K., and Jahn, T.P. (2007). Specific aquaporins facilitate the diffusion of hydrogen peroxide across membranes. *J Biol Chem* 282, 1183-1192.
- Blair, J.M., Webber, M.A., Baylay, A.J., Ogbolu, D.O., and Piddock, L.J. (2015). Molecular mechanisms of antibiotic resistance. *Nature reviews Microbiology* 13, 42-51.
- Borst, P., and Elferink, R.O. (2002). Mammalian ABC transporters in health and disease. *Annual review of biochemistry* 71, 537-592.
- Bublitz, M., Morth, J.P., and Nissen, P. (2011). P-type ATPases at a glance. *Journal of Cell Science* 124, 3917-3917.
- Cannon, R.D., Lamping, E., Holmes, A.R., Niimi, K., Baret, P.V., Keniya, M.V., Tanabe, K., Niimi, M., Goffeau, A., and Monk, B.C. (2009). Efflux-mediated antifungal drug resistance. *Clinical microbiology reviews* 22, 291-321, Table of Contents.
- Chang, G. (2003). Multidrug resistance ABC transporters. *FEBS Letters* 555, 102-105.
- Choudhury, H.G., Tong, Z., Mathavan, I., Li, Y., Iwata, S., Zirah, S., Rebuffat, S., van Veen, H.W., and Beis, K. (2014). Structure of an antibacterial peptide ATP-binding cassette transporter in a novel outward occluded state. *Proc Natl Acad Sci U S A* 111, 9145-9150.
- Cocucci, E., Kim, J.Y., Bai, Y., and Pabla, N. (2017). Role of Passive Diffusion, Transporters, and Membrane Trafficking-Mediated Processes in Cellular Drug Transport. *Clinical pharmacology and therapeutics* 101, 121-129.

- Dawson, R.J., and Locher, K.P. (2006). Structure of a bacterial multidrug ABC transporter. *Nature* 443, 180-185.
- Decottignies, A., Grant, A.M., Nichols, J.W., de Wet, H., McIntosh, D.B., and Goffeau, A. (1998). ATPase and multidrug transport activities of the overexpressed yeast ABC protein Yor1p. *J Biol Chem* 273, 12612-12622.
- Decottignies, A., Kolaczowski, M., Balzi, E., and Goffeau, A. (1994). Solubilization and characterization of the overexpressed PDR5 multidrug resistance nucleotide triphosphatase of yeast. *Journal of Biological Chemistry* 269, 12797-12803.
- Decottignies, A., Lambert, L., Catty, P., Degand, H., Epping, E.A., Moye-Rowley, W.S., Balzi, E., and Goffeau, A. (1995). Identification and characterization of SNQ2, a new multidrug ATP binding cassette transporter of the yeast plasma membrane. *J Biol Chem* 270, 18150-18157.
- Decottignies, A., Owsianik, G., and Ghislain, M. (1999). Casein kinase I-dependent phosphorylation and stability of the yeast multidrug transporter Pdr5p. *The Journal of biological chemistry* 274, 37139-37146.
- Denning, D.W., and Hope, W.W. (2010). Therapy for fungal diseases: opportunities and priorities. *Trends in microbiology* 18, 195-204.
- Dou, W., Zhu, J., Wang, T., Wang, W., Li, H., Chen, X., and Guan, W. (2016). Mutations of charged amino acids at the cytoplasmic end of transmembrane helix 2 affect transport activity of the budding yeast multidrug resistance protein Pdr5p. *FEMS Yeast Research*, 1567-1364.
- Downes, M.T., Mehla, J., Ananthaswamy, N., Wakschlag, A., Lamonde, M., Dine, E., Ambudkar, S.V., and Golin, J. (2013). The transmission interface of the *Saccharomyces cerevisiae* multidrug transporter Pdr5: Val-656 located in intracellular loop 2 plays a major role in drug resistance. *Antimicrob Agents Chemother* 57, 1025-1034.
- Eckford, P.D., and Sharom, F.J. (2008). Interaction of the P-glycoprotein multidrug efflux pump with cholesterol: effects on ATPase activity, drug binding and transport. *Biochemistry* 47, 13686-13698.
- Elmlund, D., Le, S.N., and Elmlund, H. (2017). High-resolution cryo-EM: the nuts and bolts. *Curr Opin Struct Biol* 46, 1-6.
- Engelman, D.M. (2005). Membranes are more mosaic than fluid. *Nature* 438, 578-580.

Ernst, R., Kueppers, P., Klein, C.M., Schwarzmüller, T., Kuchler, K., and Schmitt, L. (2008). A mutation of the H-loop selectively affects rhodamine transport by the yeast multidrug ABC transporter Pdr5. *Proc Natl Acad Sci U S A* *105*, 5069-5074.

Ernst, R., Kueppers, P., Stindt, J., Kuchler, K., and Schmitt, L. (2010). Multidrug efflux pumps: substrate selection in ATP-binding cassette multidrug efflux pumps--first come, first served? *The FEBS journal* *277*, 540-549.

Furman, C., Mehla, J., Ananthaswamy, N., Arya, N., Kulesh, B., Kovach, I., Ambudkar, S.V., and Golin, J. (2013). The deviant ATP-binding site of the multidrug efflux pump Pdr5 plays an active role in the transport cycle. *J Biol Chem* *288*, 30420-30431.

Golin, J., and Ambudkar, S.V. (2015). The multidrug transporter Pdr5 on the 25th anniversary of its discovery: an important model for the study of asymmetric ABC transporters. *Biochem J* *467*, 353-363.

Golin, J., Barkatt, A., Cronin, S., Eng, G., and May, L. (2000). Chemical specificity of the PDR5 multidrug resistance gene product of *Saccharomyces cerevisiae* based on studies with tri-n-alkyltin chlorides. *Antimicrob Agents Chemother* *44*, 134-138.

Golin, J., Kon, Z.N., Wu, C.P., Martello, J., Hanson, L., Supernavage, S., Ambudkar, S.V., and Sauna, Z.E. (2007). Complete inhibition of the Pdr5p multidrug efflux pump ATPase activity by its transport substrate clotrimazole suggests that GTP as well as ATP may be used as an energy source. *Biochemistry* *46*, 13109-13119.

Gottesman, M.M., Fojo, T., and Bates, S.E. (2002). Multidrug resistance in cancer: role of ATP-dependent transporters. *Nat Rev Cancer* *2*, 48-58.

Gottesman, M.M., and Pastan, I. (1988). The multidrug transporter, a double-edged sword. *J Biol Chem* *263*, 12163-12166.

Gupta, R.P., Kueppers, P., Hanekop, N., and Schmitt, L. (2014). Generating symmetry in the asymmetric ATP-binding cassette (ABC) transporter Pdr5 from *Saccharomyces cerevisiae*. *J Biol Chem* *289*, 15272-15279.

Hansch, C., Leo, A., and Hoekman, D. (1995). Exploring QSAR. Hydrophobic, electronic, and steric constants. ACS Professional Reference Book. ACS, Washington.

Higgins, C.F. (2001). ABC transporters: physiology, structure and mechanism--an overview. *Research in microbiology* *152*, 205-210.

- Higgins, C.F. (2007). Multiple molecular mechanisms for multidrug resistance transporters. *Nature* *446*, 749-757.
- Higgins, C.F., and Linton, K.J. (2004). The ATP switch model for ABC transporters. *Nat Struct Mol Biol* *11*, 918-926.
- Hoffman, M.M., and Roepe, P.D. (1997). Analysis of ion transport perturbations caused by hu MDR 1 protein overexpression. *Biochemistry* *36*, 11153-11168.
- Hofmann, S., Januliene, D., Mehdipour, A.R., Thomas, C., Stefan, E., Bruchert, S., Kuhn, B.T., Geertsma, E.R., Hummer, G., Tampe, R., *et al.* (2019). Conformation space of a heterodimeric ABC exporter under turnover conditions. *Nature* *571*, 580-583.
- Hohl, M., Briand, C., Grutter, M.G., and Seeger, M.A. (2012). Crystal structure of a heterodimeric ABC transporter in its inward-facing conformation. *Nat Struct Mol Biol* *19*, 395-402.
- Hollenstein, K., Dawson, R.J., and Locher, K.P. (2007). Structure and mechanism of ABC transporter proteins. *Curr Opin Struct Biol* *17*, 412-418.
- Hovers, J., Potschies, M., Polidori, A., Pucci, B., Raynal, S., Bonnete, F., Serrano-Vega, M.J., Tate, C.G., Picot, D., Pierre, Y., *et al.* (2011). A class of mild surfactants that keep integral membrane proteins water-soluble for functional studies and crystallization. *Mol Membr Biol* *28*, 171-181.
- International Transporter, C., Giacomini, K.M., Huang, S.M., Tweedie, D.J., Benet, L.Z., Brouwer, K.L., Chu, X., Dahlin, A., Evers, R., Fischer, V., *et al.* (2010). Membrane transporters in drug development. *Nature reviews Drug discovery* *9*, 215-236.
- Janas, E., Hofacker, M., Chen, M., Gompf, S., van der Does, C., and Tampe, R. (2003). The ATP hydrolysis cycle of the nucleotide-binding domain of the mitochondrial ATP-binding cassette transporter Mdl1p. *J Biol Chem* *278*, 26862-26869.
- Jardetzky, O. (1966). Simple allosteric model for membrane pumps. *Nature* *211*, 969-970.
- Jones, P.M., and George, A.M. (2009). Opening of the ADP-bound active site in the ABC transporter ATPase dimer: evidence for a constant contact, alternating sites model for the catalytic cycle. *Proteins* *75*, 387-396.
- Jones, P.M., and George, A.M. (2013). Mechanism of the ABC transporter ATPase domains: catalytic models and the biochemical and biophysical record. *Crit Rev Biochem Mol Biol* *48*, 39-50.

- Jungwirth, H., and Kuchler, K. (2006). Yeast ABC transporters - A tale of sex, stress, drugs and aging. *FEBS Lett* 580, 1131-1138.
- Katzmann, D.J., Hallstrom, T.C., Voet, M., Wysock, W., Golin, J., Volckaert, G., and Moylerowley, W.S. (1995). Expression of an Atp-Binding Cassette Transporter-Encoding Gene (Yor1) Is Required for Oligomycin Resistance in *Saccharomyces-Cerevisiae*. *Mol Cell Biol* 15, 6875-6883.
- Kim, R.B. (2006). Transporters and Drug Discovery: Why, When, and How. *Molecular Pharmaceutics* 3, 26-32.
- Kimura, Y., Kioka, N., Kato, H., Matsuo, M., and Ueda, K. (2007). Modulation of drug-stimulated ATPase activity of human MDR1/P-glycoprotein by cholesterol. *Biochem J* 401, 597-605.
- Kolaczowska, A., and Goffeau, A. (1999). Regulation of pleiotropic drug resistance in yeast. Drug resistance updates : reviews and commentaries in antimicrobial and anticancer chemotherapy 2, 403-414.
- Kolaczowski, M., Michel, v.d.R., Cybularz-Kolaczowska, A., Soumillon, J.P., Konings, W.N., and Andre, G. (1996). Anticancer Drugs, Ionophoric Peptides, and Steroids as Substrates of the Yeast Multidrug Transporter Pdr5p. *Journal of Biological Chemistry* 271, 31543-31548.
- Kontoyiannis, D.P., and Lewis, R.E. (2002). Antifungal drug resistance of pathogenic fungi. *The Lancet* 359, 1135-1144.
- Krasowska, A., Lukaszewicz, M., Bartosiewicz, D., and Sigler, K. (2010). Cell ATP level of *Saccharomyces cerevisiae* sensitively responds to culture growth and drug-inflicted variations in membrane integrity and PDR pump activity. *Biochemical and biophysical research communications* 395, 51-55.
- Kueppers, P., Gupta, R.P., Stindt, J., Smits, S.H., and Schmitt, L. (2013). Functional impact of a single mutation within the transmembrane domain of the multidrug ABC transporter Pdr5. *Biochemistry* 52, 2184-2195.
- Lage, H. (2003). ABC-transporters: implications on drug resistance from microorganisms to human cancers. *Int J Antimicrob Agents* 22, 188-199.
- Lamping, E., Baret, P.V., Holmes, A.R., Monk, B.C., Goffeau, A., and Cannon, R.D. (2010). Fungal PDR transporters: Phylogeny, topology, motifs and function. *Fungal Genet Biol* 47, 127-142.
- Lee, J.Y., Kinch, L.N., Borek, D.M., Wang, J., Wang, J., Urbatsch, I.L., Xie, X.S., Grishin, N.V., Cohen, J.C., Otwinowski, Z., *et al.* (2016). Crystal structure of the human sterol transporter ABCG5/ABCG8. *Nature* 533, 561-564.

- Leppert, G., McDevitt, R., Falco, S.C., Van Dyk, T.K., Ficke, M.B., and Golin, J. (1990). Cloning by gene amplification of two loci conferring multiple drug resistance in *Saccharomyces*. *Genetics* *125*, 13-20.
- Livnat-Levanon, N., A, I.G., Ben-Tal, N., and Lewinson, O. (2016). The uncoupled ATPase activity of the ABC transporter BtuC2D2 leads to a hysteretic conformational change, conformational memory, and improved activity. *Scientific reports* *6*, 21696.
- Locher, K.P. (2016). Mechanistic diversity in ATP-binding cassette (ABC) transporters. *Nat Struct Mol Biol* *23*, 487-493.
- Locher, K.P., Lee, A.T., and Rees, D.C. (2002). The *E. coli* BtuCD structure: a framework for ABC transporter architecture and mechanism. *Science* *296*, 1091-1098.
- Mahe, Y., Lemoine, Y., and Kuchler, K. (1996). The ATP binding cassette transporters Pdr5 and Snq2 of *Saccharomyces cerevisiae* can mediate transport of steroids in vivo. *J Biol Chem* *271*, 25167-25172.
- Mandala, M., Serck-Hanssen, G., Martino, G., and Helle, K.B. (1999). The fluorescent cationic dye rhodamine 6G as a probe for membrane potential in bovine aortic endothelial cells. *Analytical Biochemistry* *274*, 1-6.
- Manolaridis, I., Jackson, S.M., Taylor, N.M.I., Kowal, J., Stahlberg, H., and Locher, K.P. (2018). Cryo-EM structures of a human ABCG2 mutant trapped in ATP-bound and substrate-bound states. *Nature* *563*, 426-430.
- Meyers, S., Schauer, W., Balzi, E., Wagner, M., Goffeau, A., and Golin, J. (1992). Interaction of the yeast pleiotropic drug resistance genes PDR1 and PDR5. *Current genetics* *21*, 431-436.
- Milewski, S., Mignini, F., Prasad, R., and Borowski, E. (2001). Unusual susceptibility of a multidrug-resistant yeast strain to peptidic antifungals. *Antimicrob Agents Chemother* *45*, 223-228.
- Müller, F., Ackermann, P., and Margot, P. (2011). *Fungicides, Agricultural*, 2. Individual Fungicides.
- Muller, M., Bakos, E., Welker, E., Varadi, A., Germann, U.A., Gottesman, M.M., Morse, B.S., Roninson, I.B., and Sarkadi, B. (1996). Altered drug-stimulated ATPase activity in mutants of the human multidrug resistance protein. *J Biol Chem* *271*, 1877-1883.
- Neuhaus, H.E., and Wagner, R. (2000). Solute pores, ion channels, and metabolite transporters in the outer and inner envelope membranes of higher plant plastids. *Biochimica et biophysica acta* *1465*, 307-323.

- Oancea, G., O'Mara, M.L., Bennett, W.F., Tieleman, D.P., Abele, R., and Tampe, R. (2009). Structural arrangement of the transmission interface in the antigen ABC transport complex TAP. *Proc Natl Acad Sci U S A* *106*, 5551-5556.
- Oldham, M.L., Davidson, A.L., and Chen, J. (2008). Structural insights into ABC transporter mechanism. *Curr Opin Struct Biol* *18*, 726-733.
- Oswald, C., Holland, I.B., and Schmitt, L. (2006). The motor domains of ABC-transporters. What can structures tell us? *Naunyn Schmiedebergs Arch Pharmacol* *372*, 385-399.
- Paumi, C.M., Chuk, M., Snider, J., Stagljar, I., and Michaelis, S. (2009). ABC transporters in *Saccharomyces cerevisiae* and their interactors: new technology advances the biology of the ABCC (MRP) subfamily. *Microbiology and molecular biology reviews* : MMBR *73*, 577-593.
- Perozo, E., Cortes, D.M., Sompornpisut, P., Kloda, A., and Martinac, B. (2002). Open channel structure of MsCL and the gating mechanism of mechanosensitive channels. *Nature* *418*, 942-948.
- Pfaller, M.A., and Diekema, D.J. (2007). Epidemiology of invasive candidiasis: a persistent public health problem. *Clinical microbiology reviews* *20*, 133-163.
- Pomorski, T.G., and Menon, A.K. (2016). Lipid somersaults: Uncovering the mechanisms of protein-mediated lipid flipping. *Progress in lipid research* *64*, 69-84.
- Prasad, R., Banerjee, A., Khandelwal, N.K., and Dhamgaye, S. (2015). The ABCs of *Candida albicans* Multidrug Transporter Cdr1. *Eukaryot Cell* *14*, 1154-1164.
- Prescher, M., Kroll, T., and Schmitt, L. (2019). ABCB4/MDR3 in health and disease - at the crossroads of biochemistry and medicine. *Biol Chem*.
- Reich-Slotky, R., Panagiotidis, C., Reyes, M., and Shuman, H.A. (2000). The detergent-soluble maltose transporter is activated by maltose binding protein and verapamil. *J Bacteriol* *182*, 993-1000.
- Roepe, P. (2000). What is the Precise Role of Human MDR 1 Protein in Chemotherapeutic Drug Resistance. *Current Pharmaceutical Design* *6*, 241-260.
- Roepe, P.D., Wei, L., Hoffman, M.M., and Fritz, F. (1996). Altered drug translocation mediated by the MDR protein: Direct, indirect, or both? *Journal of Bioenergetics and Biomembranes* *28*, 541-555.

- Rogers, B., Decottignies, A., Kolaczowski, M., Carvajal, E., Balzi, E., and Goffeau, A. (2001). The pleiotropic drug ABC transporters from *Saccharomyces cerevisiae*. *J Mol Microb Biotech* 3, 207-214.
- Rosenberg, M.F., Kamis, A.B., Callaghan, R., Higgins, C.F., and Ford, R.C. (2003). Three-dimensional structures of the mammalian multidrug resistance P-glycoprotein demonstrate major conformational changes in the transmembrane domains upon nucleotide binding. *J Biol Chem* 278, 8294-8299.
- Sa-Correia, I., dos Santos, S.C., Teixeira, M.C., Cabrito, T.R., and Mira, N.P. (2009). Drug:H⁺ antiporters in chemical stress response in yeast. *Trends in microbiology* 17, 22-31.
- Saier, M.H., Jr. (2000). A functional-phylogenetic classification system for transmembrane solute transporters. *Microbiology and molecular biology reviews* : MMBR 64, 354-411.
- Sauna, Z.E., Bohn, S.S., Rutledge, R., Dougherty, M.P., Cronin, S., May, L., Xia, D., Ambudkar, S.V., and Golin, J. (2008). Mutations define cross-talk between the N-terminal nucleotide-binding domain and transmembrane helix-2 of the yeast multidrug transporter Pdr5: possible conservation of a signaling interface for coupling ATP hydrolysis to drug transport. *J Biol Chem* 283, 35010-35022.
- Scaduto, R.C., and Grotyohann, L.W. (1999). Measurement of mitochondrial membrane potential using fluorescent rhodamine derivatives. *Biophys J* 76, 469-477.
- Schmitt, L., and Tampe, R. (2002). Structure and mechanism of ABC transporters. *Curr Opin Struct Biol* 12, 754-760.
- Seddon, A.M., Curnow, P., and Booth, P.J. (2004). Membrane proteins, lipids and detergents: not just a soap opera. *Biochimica et biophysica acta* 1666, 105-117.
- Servos, J., Haase, E., and Brendel, M. (1993). Gene SNQ2 of *Saccharomyces cerevisiae*, which confers resistance to 4-nitroquinoline-N-oxide and other chemicals, encodes a 169 kDa protein homologous to ATP-dependent permeases. *Molecular & general genetics* : MGG 236, 214-218.
- Sharom, F.J. (1997). The P-Glycoprotein Efflux Pump: How Does it Transport Drugs? *Journal of Membrane Biology* 160, 161-175.
- Shukla, S., Abel, B., Chufan, E.E., and Ambudkar, S.V. (2017). Effects of a detergent micelle environment on P-glycoprotein (ABCB1)-ligand interactions. *J Biol Chem* 292, 7066-7076.

- Singh, H., Velamakanni, S., Deery, M.J., Howard, J., Wei, S.L., and van Veen, H.W. (2016). ATP-dependent substrate transport by the ABC transporter MsbA is proton-coupled. *Nat Commun* 7, 12387.
- Sorum, B., Torocsik, B., and Csanady, L. (2017). Asymmetry of movements in CFTR's two ATP sites during pore opening serves their distinct functions. *Elife* 6.
- Steingold, K.A., Cefalu, W., Pardridge, W., Judd, H.L., and Chaudhuri, G. (1986). Enhanced Hepatic Extraction of Estrogens Used for Replacement Therapy. *J Clin Endocr Metab* 62, 761-766.
- Sugano, K., Kansy, M., Artursson, P., Avdeef, A., Bendels, S., Di, L., Ecker, G.F., Faller, B., Fischer, H., Gerebtzoff, G., *et al.* (2010). Coexistence of passive and carrier-mediated processes in drug transport. *Nature reviews Drug discovery* 9, 597-614.
- Tanabe, K., Bonus, M., Tomiyama, S., Miyoshi, K., Nagi, M., Niimi, K., Chindamporn, A., Gohlke, H., Schmitt, L., Cannon, R.D., *et al.* (2019). FK506 Resistance of *Saccharomyces cerevisiae* Pdr5 and *Candida albicans* Cdr1 Involves Mutations in the Transmembrane Domains and Extracellular Loops. *Antimicrob Agents Chemother* 63.
- Taylor, N.M.I., Manolaridis, I., Jackson, S.M., Kowal, J., Stahlberg, H., and Locher, K.P. (2017). Structure of the human multidrug transporter ABCG2. *Nature* 546, 504-509.
- Trounce, I., and Wallace, D.C. (1996). Production of transmitochondrial mouse cell lines by cybrid rescue of rhodamine-6G pre-treated L-cells. *Somatic cell and molecular genetics* 22, 81-85.
- Velamakanni, S., Yao, Y., Gutmann, D.A., and van Veen, H.W. (2008). Multidrug transport by the ABC transporter Sav1866 from *Staphylococcus aureus*. *Biochemistry* 47, 9300-9308.
- Vermitsky, J.P., and Edlind, T.D. (2004). Azole resistance in *Candida glabrata*: coordinate upregulation of multidrug transporters and evidence for a Pdr1-like transcription factor. *Antimicrob Agents Chemother* 48, 3773-3781.
- Wang, J., Grishin, N., Kinch, L., Cohen, J.C., Hobbs, H.H., and Xie, X.S. (2011). Sequences in the nonconsensus nucleotide-binding domain of ABCG5/ABCG8 required for sterol transport. *J Biol Chem* 286, 7308-7314.
- Ward, A., Reyes, C.L., Yu, J., Roth, C.B., and Chang, G. (2007). Flexibility in the ABC transporter MsbA: Alternating access with a twist. *Proc Natl Acad Sci U S A* 104, 19005-19010.
- Yan, N. (2013). Structural advances for the major facilitator superfamily (MFS) transporters. *Trends in biochemical sciences* 38, 151-159.

Yang, R., Cui, L., Hou, Y.-x., Riordan, J.R., and Chang, X.-b. (2003). ATP Binding to the First Nucleotide Binding Domain of Multidrug Resistance-associated Protein Plays a Regulatory Role at Low Nucleotide Concentration, whereas ATP Hydrolysis at the Second Plays a Dominant Role in ATP-dependent Leukotriene C₄ Transport. *Journal of Biological Chemistry* 278, 30764-30771.

Ziegler, M.L., and Davidson, R.L. (1981). Elimination of mitochondrial elements and improved viability in hybrid cells. *Somatic cell genetics* 7, 73-88.

A. Curriculum Vitae

Personal Data

Name	Manuel Wagner
Date of Birth	September 10, 1987
Place of Birth	Mettingen

University Education

July 2014 – recent	Doctorate Heinrich-Heine-University Düsseldorf Institute of Biochemistry Prof. Dr. Lutz Schmitt <i>In vitro analysis of the ABC transporter Pdr5</i>
October 2012 – June 2014	Master of Science – Chemistry and Business Administration Heinrich-Heine-University Düsseldorf Institute of Biochemistry Prof. Dr. Lutz Schmitt <i>Establishment of a Heterologous Expression of the Dehydratase NisB</i>
April 2012 – August 2012	Study Abroad Western Washington University, Bellingham, USA Non-Degree Program, Intensive English Program, Anthropology

October 2008 – February 2012

Bachelor of Science – Chemistry and Business Administration

Heinrich-Heine-University Düsseldorf

Institute of Biochemistry

Prof. Dr. Lutz Schmitt

Alanin-scanning Mutagenesis of the Nisin Cyclization Reaction

Civilian Service

July 2007 – August 2008

terre des hommes Deutschland e.V.,
Osnabrück

School Education

August 2000 – July 2007

Diploma from German secondary school
qualifying for university admission (*Abitur*)
Gymnasium Bad Iburg

Awards and Scholarships

April 2018

Fellowship

ABC2018 Fellow 7th FEBS Special Meeting on
ABC Proteins

August 2012

Honor Roll in the IEP at Western Washington
University, Summer Quarter 2012

July 2012

Scholarship

Joe and Anneliese Zauchner Scholarship at
Western Washington University

June 2012

Honor Roll in the IEP at Western Washington
University, Spring Quarter 2012

Publications

- 2019 **Wagner, M.**, Smits, S. H., & Schmitt, L. (2019). In vitro NTPase activity of highly purified Pdr5, a major yeast ABC multidrug transporter. *Scientific reports*, 9(1), 7761.
- 2017 **Wagner, M.**, Doehl, K., & Schmitt, L. (2017). Transmitting the energy: interdomain cross-talk in Pdr5. *Biological chemistry*, 398(2), 145-154.
- 2014 AlKhatib, Z., Lagedroste, M., Zschke, J., **Wagner, M.**, Abts, A., Fey, I., ... & Smits, S. H. (2014). The C-terminus of nisin is important for the ABC transporter Nis FEG to confer immunity in *Lactococcus lactis*. *Microbiologyopen*, 3(5), 752-763.

B. Acknowledgments

Mein ganz besonderer Dank gilt meinem Doktorvater Prof. Dr. Lutz Schmitt. Danke, dass du es mir ermöglicht hast, diese Arbeit anzufertigen und dabei immer mit Rat und Tat zur Seite standst. Besonders in den doch manchmal tiefen Tiefen, die es gab, stand immer deine Tür offen und du hattest eine zündende Idee. Die Möglichkeiten, die du mir geboten hast, dieses spannende Projekt zu realisieren und die Begeisterung, die du immer dafür gezeigt hast, sind etwas ganz Besonderes und ich werde mich immer gerne an diese wichtige und besondere Zeit zurückerinnern!

Des Weiteren danke ich Dr. Sander Smits. Du hast in den Momenten, in denen der Frust groß war immer gewusst, wie du mich wieder auf die Beine bringen konntest, ob mit Witz oder Rat. In den zahllosen Meetings hast du es stets verstanden, mich und uns auf das Wesentliche zurück zu führen, wenn die Fantasie mal wieder mit uns durchging. Die morgendliche Tasse Kaffee und die offenen und produktiven Gespräche, genauso wie der Spaß für den du zu haben warst, werden in guter Erinnerung bleiben.

Bei PD Dr. Ulrich Schulte danke ich, mich mit der Materie der Biochemie vertraut zu machen. Ohne dich wäre ich nie zur Biochemie gekommen. Darüber hinaus warst du immer ansprechbar, wenn mein biochemisches Wissen mal nicht ausgereicht hat oder organisatorische Fragen aufgekommen sind und wusstest stets in deiner ruhigen und besonnenen Art zu helfen.

Hiermit danke ich Prof. Dr. Georg Groth für die freundliche Übernahme des Korreferats meiner Arbeit.

Den Kooperationspartnern Prof. Dr. Ben F. Luisi und Prof. Dr. John Golin danke ich für eine erfolgreiche und interessante Zusammenarbeit. Zudem möchte ich Prof. Dr. Ben F. Luisi und Prof. Dr. Bert Poolman für ihre große Gastfreundschaft danken, sowie ihre Bereitschaft Wissen zu teilen und mir einen interessanten Einblick in die Forschung in ihren Instituten zu ermöglichen.

Martin, dir danke ich, dass du schwierige Zeiten erträglicher, frustrierende Zeiten auch mal unerträglicher und gute Zeiten besser gemacht hast, mit deinen Witzen und auch

aufbauenden Worten. Die fachlichen Gespräche werden genauso in Erinnerung bleiben, wie das morgendliche Pumpen, das abendliche Zocken oder Bierchen.

Tobias und Jens, euch danke ich, dass ihr euer Wissen und Enthusiasmus für die Wissenschaft und den Whisky mit mir geteilt habt. Beides hat manchmal auch Kopfschmerzen bereitet. Jens, dir danke ich auch dafür, dass du mich während der Masterarbeit mit dem Biacore auf die Frustrationen der Doktorzeit vorbereitet hast.

Danke Isabelle, Olivia, Julia für eure offene und lustige Art und fürs Ausrasten, wenn es sein musste. Ihr haltet die Truppe am Laufen. Passt auf, dass Tim nicht noch mehr runterfallen lässt. Tim, danke für so manchen Lacher und gute Labor- und Büronachbarschaft.

Den „Neuen“, Florestan, Manuel, Zohreh, Alexandra, Vivien und Stefanie, die inzwischen gar nicht mehr so neu sind, danke ich für eine tolle Atmosphäre am und neben dem Institut. Allen, aber natürlich besonders der neuen Pdr5 Chefin Stefanie, wünsche ich das Beste für die Zukunft.

Silke und Martina, danke euch, dass ihr euch stets um alles und alle kümmert und den Betrieb in Gang haltet.

Ich danke der „alten“ Truppe (zu der ich mich inzwischen auch schon zähle) rund um Marcel, Sven und Michael. Ihr habt mich die meisten Jahre während dieser Arbeit begleitet, habt Leid und Freud mit mir geteilt und viele schöne Momente verbracht. Das wird auf ewig in Erinnerung bleiben.

Auch möchte ich meinen ehemaligen Kollegen Rebecca, Katja, Ricarda, Diana, Iris, André und Christian für eine tolle Zeit danken.

Der Arbeitsgruppe von Alexej mit Athanasios, Michael und Maryna danke ich für den frischen Wind, den sie ins Institut gebracht haben, mit interessanten Gesprächen und viel positiver Stimmung.

Ganz besonderer Dank gilt meiner Familie, meiner Freundin und auch meinen Freunden, die mich über die gesamte Zeit mit viel Kraft, Verständnis und Liebe unterstützt haben. Ich danke

euch für eure Geduld und dass ihr immer an mich geglaubt habt. Ohne euch wäre all dies nicht möglich gewesen.

C. Declaration

Ich versichere an Eides Statt, dass die Dissertation von mir selbständig und ohne unzulässige fremde Hilfe unter Beachtung der „Grundsätze zur Sicherung guter wissenschaftlicher Praxis an der Heinrich-Heine-Universität Düsseldorf“ erstellt worden ist. Die Dissertation wurde in der vorgelegten oder in ähnlicher Form noch bei keiner anderen Fakultät eingereicht. Ich habe bisher keine erfolglosen und erfolgreichen Promotionsversuche unternommen.

(Ort, Datum)

(Manuel Wagner)